Morphotectonic architecture and evolution of the postulated microcontinental blocks and deep offshore regions adjacent to the southwestern continental margin of India and its conjugate regions of Madagascar

A Thesis submitted in partial fulfillment for the Degree of

DOCTOR OF PHILOSOPHY

In the School of Earth, Ocean and Atmospheric Sciences

Goa University

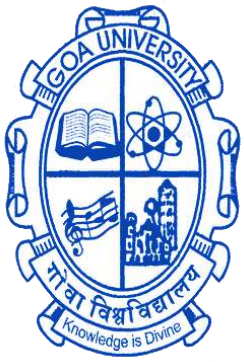

By

Bijesh C. M.

School of Earth, Ocean and Atmospheric Sciences, Goa University,

Taleigao Plateau, Goa, India- 403206

&

National Centre for Polar and Ocean Research

Headland Sada, Vasco-da-Gama, Goa, India-403804

May 2022

DECLARATION

I, Bijesh C. M., hereby declare that this thesis represents work which has been carried out by me and that it has not been submitted, either in part or full, to any other University or Institution for the award of any research degree.

Place: Taleigao Plateau.

Date: 09-05-2022

Bijesh C. M.

CERTIFICATE

I hereby certify that the above Declaration of the candidate, Bijesh C. M., is true and the work was carried out under my supervision.

Dr. Yatheesh Vadakkeyakath

(Research Guide)

Principal Scientist

CSIR-National Institute of Oceanography

Dona Paula, Goa

DECLARATION FOR INCORPORATION OF REVIEWERS COMMENTS

I, Bijesh C. M., hereby declare that all suggestions from the reviewers have been incorporated in the thesis entitled “Morphotectonic architecture and evolution of the postulated microcontinental blocks and deep offshore regions adjacent to the southwestern continental margin of India and its conjugate regions of Madagascar”.

Place: Taleigao Plateau Bijesh C. M.

Acknowledgment

I frequently ponder the path of my research field following my post-graduation. Initially, entering the research field was not my deliberate choice, but I was later afforded the opportunity to pursue a PhD. Now, the time has come to bring the current phase of my research career to a close.

I have done my master's dissertation with ***Dr. Yatheesh Vadakkeyakath****, Principal scientist from CSIR-National Institute of Oceanography, Goa. Since then he has been a true mentor in my research career. After working in various institutes, finally I got a chance to pursue the PhD under his guidance. His perfectionism in the field of research work is the main thing I admire. I take this opportunity to express my sincere gratitude towards him for his valuable support in my personal life and guidance during my entire research career.*

One of the major breakthroughs in my career is that I joined as a Project Scientist at National Center for Polar and Ocean Research as a member of EEZ Group, led by ***Dr. John Kurian P****. (Scientist F, NCPOR). Without his consent and continuous support, this work would not have been finished in a better way. The EEZ data that he was ready to share with me was a great appreciation for this research work. The immense support he has given during this entire time is unremarkable. I am very much grateful for his support, encouragement and work freedom at NCPOR during this period.*

I express my gratitude to ***Dr. M. Ravichandran****,* ***Mr. Mirza Javed Beg*** *(former Directors, NCPOR, Goa), and,* ***Dr. Thamban Meloth*** *(Director, NCPOR) for allowing me to do this PhD work and providing necessary facilities in the Institute. I am grateful to* ***Prof. Sunil Kumar Singh*** *(Director CSIR-NIO, Goa) for his support. I am thankful to* ***Prof. H. B. Menon****, Former Dean & Vice Chancellor, Goa University;* ***Prof. C. U. Rivonker****, The Dean;* ***Prof. Vishnu Murty Matta****, Vice Dean (Research);* ***School of Earth, Ocean and Atmospheric Sciences*** *and the* ***Administrative Staff*** *for their support to ease the registration and official formalities in the department.*

I wish to express my sincere acknowledgement to ***Prof. G. N. Nayak*** *and* ***Dr. K. A. Kamesh Raju****, my advisors, and Doctoral Committee Members for their valuable evaluation and suggestions in the progress of my research in a productive and affable manner. Their*

critical feedback during the different stages of the research work helped me to improve the results of the study. Special thanks to Prof. Nayak for his guidance in the University procedures and formalities.

I extend my gratitude to the ***Ministry of Earth Sciences (MoES****), New Delhi,* ***Directorate General of Hydrocarbon (DGH)****, India for the permission to use the data. I thank the* ***Administration Section, Library and IT Section at NCPOR****, Goa for their assistance as and when required. The Data Center at CSIR-NIO, Goa is acknowledged. I express my sincere thanks to Mr. Abhishek Tyagi (Scientist, NCPOR), Smita, Sradha, Suman & Sacchi (EEZ Lab, NCPOR) for their support and help.*

Within this time, I have spent almost 370 days onboard research vessels like ORV Sagar Kanya and MGS Sagar. I express my thanks to the scientific as well as ship crew who participated in various cruises onboard different research vessels for the acquisition of marine geophysical data under the EEZ Program.

I feel fortunate to have a lot of friends in the NCPOR who made these seven years truly memorable. I extend my love to Solly, Susanth, Subeesh, Prajith, Linsy, Chanku, Nisha, Femi, Hari, Mahesh, Preethi, Shafeeq, Lathika, Midhun, Sarath Chandraprasad, Bincy, Sulfi, Sarun, Rahul Yadav, Sibin and Sreerag.

I have enjoyed the days I spent in NIO with my friends since my M.Sc. dissertation time. I will always remember those moments and express my love to Nikhil, Sethu, Savio, Jismy, Navaneeth, Gokul, Robin, Benitha, Saira, Zeba, Ashita, Teesha, Anoop, Sherin, Tyson, Ajeesh, Shuhail, Rasiq, Rashith, Yasar, Shanas, Gautham, Jishad and Yadhu.

Love for my friends who have always supported me when things go disheartening; Sruthi, Reshmi, Vrinda and Twinkle.

Dear "Kochu", your memories are always with me.

I express my respect and love to Chittooramma, Mummy, and Saradamma.

I thank Achan, Amma, Lekha, Sajith, Anikha, Abhi and Viswajith for their support.

Lots of love to Aswini, thanks for always being there for me.

Bijesh C. M.

Dedicated to:

My dear sister Lekha

Table of Contents

List of Tables

List of Figures

PREFACE

The formation of the Indian Ocean and its adjacent continental margins were resulted by the breakup and spreading of the eastern sector of the Gondwanaland. The rifting followed by drifting of the continental blocks (Africa, Madagascar, Antarctica, India, Australia and Arabia) caused formation of various ocean basins in the Indian Ocean. Most of the Indian Ocean regions were studied through the geo-scientific investigations during the International Indian Ocean Expedition (IIOE) in the 1960s. Contemporarily, the concept of seafloor spreading was getting accepted into the theory of plate tectonics. Based on this concept and preliminary geophysical data collected during IIOE, researchers proposed a broad plate tectonic evolutionary history for the Indian Ocean by providing large-scale plate reconstruction models. Subsequently, various researchers improved the identifications of magnetic anomalies in different ocean basins, and provided improved models for describing the sectoral plate tectonic evolution.

In the revised plate tectonic evolution model published by Bhattacharya and Yatheesh (2015), several postulated continental blocks (Northern Madagascar Ridge, Alleppey-Trivandrum Terrace Complex, Laccadive Plateau, Laxmi Ridge, and the Saurashtra Volcanic Platform) were accommodated as intervening continental slivers between India and Madagascar in their pre-breakup scenario. This proposal is mainly based on the existing information, the shape and fitting of these features in the tectonic evolutionary model. The detailed understanding of the crustal architecture of these postulated microcontinental blocks are yet to be confidently established. In addition, the southwestern continental margin of India and its adjacent regions have experienced various geodynamic events that might have created imprints over the onshore as well as offshore regions, and the detailed morphological study on this aspect is awaiting. The present study mainly deals with the detailed understanding of the geomorphological signatures and morphotectonic architecture of the postulated continental slivers in the southwestern continental margin of India and its conjugate region of Madagascar. The data used for this study mainly consists of high-resolution multibeam bathymetry data, sea-surface gravity, magnetic and bathymetry profiles; satellite-derived gravity data; multichannel seismic sections; published seismic reflection and refraction results; and the geographic extent of the offshore and onshore

tectonic elements. The contents of the present study have been organised in eight chapters as given below:

Chapter 1 comprises the present understanding on the large-scale plate tectonic evolutionary history of the Indian Ocean and general idea on the major physiographic features in the Western Indian Ocean. Further, details about study area in the present work and brief description of research questions and its scope has been introduced.

Chapter 2 delivers a review of the existing knowledge about the tectonics and overall geological framework of the conjugate onshore and offshore regions from the southwestern part of India and southeastern part of Madagascar.

Chapter 3 provides a detailed information on the various data used in the current study and the methodology followed for analysis and interpretation. The methodology and the software packages used for multibeam data processing, integrated gravity and magnetic forward modelling and plate tectonic reconstruction models have been concisely explained.

Chapter 4 presents the morphotectonic characteristics of the southwestern continental margin of India and the adjacent deep offshore regions using an up-to-date compilation of marine geophysical data. The updated bathymetric map of the study area highlights 33 bathymetric high features, consisting of 14 seamounts, 8 hills, 3 knolls, 2 guyots and 6 plateaus. Sub-seafloor configuration has been analyzed from the selected bathymetric features using seismic reflection sections. The inferred basement configuration suggests that some of the bathymetric features might represent volcanic extrusives while others might represent basement highs associated with bulging of sediment layers over the subsurface volcanic intrusive. The sea-surface gravity signatures of the selected features suggest a characteristic relatively high gravity anomaly superimposed over a regional negative anomaly. The magnetic anomalies over the bathymetric high features exhibits complex behaviour and it is difficult to correlate this only with the topography. Both negative and positive magnetic anomalies are observed over the features, superimposed over the regional magnetic signatures. Based on the proximity to the St. Mary Islands and the Ezhimala Igneous Complex, which are considered to be products of the Marion hotspot, it is considered that the bathymetric highs located in the southwestern continental slope of India and along-strike of Chain-Kairali Escarpment were formed by the Marion hotspot volcanism. The bathymetric

features in the Laccadive Basin and eastern part of the Laccadive Plateau are in the proximity of the Réunion hotspot track and therefore the genesis of these features are attributed to the Réunion hotspot volcanism.

Chapter 5 explains the integrated geophysical study carried out for understanding the geophysical signatures and evaluation of the postulated continental nature of the Laccadive Plateau. The overall morphology of the Laccadive Plateau has been explained from the high-resolution multibeam bathymetry data. The block-faulted nature of the basement representing the proposed Cannanore Rift System on the central part of the Laccadive Plateau is clearly visible from the available multichannel seismic reflection sections. Sea-surface gravity and magnetic profiles cutting across the Laccadive Plateau and Laccadive Basin are analysed to establish the geophysical signatures. Integrated forward modelling of the gravity and magnetic profiles over Laccadive Plateau suggests that the Laccadive Plateau can be reasonably explained in terms of a continental sliver intermingled with volcanic intrusives.

Chapter 6 deals with the geophysical investigation on the bathymetric highs located west of the Laccadive Plateau, using high-resolution multibeam bathymetric, gravity and magnetic data. The bathymetric map suggests the presence of a nearly elliptical bathymetric high complex consisting of three seamounts and several linear ridge-like features surrounding a region of nearly flat seafloor measuring ~ 50 km x 30 km. This bathymetric high complex is referred to as the Sagar Kanya Bathymetric High Complex (SKBHC), constituting Sagar Kanya-1 (SK-1), Sagar Kanya-2 (SK-2) and Sagar Kanya-3 (SK-3) seamounts. The free-air gravity anomalies of the Sagar Kanya Bathymetric High Complex are correlated with topography in general, with their maximum corresponding to the locations of the summit of the seafloor features. The magnetic anomalies over the study area are complex, consisting of several positive and negative magnetic anomalies. The morphology of the Sagar Kanya Bathymetric High Complex appears to qualify to be considered as the rim surrounding the summit caldera of a large extinct submarine volcano, referred to as the Sagar Kanya Volcano. Considering the tectonic framework of the western continental margin of India and the adjacent deep ocean basins, the genesis of these phases of volcanism has been attributed to the Réunion hotspot.

Chapter 7 examines the proposed conjugate nature of Northern Madagascar Ridge and Alleppey-Trivandrum Terrace Complex in terms of geophysical signatures and the derived crustal model. Comparison of the crustal configuration derived for these features reveal that both these features can be explained in terms of thinned continental crust intermingled with volcanic intrusives. Therefore, based on these observations derived from the integrated interpretation of geophysical data, complemented by the postulated juxtaposition observed from the plate tectonic reconstruction, it support the earlier interpretation that the NMR and ATTC represent conjugate features that was proposed based on the fitting of shape and size of the bathymetric notch observed in the southeastern continental margin of Madagascar with a bathymetric protrusion observed in the southwestern continental margin of India in the India-Madagascar pre-drift scenario. These features remained as a single unit prior to ~ 88 Ma and subsequently got separated during the India-Madagascar breakup.

Chapter 8 summarizes the main findings and highlights the results from the thesis. A discussion on the scope of future work also has been discussed in this chapter.

A complete list of references of the works cited has been provided in alphabetical order at the end of the thesis. Also, a copy of major results from the thesis published in scientific journals are annexed.

Chapter 1

General Background

1.1 Introduction

The Indian Ocean (Figure 1.1), which represents the third largest ocean, is considered as the least studied region compared to the Pacific and Atlantic oceans in terms of marine geophysical investigations. The Indian Ocean is bordered by Africa and Arabia in the west; Iran, Pakistan, India and Bangladesh in the north; Burma, Thailand, Malaysian Peninsula, Andaman-Nicobar-Sumatra Trench and Australia in the east and Antarctica in the south. In terms of plate tectonics, the Indian Ocean encompasses the Indo-Australian Plate, the Arabian Plate, the African Plate and the Antarctic Plate (Figure 1.2). Broadly, the formation of the Indian Ocean is resulted by the breakup and spreading of the eastern sector of the Gondwanaland. The rifting followed by drifting of the continental blocks (Africa, Madagascar, Arabia, India, Australia and Antarctica) caused formation of various deep ocean basins and the associated continental margins in the Indian Ocean. Most of the Indian Ocean region was studied through the geo-scientific investigations during the International Indian Ocean Expedition (IIOE) in the 1960s. Contemporarily, the concept of seafloor spreading was getting accepted into the theory of plate tectonics. Based on this concept and preliminary geophysical data collected during IIOE, researchers proposed large-scale plate tectonic reconstruction models to depict broad plate tectonic evolution for the Indian Ocean (McKenzie and Sclater, 1971; Norton and Sclater, 1979; Besse and Courtillot, 1988; Scotese et al., 1988). As far as the Western Indian Ocean is concerned, subsequent researchers (e.g. Bhattacharya et al., 1994a; Malod et al., 1997; Bernard and Munschy, 2000; Chaubey et al., 2002a; Royer et al., 2002; Yatheesh et al., 2009; Fournier et al., 2010; Eagles and Wibisono, 2013; Cande et al., 2010; Shuhail et al., 2018; Yatheesh et al., 2019) improved the identifications of magnetic anomalies and estimation of age of the oceanic crust in different ocean basins, and provided improved models for describing the sectoral plate tectonic evolution. Recently, Bhattacharya and Yatheesh (2015) evaluated all the magnetic anomaly identifications and provided a revised plate tectonic reconstruction model for early

opening history of the Arabian Sea by accommodating the several postulated microcontinental blocks and the identified now-extinct spreading centres. However, a detailed marine geophysical investigation to understand the morphotectonic architecture of these postulated microcontinental blocks and the geomorphological and geophysical signatures of the various features formed as a result of subsequent evolution of these regions are still awaited.

In this chapter, the geographical extent of the study area has been presented followed by a brief description of the major physiographic and structural features in the sector of the Western Indian Ocean from the southwestern continental margin of India to the southeastern continental margin of Madagascar. In addition, a brief description has been provided on the large-scale plate tectonic evolution of the Western Indian Ocean. At the end of this chapter, the objectives and scope of the study have been introduced.

1.2 Study Area: The Western Indian Ocean

The study area (Figure 1.3) mainly constitutes the major part of the Western Indian Ocean, covering the southwestern continental margin of India, southeastern continental margin of Madagascar and the deep ocean basins adjacent to these regions.

1.3 Major Tectonic Features in the Western Indian Ocean

The most dominant bathymetric features of the Western Indian Ocean are the active mid-oceanic ridges, a large number of aseismic ridges or submarine plateaus, seamounts, islands and deep ocean basins. A brief description of these features has been provided in this section.

1.3.1 Mid-Oceanic Ridge System (MORs)

The Western Indian Ocean mainly represents three branches of the active mid-oceanic ridge system, the northern branch consisting of the Central Indian Ridge (CIR), the Carlsberg Ridge (CR) and the Sheba Ridge (SR), the western branch representing the Southwest Indian Ridge (SWIR) and the eastern branch representing the Southeast Indian Ridge (SEIR). These three branches of the mid-oceanic ridges, forming the divergent boundaries between Indian, African, and

Antarctic plates (Figure 1.2), appear to converge near 25.5°S, 70°E in the form of a ridge-ridge-ridge triple junction, referred to as the Rodrigues Triple Junction (RTJ). The Central Indian Ridge lies between Rodrigues Triple Junction and the equator, broadly forming a nearly north-south lineation. The Carlsberg Ridge is the northwest-southeast trending ridge segment, which lies between the equator and the Owen Fracture Zone (OFZ). The Sheba Ridge in the Gulf of Aden forms an offset extension of the Carlsberg Ridge and it connects the East African Rift Valley and the Red Sea Spreading Centre (RSSC). The NE-SW trending Southwest Indian Ridge starts from the Rodrigues Triple Junction and joins the southern part of the Mid-Atlantic Ridge System at the Bouvet Triple Junction near 55°S and 1°W. The NW-SE trending Southeast Indian Ridge starts from the Rodrigues Triple Junction and extends southeastward to join the Pacific-Antarctic Mid-oceanic Ridge System south of Australia.

1.3.2 Submarine Plateaus and Aseismic Ridges

Apart from the mountainous zones of the seismically active mid-oceanic ridge system, the Western Indian Ocean also contains a number of prominent topographic features, which project high above the ocean floor (Figure 1.3). These features are morphologically elongated in nature and are wholly submarine, but a few of them rise above sea level and appear as islands. The major aseismic ridges or submarine plateaus in the Western Indian Ocean are the Laxmi Ridge (LXR), the Laccadive-Chagos Ridge (LCR), the Comorin Ridge (CMR), the Seychelles-Mascarene Plateau (SMP), the Madagascar Ridge (MDR), and the Mozambique Ridge (MZR). The Laxmi Ridge is an aseismic basement high feature, consisting of a ~ NW-SE and an E-W trending segments, located off the northwestern continental margin of India. The Laccadive-Chagos Ridge is a slightly arcuate major elongated aseismic feature, which extends to about 2500 km approximately along 73°E meridian between 14°N and 9°S. The Comorin Ridge extends towards south from the Cape Comorin for about 500 km and possess an average relief of about 1000 m. The Seychelles-Mascarene Plateau complex is an arcuate system of wide, partially isolated shallow banks (Seychelles Bank, the Saya de Malha Bank, the Nazareth Bank, the Cargados Bank and Caragos Bank), small islands (Mauritius Island and Réunion Island),

and it is located in the areas between Madagascar Island and the segment of the Central Indian and Carlsberg ridges. The Rodrigues Ridge is a narrow, linear ~ 250 km long volcanic ridge that intersects the Mascarene Plateau perpendicularly about 200 km north. The Madagascar Ridge is an aseismic, elongated basement high feature, appearing as southward extension of the Madagascar Island.

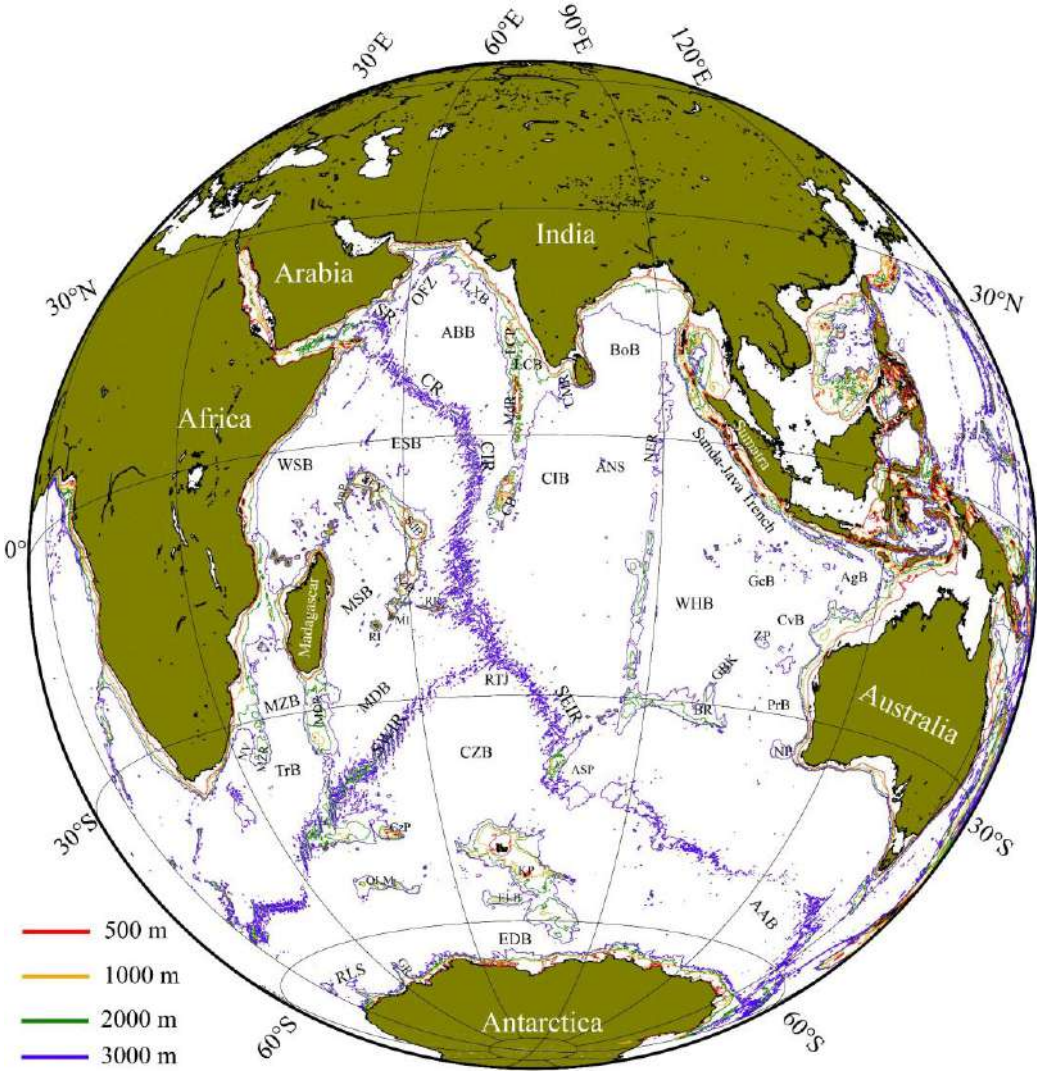

Figure 1.1: Physiographic map of the Indian Ocean with selected bathymetric contours of 200, 1000, 2000 and 3000 metres. Abbreviations used are provided in Table 1.1.

Table 1.1**:** Abbreviations used in the present study.

Ocean Basins		**Aseismic Ridges / Submarine Plateaus**	
AAB	Australian-Antarctic Basin	AmP	Amirante Plateau
ABB	Arabian Basin	BR	Broken Ridge
AgB	Argo Basin	CB	Chagos Bank
BoB	Bay of Bengal	CMR	Comorin Ridge
CIB	Central Indian Basin	CzP	Crozet Plateau
CvB	Cuvier Basin	ELB	Elan Bank
CZB	Crozet Basin	GBK	Gulden Draak and Batavia knolls
EDB	Enderby Basin	GR	Gunnerus Ridge
ESB	Eastern Somali Basin	KP	Kerguelen Plateau
GcB	Gascoyne Basin	LCP	Laccadive Plateau
MDB	Madagascar Basin	MDR	Madagascar Ridge
MSB	Mascarene Basin	MdR	Maldive Ridge
MZB	Mozambique Basin	NMR	Northern Madagascar Ridge
NV	Natal Valley	NP	Naturaliste Plateau
PrB	Perth Basin	NzB	Nazareth Bank
RLS	Riiser Larsen Sea	RR	Rodriguez Ridge
TrB	Transkei Basin	SdB	Saya de Malha Bank
WCIB	Western Central Indian Basin	SEY	Seychelles Plateau
WHB	Wharton Basin	WP	Wallaby Plateau
LCB	Laccadive Basin	ZP	Zenith Plateau
LXB	Laxmi Basin	ATTC	Alleppey-Trivandrum Terrace Complex
Mid-ocean Ridges		LAX	Laxmi Ridge
CIR	Central Indian Ridge	**Seamounts / Islands**	
CR	Carlsberg Ridge	ASP	Amsterdam & Saint Paul islands
SEIR	Southeast Indian Ridge	MI	Mauritius Island
SR	Sheba Ridge	RI	Réunion Island
SWIR	Southwest Indian Ridge	ANS	Afanasy Nikitin Seamount
RSSC	Red Sea Spreading Centre	OLM	Ob, Lena, Marion Dufresne seamount chain

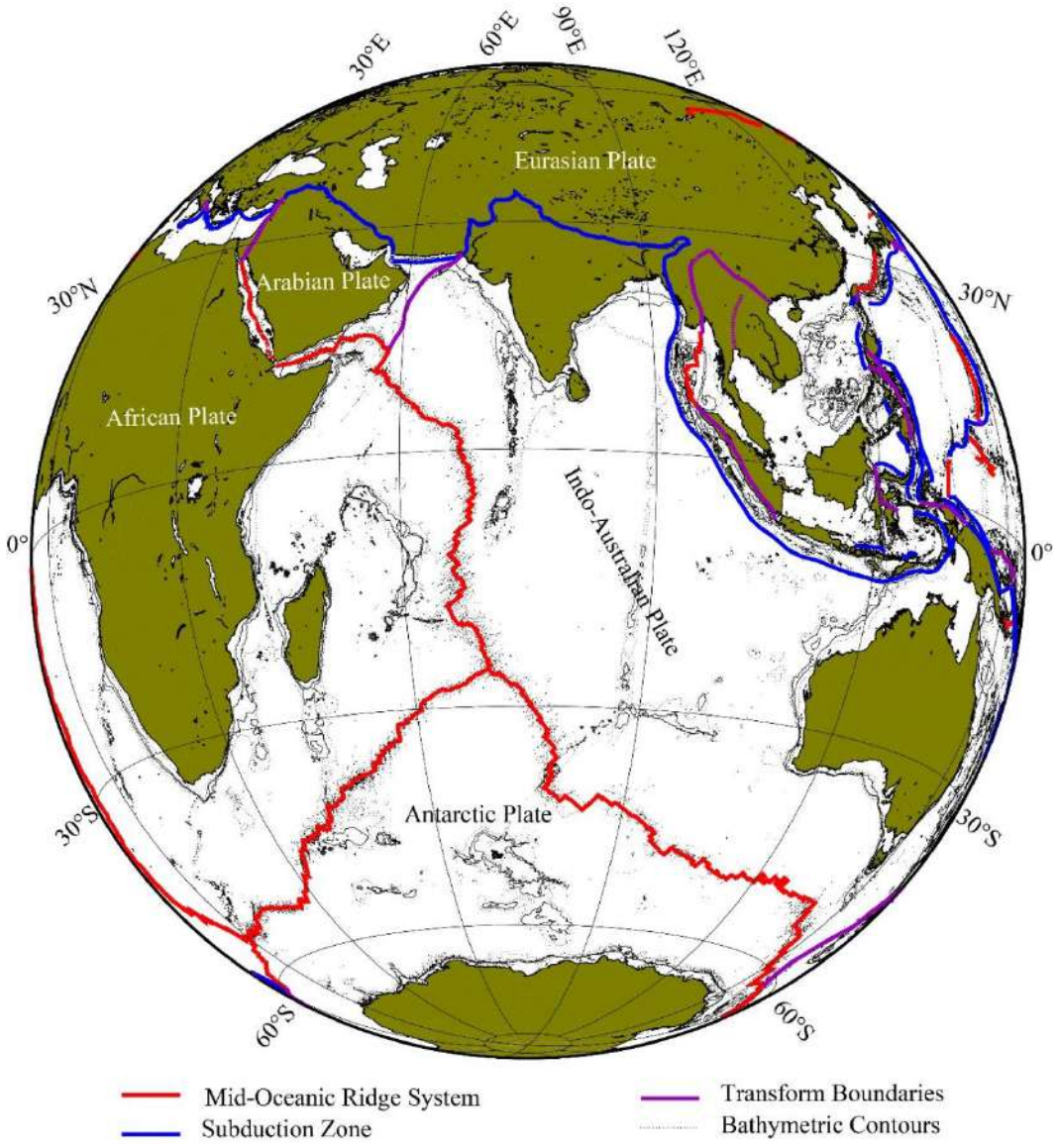

Figure 1.2: Major lithospheric plates in the Indian Ocean demarcated by the divergent, convergent and transform boundaries.

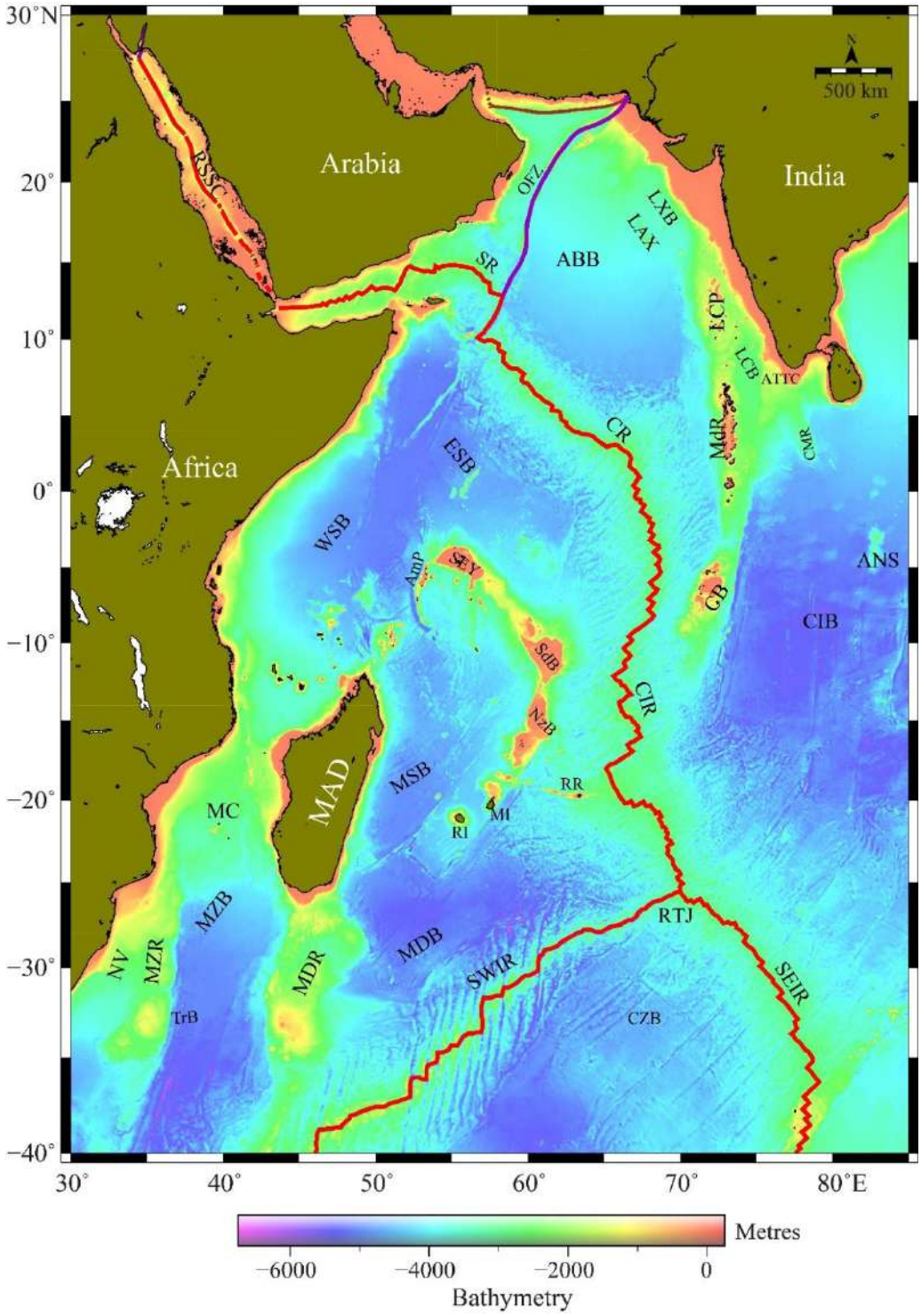

Figure 1.3: Bathymetric map of the Western Indian Ocean depicted by global bathymetric grid (GEBCO Compilation Group, 2020), showing the major features and domains. Other details are as in the Figures 1.1, 1.2, and Table 1.1.

1.3.3 Seamounts

Seamounts on the ocean floor are good indicators of the passage of the oceanic crust over loci of magma generation and this will help in the understanding of evolutionary history of ocean basins. The Geological and Geophysical Atlas of the Indian Ocean (Udintsev et al., 1975) and the later studies testified the presence of several seamounts in the Indian Ocean. However, very few of them are methodically studied and only scarce information is available about them in the public domain. Among these, the Error Seamount (Matthews, 1966; Ramana et al., 1987), Sagar Kanya Seamount (Bhattacharya and Subrahmanyam, 1991), Laxmi Basin seamount chain (Bhattacharya et al., 1994b), and the Afanasy Nikitin Seamount (Curray and Munasinghe, 1991) were characterized in terms of geomorphology and geophysical signatures from previous studies. The Error Seamount is located approximately at the northwestern boundary of the Carlsberg Ridge and it can be considered as a part of the Owen Fracture Zone system. The Sagar Kanya Seamount is located about 200 km west of the Laccadive Plateau with a total relief of 2464 m from the adjacent seafloor. The Laxmi Basin seamount chain, which consists of Raman Seamount, Panikkar Seamount and Wadia Guyot, lies approximately along the axial part of the Laxmi Basin.

1.3.4 Deep Ocean Basins

The surrounding continents, mid-oceanic ridges and the aseismic ridges divide the Western Indian Ocean into a number of deep ocean basins (Figure 1.3). Most of these basins were created by seafloor spreading through the presently active mid-oceanic ridges while the others were formed by the past episodes of seafloor spreading representing now-extinct spreading centres. These basins mainly consist of the Arabian Basin, the Eastern Somali Basin, the Laxmi Basin, the Gop Basin, the Laccadive Basin, the Central Indian Basin, the Crozet Basin, the Madagascar Basin, the Mascarene Basin, the Western Somali Basin, the Mozambique Basin, the Natal Valley, and the Transkei Basin. The Arabian Basin is bordered by the Owen Fracture Zone in the west, the Carlsberg Ridge in the south, the E-W trending segment of the Laxmi Ridge and the Gop Basin in the north and the NW-SE trending segment of the Laxmi Ridge and the Laccadive Plateau in the east. The Eastern Somali Basin, which represents the conjugate of the Arabian Basin, lies

between the Carlsberg Ridge in north; the northern part of the Seychelles-Mascarene Plateau in the south; the Central Indian Ridge in the east, and the Chain Ridge in the west. The Laxmi Basin is bordered by the western continental slope of India in the east and the NW-SE trending segment of the Laxmi Ridge in the west. The Gop Basin is located between the Saurashtra Volcanic Platform in the north and the E-W trending segment of the Laxmi Ridge in the south. The triangular shaped Laccadive Basin is bounded between the Laccadive Plateau in the west and the southwestern continental slope of India in the east. The Central Indian Basin is bordered by the southern part of the Central Indian Ridge, the Chagos Bank and the Maldive Ridge in the west; the Ninetyeast Ridge in the east; the Southeast Indian Ridge in the south and by the Bay of Bengal in the north. The Crozet Basin is located between the Southwest Indian Ridge in the northwest, the Southeast Indian Ridge in the northeast and the Ob, Lena and Marion Dufresne seamount chain in the south. The Madagascar Basin is located between the southwest Indian Ridge in the south, the Central Indian Ridge in the east and the Madagascar Ridge in the west. The Mascarene Basin, considered as the northwestern extension of the Madagascar Basin, locates between the Madagascar Island and the Seychelles-Mascarene Plateau. The Western Somali Basin is bordered by east coast of Africa in the west and northwest. The Mozambique Basin is one of the oldest basins in the Indian Ocean that is located between the N-S trending Madagascar and Mozambique ridges. The highly sedimented Owen Basin is bounded between the Gulf of Oman in the North, Sheba Ridge in the south, Arabian continental margin in the west, and Owen Fracture Zone in the east.

1.4 Large-scale Plate Tectonic Evolution of the Western Indian Ocean

The geomagnetic investigations carried out in the Indian Ocean could provide large-scale plate tectonic reconstruction model to illustrate the plate tectonic history of the Indian Ocean based on the identification of seafloor spreading type magnetic anomalies, delineation of fracture zone traces, and the paleomagnetic studies of the continental rocks (McKenzie and Sclater, 1971; Norton and Sclater, 1979; Besse and Courtillot, 1988; Scotese et al., 1988). This large-scale plate tectonic reconstruction model suggests that the present day configuration of continents, continental fragments and ocean basins were created by breakup and dispersal of a

super continent named “Pangea”. The Pangea was surrounded by the universal ocean “Panthalassa” (the ancestral Pacific) and eastern shores of Pangea were caved by a triangular sea called “Paleo-Tethys”. Around 200Ma, The Pangean Supercontinent began to split, first to Laurasia (northern part) and Gondwanaland (southern part) and the origin of the Indian Ocean is related to the fragmentation and dispersal of Gondwanaland. The Gondwanaland constitute the present-day South America, Africa, Arabia, Madagascar, Sri Lanka, India, Antarctica and Australia as major blocks. Major episodes of this plate tectonic evolution can be summarized into six different stages (Figure 1.4) as discussed below:

Stage 1: The break-up of Gondwanaland seems to have caused by the interaction of succession of hotspots and mantle plumes. The Karoo megaplume was the cause of the first split of Gondwanaland, and the breakup of Gondwanaland started by a rifting episode, which was initiated earlier than 152 Ma (Late Jurassic). As a result of this breakup, the Gondwanaland was divided into two blocks, West and East Gondwanaland (Figure 1.4a). The West Gondwanaland consisted of Africa, Arabia and South America; while the East Gondwanaland consisted of Antarctica, Australia, New Zealand, Madagascar, Seychelles, India and Sri Lanka. Gradually, East Gondwanaland moved southward relative to the West Gondwanaland and resulted in the opening of major ocean basins, such as the Mozambique Basin, the Riiser Larsen Sea, the Western Somali Basin and probably the Northern Somali Basin.

Stage 2: Further breakup of the East Gondwanaland commenced at about 133 Ma (Early Cretaceous), and the conjoined Antarctica-Australia block rifted and drifted away from Madagascar- Seychelles-India continental block (Figure 1.4b). These events resulted in the formation of the Bay of Bengal and the Enderby Basin.

Stage 3: The seafloor spreading event continued in a uniform fashion for about 15 m.y. followed by the separation of the Madagascar-Seychelles-India block from Australia-Antarctica block, after which the spreading between Africa-Arabia and Madagascar-Seychelles-India blocks occurred. About chron M0 (~ 118 Ma), spreading in the Western and Northern Somali Basin stopped, and resulted in the joining of Madagascar-Seychelles-India block to the African plate. About 30 m.y. later, due to the influence of Marion hotspot (~ 88 Ma) rifting was initiated between Madagascar and Seychelles-India blocks and shortly before 83 Ma, the seafloor

spreading detached Madagascar fully from Seychelles-India block resulting in the opening of the Mascarene Basin (Figure 1.4c). These events established a three plate system with a triple junction (Indian Ocean Triple junction) at 55°S in the Western Indian Ocean.

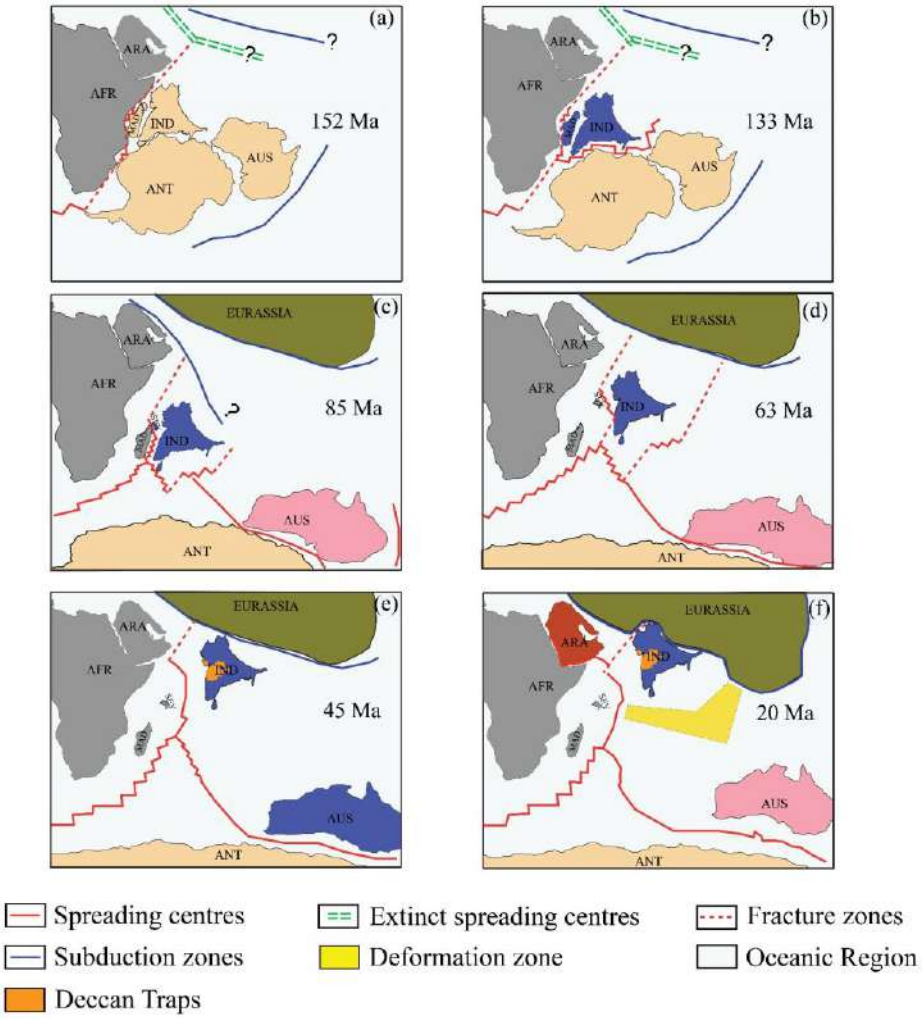

Figure 1.4: Schematic diagrams illustrating the large-scale plate tectonic evolution of the Western Indian Ocean in fixed Africa reference frame (modified after Yatheesh et al., 2013a). (a) Reconstruction at 152 Ma; (b) Reconstruction at 133 Ma; (c) Reconstruction at 85 Ma; (d) Reconstruction at 63 Ma; (e) Reconstruction at 45 Ma; (f) Reconstruction at 20 Ma. ANT: Antarctica; AFR: Africa; ARA: Arabia; IND: India; MAD: Madagascar; SEY: Seychelles; AUS: Australia.

Stage 4: During the northward drift of Seychelles-India block (Figure 1.4d), widespread volcanism took place over the Indian landmass and created the Deccan Trap flood basalt related to the Réunion hotspot activity (around 69-65 Ma, Duncan, 1990). Simultaneously an increase in spreading rate of the Madagascar and Mascarene basins occurred and resulted a rapid northward drift for Indian block. While continuing the northward drift, adjacent offshore regions came under the influence of Réunion hotspot and resulted in the formation of the Laccadive-Chagos Ridge and reorientation of the close by spreading centres. Around anomaly C28n (~ 63 Ma, Late Paleocene), spreading in the Mascarene Basin gradually stopped and formation of new spreading centre, the Paleo-Carlsberg Ridge got initiated resulting in the opening of the conjugate Arabian and Eastern Somali basins.

Stage 5: At around 55-50 Ma, Indian block is believed to have collided with the Kohistan-Ladakh Island Arc System and the Carlsberg, Central Indian and the Southeast Indian ridges experienced a slowing down of the spreading rate (Figure 1.4e). As a consequence of the continued collision between India and Eurasia, substantial crustal shortening took place along the northern border of Indian Plate and the plate boundaries in the Indian Ocean began to assume present-day spreading scenario (~ 40 Ma).

Stage 6: The spreading along the Carlsberg Ridge propagated westward between Africa and Arabia and initiated spreading along the Sheba Ridge and opened the Gulf of Aden during the late Miocene time. Another important event that might have started at ~ 20 Ma and still ongoing is the development of a wide deformed area in the Central Indian and Wharton basins (Figure 1.4f).

1.5 Objectives and Scope of the study

Bhattacharya and Yatheesh (2015) evaluated all the magnetic anomaly identifications and the geophysical signatures of the various offshore tectonic elements from the conjugate continental margins of India, Seychelles and Madagascar and the adjacent deep ocean basins, and provided a revised plate tectonic reconstruction model for describing the early opening of the Arabian Sea. In this model, several postulated microcontinental blocks (the Northern Madagascar Ridge, the Alleppey-Trivandrum Terrace Complex, the Laccadive Plateau, the Laxmi Ridge, the Seychelles Plateau, and the Saurashtra Volcanic Platform) were

accommodated as intervening continental slivers between India and Madagascar in their pre-breakup scenario. This postulation is mainly based on the existing information on the geophysical signatures and the shape and fitting of these features in the plate tectonic reconstruction model in their pre-drift scenario. However, the detailed understanding of the crustal architecture of these postulated microcontinental blocks are yet to be confidently established. In addition, the southwestern continental margin of India and its adjacent regions have experienced various geodynamic events that might have created imprints over the onshore as well as offshore regions, and the detailed morphological study on this aspect is still awaited. The present study mainly deals with the detailed understanding of the geomorphological and geophysical signatures of these features and morphotectonic architecture of the postulated continental blocks in the southwestern continental margin of India and its conjugate region of Madagascar. In this context, the present study focuses to address the following objectives:

- To understand geomorphology of the southwestern continental margin of India and the adjacent deep offshore regions
- To evaluate the postulated continental nature of the Laccadive Plateau and arrive at a crustal structure model based on integrated analysis of geophysical data
- To derive the crustal architecture of the Northern Madagascar Ridge and examine its proposed conjugate nature with the Alleppey-Trivandrum Terrace Complex
- To decipher detailed plate tectonic evolution of the southwestern continental margin of India and the adjacent deep offshore regions

For accomplishing these objectives, the study utilized high-resolution multibeam bathymetry data, sea-surface gravity, magnetic and bathymetry profiles; satellite-derived free-air gravity data; GEBCO global bathymetric grids and isobaths, multichannel seismic sections; published seismic reflection and refraction results; the geographic extent of the offshore and onshore tectonic elements; and the available published rotation parameters that constrain the relative motion among the associated continental blocks.

Chapter 2

Geological Framework

2.1 Introduction

The conjugate continental margins of India and Madagascar and their adjoining deep offshore regions were formed due to the rift-drift processes among various continental blocks that constitute the East Gondwanaland. The previous geophysical as well as geological studies carried out in these regions have detailed the existence of several tectonic elements that were used to constrain the present understanding on crustal structure and plate tectonic evolution of these regions. To examine and validate the results of the present study, presently available information on the structure and tectonic settings of the conjugate onshore and offshore regions adjacent to the southwestern part of India and southeastern part of Madagascar have been compiled and presented in this chapter.

2.2 Tectonic elements of the southwestern Indian mainland and its adjoining oceanic regions

2.2.1 Features on the Southwestern Indian mainland

The Indian subcontinent encompasses Himalayan mountain ranges in the north, Indo-Gangetic plain in the middle and Peninsular India in the south (Figure 2.1). The Indian shield is a combination of Precambrian metamorphic terrains with an age range of 3.6-2.6 Ga, one of the oldest cratonic blocks of the world (Sharma, 2009) and Deccan Trap or Deccan Volcanic Province (DVP). The Peninsular shield can be divided into Southern Granulite Terrain (SGT), Western Dharwar Craton (WDC), Eastern Dharwar Craton (EDC), Eastern Ghat Mobile Belt (EGMB), Bastar Craton and Singhbhum Craton (Figure 2.1). Since the main focus of the present study is the southwestern continental margin of India, emphasis is given for Southern Granulite Terrain, Western Dharwar Craton and Deccan Trap, which form a major part of the southwestern Indian mainland.

The Southern Granulite Terrane of India (Figure 2.1) is one among the few terranes that has preserved the Archean crust in the world, believed to have a lower-crustal origin (Tewari et. al., 2018). The SGT consisting of several granulite blocks,

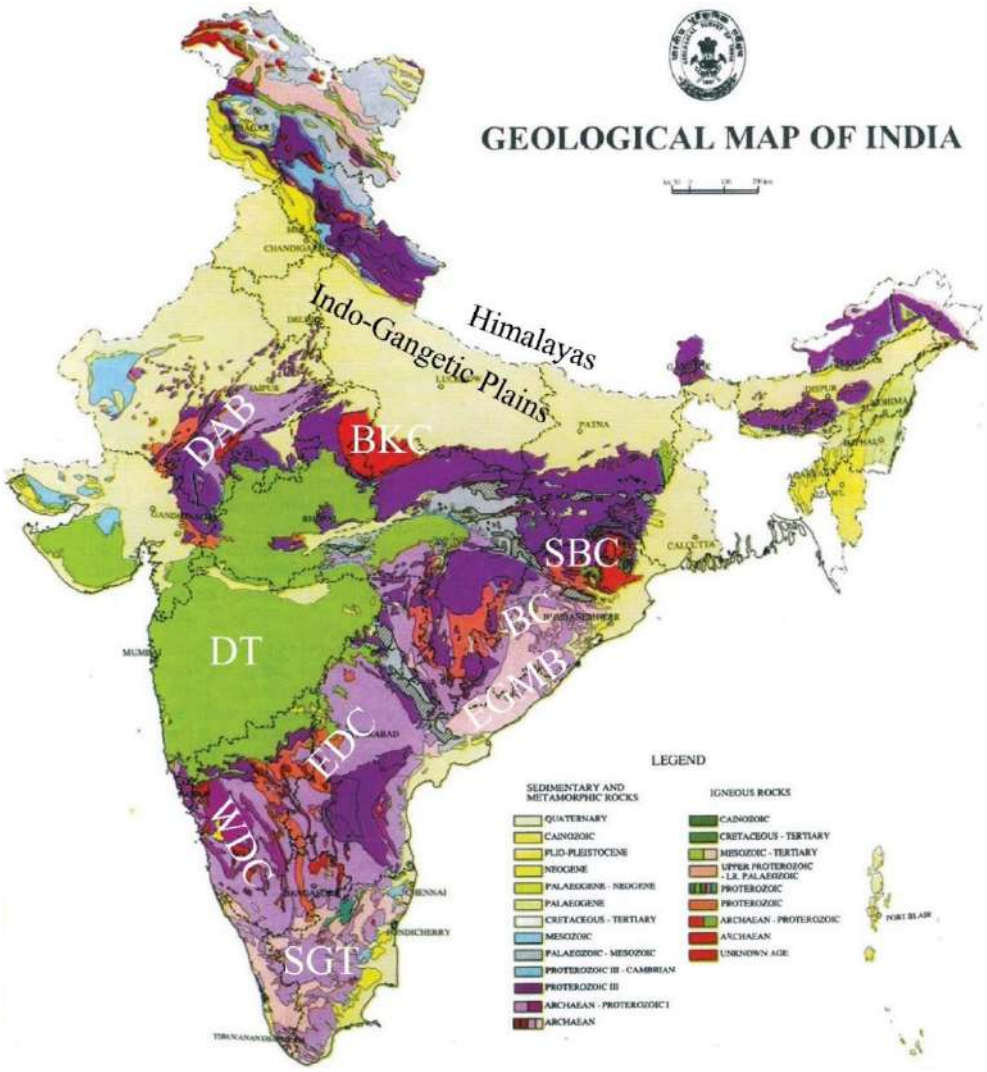

Figure 2.1: Geological Map of India (modified after GSI, 1999 as reproduced in Naqvi, 2005). SGT: Southern Granulite Terrain; EGMB: Eastern Ghat Mobile Belt; WDC: Western Dharwar Craton; EDC: Eastern Dharwar Craton; BKC: Bundelkand Craton; BC: Bastar Craton; DT: Deccan Traps; SBC: Singbhum Craton; DAB: Delhi-Aravalli Fold Belt.

which are separated by numerous shear zones/suture zones (Chetty 2017, 2021). The Achankovil Shear Zone (AKSZ) having ~ 100km length and 10-20km width, dissects the southern Trivandrum Block from the northern Madurai Block (Figure 2.2). A recent study (Praharaj et al., 2021) proposed that the structural-chronological contrasts between these two blocks imply the AKSZ to be a Pan-African terrain boundary shear zone system that is continuous with the Ranotsara Shear Zone in Madagascar. Deep seismic imaging study carried out in this domain

(Mandal et al., 2021) identified a unique south-dipping reflection fabric extending from the surface to upper mantle depth that can be resulted due to the subduction-accretion process of Madurai and Trivandrum blocks during the East African Orogen.

The Trivandrum Block and Achankovil Shear Zone are collectively called as Kerala Khondalite Belt (KKB). Further north, 400 km long Palghat Cauvery Shear Zone (PCSZ) divides the Nilgiri Block and Billigiri Rangan Block and Madurai Block (Ishwar-Kumar et al., 2013; Collins et al., 2014; Ratheesh-Kumar et al., 2016). The Mercara Suture Zone and Moyar Shear Zone in north and south respectively borders the Coorg Block (Santhosh et al., 2015). These shear zones/ suture zones are vital in the perspective of India-Madagascar pre-drift juxtaposition, as they are often considered to be conjugate of several correlatable shear zones/suture zones in Madagascar and India. The Archean Dharwar Craton is the northern limit of the SGT (Figure 2.1) and the northern limit of Dharwar Craton is Narmada-Son-Godavari Rift system (Naqvi, 2005). The N-S trending Closepet Granite divides the Dharwar Craton into Western Dharwar Craton (WDC) and Eastern Dharwar Craton (EDC) (Friend and Nutman, 1991). Among this, WDC is older than the EDC constituting Mesoarchean rocks (Naqvi, 2005). The Archean domains of WDC shows thick mafic and EDC shows thin felsic nature for the crust with magmatic underplating (Saikia et al., 2017). The Eastern Ghat Mobile Belt (EGMB) forms the eastern boundary of the EDC.

Continental Flood Basalts (CFB) are formed by some of the major magmatic events in the Earth history, with intrusion and eruption of very large area of basaltic magma over a short period (~1–5 Ma, Mital et al., 2021). CFB eruptions are often associated with crustal extension and continental rifting (White and McKenzie, 1995). Continental flood basalts covering about one million cubic kilometres, which can be considered as one of the largest volcanic provinces, masks the major portion of the deeper geology of the western India. The Deccan Volcanic Province (DVP) / Deccan Flood Basalt (DFB) / Deccan Trap (DT) mainly consists of tholeiitic lava flows resulted by Réunion hotspot volcanic activity prevailed within the Indian subcontinent during late Cretaceous-early Tertiary time (Morgan, 1972, 1981; Courtillot et al., 1986; Duncan, 1990).

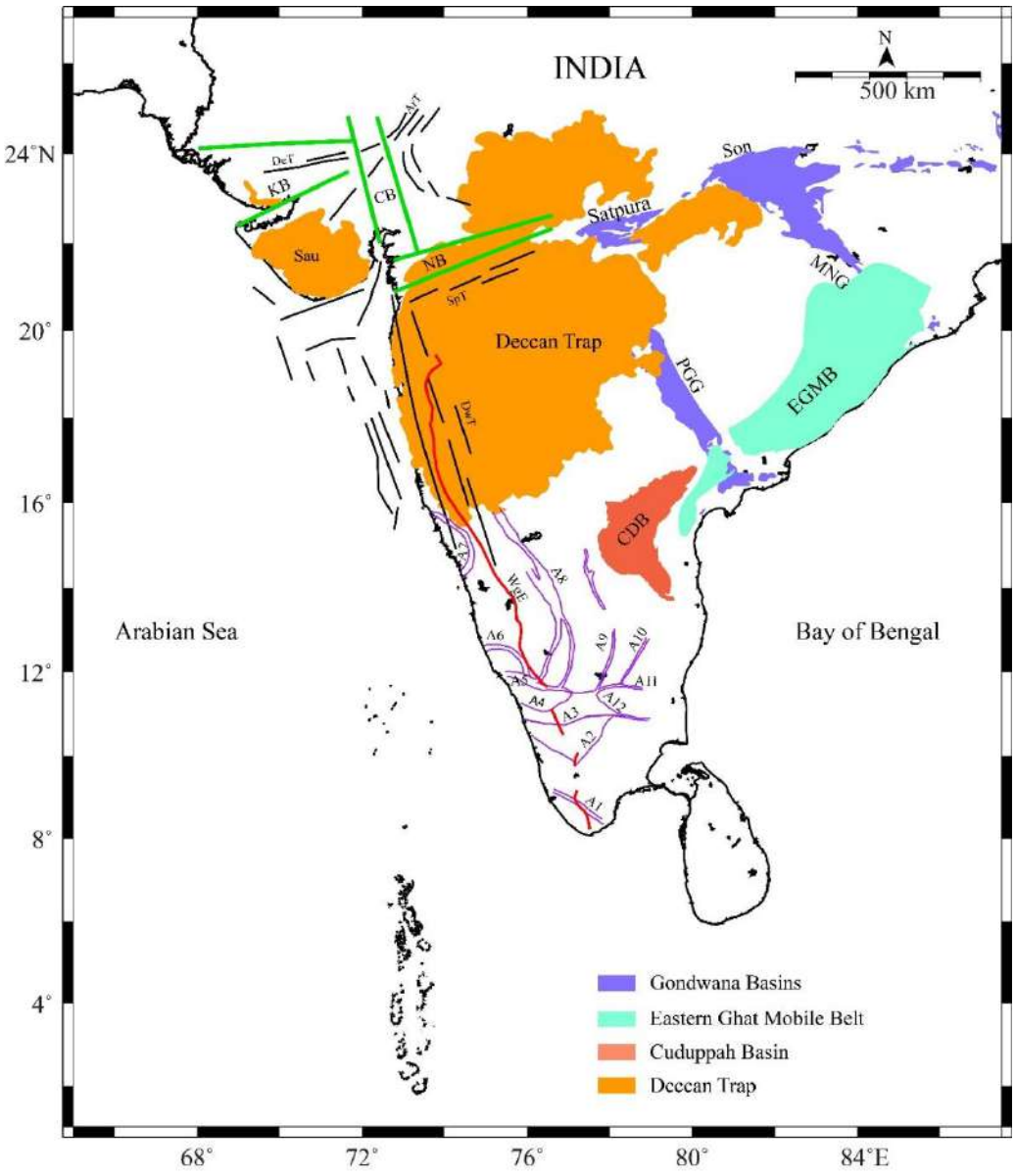

Figure 2.2: Geological domains and structural features on Indian mainland (compiled from Biswas, 1982; Bhattacharya and Subrahmanyam, 1986; Chakraborty and Ghosh., 2005; Sharma, 2009; Ghatak and Basu, 2011; Ishwar-Kumar et al., 2013; Bhattacharya and Yatheesh, 2015; Shuhail, 2018). Thick green lines and black lines represent the boundaries of rift grabens on the western margin of India and the structural trends, respectively. Thin pink lines represent the shear zones. The abbreviations used are as in Table 2.1.

Table 2.1: Abbreviations used for representing the onland geological features in both Indian and Madagascar Side.

Indian Side		CG	Cambay Rift Basin
A1	Achankovil Shear Zone	MNG	Mahanadi Graben
A2	Karur-Kambum-Painavu-Trichur Shear Zone	Sau	Saurashtra Peninsula
A3	Palghat-Cauvery Shear Zone	DwT	Dharwar Trend
A4	Bhavani Shear Zone	DeT	Delhi Trend
A5	Moyar Shear Zone	NB	Narmada Rift Basin
A6	Coorg Shear Zone	KG	Kutch Rift Basin
A7	Kumta Shear Zone	PGG	Pranhita-Godavari Graben
A8	Chtiradurga Shear Zone	**Madagascar Side**	
A9	Mettur-Kolar Shear Zone	B1	Ampanihy Shear Zone
A10	Nallamalai Shear Zone	B2	Bereketa Shear Zone
A11	Salem-Attur Shear Zone	B3	Tranomaro Shear Zone
A12	Cauvery Shear Zone	B4	Ranotsara Shear Zone
WgE	Western Ghat Escarpment	B5	Angavo Shear Zone
SpT	Satpura Trend	B6	Betsimisaraka Suture Zone
ArT	Aravalli Trend	AgE	Angavo Escarpment

Even though the exact age of the volcanic extrusion is not confirmed, several studies explain an age span of 69-64 Ma (Venkatesan et al., 1986), 68.5–66.5 Ma in Western Ghats (Duncan and Pyle, 1988), and 65.5+/-2.5 Ma in central India (Vandamme et al., 1991). These studies imply that the main pulse of the Réunion hotspot volcanism that affected the Indian mainland was at about 65 Ma (Courtillot et al., 1988; Bhattacharya and Yatheesh, 2015; Pande et al., 2017). The former magmatism suggests an incubation period of a primitive mantle plume before the rapid extrusion of the Deccan Volcanic Province (Basu et al., 1993; Tewari et al., 2018). Hooper et al. (2010) provided details on the chemically distinct types of dikes along the west coast of India indicating that the lithospheric extension, which led to the separation of Seychelles from the Indian Plate, began only during the final phases of the basalt eruptions. A recent geophysical study (Kumar and Chaubey,

2019), using P-wave velocity estimation, suggests that the Deccan Flood Basalt is present below sediment in the entire northwestern continental margin of India, extending up to the Laxmi and Laccadive ridges.

The Precambrian basement of the western part of India consists of three prominent orogenic trends such as the Dharwar trend, Delhi-Aravalli Fold Belt and the Satpura Fold Belt (Figure 2.2). The Dharwar trend with NNW orientation is expected to extend much towards the Deccan Volcanic Province (Biswas, 1982; Gombos et al., 1995). The Delhi-Aravalli Fold Belt is a major segment of NW Indian shield which constitute highly folded, deformed and metamorphosed rocks of Proterozoic age (Tewari and Rao, 2003). The Aravalli fold belt runs ~ 700km with a NE-SW orientation passing through Rajasthan, Haryana and Delhi (Sharma, 2009). It is composed of Archaean basement gneiss complex (Sharma, 2009) and geochronological studies carried out suggest an age of ~ 1.7-1.8 Ga for this orogeny (Biju-Sekhar et al., 2003; Bhowmik et al., 2010). The Aravalli trend continues across the Cambay Graben into Kathiawar peninsula. The Satpura Fold Belt (SFB) oriented in ENE-WSW directions belongs to the supracrustal rocks of Sausar Group rocks (Sharma, 2009). The Satpura Fold Belt is considered as the zone of collision of Central Indian Tectonic Zone (CITZ, Mohanthy, 2010 and reference therein) and lies south of Narmada-Son lineament. These above-mentioned three major orogenic trends form the zones of deformed and weakened crust that facilitated Phanerozoic rifting (Biswas, 1982, 1987). Reactivated movements resulted during the different stages of tectonic history along these trends caused the formation of three important peri-continental rift basins, the Kutch, Cambay and Narmada basins, which borders the northern region of western continental shelf of India (Biswas, 1982). The Kutch basin extends from land to offshore situating west of the Cambay Basin, which is believed to have developed in Jurassic time along the Delhi trend. The Cambay Basin is a narrow, NNW-SSE trending, intra-cratonic rift basin along the Dharwar trend. The Narmada Basin formed along the Satpura trend in the Late Cretaceous period.

The Western Ghat Escarpment (WgE, Figure 2.2) is one of the major physiographic features in the peninsular India and a typical example of passive margin great escarpment over the globe (Kale, 2009). Various geophysical studies

have been carried out in different domains of WGE to understand its crustal structures, magmatic underplating (Devey and Lightfoot, 1986; Dubey and Tiwari, 2018), flexural unloading (Buck, 1986), and flexural response to denudation (Gunnell and Fleitout, 2000). The formation of the Western Ghat is associated with the India-Madagascar break-up process (Bhattacharya and Yatheesh, 2015). Based on the sample collected from drill hole, Radhakrishna et al. (2019) proposed igneous underplating that caused uplift of the WGE and lithosphere beneath the continental margin, while returning to normal temperatures following the Seychelles-India breakup. The "swales" or gaps are identified along this feature, and the ~ 15 km wide Palghat Gap is the most prominent among such gaps.

2.2.2 Continental shelf-slope morphology of southwestern continental margin of India

The shape as well as overall morphology of the western continental shelf-slope province (Figure 2.3) has influenced by the breakup of India-Madagascar-Seychelles block. The western Indian continental shelf runs with a ~ NNW-SSE trend, starting from Gujarat offshore in the north to southern edge of Indian Peninsula. The shelf edge is widely defined by the ~ 200 m isobaths (Naini, 1980). The shelf is ~ 345 km wide in the northern part and it gradually narrows towards the off Trivandrum region to ~ 50 km (Faruque and Ramachandran, 2014). The shelf province is suggested to have several coast parallel, horst-graben structures, with the same NNW-SSE Dharwar trend, and these features are considered to represent as the result of Dharwarian basement grain parallel rifting episode that occurred during the India-Madagascar breakup period (Biswas, 1989; Gombos et al., 1995). The western continental shelf of India is divided into several sub-basins such as the Kutch-Surat Basin, the Ratnagiri Basin, the Konkan Basin and the Kerala Basin. These basins are divided based on the presence of anticline structures called as the Saurashtra Arch, the Vengurla Arch and the Tellicherry Arch, from north to south (Biswas, 1989). Unlike the continental shelf, the continental slope province is narrower in the north and it get widens towards the south. In the southwestern region, the mid-continental slope is characterized with the presence of an anomalous bathymetric high feature referred to as the Alleppey-Trivandrum Terrace Complex, with its western limit marked by a sharp drop of the seafloor,

referred to as the Chain-Kairali Escarpment (Yatheesh et al., 2006, 2013b; Bhattacharya and Yatheesh, 2015).

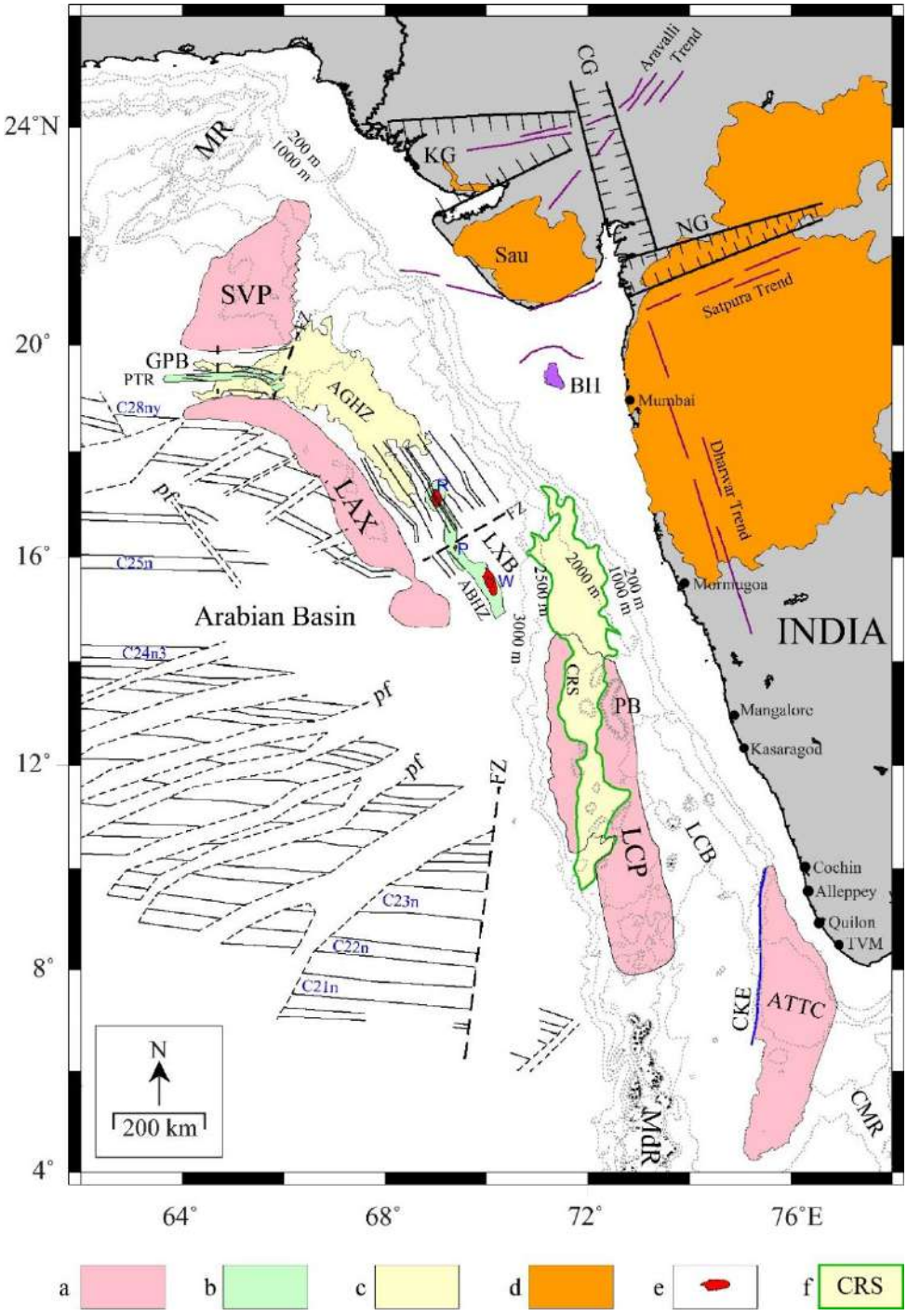

Figure 2.3: Tectonic fabric map of the western continental margin of India and the adjacent regions (modified after Bhattacharya and Yatheesh (2015)). The continuous black lines, thick dashed lines and the dotted lines represent the magnetic lineations, fracture zones and

pseudofaults, respectively. The hachured thick black lines represent postulated boundaries of rift graben basins onland and the magenta lines represent onshore and offshore structural trends. ATTC: Alleppey-Trivandrum Terrace Complex; CKE: Chain-Kairali Escarpment; ABHZ: Axial basement high representing the Panikkar Ridge in the Laxmi Basin; PTR: Palitana Ridge; CG: Cambay Rift Graben; KG: Kutch Rift Graben, NG: Narmada Rift Graben; LCP: Laccadive Plateau; MdR: Maldive Ridge; CMR: Comorin Ridge; PB: Padua Bank; LXB: Laxmi Basin; GPB: Gop Basin; LCB: Laccadive Basin; Sau: Saurashtra; TVM: Trivandrum; MR: Murray Ridge; SVP: Saurashtra Volcanic Platform; BH: Bombay High; Explanation of items of the legend - (a) Continental slivers; (b) Extent of axial basement high zones representing the extinct spreading centres in the Laxmi and Gop basins; (c) anomalous gravity high zone (AGHZ); (d) extents of Deccan Flood Basalts; (e) Seamounts in the Laxmi Basin, R Raman Seamount; P Panikkar Seamount; W Wadia Guyot; (f) Cannanore Rift System.

2.2.3 Laxmi and Gop basins

The Laxmi and Gop basins are situated between the Laxmi Ridge and continental margins of India and Pakistan, respectively (Figure 2.3). These deep offshore basins are believed to have formed as a result of breakup of Seychelles-Laxmi Ridge block from Indian continental block. The Laxmi Basin is bounded by the NW-SE trending segment of the Laxmi Ridge in the west and the western continental slope of India in the east (Bhattacharya et al., 1994a). Different views exist about the nature of crust underlying the Laxmi Basin. Some researchers (Naini and Talwani, 1982; Kolla and Coumes, 1990; Todal and Eldholm, 1998; Krishna et al., 2006) explained as thinned continental crust intruded with volcanics, based on semi-continental crustal thickness and lack of identifiable seafloor spreading magnetic anomalies. On the other hand, others considered oceanic crust based on the occurrence of hyperbolic reflection which is typical in the case of oceanic crust (Biswas et al., 1988), identification of well correlatable magnetic anomalies symmetric about a central negative magnetic anomaly (Bhattacharya et al., 1994a), presence of seaward dipping reflectors in the western and eastern limits of Laxmi

Basin (Corfield et al., 2010; Siawal et al., 2014; Misra et al., 2015), and the combined forward modelling of the sea-surface gravity and magnetic data constrained by seismic reflection and refraction results (Yatheesh, 2007). Recently, Pandey et al. (2019) carried out geochemical and isotopic studies using the igneous crust in Laxmi Basin obtained through International Ocean Discovery Program (IODP) Expedition 355 and suggested occurrence of relict subduction initiation event in the Laxmi Basin. Contradicting to this, Clift et al. (2020) proposed a simple volcanic rifting episode for opening of the Laxmi Basin using the same geochronological and geochemical data. Based on an independent geochemical investigation using the same samples drilled during IODP Expedition 355, Radhakrishna et al. (2021) proposed that the basement rocks represent continental rift basalt which is contrasting from the Deccan and Madagascan basalts.

The Gop Basin is the deep offshore basin located between the E-W trending segment of the Laxmi Ridge and the Saurashtra Volcanic Platform (Yatheesh et al., 2009; Bhattacharya and Yatheesh, 2015). The Gop Basin is considered to have underlain by oceanic crust based on the identification of seafloor spreading type magnetic anomalies (Malod et al., 1997; Yatheesh, 2007; Collier et al., 2008; Yatheesh et al., 2009), derived crustal velocity structure using wide angle seismic reflection data (Collier et al., 2004, 2009; Minshull et al., 2008) and the combined forward modelling of gravity and magnetic anomalies complemented with seismic constraints (Yatheesh, 2007; Yatheesh et al., 2009). Recently, based on the estimated effective elastic thickness and crustal stretching factor, Rao et al. (2018) proposed a continental nature for the Gop Basin. Although most of the researchers have broad agreement that the Gop Basin is underlain by oceanic crust, there exist different views on the identification of magnetic anomalies and the location of the extinct spreading centre (Malod et al., 1997; Collier et al., 2008; Yatheesh et al., 2009; Ramana et al., 2015; Bhattacharya and Yatheesh, 2015). These varied identifications suggest opening of the Gop Basin ranging between 79 and 64.7 Ma and the cessation of seafloor spreading ranging from 69 to 56.4 Ma. Radhakrishna et al. (2021), based on their geochemical results, suggested that the basalt eruption occurred at ~ 75 Ma caused the igneous underplating and this event triggered the opening of the Gop Basin. Collier et al. (2008) proposed a basement high existing ~ 50 km north of the Palitana Ridge as the extinct spreading centre, while Yatheesh

et al. (2009) inferred the Palitana Ridge as the extinct spreading centre in the Gop Basin.

2.2.4 Laxmi Basin Seamount Chain

Swath bathymetric survey carried out in the Laxmi Basin revealed the existence of a ~ 250 km long and NNW-SSE trending seamount chain in its axial part (Bhattacharya et al., 1994b). This consists of the Raman Seamount, the Panikkar Seamount and the Wadia Guyot from north to south. The Raman Seamount possesses N-S elongation with an elliptical shape, occupying basal area of ~ 660 sq. km. The Raman Seamount has a total relief of 1505 m from the adjacent seafloor and this feature is marked with a secondary peak. The Panikkar Seamount is an arcuate shaped feature with a maximum height of 1068 m, having multiple peaks. The Wadia Guyot is the largest among these three seamounts with a rhomboid shape, occupying a basal area of 1210 sq. km with height of 1461m. All these anomalous bathymetric highs are characterized by gully-like patterns along the flanks that might have resulted due to the sub-areal erosion. Probable genesis of the seamount chain is attributed with an anomalous volcanism caused by the interaction of Réunion hotspot and the now-extinct spreading centre in the Laxmi Basin when they were in close vicinity around 65 Ma (Bhattacharya et al., 1994a). The Panikkar Seamount is associated with several caldera-like features, corroborating the volcanic origin for the Laxmi Basin seamount chain (Savio et al., 2022).

2.2.5 Laxmi Ridge

The Laxmi Ridge is an aseismic basement high feature, having a NW-SE and an E-W trending segments, bordering the western limit of the Laxmi Basin, southern limit of the Gop Basin and the northern/northeastern limit of the Arabian Basin (Figure 2.3). This feature is presented as a bathymetric high in the southern end, but its bathymetric signature is not evident north of 18°30’N. Interestingly, Laxmi Ridge is characterized by a broad negative free-air gravity anomaly (~ 50 mGal), although it is expressed as a basement high feature. Many authors proposed a continental origin for the crust underlying the Laxmi Ridge. The interpretations of the continental nature of the Laxmi Ridge were mainly based on the velocity-

depth structure derived from sonobuoy seismic refraction results (Naini, 1980; Naini and Talwani, 1982), identification of crustal thickness and Moho depth deduced from wide-angle seismic reflection results (Collier et al., 2004, 2009; Minshull et al., 2008), gravity modelling integrated with seismic information (Krishna et al., 2006; Yatheesh, 2007; Yatheesh et al., 2009), admittance analysis of gravity data (Bansal et al., 2005) and the presence of seaward dipping reflectors (SDRs) on both the landward and seaward sides of the Laxmi Ridge (Corfield et al., 2010; Calvès et al., 2011; Siawal et al., 2014). However, Todal and Eldholm (1998) suggested that Laxmi Ridge is a marginal high complex, consisting of both continental and oceanic crust based on gravity modelling and plate tectonic reconstruction. Based on the analysis of deep penetrated seismic reflection data and forward gravity modelling, Misra et al. (2015) proposed that the Laxmi Ridge is composed of oceanic crust formed at a fossil spreading centre. Recently, Mishra et al. (2020) supported a continental nature for Laxmi Ridge from the integrated analysis of the geophysical data and proposed that the Laxmi Ridge extend towards the Laccadive Plateau.

2.2.6 Arabian and Eastern Somali basins

The Arabian and Eastern Somali basins are the conjugate basins formed by seafloor spreading through the Carlsberg Ridge (Figure 2.3). These conjugate basins are bordered by the Laxmi Ridge, the Seychelles Plateau, the Chain Ridge-Owen Fracture Zone System and the Laxmi-Laccadive ridges, respectively, in the north, south, west and east. The NW-SE trending anomaly C27n (~ 61 Ma) is the oldest magnetic anomaly identified in the Eastern Somali Basin north of Seychelles Plateau (Chaubey et al., 2002a). Similarly, on the Indian side, oldest anomaly C28n (~ 62.5 Ma) is identified south of the Laxmi Ridge (Chaubey et al., 2002a). Several studies revealed the existence of oblique offsets of magnetic anomaly lineations, which are indications of ridge propagation associated with pseudo-faults in these conjugate basins (Miles and Roest 1993; Chaubey et al., 1998, 2002a; Dyment, 1998; Royer et al., 2002). These studies came up with three major episodes of ridge propagation between chrons C28ny (~ 62.5 Ma) and C21ny (~ 42.54 Ma) for the Arabian and Eastern Somali basins. Recent studies mapped magnetic lineations and associated fracture zones during the period corresponding to chrons C1no (0.78 Ma) and C6no (~ 20.13 Ma) in these conjugate basins (Merkouriev and DeMets, 2006).

2.2.7 Laccadive-Chagos Ridge

The Laccadive-Chagos Ridge (LCR) is a slightly arcuate, elongated aseismic bathymetric high feature extending about 2500 km between 14°N and 9°S. The Laccadive-Chagos Ridge is divided into three segments as Laccadive Plateau (LCP), the Maldive Ridge (MdR) and the Chagos Bank (CB), from north to south, based on the presence of several relatively deep saddle-like features (Bhattacharya and Chaubey, 2001). A few hypotheses regarding the formation of LCR includes, a leaky transform fault (Fisher et al., 1971; Sclater and Fisher, 1974), a zone of transition between oceanic crust and continental crust in western and eastern parts, respectively (Narain, 1968), hotspot trail (Whitmarsh, 1974; Duncan, 1981; Morgan, 1981), a composite structural elements of various origin (Avraham and Bunce, 1977; Sreejith et al., 2019) and crack propagation (Sheth, 2005). Among these, the hotspot genesis seems to have wide acceptance for the genesis of the entire Laccadive-Chagos Ridge. However, several studies proposed that the Laccadive Plateau is a continental sliver. This postulation was mainly based on (a) the interpretation of crustal thickness from seismic refraction studies (Babenko et al., 1981; Naini and Talwani, 1982); (b) the presence of rotated fault blocks that represents extensional tectonic activity (Murty et al., 1999); (c) the presence of seaward dipping reflectors (SDRs) west of the Laccadive Plateau (Ajay et al., 2010), (d) crustal configuration derived from the forward modelling of gravity data (Chaubey et al., 2002b; Ajay et al., 2010; Nair et al., 2013) and (e) the presence of a complex block-faulted basement structure, constituting system of grabens, half grabens and single normal faults, which are grouped into a rift system, referred as the Cannanore Rift System (Bhattacharya and Yatheesh, 2015; DGH, 2014). Bhattacharya and Yatheesh, (2015) could accommodate the Laccadive Plateau as an intervening continental sliver between India and Madagascar in a close-fit India-Madagascar juxtaposition model. Based on the analysis of gravity data, Kumar et al. (2020) observed the structural pattern with the continental trends and moderate crustal thickness for the Laccadive Plateau suggesting thinned continental crustal nature.

The middle segment of the LCR is referred as the Maldive Ridge, which extends between 7°N and 1°S. Seismic reflection studies inferred that ~ 5 km thick sedimentation is underlain by a faulted basement in the deep basin associated with

the northern domain of the crestal region of Maldive Ridge (Avraham and Bunce, 1977). Based on the analysis of crustal thickness, Moho variations and Curie depth, Kunnummal and Anand (2022) proposed that the Maldive Ridge was formed close to the spreading centre. The southernmost part of Laccadive-Chagos Ridge is the Chagos Bank, which extends south of 4°S. Drilling results from the northern part of the Chagos Bank indicate basaltic basement with age of 49 Ma (Middle Eocene, Duncan and Hargraves, 1990).

2.2.8 Laccadive Basin

The Laccadive Basin is the narrow, triangular basin situated between southwestern continental slope of India in the east and the Laccadive Plateau in the west (Figure 2.3). This basin extends from ~ 16°N where the northern edge of the Laccadive Plateau joins the continental slope of India, and towards south, the Laccadive Basin opens to the Central Indian Basin (Bhattacharya and Chaubey, 2001). The Laccadive Basin is narrow in the northern part and get widens towards south (~ 215 km) within the water depth of ~ 2000 m to ~ 2800 m. The nature of crust underlying the Laccadive Basin is still ambiguous. Based on the presence of rotated fault blocks representing half grabens, it is suggested that the Laccadive Basin represents a failed rift comprising of stretched continental crust intermixed with volcanics (Chaubey et al., 2002b). Interpreting the occurrence of SDRs west of Laccadive Plateau, and the crustal structure derived from the forward modelling of the gravity data, Ajay et al. (2010) proposed a continental nature for the Laccadive Basin. Based on the analysis of gravity and magnetic anomalies, Yatheesh et al. (2013b) proposed that the Laccadive Basin region could be interpreted as thinned continental crust or an anomalously thick oceanic crust. Based on the analysis of sea-surface magnetic and gravity anomalies, Shuhail (2018) inferred that the Laccadive Basin is underlain by oceanic crust formed by seafloor spreading between India and the Laccadive Plateau. The magnetic anomalies in the Laccadive Basin have been interpreted to represent the seafloor spreading type magnetic anomaly sequence of chrons C31no (68.73 Ma) to C28ny (62.5 Ma) proposing the commencement and cessation of seafloor spreading in the Laccadive Basin at ~ 68.7 Ma and 62.5 Ma, respectively.

2.3 Tectonic elements from Madagascar and adjacent ocean basins

2.3.1 Features on the Madagascar mainland

The Precambrian of Madagascar can be divided as northern and southern Madagascar by a major shear zone called as the Ranotsara Shear Zone (Figure 2.4). Major tectonic units of northern Madagascar constitute Antongil-Masora Block and Antananarivo Block (Collins and Windley, 2002) alongwith Itremo Sheet, Tsaratanana Sheet and Bemarivi Belt. The southern Madagascar consists of six tectonic units as Vohibory Belt, Ampanihy Belt, Bekily Belt, Betroka Belt, Tranomaro Belt and Dauphin-Anosyan Belt, from west to east (Windley et al., 1994). The Antongil-Masora Block, is composed of ~ 3.2 Ga old gneiss with Late Archaean granites (Collins and Windley, 2002). The Antananarivo Block which covers the central part of Madagascar is the largest tectonic block bearing ~ 2.5 Ga old gneiss with interlayered granites, syenite and gabbros of 824-719 Ma (Kroener et al., 2000; Collins and Windley, 2002). Angavo Shear Zone is the ~ 800 km long, ~ 20-60 km wide, N-S trending belt of deformed rocks instituted with Antananarivo Block (Raharimahefa et al., 2013). Approximately 1000 km long and steep escarpment termed as the Angavo Escarpment is present parallel to the Angavo Shear Zone, which was proposed to evolve during India-Seychelles-Madagascar separation (Gunnell and Harbor, 2008). This is considered as the conjugate of the Western Ghat Escarpment in the Indian Peninsula. A recent study (Armistead et al., 2020) carried out in the eastern Madagascar suggests that orogenic deformation is syn to post - 550 Ma time, and possibly formed with respect to final cessation of the Mozambique Basin along the Betsimisaraka Suture Zone that amalgamated Madagascar with the Dharwar Craton of India.

The Ranotsara Shear Zone have been accounted a significant role in the India-Madagascar juxtaposition and the respective reconstruction of Gondwanaland (Katz and Premoli, 1979; Agrawal et al., 1992; Windley et al., 1994, Menon and Santosh, 1995; Rogers et al., 1995; Yoshida et al., 1999). For example, Ranotsara Shear Zone is considered as conjugate to the Achankovil Shear Zone and Betsimisaraka Shear Zone with the Moyar shear zone (Braun and Kriegsman, 2003). Counter to this observation, Tucker et al. (2011) proposed the correlation

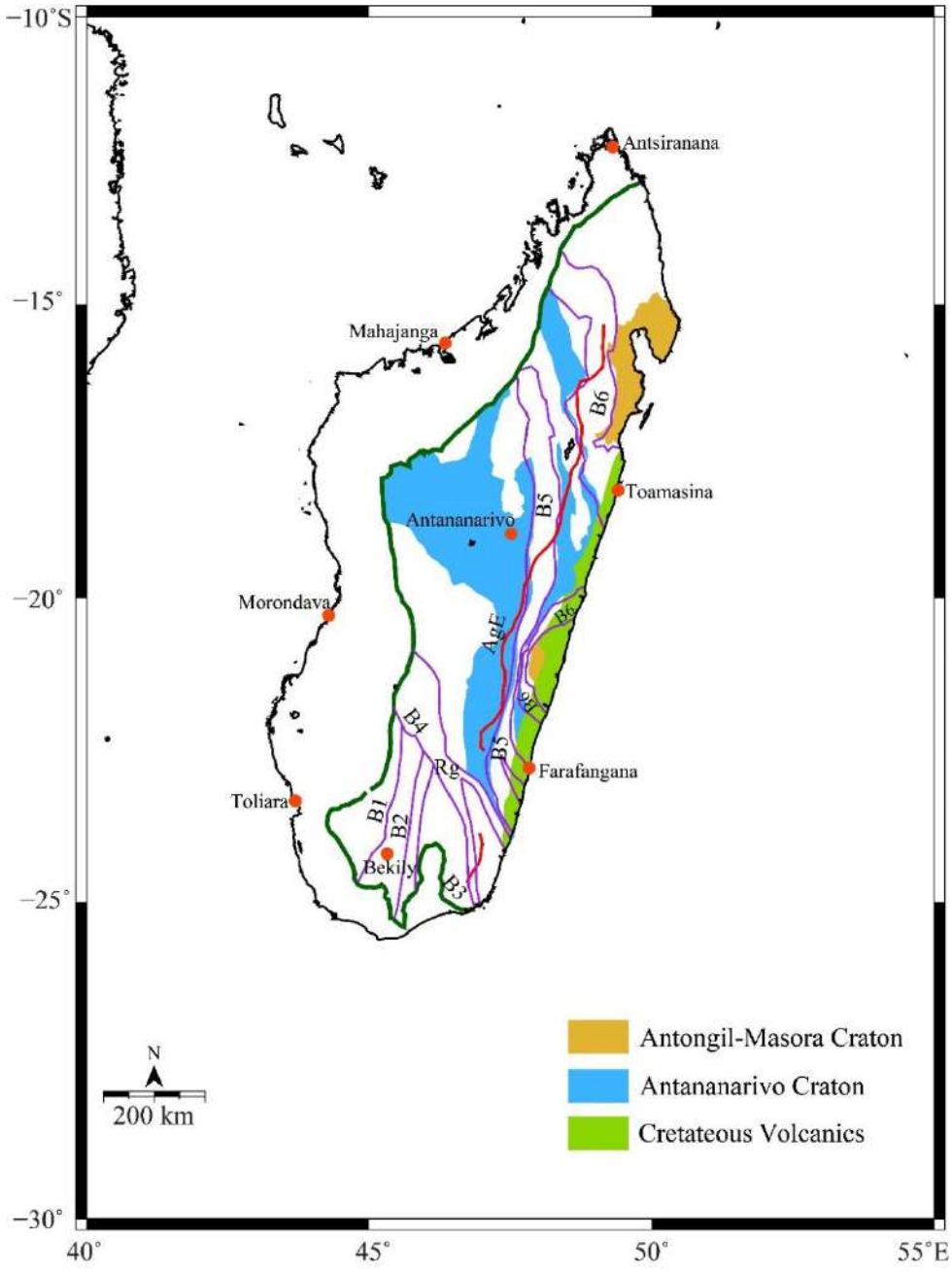

Figure 2.4: Geological domains and structural features on Madagascar mainland (compiled from Collins and Windley, 2002; Ishwar-Kumar et al., 2013; Ratheesh-Kumar et al., 2015; and Bhattacharya and Yatheesh, 2015; Shuhail, 2018). Green coloured thick line represents the Precambrian boundary of Madagascar. Red coloured thick line represents Angavo Escarpment (AgE). Pink lines represents shear zones. Other details are as in Table 2.1.

Among Angavo Shear Zone to the Moyar shear zone. Some researchers proposed Ranotsara Shear Zone is conjugate with Palghat-Cauvery Shear Zone (Janardhan, 1999) or with the Karur-Kambum-Painavu-Trichur Shear Zone (Collins and Windley, 2002). With the help of integrated geochemical and geochronological investigations the possibility for the extension of the Betsimisaraka Suture Zone in the Madagascar side with the Kumta Suture Zone, which re-enters southern India as Mercara (Coorg) Suture Zone has been proposed (Ishwar-Kumar et al., 2013; Santosh et al., 2015). A recent study (Schreurs et al., 2010), based on remote sensing data and field investigations, proposed that Ranotsara Shear Zone is not a megascale intracrustal shear zone that cut-across the entire basement of southern Madagascar, and hence Ranotsara Shear Zone cannot be considered as a piercing point for correlation in Gondwana reconstruction.

2.3.2 Eastern continental margin of Madagascar

The eastern continental shelf of Madagascar (Figure 2.5) is generally narrow, with an average width of ~ 25 km. Along the northeast margin, no shelf is observed at some places. The narrow shelf between Fort Dauphin and the Bay of Antongil appears as a fault escarpment. The escarpment dips steeply up to 1800 m, and the continental slope lies along the fault plane. Pepper and Everhart (1963) proposed that the Bay of Antongil, which is bordered on each side by a fault trending northwestward along its shore, is possibly a down-faulted block trending at an acute angle to the main coastal fault. Previous researchers (Barron, 1987; Lawver et al., 1998) considered this straight slope as a proof for transform motion between India and Madagascar.

2.3.3 Seychelles-Mascarene Plateau Complex

The Seychelles-Mascarene Plateau (SMP) is situated between the Madagascar Island and the Central Indian-Carlsberg ridges (Figure 2.5). The SMP is an arcuate, ~ 2600 km long feature, which consists of numerous banks and small islands. The SMP mainly comprises of the Amirante Plateau, Seychelles Bank, Mascarene Plateau (comprising the Saya de Malha Bank, Nazareth Bank, Cargados Carajos Bank and the Mauritius Island) and the Réunion Island. The Amirante Plateau is the northwestern end of this complex feature, with an arcuate shape and 400 km length, extending towards south. The western flank of the Amirante Plateau

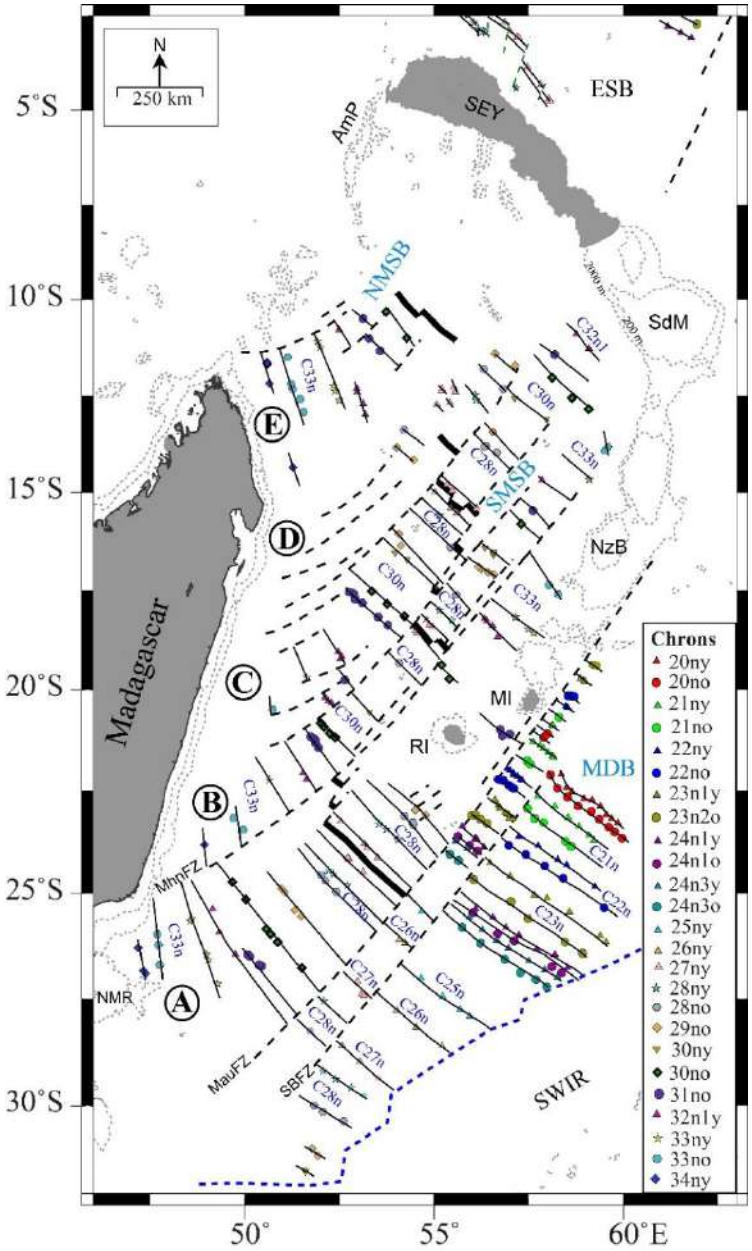

Figure 2.5: Tectonic fabric map of the eastern continental margin of Madagascar and the adjacent deep offshore regions (after Shuhail et al. (2018)). The thick black lines represent extinct spreading axis. The compartments from A to D fall in the Southern Mascarene Basin (SMSB) and the compartment E falls within the Northern Mascarene Basin (NMSB). NMR: Northern Madagascar Ridge; SEY: Seychelles Plateau; MauFZ: Mauritius Fracture Zone: MhnFZ: Mahanoro Fracture Zone; SBFZ: Southern Boussole Fracture Zone. Other details are as in Figures 1.1, 2.3 and Table 1.1.

is continued to a deep sediment filled trough called Amirante Trough. The Amirante Plateau along with the Amirante Trough have been considered as a result of short term subduction event in which Amirante Trough characterises the subduction trench (Mart, 1988).

The Seychelles Bank occupies the area between 4°S and 6°S latitudes and 54°E and 57°E longitudes with its flat top lying about 50 m water depth. The Seychelles Bank comprise of three major islands, Mahe, Praslin and Silhouette islands. Radiometric age determination of rocks collected from these islands indicates the presence of Upper Precambrian hornblende granite, preserved about 650 Ma (Baker and Miller, 1963). Seismic refraction studies propose that the Seychelles Bank has a three-layered density structure with an overall crustal thickness of more than 30 km (Plummer and Belle, 1995), and therefore, the Seychelles Bank is considered as a continental fragment. Bhattacharya and Yatheesh (2015) considered that the continental crust underlying the Seychelles Bank extend further southeast to a part of the Seychelles-Saya de Malha saddle and they considered this extent to define the Seychelles Plateau microcontinental block.

The Mascarene Plateau includes the Saya de Malha Bank, the Nazareth Bank, the Cargados Carajos Bank and the Mauritius Island (Figure 2.5). These banks lie at a water depth of 50 m and carry coral reef over the body, and with steep scarp. Industrial drilling over the Saya de Malha Bank revealed the presence of olivine tholeiitic basalt of age 45 Ma and over the Nazareth Bank corresponds to the 31 Ma (Duncan and Hargraves, 1990). Mauritius Island is believed to be formed as a result of three phases of volcanic eruption related Réunion hotspot activity (Duncan and Hargraves, 1990). Torsvik et al. (2013) proposed a Palaeoproterozoic and Neoproterozoic time for the zircon xenocrysts recovered from the Mauritian beach sands, and proposed continental origin for the Mauritius Island. The Réunion Island constitutes two amalgamated volcanoes called Piton des Neiges and Piton de La Fournaise. The Réunion Island bears mainly basaltic rocks and the oldest rock found is about 2 Ma.

2.3.4 Madagascar Ridge

The Madagascar Ridge (MDR) is an aseismic, bathymetric high feature extending from south of Madagascar Island between 26°S to 36°S. The marine

geoscientific studies carried out in this region are sparse and only the results of three such studies (Goslin et al., 1980, 1981; Sinha et al., 1981; Sato et al., 2022) are available in the public domain. The Madagascar Ridge exhibits an overall length of 1300 km with N-S elongation and a width of 600 km. Based on the geophysical data analysis, Goslin et al. (1980) proposed that the Madagascar Ridge constitute two different domains along 31°S. The segment of the Madagascar Ridge located north of 31°S exhibits a complex basement structure and irregular bathymetric expression, while the segment south of 31°S shows more subdued bathymetry with a uniform sedimentation (Goslin et al., 1981). Composition of Madagascar Ridge is of porphyritic low alkali basalts with manganese encrustation and seismic reflection and refraction studies reveal that the Madagascar Ridge is covered by the sediment deposits (Goslin et al., 1980). Based on the analysis of geophysical data, Goslin et al. (1980) favoured oceanic crust for the entire length of the Madagascar Ridge. Using forward modelling and seismic refraction studies Sinha et al. (1981) suggested that the northern part of the Madagascar Ridge is underlain by thickened oceanic crust with a thickness of 20-25 km, while the velocity-depth distribution of the southern domain is closely related to that of mean oceanic crust. Later, Storey et al. (1995) proposed that the Madagascar Ridge is a result of volcanic emplacement related to the motion of the African plate over Marion hotspot since 90 Ma. Bhattacharya and Chaubey (2001) opined that the crust underlying the northern domain can be considered to be anomalous, as it has neither purely continent nor oceanic affinity. Based on the plate tectonic reconstruction of the Western Indian Ocean, Yatheesh et al. (2006) inferred that the northern domain of the Madagascar Ridge and the Alleppey-Trivandrum Terrace Complex located in the southwestern continental margin of India represents conjugate features in the India-Madagascar pre-drift scenario. Sato et al. (2022) considered the southern Madagascar Ridge and Del Cano Rise as a single entity, created due to Marion hotspot volcanism around the actively spreading Southwest Indian Ridge, that got separated around Chron C30ny (~ 65.6 Ma).

2.3.5 Madagascar Basin

The Madagascar Basin is situated between the Southwest Indian Ridge, the Madagascar Ridge, the Mascarene Basin and the southern sector of the Central Indian Ridge (Figure 2.5). Various geophysical studies (Schlich, 1982; Patriat,

1987; Cande et al., 2010; Yatheesh et al., 2019) carried out in this region identified magnetic anomaly sequence of chrons C30ny to C1n (~ 65.58 to 0.0 Ma). The oldest anomaly C30ny (~ 65.58 Ma) was found in the southern Madagascar Basin close to the Madagascar Ridge. The anomaly C20ny (~ 66 Ma) was reported from the south of Mauritius Island. The DSDP sites 245 located in the close proximity of anomaly C29n (~ 64Ma) has sampled basaltic basement and the age was inferred to be ~ 63.6-66.4 Ma (Early Paleocene). The Madagascar Basin is formed by seafloor spreading through the Central Indian Ridge, and its conjugate ocean basin is the Western Central Indian Basin.

2.3.6 Mascarene Basin

The Mascarene Basin (Figure 2.5) is located between the arcuate Seychelles-Mascarene Plateau and the eastern continental margin of Madagascar. A boundary linking the northern tip of the Madagascar Island, the Farquhar Group of Islands, the Amirante Plateau and the Seychelles Bank borders the northwestern part, and its southeastern extent is defined by the Mauritius Fracture Zone. The DSDP site 239, which is located in the southern Mascarene Basin encountered the oldest sediment followed by a basaltic basement of age ~ 71 Ma (Schlich, 1982). The magnetic anomaly identification carried out by various researchers (Dyment 1991; Sahabi, 1993; Bernard and Munschy 2000; Eagles and Wibisono, 2013) reported the presence of symmetric sequence of magnetic anomalies 34 through 26 in the Mascarene Basin. The Mascarene Basin can be considered as two domains, the Northern Mascarene Basin and the Southern Mascarene Basin. The Southern Mascarene Basin is broader compared to the oceanic crust in the Northern Mascarene Basin (Bhattacharya and Yatheesh, 2015). Geologically it appears as the Mascarene Basin is a continuation of the Madagascar Basin located in the south. The revised plate tectonic model and magnetic lineation identifications (Shuhail et al., 2018) proposed that spreading direction in the Mascarene Basin changed from ~E-W to ~NE-SW direction around C33ny (~73.62 Ma).

2.4 Dated volcanism in the areas related to the present study

The Indian and its conjugate Madagascar mainland as well as the adjoining offshore regions have experienced different episodes of volcanic activities (related

to the Marion and the Réunion hotspots) and hence their imprints are well recorded in these regions. Presently available information on the locations and ages of the volcanic rocks in and around the Indian mainland, the adjacent offshore regions and its conjugate region of Madagascar side are given in Figure 2.6.

The peninsular India and the eastern Madagascar contains the traces of the Marion hotspot volcanism. The Cretaceous volcanics/intrusive rocks recovered from the east coast of Madagascar is reported an age estimate of ~ 83-92 Ma (Storey et al., 1995; Torsvik et al., 1998; 2000). Volcanics with similar age (80-90 Ma), representing the Marion hotspot activity, has also been recovered from the Indian side. These volcanics from Indian side mainly consists of mafic dykes of Huliyardurga, Karnataka (Kumar et al., 2001), felsic volcanic rocks of St. Mary Islands (Valsangkar et al., 1981; Pande et al., 2001; Melluso et al., 2009), the Ezhimala Igneous Complex (Mohan et al., 2016), the North Kerala Dykes (Radhakrishna et al., 1999), and the Sarnu-Dandali complex, Rajasthan (Sheth et al., 2017).

The second phase of volcanism due to the Réunion hotspot activity has resulted in the formation of tholeiitic Deccan Flood Basalts which spread around an area of ~ 500,000 sq. km. along the central and western India (Figure 2.6). Maximum thickness of this DFB is observed near the western coastal regions and it reaches up to 1800 meters (Patro and Sarma, 2007). It is suggested that the bulk of DFB was created during ~ 65-66 Ma, corresponding to the C30n-C29r-C29n magnetic polarity reversal sequence (Courtlllot et al., 1986; Vandamme et al., 1991; Hooper, 1999; Sen, 2001). However, Pande (2002), based on the available paleo-magnetic information, proposed that DFB activity was not continuous, instead, it took place as distinct eruption and quiescence within the period of ~ 69 to ~ 63 Ma. The most intense eruption was expected to occur around 67 Ma corresponding to chron C30r. Recent studies based on radiometric age estimation from the Khatkopar-Pawai tholeiitic sequence containing both flows and dykes reported an age of 62.5 Ma (Pande et al., 2017). The volcanic occurrence in the Seychelles Plateau, Amboronola volcanics and its offshore regions contains the imprints of Réunion hotspot related volcanism. Some of these are the ~ 69-73 Ma aged tholeiitic dykes of Praslin Island, ~ 60-63 Ma aged alkaline rocks of the Silhouette and North

Island, emplaced during chron C28n (Plummer and Belle, 1995; Ganerod et al., 2011). Shellnutt et al. (2017) recently reported the occurrence of volcanics of age with ~ 62-67 Ma from the Silhouette Island.

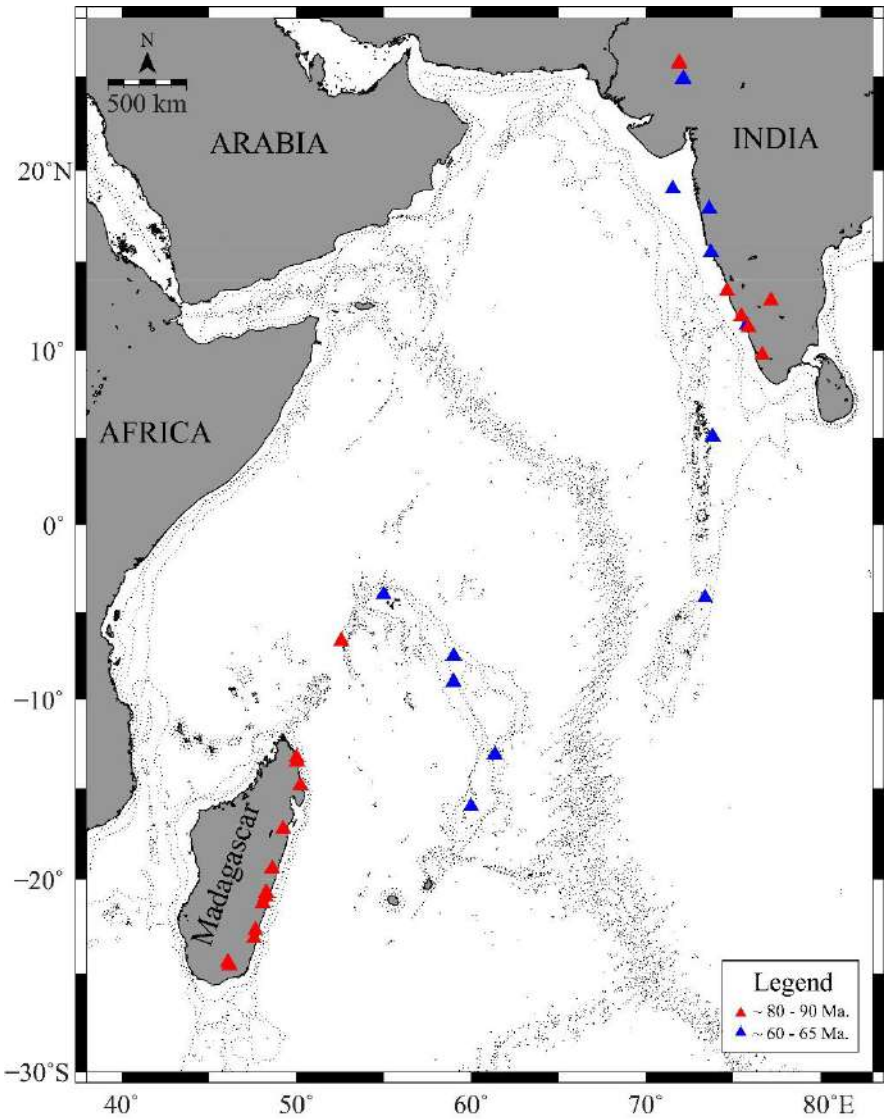

Figure 2.6: Map of Indian Ocean and surrounding continents showing locations of the published dated volcanics related to the Marion and Reunion hotspot activities, marked with red and blue symbols, rspectively (Compiled from Duncan and Hargraves, 1990; Storey et al., 1995; Radhakrishna and Joseph, 2012; Sen et al., 2012; Sheth et al., 2017; Pande et al., 2017; Shellnutt et al., 2017).

Chapter 3

Data and Methodology

3.1 Introduction

The major datasets used in the present study are; high-resolution multibeam bathymetry data, multi-channel seismic reflection data, sea-surface gravity, magnetic and bathymetric profiles, satellite-derived free air gravity data, GEBCO global bathymetric grids and contours, published information on geographical extent of the onshore and offshore tectonic elements, published seismic reflection sections and seismic refraction information, and the rotation parameters that constrain the relative motion among various continental blocks associated with early opening of the Arabian Sea. The methods of forward modelling of gravity and magnetic data and plate tectonic reconstruction have been used as the interpretation tools during the research work. In this chapter, the types and sources of these data used and methodology adopted for interpretation have been described.

3.2 Datasets used in this study

3.2.1 High-resolution multibeam bathymetry data

A large volume of multibeam bathymetry data has been used in the present study for understanding morphotectonic characteristics of the southwestern continental margin of India and the adjacent deep offshore regions. The high-resolution multibeam bathymetry database compiled for the present study consists of the data acquired during twenty six cruises conducted by National Centre for Polar and Ocean Research (NCPOR), Goa and one cruise by CSIR-National Institute of Oceanography (CSIR-NIO), Goa, under the project "Geoscientific Studies of Exclusive Economic Zone of India". The details of the cruises in which multibeam bathymetry data have been collected are given in Table 3.1 and the location of the respective cruises are given in Figure 3.1. Technical specifications (such as make, frequency, beam angle, beam width, etc.) of the Multibeam Echosounder System used for the surveys onboard various research vessels are given in the Table 3.2.

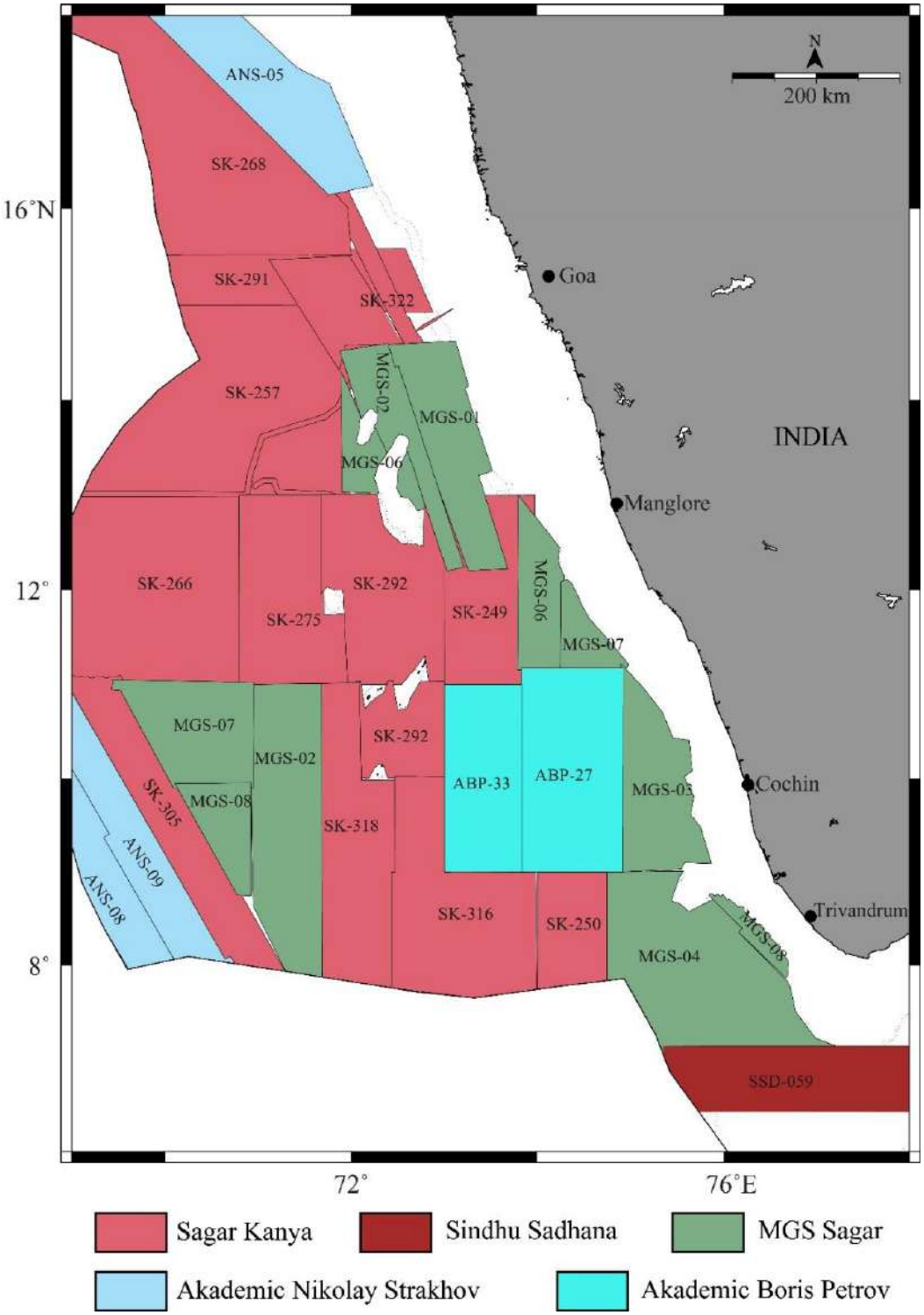

Figure 3.1: Area-wise details of the multibeam bathymetry data collected through different cruises in the Arabian Sea region that is used in the present study. Other details are as in Table 3.1.

Table 3.1: Details of the cruises/marine geophysical datasets used in the present study.

Sl. No.	Cruise ID	Vessel	Year	B	G	M	Source
(a) Southwestern continental margin of India and adjacent deep ocean basins							
1	SK-221	O R V Sagar Kanya	2005	×	✓	✓	NCPOR
2	ABP-27	Akademic Boris Petrov	2007	✓	×	×	NCPOR
3	SK-249	O R V Sagar Kanya	2008	✓	×	×	NCPOR
4	SK-250	O R V Sagar Kanya	2008	✓	×	×	NCPOR
5	ABP-33	Akademic Boris Petrov	2008	✓	×	×	NCPOR
6	SK-257	O R V Sagar Kanya	2009	✓	×	×	NCPOR
7	SK-266	O R V Sagar Kanya	2009-10	✓	×	×	NCPOR
8	SK-268	O R V Sagar Kanya	2010	✓	×	×	NCPOR
9	SK-275	O R V Sagar Kanya	2010	✓	×	×	NCPOR
10	SK-291	O R V Sagar Kanya	2011	✓	×	×	NCPOR
11	SK-292	O R V Sagar Kanya	2012	✓	×	×	NCPOR
12	SK-305	O R V Sagar Kanya	2013	✓	×	×	NCPOR
13	ANS-08	RV-AN Strakhov	2013	✓	×	×	NCPOR
14	ANS-08	RV-AN Strakhov	2013	✓	×	×	NCPOR
15	ANS-09	RV-AN Strakhov	2013	✓	×	×	NCPOR
16	SK-305	O R V Sagar Kanya	2013	✓	×	×	NCPOR
17	SK-316	O R V Sagar Kanya	2014	✓	×	×	NCPOR
18	SK-318	O R V Sagar Kanya	2014-15	✓	×	×	NCPOR
19	SK-322	O R V Sagar Kanya	2015	✓	×	×	NCPOR
20	MGS-01	MGS Sagar	2015	✓	✓	×	NCPOR
21	MGS-02	MGS Sagar	2015	✓	✓	✓	NCPOR
22	MGS-03	MGS Sagar	2016	✓	✓	✓	NCPOR
23	MGS-04	MGS Sagar	2016	✓	✓	✓	NCPOR
24	MGS-06	MGS Sagar	2016	✓	✓	✓	NCPOR
25	MGS-07	MGS Sagar	2016	✓	✓	✓	NCPOR
26	MGS-08	MGS Sagar	2016	✓	✓	✓	NCPOR
27	SK-365	O R V Sagar Kanya	2020	✓	×	×	NCPOR
28	SSD-059	O R V Sindhu Sadhana	2018	✓	×	×	NIO
29	jc130	R/V Jean Charcot	1983-84	×	×	✓	NCEI
30	jc02	R/V Jean Charcot	1984	×	×	✓	NCEI
31	mdu57	R/V Marion Dufresne	1988	×	×	✓	NCEI
32	cn006	R/V Chain	1971	×	×	✓	NCEI
33	rc1708	R/V Robert Conrad	1974	×	×	✓	NCEI
34	um6080	R/V Umitaka Maru	1968-68	×	×	✓	NCEI
35	ve2902	R/V Vema	1971-72	×	×	✓	NCEI
36	wi815	USNS Wilkes	1978	×	×	✓	NCEI
37	wi821	USNS Wilkes	1978	×	×	✓	NCEI
38	wi827	USNS Wilkes	1978	×	×	✓	NCEI
39	wi828	USNS Wilkes	1978	×	×	✓	NCEI
40	ve2010	R/V Vema	1964	✓	✓	✓	NCEI
41	ve3410	R/V Vema	1977	✓	✓	✓	NCEI
(b) Northern Madagascar Ridge and the adjoining regions							
42	mdu11	Marion Dufresne	-	✓	✓	✓	NCEI
43	mdu23	Marion Dufresne	-	✓	✓	✓	NCEI
44	md09	Marion Dufresne	-	✓	×	✓	NCEI
45	di101	R/V Discovery	1979	×	✓	✓	NCEI
46	at9305	Atlantis II	1976	✓	×	✓	NCEI
47	ve2904	R/V Vema	1972	✓	✓	✓	NCEI
48	jr114	R/V JOIDES Resolution	1987	×	✓	×	NCEI

B: Multibeam Bathymetry; G: Gravity; M: Magnetic

Table 3.2: Details of the specifications of the MBES system used onboard various research vessel.

Vessel	**ORV Sagar Kanya (SK)**	**RV-Akademik Boris Petrov (ABP)**	**RV-Akademik Nikolaj Strakhov (ANS)**	**RV-MGS Sagar (MGS)**
Make	L3-Comm. Elac-Nautik	Atlas Elektronik	Reson	Reson
Model	SB3012	Hydrosweep-DS2	SeaBat 7150	SeaBat 7150
Frequency of operation	12 kHz	15 kHz	12 kHz / 24 kHz	12 kHz / 24 kHz
Number of Beams	201	240	234	234
Swath Coverage	Upto 5 x Depth	Upto 3.5 x Depth	Upto 5 x Depth	Upto 5 x Depth
Angular Coverage	Upto 140°	Upto 120°	Upto 150°	Upto 150°
Beam Width	2°	2.3°	2°	2°
Depth of performance	Upto 11,000m	Upto 10,000m	Upto 10,000m/ 6000m	Upto 10,000m/ 6000m
Acquisition software	Hydrostar	Hydromap Online	PDS2000	PDS2000

Processing of the multibeam bathymetry (MB) data includes the removal of erroneous depth, data editing and visualization. The MB data is corrected for the vessel movements as a result of sea state causing roll, pitch, heave etc. It is well known that sound velocity in the water column varies with varying salinity, temperature and pressure. So accurate bathymetric measurements can be made only

if these changes are taken into consideration. During the survey, sound velocity profiles were collected in regular intervals of time and refraction corrections were applied for the MB data in real-time or during post processing stage. Processing of the MB data has been carried out using Caris Hips and Sips software, which is a designated software for bathymetric data processing and visualization. Spurious depth soundings and spikes are removed at the last stage of post-processing. Finally, all the cruise data has been merged together to make a bathymetric grid which is used for further interpretation. Fledermaus software also has been extensively used for the visualization and interpretation of the bathymetry data.

3.2.2 Sea-surface magnetic and gravity data

Sea-surface magnetic and gravity data from the southwestern continental margin of India and its conjugate region of Madagascar have been compiled and utilized for the present study. Major source of underway geophysical data in the SWCMI region is from National Centre for Polar and Ocean Research, Goa and CSIR-National Institute of Oceanography, Goa. Apart from these indigenous datasets, public domain data available from the National Centers for Environmental Information (NCEI), Boulder, Colorado, USA (https://www.ngdc.noaa.gov/mgg/mggd.html) has also been compiled and used. Free-air gravity anomaly has been deduced by applying normal and Eötvös corrections to the raw data. The total field magnetic data were reduced to residual magnetic anomalies by applying International Geomagnetic Reference Field (IGRF) for the corresponding epoch. The locations of sea-surface gravity and magnetic profiles used in the present study in the Indian side and its conjugate Madagascar side are given in Figures 3.2 and 3.3, respectively, and the cruise details are given in Table 3.1.

3.2.3 Satellite-derived free-air gravity anomalies

The satellite derived free-air gravity anomalies have been used as a supporting information for identifying various seafloor and basement features in the present study. The latest version of satellite-derived free air gravity anomaly data grid (Sandwell et al., 2014) is obtained from the web portal ftp://topex.ucsd.edu/pub/global_grav_1min, which is maintained by Scripps Institution of Oceanography, University of California San Diego, USA. This is

version 30.1 of the satellite-derived free-air gravity anomaly grid, with a spatial resolution of 1 arc minute.

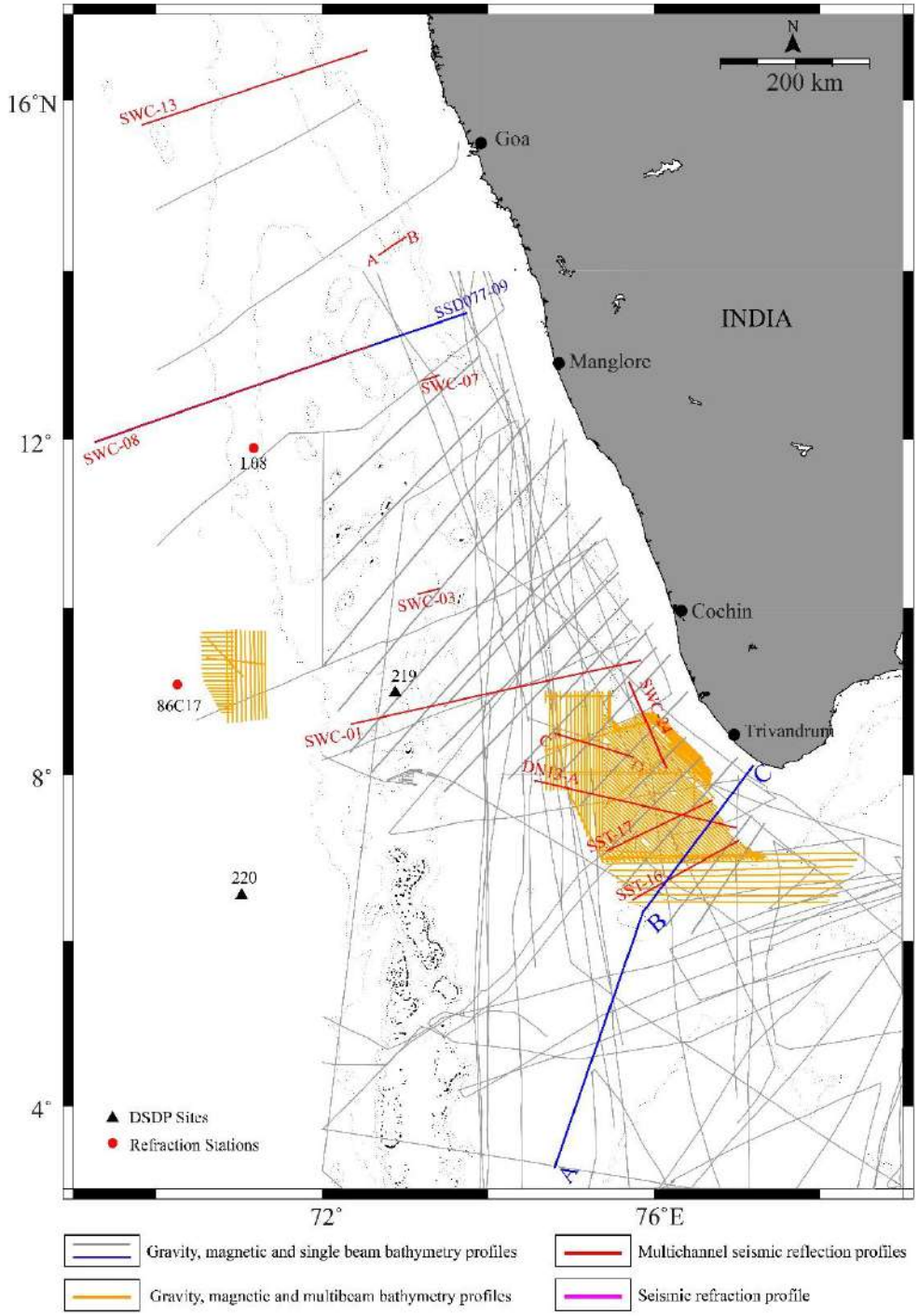

Figure 3.2: Map showing the marine geophysical track-line locations in the SWCMI and the adjacent deep ocean basins that is used for the present study. Other details are given in Table 3.1.

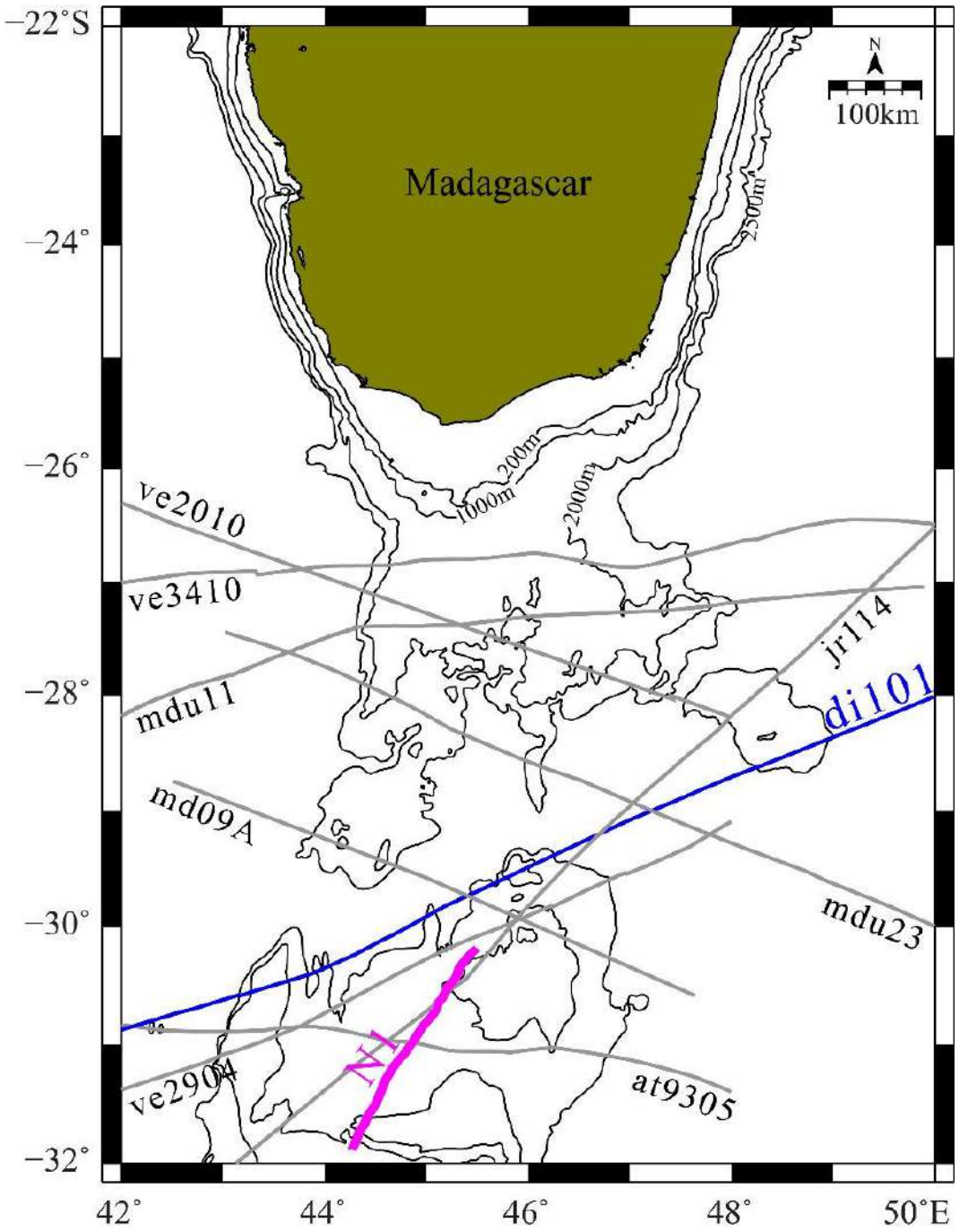

Figure 3.3: Map showing the marine geophysical track-line locations in the northern Madagascar Ridge that is used for the present study. N1 is the location of available seismic refraction station (Goslin et al., 1980). Other details are given in Figure 3.2 and Table 3.1.

3.2.4 Global bathymetric data

A global bathymetric grid for the world ocean combined with land topography has been prepared and released by the General Bathymetric Chart of the Oceans (GEBCO). This data has been used for understanding broad morphology of the study area and to aid the interpretation in the gap areas where multibeam bathymetry data is not available. GEBCO_2014 has a resolution of 30 arc seconds (Weatherall et al., 2015) and GEBCO_2020 (GEBCO Compilation Group, 2020) has a resolution of 15 arc seconds integrating the publically available latest versions of regional bathymetric compilations from the different sectors of the global ocean. The gridded data have been downloaded from https://www.gebco.net/data_and_products/gridded_bathymetry_data/. Together with the bathymetric grid, the isobaths extracted from the CD ROM database titled "The Centenary Edition of the GEBCO Digital Atlas (GDA)" also has been used (IOC-IHO-BODC, 2003).

3.2.5 Seismic reflection profiles

The seismic reflection sections provide the sub-seafloor information including sediment stratigraphy, occurrence of major tectonic elements, and basement characteristics. A fresh set of 2D multichannel seismic data along with the published seismic information in the SWCMI and the adjacent deep ocean basins has been used for the present study. The locations of the seismic sections presented in the study are given in Figure 3.2. The seismic reflection database used for the present study consists of the multichannel seismic reflection data available from Directorate General of Hydrocarbon (DGH), India (SWC profiles, SST profiles) and single / multichannel seismic sections available from published literature (Whitmarsh, 1974; Rao et al., 2010; Yatheesh et al., 2013b; Nathaniel, 2013), to understand the sediment and basement characteristics of the bathymetric highs in the SWCMI and the Alleppey-Trivandrum Terrace Complex region.

3.2.6 Seismic refraction information

The published seismic refraction information has been used as constraints for the two-dimensional forward modelling of gravity and magnetic data. In the Indian side, the velocity-depth information available from the sonobuoy seismic refraction experiment (Naini, 1980; Naini and Talwani, 1982) have been compiled

and used while carrying out forward modeling of gravity profiles from the southwestern continental margin of India and the adjacent deep ocean basins. The locations of these refraction stations are given in Figure 3.2. In the Madagascar side, velocity-depth information (Goslin et al., 1980) from the N1 profile located on the Northern Madagascar Ridge has been compiled and used while carrying out forward modeling of gravity profiles over the Northern Madagascar Ridge and the adjoining regions. The location of this seismic refraction profile (N1) is shown in Figure 3.3.

3.2.7 Total rotation parameters constraining relative plate motions

The total rotation parameters represent the set of values which define relative movement of plates over spherical surface in a fixed reference frame. These parameters consist of Euler pole (defined by latitude and longitude) and Euler angle defining the movement of a moving plate from a fixed plate. Since the study involves evaluation of the conjugate nature of features in the plate tectonic reconstruction models proposed based on the previous studies and explaining the genesis of various tectonic elements identified from the present study in terms of plate tectonic evolution of the study area, all the available (Bhattacharya and Yatheesh, 2015; Shuhail, 2018; Shuhail et al., 2018; Yatheesh et al., 2020) rotation parameters describing these relative motions are compiled. While compiling these data, for consistency, the age corresponding to all the chrons were reassigned based on Cande and Kent (1995) geomagnetic polarity reversal timescale.

3.2.8 Geographical extent of the other offshore and onshore tectonic elements

The Precambrian trends, rift grabens, and the location of volcanics from the SWCMI and its conjugate region of Madagascar have been compiled for examining the plate tectonic reconstruction scenario. These constraints are examined and incorporated while developing plate tectonic reconstruction models depicting the plate tectonic evolution of the SWCMI and its conjugate regions. These tectonic elements mainly comprise of the coastlines, continent-ocean boundaries, aseismic ridges, present and extinct spreading centres, trenches, fracture zones and the postulated microcontinents. The extent of these various onshore and offshore tectonic elements used in the present study are given in Figure 3.4.

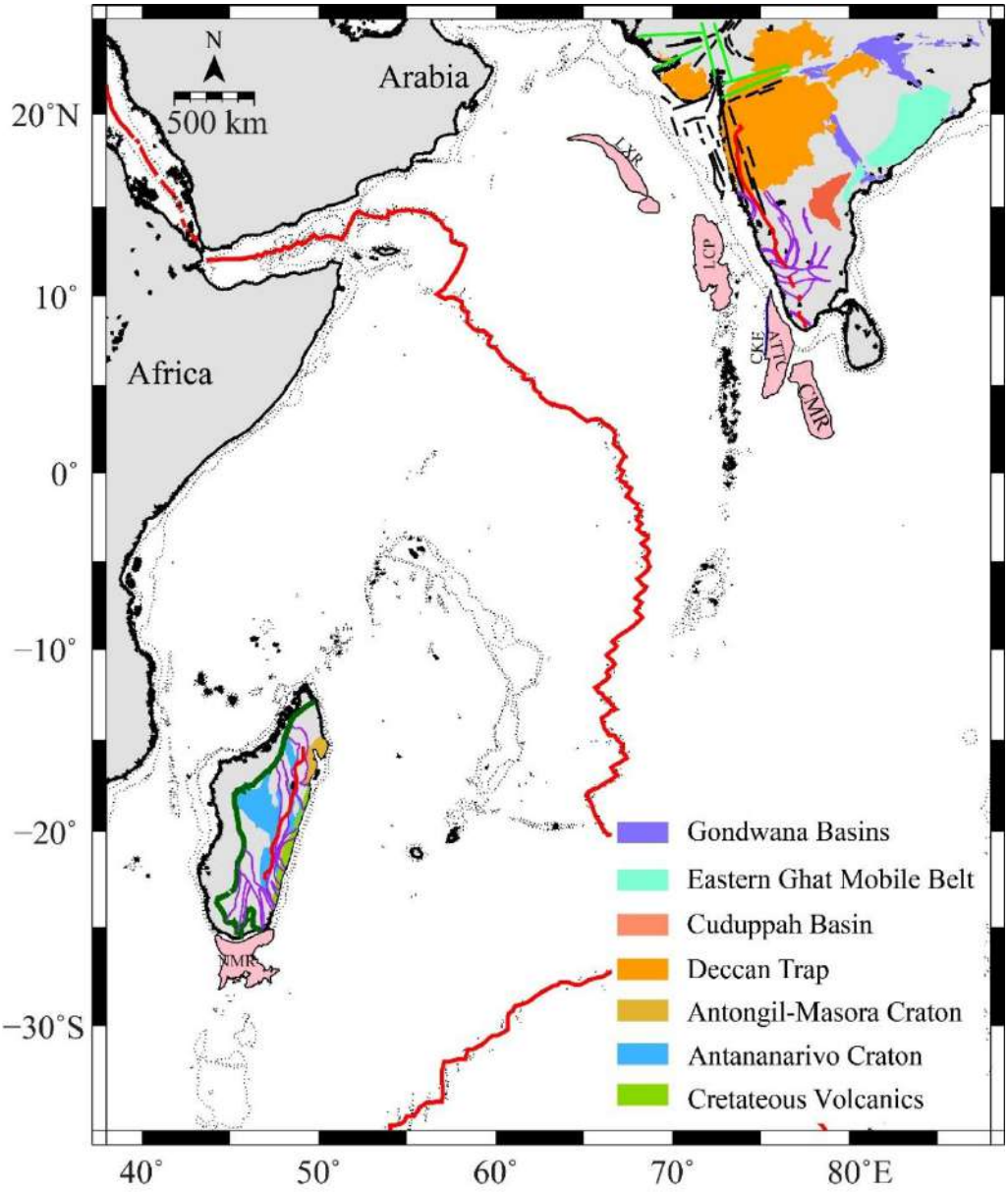

Figure 3.4: Map delineating the extent of various onshore and offshore tectonic elements from the western Indian Ocean and the adjoining landmasses presented in this study. Other details are as in the Figures 2.2, 2.3, 2.4 and 2.5.

3.3 Methodology

3.3.1 Classification of seafloor morphology

The present study mainly characterizes the bathymetric high features in the SWCMI from the bathymetry map generated using high resolution multibeam bathymetry data. The identification and classification of these features are performed by visual interpretation of the bathymetric data using Caris Hips & Sips

and Fledermaus software based on which one can visualize 2D and 3D perspective of the data. In the present study, classification of the seafloor features is carried out based on the criteria of International Hydrographic Organization (IOC-IHO, 2013). These features were further analyzed to infer their morphological characteristics and the morphometric parameters.

3.3.2 Forward modelling of gravity and magnetic anomalies

The forward modelling of gravity and magnetic anomaly profiles are attempted to derive a geologically reasonable crustal model for the Northern Madagascar Ridge, the Alleppey-Trivandrum Terrace Complex, the Sagar Kanya Bathymetric High Complex and the Laccadive Plateau. The forward modelling of gravity and magnetic anomalies caused by two-dimensional bodies is carried out by the method proposed by Talwani et al. (1959) and Talwani and Heirtzler (1964), respectively. In the present study, the gravity and magnetic modeling is achieved using the commercially available interactive GM-SYS software, a product of Northwest Geophysical Associates, Inc, in which the gravity response for the given 2D body is computed based on the method of Talwani et al. (1959) and magnetic response is computed based on the method of Talwani and Heirtzler (1964).

a) Computation of gravity anomalies over 2-D bodies

The purpose of a gravity modelling is to obtain a geologically possible crustal structure which is compatible with the existing geological constraints and the observed gravity anomalies. For deriving this model, the following procedures were adopted:

i) A preliminary crustal model is constructed by incorporating all available bathymetric, seismic reflection and refraction information.

ii) The main crustal units (oceanic crust layer-2 and layer-3, upper and lower continental crust, sediment layer) are identified and the average interval velocities are assigned for each unit wherever geological/geophysical information are available. Wherever precise information is not available, standard velocity have been assigned for the oceanic and continental crustal blocks.

iii) From the velocity-density relationship of Ludwig et al. (1970) and Brocher (2005), layer densities are assumed for these crustal and sedimentary units.

iv) Considering each of these crustal units as separated body defined by a coordinated bounding polygon with constant density, the composite gravity anomaly for the crustal section is computed as a sum of anomalies for all these separate bodies.

v) The initial crustal model is refined by trial and error, to obtain an acceptable model which gives reasonably good fit between the observed and computed gravity anomalies.

b) Computation of magnetic anomalies over 2-D bodies

Once a reasonably good fit for gravity profile is obtained, modelling of magnetic anomaly is carried out as given in the following steps:

i) Initial magnetized bodies are created within the crustal units derived based on gravity modelling and the magnetic properties (strike of the body, magnetic susceptibility, remnant inclination, remnant declination, remnant magnetization, present day inclination, present day declination, and present day magnetization) are assigned.

ii) Similar to the gravity modelling, magnetic response of the given crustal section is computed for the entire magnetic profile.

iii) The crustal model is further refined by several iterations by keeping magnetization information fixed and by slightly changing the extent of the bodies till obtaining a good fit between observed and computed magnetic anomalies.

3.3.3 Plate tectonic reconstruction

The plate tectonic reconstruction (paleogeographic reconstruction) is the process of restoring lithospheric plates back to the relative positions they occupied in the geological past. In the present study, plate tectonic reconstruction has been used to evaluate the conjugate nature of features in the plate tectonic reconstruction models proposed based on the previous studies and explaining the genesis of various tectonic elements identified from the present study in terms of plate tectonic evolution of the study area. In the present study, the plate tectonic reconstruction models have been generated using the GPlates software (Boyden et al., 2011), which is an open-source plate reconstruction software developed by the University

of Sydney, Australia, the California Institute of Technology, USA and the Norwegian Geological Survey, Norway.

3.3.4 Preparation of maps

The present study consists of generating large number of maps including color-coded 2D, 3D, contour maps and profile plots for carrying out the interpretation. All these maps are prepared using the Generic Mapping Tools (GMT) software (Wessel et al., 2013). The plate tectonic reconstruction geometries derived using the GPlates software used with the GMT for generating plate tectonic reconstruction models. The seismic sections have been interpreted and presented using the Seismic Unix software.

Chapter 4

Morphotectonic characteristics, distribution and probable genesis of bathymetric highs off southwest coast of India

4.1 Introduction

Bathymetric high features are important submarine physiographic features, which have been a subject of interest in geophysical, geological, oceanographic and biological aspects. Detailed investigations of the bathymetric features are important because such studies can provide vital clues for understanding the evolution of deep ocean basins and the adjacent continental margins as well as identification of economically important mineral deposits. Research focused on the morphological and geophysical aspects of the bathymetric high features were widely conducted in the world ocean (Menard, 1964; Smith and Jordan., 1988; Wessel, 2001; Wessel et al., 2010; Harris et al., 2014). Various hypotheses were proposed for the formation of these bathymetric high features, mainly, hotspot activity, ridge-hotspot interaction, ridge parallel faulting, off axis volcanism and propagating fracture (Fornari et al., 1984; Duncan and Clauge, 1985; Fornari et al., 1988; Shen et al., 1993; Clauge et al., 2000; Clouard et al., 2003; Das et al., 2007).

In the Indian Ocean, extensive studies of geomorphologic features were carried out in the Central Indian Basin (Kodagali, 1989, 1992, 1998; Mukhopadhyay and Khadge, 1990; Mukhopadhyay and Batiza, 1994; Das et al., 2005, 2007; Iyer, 2009; Iyer et al.,2012), however, such studies of morphological features are comparatively sparse in the Western Indian Ocean except a few in the Arabian Sea (Bhattacharya and Subrahmanyam, 1991; Bhattacharya et al., 1994b; Mukhopadhyay et al., 2008; Rao et al., 2010). Bhattacharya and Subrahmanyam (1991) carried out detailed geophysical study over the Sagar Kanya Seamount in the Arabian Basin and provided crustal configuration and probable genesis for this seamount. Bhattacharya et al. (1994b) mapped a seamount chain in the Laxmi Basin, consisting of the Raman Seamount, Panikkar Seamount and Wadia Guyot. Subsequently, Mukhopadhyay et al. (2008) and Rao et al. (2010) studied bathymetric highs in the mid continental slope region of the southwestern continental margin of India (SWCMI). However, such detailed geomorphologic

studies were not undertaken in the Laccadive Basin and the adjacent areas (Figure 4.1), which consists of several prominent bathymetric highs. In the present study, attempt has been made to map these bathymetric features in the Laccadive Basin, eastern part of the Laccadive Plateau and the southwestern continental margin of India and then to discuss their distribution and probable mode of emplacement.

4.2 Seafloor morphology from multibeam bathymetry data

The updated bathymetric map (Figure 4.1) of the study region covers an area of ~ 2,34,000 sq.km. This high-resolution bathymetric map shows the presence of 33 distinct bathymetric highs with varying size and height. These seafloor features have been classified into different categories such as seamounts, hills, knolls, guyots and plateaus, following the classification scheme of International Hydrographic Organization (IOC-IHO, 2013). The morphological characteristics of these features are inferred and their morphometric parameters have been derived. Locations of the identified features have been shown in Figures 4.1 and 4.2 and their morphometric characteristics are presented in Figure 4.3. The derived morphometric parameters, which mainly consist of height, basal area, basal width, slope angle, flatness and height-width ratio, are detailed in Table 4.1. In this section, detailed description of geomorphology of the identified bathymetric features and their morphometric characteristics are provided.

4.2.1 Seamounts

Seamounts are distinct generally equi-dimensional elevation greater than 1000 m above the surrounding relief as measured from the deepest isobath that surrounds most of the feature (IOC-IHO, 2013). From the updated bathymetric map of the study area, 14 seamounts (S1 to S14, as shown in Figure 4.1 and Table 4.1), with varying height of 1045-2260 m from the surrounding seafloor, were identified. Among these, 12 seamounts (S2 to S11 and S13 to S14) are located in the eastern sector of the Laccadive Plateau and the adjacent region of the Laccadive Basin, while two seamounts (S1 and S12) are located close to the southwestern continental slope of India. Most of these features are with single peak along the summit, but seamounts S9, S12 and S14 are characterized by four, two and three peaks, respectively. Seamount S3, a conical feature, has least basal extent (~53 sq.km) and seamount S13 has maximum basal extent (~ 904 sq.km). Seamount S11, which has

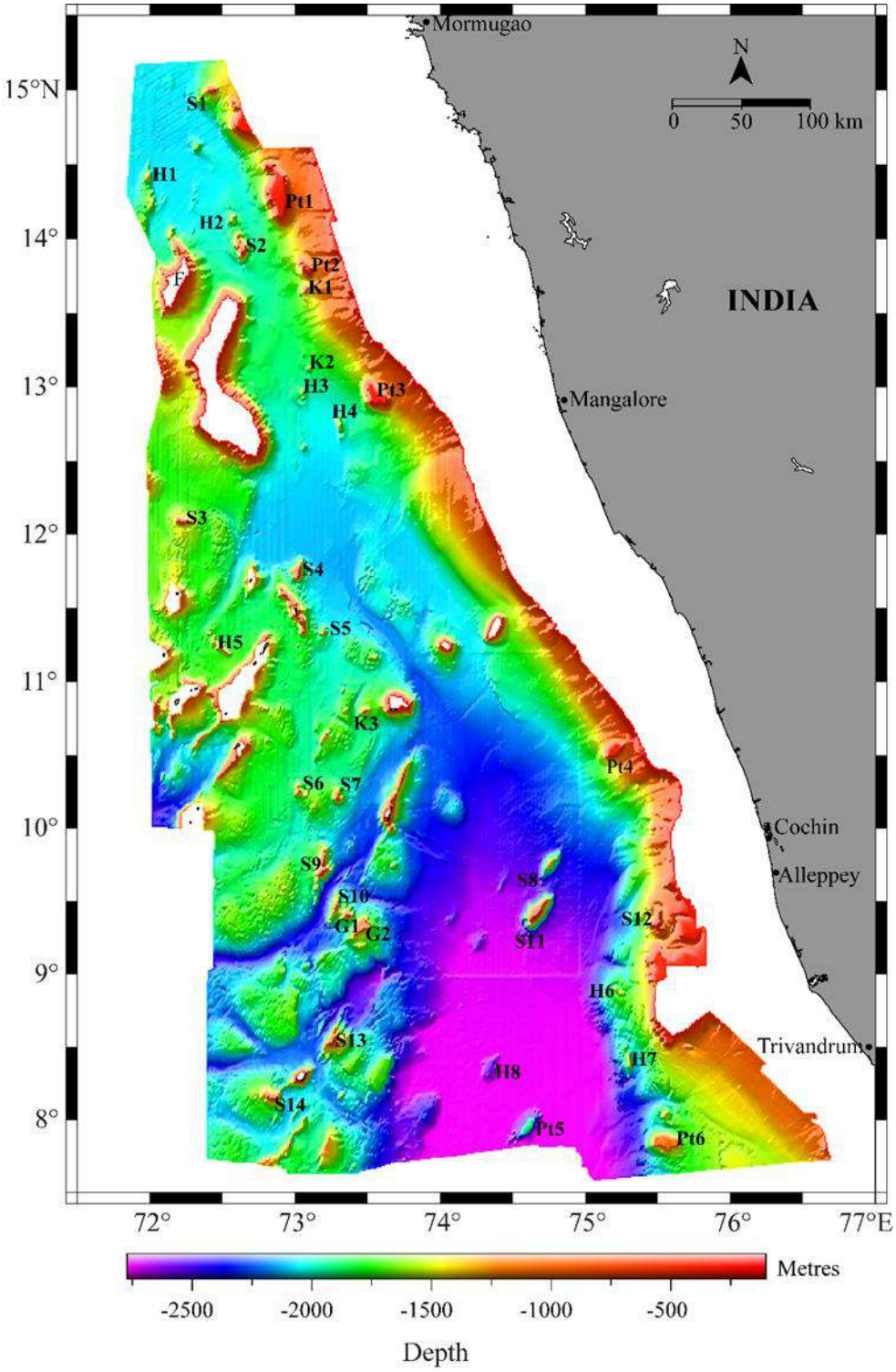

Figure 4.1: The updated high-resolution bathymetric map of the study area, showing the locations of the bathymetric high features identified in the present study. Morphometric details of these features are provide in Table 4.1.

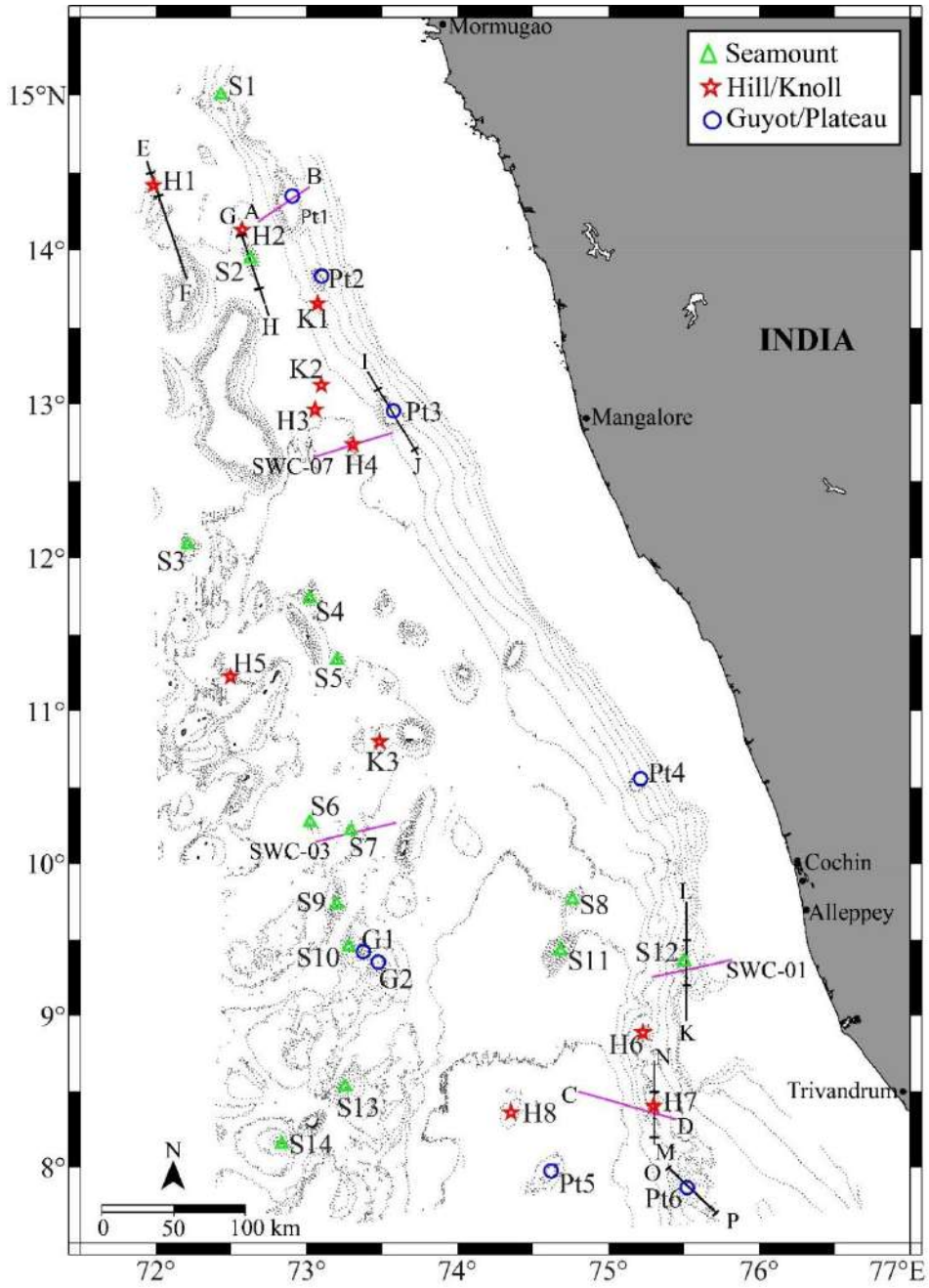

Figure 4.2: The updated bathymetric contour map (with 250 m interval) of the study area, showing the locations of the bathymetric high features identified in the present study. Pink lines represent locations of the reflection seismic sections presented in Figure. 4.10. Black lines represent locations of sea-surface bathymetry, gravity and magnetic profiles presented in Figure 4.10 (profile plots). Black cross marks on these lines represent the extent of the profiles shown in Figure 4.9.

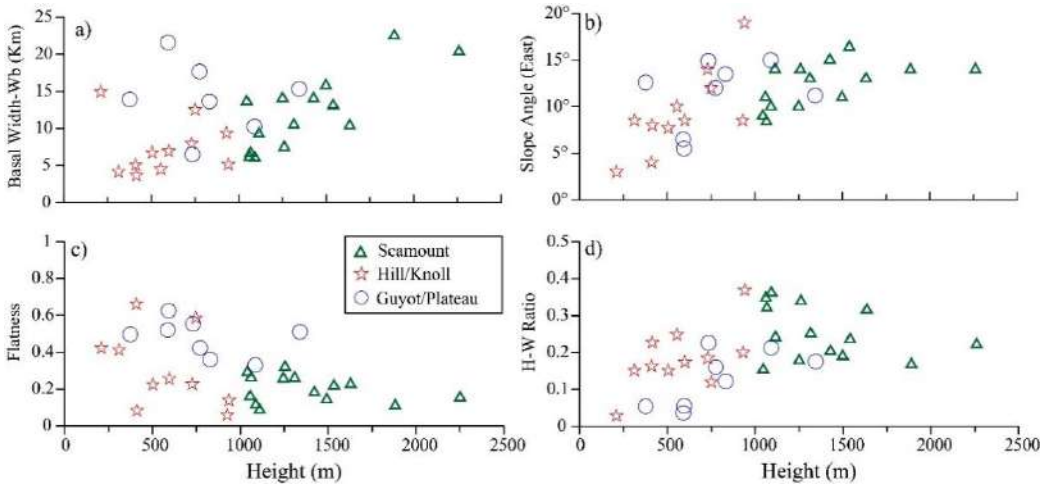

Figure 4.3: Plots of (a) height versus basal width (Wb), (b) height versus slope angle, (c) height versus flatness and (d) height versus H-W ratio of identified bathymetric high features. Morphometric details are given in Table 4.1.

maximum height (2260 m), shows (Figure 4.3) significantly large slope angle and basal width but less flatness. The plot of basal width against height for the seamounts shows that height increases (1000 to 1500 m) roughly with increasing basal width (7 to 17 km) for the seamounts (Figure 4.3). The 3D bathymetric images of the all identified seamounts, are presented in Figure 4.4.

4.2.2 Hills and Knolls

Hills are distinct elevations generally of irregular shape, less than 1000 m above the surrounding relief as measured from the deepest isobath that surrounds most of the feature (IOC-IHO, 2013). On the other hand, Knolls are distinct elevations with a rounded profile less than 1000 m above the surrounding relief as measured from the deepest isobath that surrounds most of the feature (IOC-IHO, 2013). The bathymetric map reveals the presence of clearly distinguishable 8 hills (H1 to H8) and 3 knolls (K1 to K3). These identified features are presented in Figure 4.1 and their morphometric details are given in Table 4.1. Most of the hills and knolls are characterized by an increase in basal width and slope angle against increasing height (Figure 4.3). The hills H1 to H5 and H8 are situated in relatively flat seafloor. The basal depth of hills H1 to H5 ranges between 1800-2000 m, while the basal depth of H8 is about 2750 m. These hills exhibit basal extents varying between 20.65 sq.km (H3) and 350 sq.km (H8), with varying height-width (H-W) ratio between

0.028 and 0.247. Three knolls, with basal depth ranging 1400-1800 m, were identified in the Laccadive Basin, with varying heights (310-940 m) and areal extents (25-100 sq.km). The 3D bathymetric images of the all identified knolls and hills are presented in Figures 4.5 and 4.6, respectively.

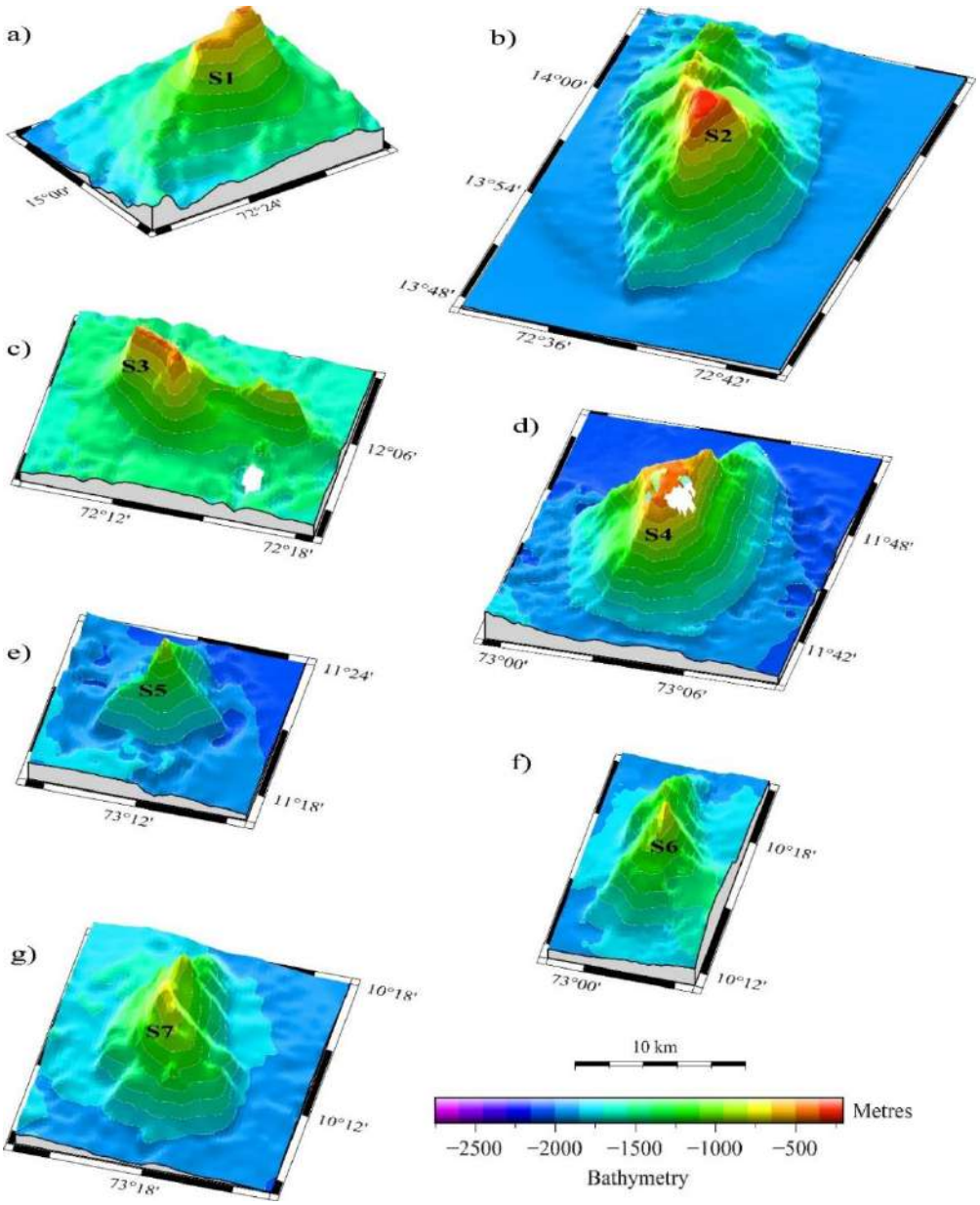

Figure 4.4: Three-dimensional images of the identified seamounts in the study area (Seamounts S1 to S7).

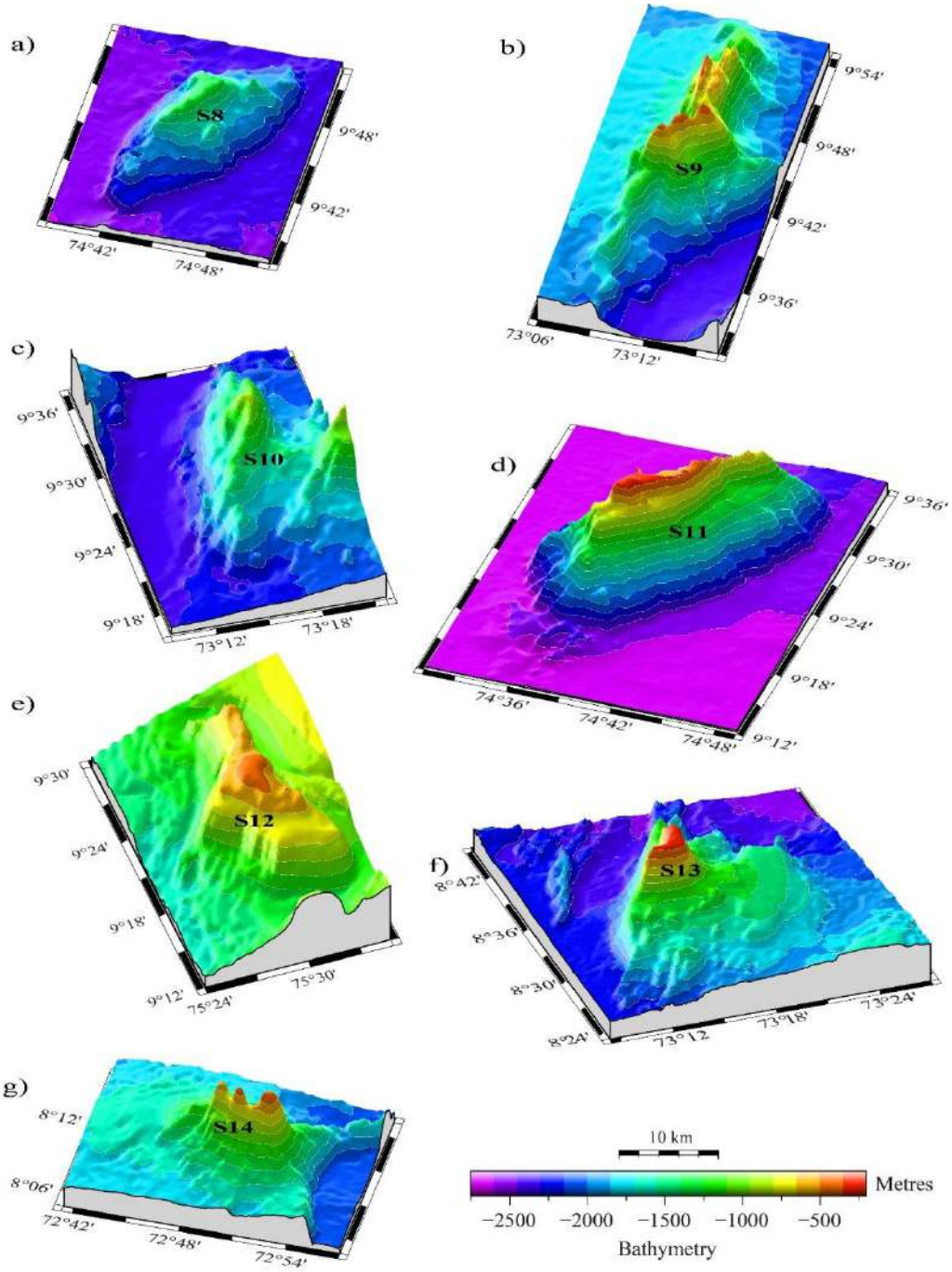

Figure 4.4contd.: Three-dimensional images of the identified seamounts in the study area (Seamounts S8 to S14).

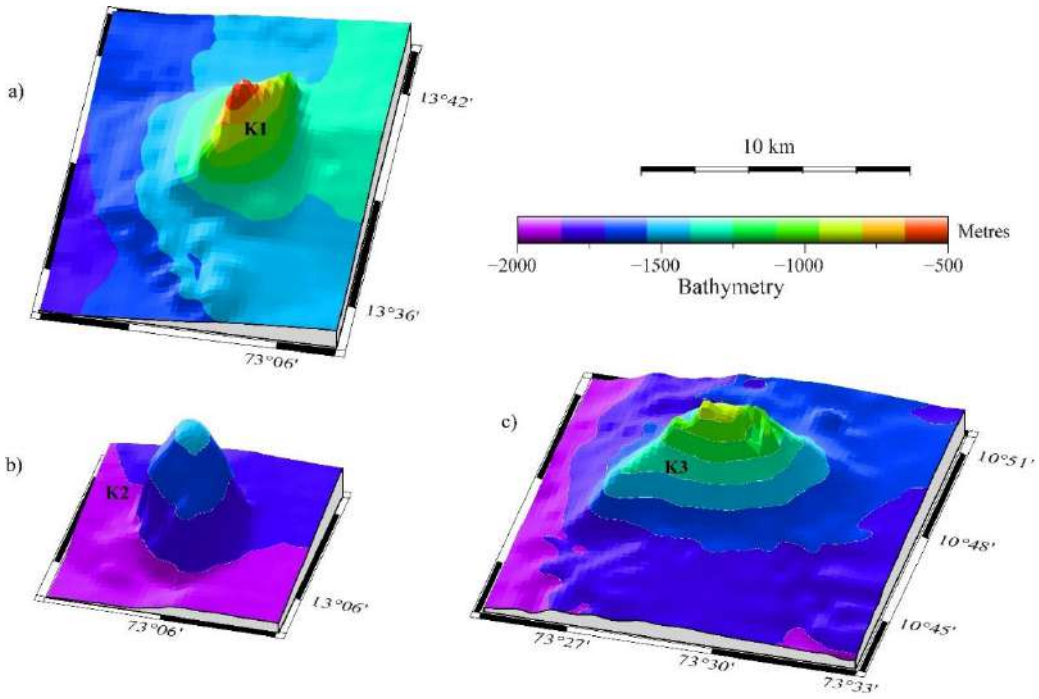

Figure 4.5: Three-dimensional images of the identified knolls in the study area.

4.2.3 Guyots and Plateaus

Guyots are seamounts with comparatively smooth flat top, and plateaus are large, relatively flat elevations that are higher than the surrounding relief with one or more relatively steep sides (IOC-IHO, 2013). The study area contains two guyots, which are located in relatively flat seafloor close to the eastern flank of the Laccadive Plateau (Figure 4.1). These guyots G1 and G2, whose basal depths are about 1800 m, show basal extent of 96 sq.km and 330 sq.km, with flatness of 0.330 to 0.510, respectively (Figure 4.3 and Table 4.1). The 3D bathymetric maps of guyots G1 and G2 are presented in Figure 4.7. From the bathymetric map, six plateaus also are identified, Pt1 to Pt6 in the study area (Figure 4.1). All the plateaus, except Pt6 are situated in the southwestern continental slope of India, while the plateau Pt5 is located in the Laccadive Basin. The plateaus in the continental slope exhibit different basal depths in the landward and seaward sides of these features. The basal depths for plateaus given in Table 4.1 represent those measured in the landward direction. These plateaus possess basal extent ranging from 123-1172 sq.km and flatness varying from 0.350-0.625 (Table 4.1). All

plateaus exhibit moderate to steep sloping flanks, showing gully patterns over both the flanks. The 3D bathymetric images maps of the all plateaus, Pt1 to Pt6 are presented in Figure 4.8.

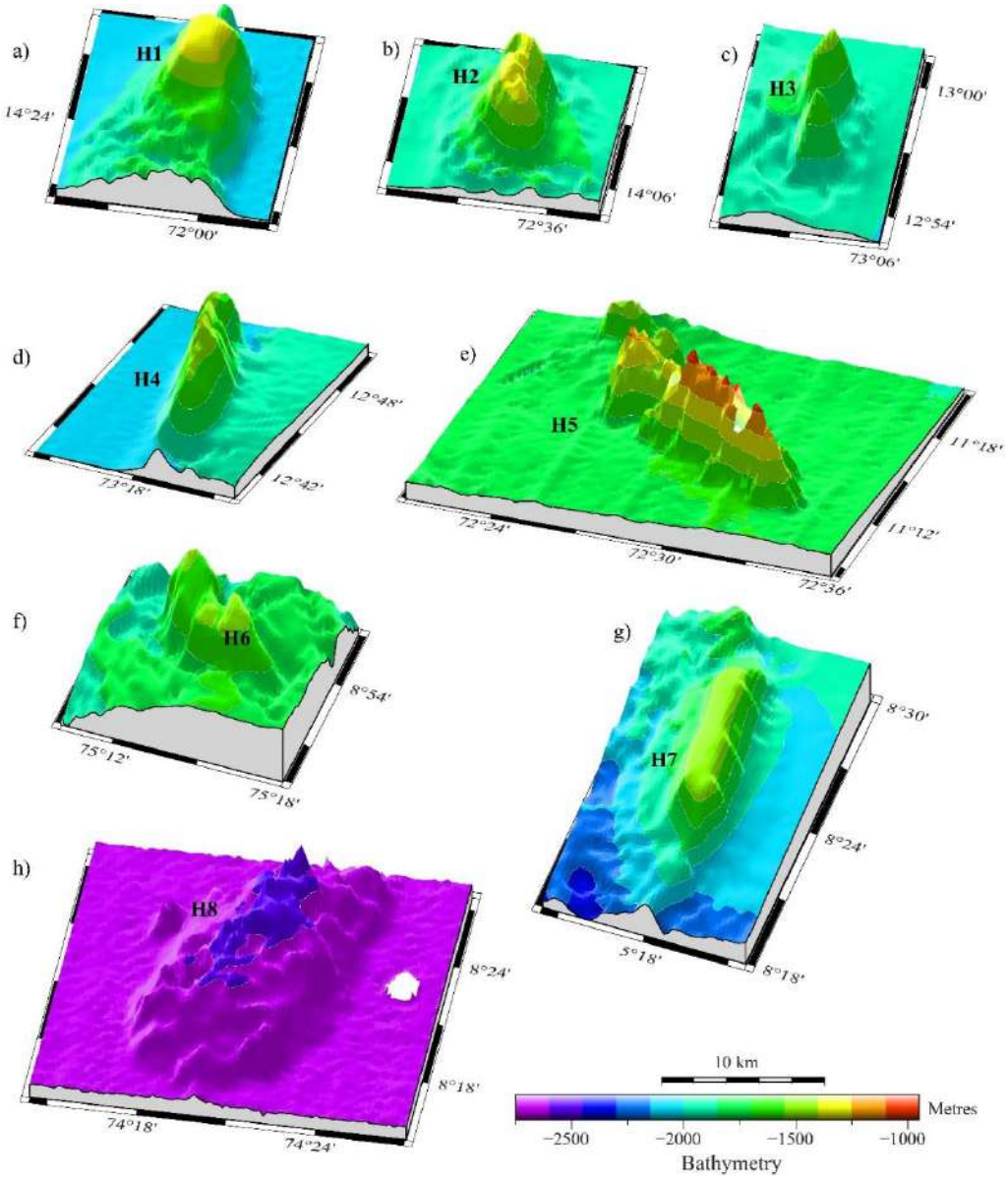

Figure 4.6: Three-dimensional images of the identified hills in the study area.

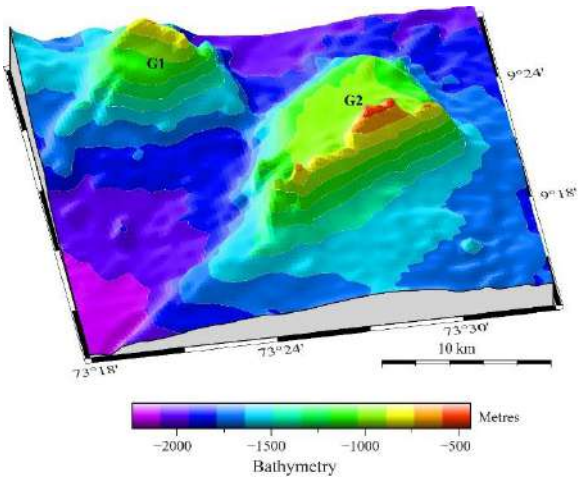

Figure 4.7: Three-dimensional images of the identified guyots in the study area.

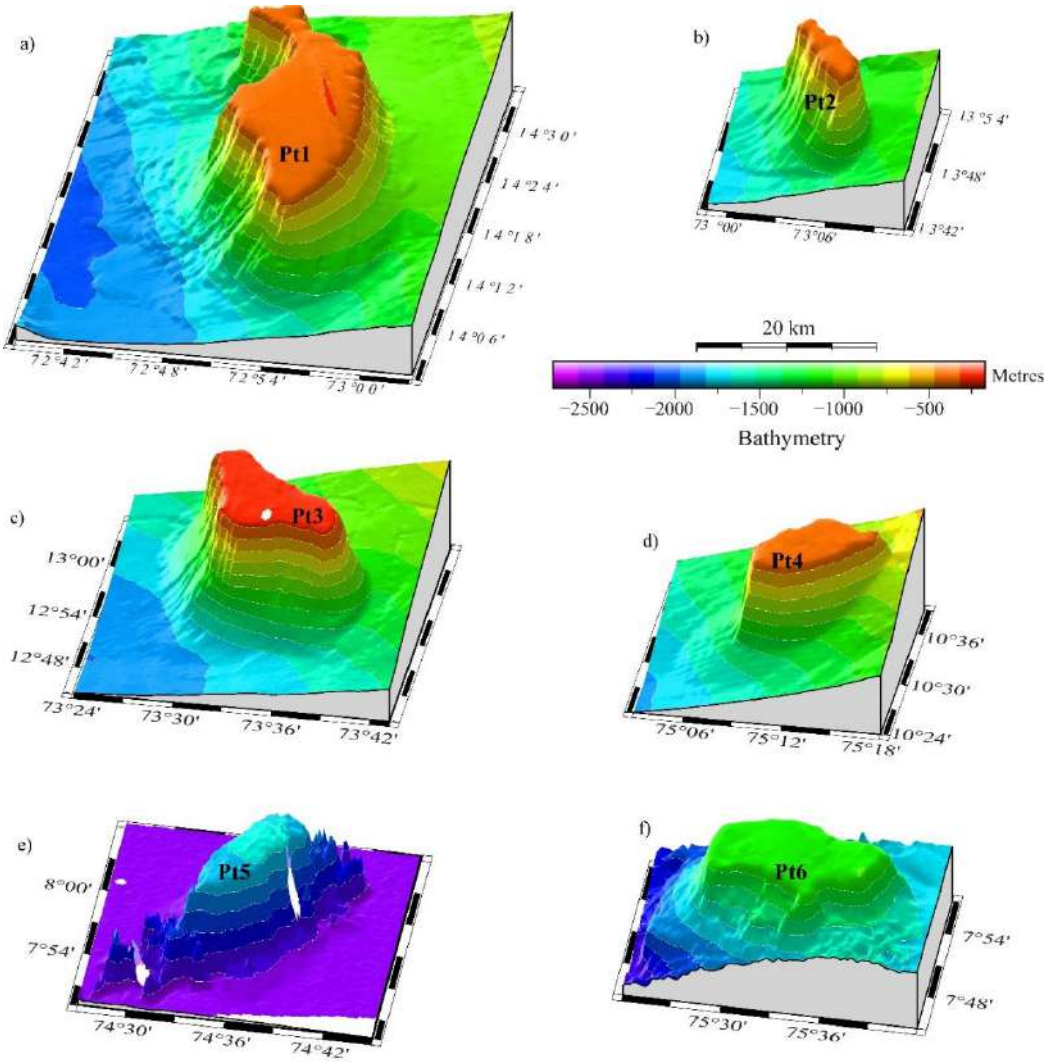

Figure 4.8: Three-dimensional images of the identified plateaus in the study area.

4.3 Sub-seafloor configuration from seismic reflection data

Three multichannel and two single channel seismic sections (Figure 4.9) are used to depict sub-seafloor configuration of the selected bathymetric features considered in the present study. The seismic sections SWC-01, SWC-03, SWC-07, AB and CD (Figures 4.1 and 4.2) cut across the bathymetric high features S12, S7, H4, Pt1, and H7, respectively. Some of these features (Pt1, H7 and S12) are located in the continental slope region, while others (H4 and S7) are located in the deep sea basin. The multichannel seismic image of the hill H4 (Figure 4.9a) and seamount S7 (Figure 4.9b) show that the flanks of these features are steep and the sediments are nearly absent on top of them. This observation suggests that both these features might represent volcanic extrusives, with a basement high piercing through the sediment surface. On the other hand, the multichannel seismic image of the seamount S12 depict (Figure 4.9c) a basement high associated with bulging of thick sediment layers (~ 2.5s TWT) on top of it, suggesting the presence of a subsurface intrusive. The single channel seismic section (Figure 4.9d) across the plateau Pt1 shows that only a thin layer of the sediments (~ 0.4s TWT) exists on top of this ~ 20 km wide bathymetric and basement highs. This feature, located in the continental

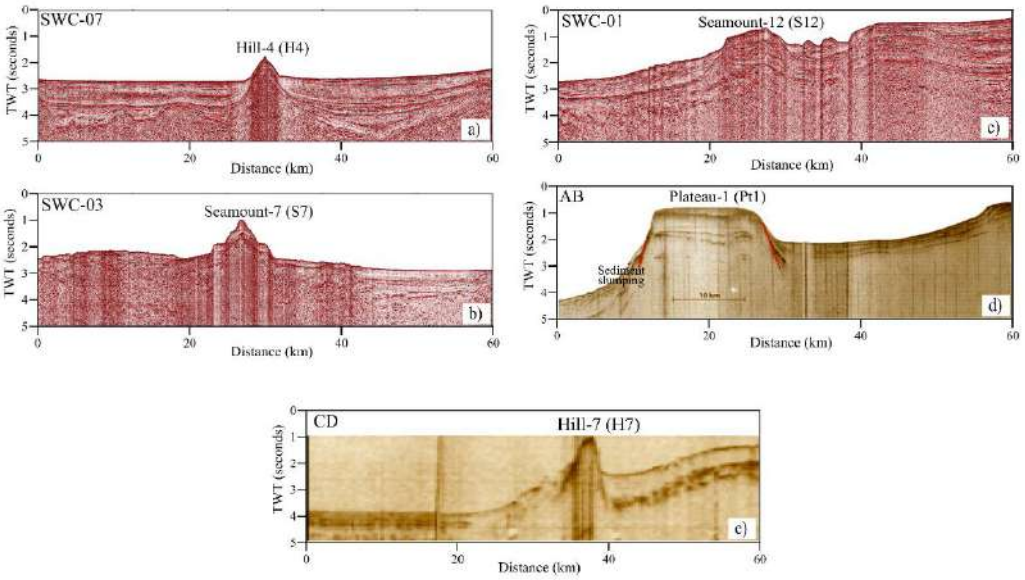

Figure 4.9: Seismic reflection sections across (a) Hill H4; (b) Seamount S7; (c) Seamount S12; (d) Plateau Pt1; and (e) Hill H7. Locations of these sections are given in Figure 4.2 as pink lines.

slope region, was earlier identified by Rao et al. (2010) and they reported that the lower half of the flanks is covered mostly by slump sediments. The hill H7 represents a bathymetric feature with steep flanks (Figure 4.9e), suggesting a volcanic extrusive. This feature represents the same bathymetric high identified by Yatheesh et al. (2013) in the Chain-Kairali Escarpment domain in the southwestern continental margin of India.

4.4 Gravity and magnetic signatures

The free-air gravity anomalies and magnetic anomalies of the selected representative bathymetric high features are presented in Figure 4.10 as colour-coded images, contours and profiles to analyze their characteristics. The free-air gravity anomalies corresponding to all the features (presented in Figure 4.10) are well-correlatable with the topography, with an observed maximum corresponding to their summit. These anomalies decrease along the flanks of the features and get superimposed on the gravity signature of the surrounding flat seafloor. The hill H1 is characterized by a broader gravity anomaly with its maximum (~ -25 mGal) over its summit (Figure 4.10a). The gravity anomaly at the summit of seamount S2 is ~-5 mGal and its base is defined by the -50 mGal contour (Figure 4.10b). The highest magnitude of free-air gravity anomaly, among all the features presented in Figure 4.10, is observed over the central part of plateau Pt3, reaching up to ~ 20 mGal, with a magnitude of ~ -70 mGal at the base of the feature (Figure 4.10c). The seamount S12 is described by free-air gravity anomalies of ~ -15 mGal for the summit and ~ -40 mGal for its base (Figure 4.10d). The hill H7 corresponds to a nearly N-S trending gravity high with free-air gravity anomaly magnitudes of ~ -15 mGal over the summit and ~ -35 mGal at the base (Figure 4.10e). The plateau Pt6 is represented as an E-W trending gravity high with ~ 5 mGal at summit and ~-30 mGal at its base (Figure 4.10f).

The northernmost region of Hill H1 is associated with an E-W trending negative magnetic anomaly with maximum intensity of -60 nT and the southernmost region of this feature is characterized by a N-S trending positive magnetic anomaly with a maximum intensity of 130 nT (Figure 4.10a). The seamount S2 is characterized by a relatively broader magnetic anomaly with two peaks, one located

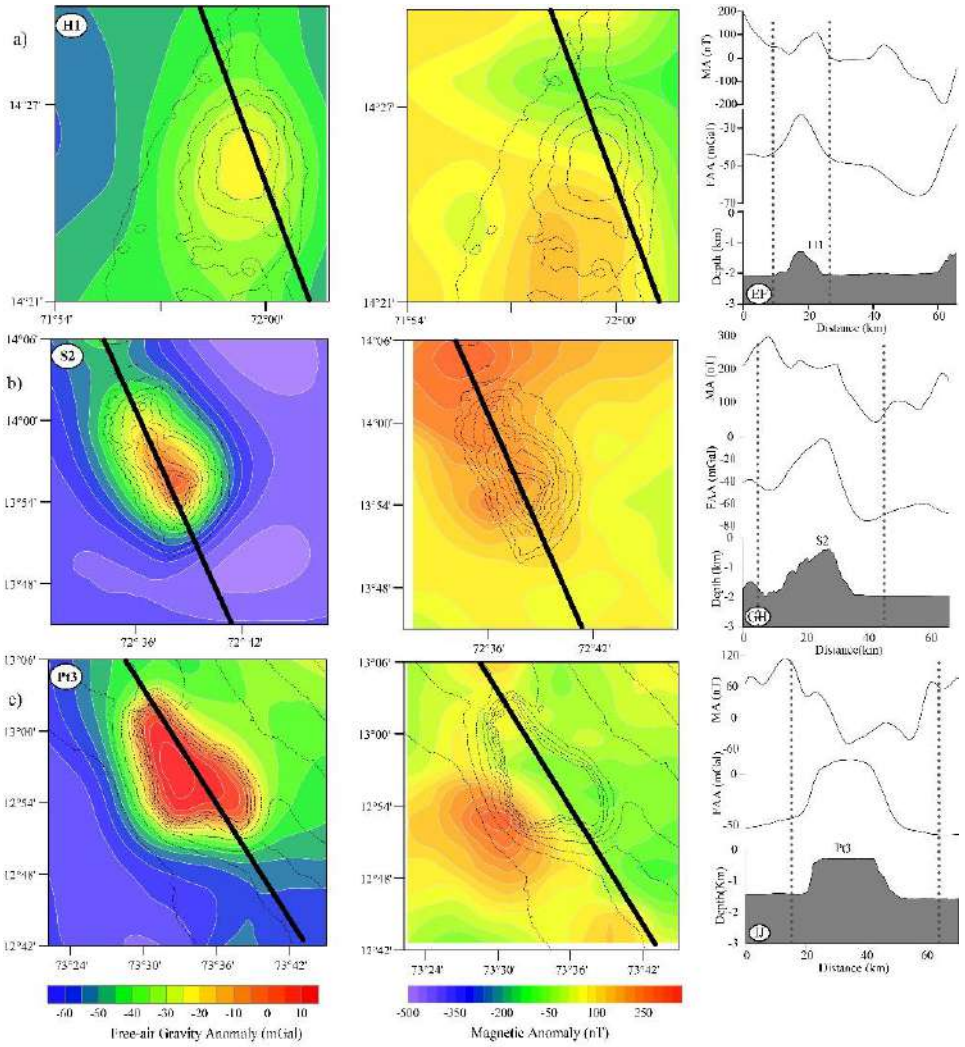

Figure 4.10: Colour-coded maps of the gravity and magnetic anomalies along with the stacked bathymetry, gravity and magnetic profiles across selected features (a) Hill H1; (b) Seamount S2; (c) Plateau Pt3; (d) Seamount S12; (e)Hill H7; (f) Plateau Pt6. The black contours represent the isobaths at 200 m interval, used to depict the extent of the bathymetric features. The white coloured lines on the gravity image represents gravity anomaly contours in 5 mGal interval and those in the magnetic image represents magnetic anomaly contours in 30nT interval. The locations of the stacked bathymetry, gravity and magnetic profiles segments within the grey dotted lines are shown as black thick lines in the colour-coded gravity and magnetic images.

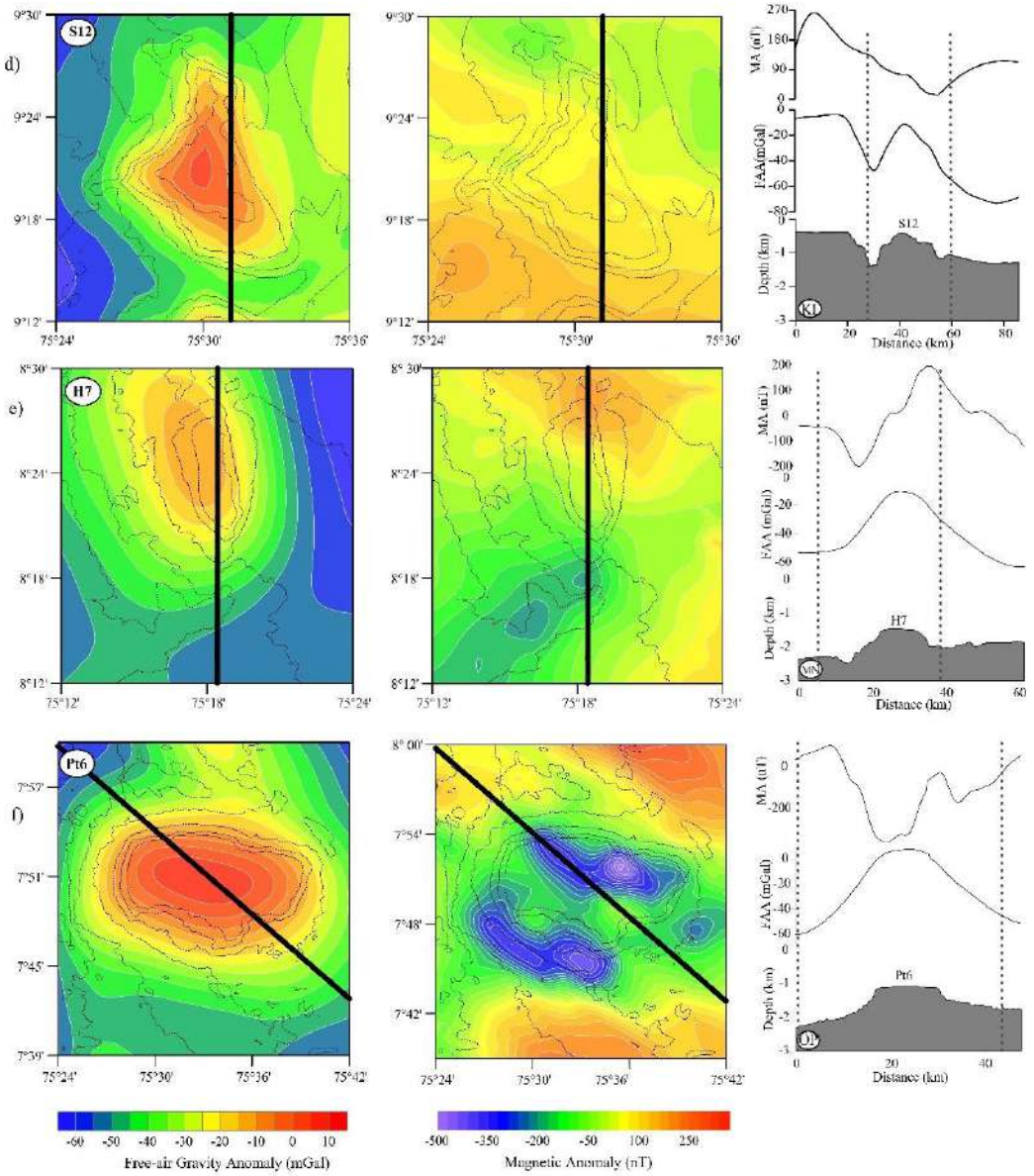

Figure 4.10contd.

closer to the northern flank and the other one located at the western flank of the seamount S2 (Figure 4.10b). The intensity of this magnetic anomaly, trending nearly NNW-SSE, gradually decreases towards southern and eastern flanks of the seamount with a sharp change in magnetic intensity from 90 nT to 60 nT from the base of the seamount to the adjacent flat seafloor. The magnetic anomaly over plateau Pt3 exhibits a nearly circular pattern (Figure 4.10c) with an observed maximum intensity corresponding to the foot of the western flank (~ 270 nT). The eastern part of the plateau Pt3 displays negative anomaly with an apparent intensity of ~ -30 nT, which gradually increases westward and northward from the summit

of the plateau. The seamount S12 exhibit a relatively flat signature of magnetic anomaly with an intensity of ~ 100 nT, with a gradual increase in intensity towards southwest and a decrease in intensity towards north in its southwestern and northern extremities, respectively (Figure 4.10d). The northernmost flank of the hill H7 coincides with a positive magnetic anomaly peak of ~ 170 nT, with a gradual decrease in intensity towards south (Figure 4.10e). The Plateau Pt6 is characterized by two negative magnetic anomalies, located on the northern and southern parts of the seamount, with intensities up to ~ -380 nT and ~ -440 nT, respectively (Figure 4.10f). The negative magnetic anomaly in the south coincides with the southern flank of the plateau, while those in the north are located on the northernmost region of the plateau summit. These two negative magnetic anomalies, trending nearly WNW-SSE, are divided by a zone of magnetic anomalies with maximum intensity of ~ -260 nT.

4.5 Probable genesis of bathymetric highs

The updated plate tectonic evolution model of the Arabian Sea (Bhattacharya and Yatheesh, 2015) suggests that the western continental margin of India was formed by the rifting and subsequent drifting among India, Seychelles and Madagascar, along with the adjacent microcontinental slivers of the Laxmi Ridge and the Laccadive Plateau. Among these, the first episode was separation of India-Laxmi Ridge-Seychelles block from Madagascar, believed to have been caused by the Marion hotspot. The evidence to this inference comes from the existence of ~ 85-92 Ma volcanics from the western side of India (Valsangkar et al., 1981; Radhakrishna et al., 1994, 1999; Torsvik et al., 2000; Anil Kumar et al., 2001; Pandey et al., 2001; Melluso et al., 2009; Radhakrishna and Joseph, 2012; Mohan et al., 2016) and the eastern side of Madagascar (Storey et al., 1995; Torsvik et al., 2000). The second episode was separation of Seychelles-Laxmi Ridge block from India, which is considered to have been initiated by oldest pulse of Réunion hotspot (at ~ 68.5 Ma) as evidenced from the existence of ~ 68.5 Ma old volcanics located north of the main Deccan Flood Basalt province (Basu et al., 1993). During this period, a break-up occurred also between the Laccadive Plateau and India. At around 65-66 Ma, the bulk of the Deccan Flood Basalt was emplaced on the Indian mainland with a large fraction of its activity during chron 29R (Courtillot et al., 1988), under the influence of the Réunion hotspot. Subsequently, the third episode

of the break-up between Seychelles and Laxmi Ridge-India block occurred shortly before 62.5 Ma, coinciding with the formation of Ghatkopar-Powai tholeiitic basalt (Pande et al., 2017) and emplacement of Raman-Panikkar-Wadia seamount chain in the Laxmi Basin (Bhattacharya and Yatheesh, 2015; Pande et al., 2017). Evidence to this comes from the oldest magnetic anomalies (chron 28ny) inferred from the conjugate Arabian and Eastern Somali basins (Miles and Roest, 1993; Chaubey et al., 2002b), formed by seafloor spreading along the Carlsberg Ridge. The spreading along the Carlsberg Ridge continued with the northward motion of Indian Plate over the Réunion hotspot and this motion caused the formation of the Laccadive-Chagos Ridge, which mainly consists of the Laccadive Plateau, Maldive Ridge and the Chagos Bank, along with the relatively deep saddle-like features.

The genesis of the bathymetric highs in the oceanic regions are generally explained in terms of hotspot activity, ridge-hotspot interaction, ridge parallel faulting, off-axis volcanism and propagating fracture, depending on the respective geological settings (Das et al., 2007 and references therein). The main geodynamic events occurred in the vicinity of the study area are the Marion and Réunion hotspots volcanism. Therefore, an attempt is made to provide a reasonable explanation for the genesis of the bathymetric highs in terms of hotspot volcanism. The bathymetric highs in the study area mainly falls in two domains, those located either in the continental slope of India or in the Laccadive Basin and the adjacent part of the Laccadive Plateau. The bathymetric features in the continental slope region are the plateaus Pt1, Pt2, Pt3, Pt4 and Pt6, hills H6 and H7, knoll K1, and seamount S12. The features, hills H6 and H7, seamount S12 and plateaus Pt4 and Pt6 are located over the Chain-Kairali Escarpment, which represents the western boundary of the thinned continental crust of the Alleppey-Trivandrum Terrace Complex (Figure 4.11). The Chain-Kairali Escarpment is interpreted (Yatheesh et al., 2013b) to represent the transform boundary formed due to the gliding between India and Madagascar during the initial stages of India-Madagascar separation, caused by the Marion hotspot volcanism. Therefore, it can be interpreted that the bathymetric features located in the relatively southern region of Alleppey-Trivandrum Terrace Complex were created by the Marion hotspot volcanism (e.g. H-7, showing the characteristics of an extrusive body in Figure 4.10e).

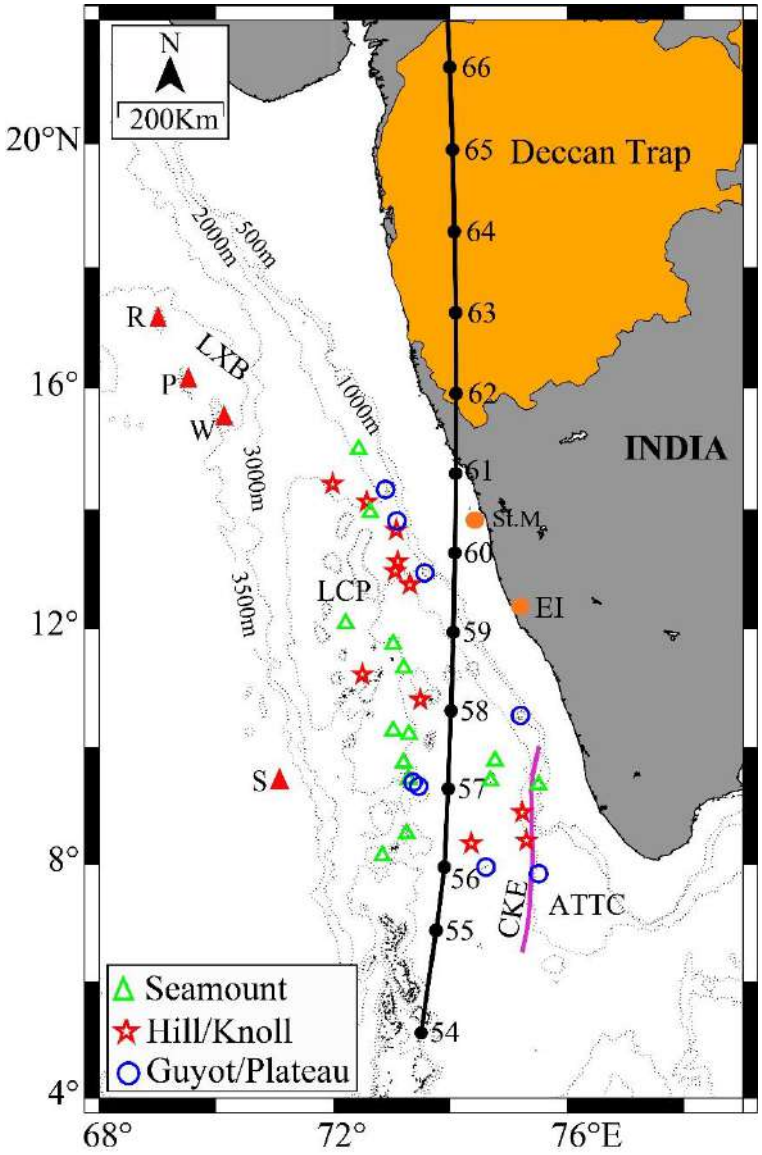

Figure 4.11: Generalized bathymetric map (GEBCO isobaths) of the study area showing locations and distribution of the bathymetric features identified in the present study. The thick black line connecting the black solid circles represents the Réunion hotspot track computed based on Müller et al. (1993). The numbers given to the solid black circles represent the ages in million years (Ma). R: Raman Seamount; P: Panikkar Seamount; W: Wadia Guyot; S: Sagar Kanya Seamount; LCP: Laccadive Plateau; CKE: Chain Kairali Escarpment; ATTC: Alleppey-Trivandrum Terrace Complex; LXB: Laxmi Basin; StM: St. Mary Islands; EI: Ezhimala Igneous Complex. Other details are as in Figure 4.1.

The plateaus Pt1, Pt2 and Pt3 and knoll K1 are located relatively north, and some of these features (plateaus Pt1 and Pt3) were interpreted by Rao et al. (2010) to represent continental slivers and horst structures formed during stretching and faulting along the southwestern continental margin of India, implying India-Madagascar break-up. However, it is reasonable to infer that these features located in the relatively northern part of the study area are very close to the Réunion hotspot (Figure 4.11) and therefore one can equally argue the genesis of these features to Réunion hotspot volcanism as well as India-Madagascar rifting, caused by the Marion hotspot volcanism. The Figure 4.11 also shows that the Réunion hotspot track is very close to the eastern part of the Laccadive Plateau and therefore, it is tempted to attribute the genesis of these bathymetric highs in the Laccadive Basin and the Laccadive Plateau to the Réunion hotspot. Since the effect of the hotspot can go over several hundreds of kilometres distance (Tolan et al., 1989; Storey et al., 1995), such an interpretation is reasonable even if the referred features in the Laccadive Basin are located not over the hotspot track exactly. This suggestion on the effect of hotspot to a larger area is also considered in the case of Sagar Kanya Seamount (Bhattacharya and Subrahmanyam, 1991) in the Arabian Sea. This seamount, which is inferred to have been formed by Réunion hotspot, is nearly 200 km away from the Réunion hotspot track.

4.6. Summary

A detailed geophysical investigation was carried out over the bathymetric high features in the Laccadive Basin and the adjacent areas to understand their distribution, morphometry, geophysical characteristics and probable genesis. The updated bathymetric map of the study area highlights identification of 33 bathymetric high features, consisting of 14 seamounts, 8 hills, 3 knolls, 2 guyots and 6 plateaus. Majority of these identified seamounts are located in the Laccadive Basin and the eastern sector of the Laccadive Plateau. Most of these seamounts are with single peak, but a few seamounts show multiple peaks. Morphometric analysis of these seamounts shows that height of the seamount increases roughly with increasing basal width. Morphology of the identified hills and knolls suggest a characteristic increase in basal width and slope angle against increasing height. Identified two adjacent guyots are located in relatively flat seafloor close to the eastern flank of the Laccadive Plateau. Most of the plateaus identified in the study

area are located in the western continental slope of India and they exhibit moderate to steep sloping flanks, showing gully pattern on both the flanks. Sub-seafloor configuration has been analyzed from the selected bathymetric features using seismic reflection sections. The inferred basement configurations suggest that some of the bathymetric features might represent volcanic extrusives while others might represent basement highs associated with bulging of sediment layers over the subsurface volcanic intrusive. The sea-surface gravity signatures of the selected features suggest a characteristic relatively high gravity anomaly superimposed over a regional negative anomaly. This relative gravity high corresponds to the summit area of the bathymetric high and this gravity anomaly reduces along its flanks. The magnetic anomalies over the bathymetric high features exhibits complex behaviour and it is difficult to correlate this only with the topography. Both negative and positive magnetic anomalies are observed over the features, superimposed over the regional magnetic signatures.

The study area is located very close to the southwestern continental margin of India, which was formed by the India-Seychelles-Madagascar break-up. The updated plate tectonic evolution model for the Arabian Sea suggests that the break-up between India and Madagascar occurred at ~ 90 Ma, believed to have been caused by the Marion hotspot, and then Seychelles-India break-up occurred at ~ 68.5 Ma, possibly caused by the earliest pulse of the Réunion hotspot (Bhattacharya and Yatheesh, 2015). Further, attempt is made to provide a reasonable answer for the genesis of the bathymetric high features in the study area, under the constraints of this tectonic setting. Majority of these features appears to have caused by the hotspot volcanism, however, at present it is not possible to conclude whether these bathymetric highs are related to the Marion hotspot volcanism or Réunion hotspot volcanism. Based on the proximity of this region to the St. Mary Islands and the Ezhimala Igneous Complex, which are considered to be a product of the Marion hotspot volcanism, it can be considered that the bathymetric highs located in the southwestern continental slope of India were formed by the Marion hotspot volcanism. But, the bathymetric features in the Laccadive Basin and eastern Laccadive Plateau are in the proximity of the Réunion hotspot track and therefore the genesis of these bathymetric features are attributed to the Réunion hotspot volcanism.

Table 4.1: Morphometric details of the bathymetric high features identified in the study area.

Feature	Centre Location (DD)	Depth (m)		Height (m) H	Length (km)		Width (km)		Area (sq.km)		H-W ratio (2H/Wb)	Flatness (Ws/Wb)	Average Slope along flanks in degrees	
		Summit	Basal		Summit	Basal	Summit (Ws)	Basal (Wb)	Summit	Basal			East	West
Seamount-1 (S1)	72.433°E, 15.001°N	464	1530	1066	5.26	11.54	1.74	6.65	9.15	76.74	0.321	0.262	8.4	13
Seamount-2 (S2)	72.629°E, 13.943°N	340	1880	1540	5.3	26.7	2.85	13.09	15.11	349.5	0.235	0.218	16.4	18.5
Seamount-3 (S3)	72.212°E, 12.087°N	440	1500	1060	3.82	8.73	0.97	6.1	3.71	53.25	0.348	0.159	11	17
Seamount-4 (S4)	73.022°E, 11.736°N	392	1890	1498	5.48	23.36	2.26	15.79	12.38	368.85	0.19	0.143	11	14
Seamount-5 (S5)	73.201°'E, 11.335°N	848	1940	1092	1.3	9.25	0.69	6.04	0.9	55.87	0.362	0.114	10	16
Seamount-6 (S6)	73.023°E, 10.271°N	540	1800	1260	8.4	16.38	2.37	7.43	19.91	121.7	0.339	0.319	14	15
Seamount-7 (S7)	73.294°E, 10.214°N	710	1825	1115	5.2	15.8	0.81	9.27	4.21	146.46	0.241	0.087	14	12
Seamount-8 (S8)	74.763°E, 9.762°N	1265	2310	1045	9.22	27.56	3.95	13.62	36.42	375.36	0.153	0.29	9	10
Seamount-9 (S9)	73.199°E, 9.732°N	300	1935	1635	15.27	40.2	2.35	10.38	35.88	417.27	0.315	0.226	13	19

Table 4.1contd.: Morphometric details of the bathymetric high features identified in the study area.

Feature	Centre Location (DD)	Depth (m)		Height (m) H	Length (km)		Width (km)		Area (sq.km)		H-W ratio (2H/Wb)	Flatness (Ws/Wb)	Average Slope along flanks in degrees	
		Summit	Basal		Summit	Basal	Summit (Ws)	Basal (Wb)	Summit	Basal			East	West
Seamount-10 (S10)	73.281°E, 9.452°N	895	2210	1315	11.87	34.2	2.73	10.48	32.41	358.41	0.251	0.26	13	17
Seamount-11 (S11)	74.684°E, 9.427°N	240	2500	2260	15.25	34.1	3.1	20.36	47.28	694.27	0.222	0.152	14	12.6
Seamount-12 (S12)	75.504°E, 9.357°N	410	1660	1250	14.34	28.4	3.6	14.05	51.62	399.02	0.178	0.256	10	7.7
Seamount-13 (S13)	73.255E, 8.531°N	208	2097	1889	6.8	40.2	2.48	22.5	16.86	904.5	0.168	0.11	14	17
Seamount-14 (S14)	72.836°E, 8.152°N	362	1790	1428	7.85	17.75	2.55	14.05	20.02	249.38	0.203	0.181	15	5
Hill-1 (H1)	71.985°E, 14.421°N	1290	2020	730	3.58	10.44	1.8	7.94	6.44	82.89	0.184	0.227	14	8.4
Hill-2 (H2)	72.572°E, 14.13°N	1271	1870	599	5.3	10.52	1.76	6.9	9.33	72.59	0.174	0.255	8.5	7.5
Hill-3 (H3)	73.057°E, 12.965°N	1491	1905	414	1.1	5.66	0.3	3.65	0.33	20.65	0.227	0.082	8	4.5
Hill-4 (H4)	73.308E, 12.740°N	1335	1889	554	1.23	14.83	0.28	4.48	0.34	66.44	0.247	0.063	10	11

Table 4.1contd.: Morphometric details of the bathymetric high features identified in the study area.														
Feature	Centre Location (DD)	Depth (m)		Height (m) H	Length (km)		Width (km)		Area (sq.km)		H-W ratio (2H/Wb)	Flatness (Ws/Wb)	Average Slope along flanks in degrees	
		Summit	Basal		Summit	Basal	Summit (Ws)	Basal (Wb)	Summit	Basal			East	West
Hill-5 (H5)	72.495°E, 11.225°	1010	1760	750	11.2	21.2	7.31	12.5	81.87	265	0.12	0.585	12	10
Hill-6 (H6)	75.229°E, 8.888°N	1500	1910	410	7.96	12.5	3.33	5.04	26.51	63	0.163	0.661	4	8
Hill-7 (H7)	75.301°E, 8.405°N	1505	2010	505	10.1	18.5	1.5	6.7	151.5	123.95	0.151	0.224	7.7	4.1
Hill-8 (H8)	74.355°E, 8.360°N	2540	2750	210	10.42	23.5	6.29	14.92	65.54	350.62	0.028	0.422	3	2
Knoll-1 (K1)	73.074°E, 13.654°N	490	1430	940	1.7	6.5	0.7	5.1	1.19	33.15	0.368	0.137	19	10
Knoll-2 (K2)	73.098°E, 13.126°N	1508	1820	312	2.6	6.1	1.7	4.13	4.42	25.19	0.151	0.412	8.5	7.5
Knoll-3 (K3)	73.485°E, 10.800°N	810	1740	930	2.02	10.7	0.55	9.35	1.11	100.05	0.199	0.059	8.5	10.5
Guyot-1 (G1)	73.364°E, 9.401°N	720	1810	1090	2.5	9.41	3.38	10.25	8.45	96.45	0.213	0.33	15	11.5
Guyot-2 (G2)	73.462°E, 9.332°N	525	1870	1345	11.2	21.6	7.82	15.32	87.58	330.91	0.176	0.51	11.2	16

Table 4.1contd.: Morphometric details of the bathymetric high features identified in the study area.

Feature	Centre Location (DD)	Depth (m)		Height (m) H	Length (km)		Width (km)		Area (sq.km)		H-W ratio (2H/Wb)	Flatness (Ws/Wb)	Average Slope along flanks in degrees	
		Summit	Basal		Summit	Basal	Summit (Ws)	Basal (Wb)	Summit	Basal			East	West
Plateau-1 (Pt1)	72.893°E, 14.331°N	325	920	595	35.4	54.3	13.5	21.6	477.9	1172.8	0.055	0.625	5.5	6.5
Plateau-2 (Pt2)	73.088°E, 13.811°N	376	1110	734	11.6	19	3.6	6.5	41.76	123.5	0.226	0.553	14.9	10.3
Plateau-3 (Pt3)	73.563°E, 12.938°N	265	1040	775	20	31.3	7.48	17.68	149.6	553.38	0.161	0.423	12	11.3
Plateau-4 (Pt4)	75.202°E, 10.537°N	370	746	376	11.65	18	6.9	13.9	80.39	250.2	0.054	0.496	12.6	11.8
Plateau-5 (Pt5)	74.609°E, 7.955°N	1888	2720	832	13.4	32.6	4.91	13.64	65.79	444.66	0.122	0.36	13.5	9.5
Plateau-6 (Pt6)	75.511°E, 7.844°N	1080	1670	590	7.1	21.3	17	32.7	120.7	696.51	0.036	0.52	6.5	7.7

Chapter 5

Morphotectonic signatures and evaluation of postulated continental nature of the Laccadive Plateau

5.1 Introduction

The Laccadive-Chagos Ridge (Figure 5.1) is a slightly arcuate aseismic ridge in the Indian Ocean, extending for about 2500 km between 12°S and 14°N. This prominent tectonic feature has been divided into three segments – the Laccadive Plateau (the northernmost segment), the Maldive Ridge (the middle segment) and the Chagos Bank (the southernmost segment), separated by deep saddle-like features (Bhattacharya and Chaubey, 2001). Different views exist for genesis of the Laccadive-Chagos Ridge as a whole, consisting of leaky transform fault (Fisher et al., 1971; Sclater and Fisher, 1974), hotspot trail (Francis and Shor, 1966; Whitmarsh, 1974; Morgan, 1981; Duncan, 1981, 1990; Ashalatha et al., 1991), composite structural elements of various origin (Avraham and Bunce, 1977; Sreejith et al., 2019), and crack propagation (Sheth, 2005). Among these, the hotspot origin hypothesis, which was formulated mainly based on the linear geometry of the feature and its north-to-south age progression records, has got broader acceptance for the genesis of the Laccadive-Chagos Ridge as a whole. However, several subsequent studies pointed out the possibility of considering the northernmost segment of the Laccadive-Chagos Ridge, i.e., the Laccadive Plateau, as continental in nature. The main observations considered to propose this inference are the velocity-depth structure and the estimated crustal thickness (Naini, 1980; Naini and Talwani, 1982; Torsvik et al., 2013), rotated fault blocks that are generally associated with regions undergoing crustal extension (Murty et al., 1999), presence of a rift system referred to as the Cannanore Rift System consisting of block-faulted basement with a system of grabens, half grabens and single normal faults (Bhattacharya and Yatheesh, 2015; DGH, 2019; Yatheesh, 2020), presence of Seaward Dipping Reflectors (SDRs) representing a continent-ocean boundary west of the Laccadive Plateau (Ajay et al., 2010), crustal configuration derived from forward modelling of gravity / magnetic profiles (Chaubey et al., 2002; Ajay et al., 2010; Nair et al., 2013; Anand et al., 2014; Mishra et al., 2020), and the effective elastic thickness estimated using gravity and bathymetry data (Chaubey et al., 2008;

Sreejith et al., 2019; Mishra et al., 2020). Further, the close-fit India-Madagascar juxtaposition model proposed by Yatheesh et al. (2006) depicted the existence of a wide gap between southern part of India and Madagascar, and demonstrated the

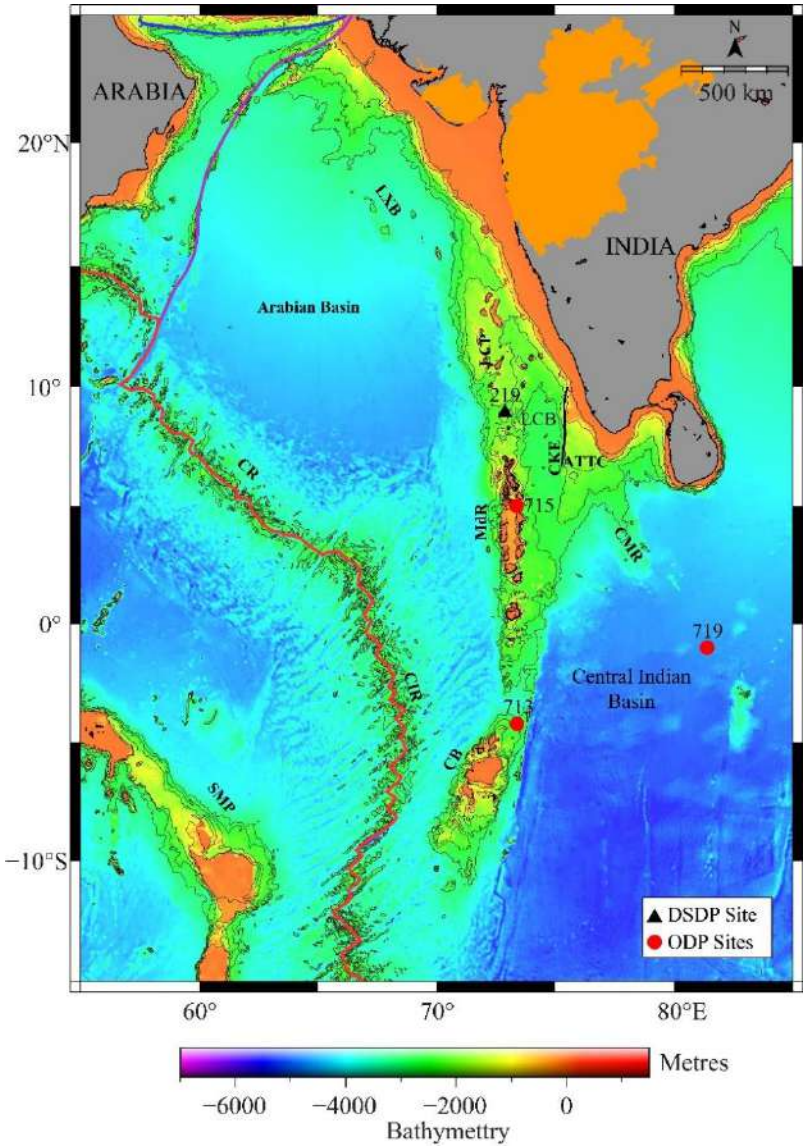

Figure 5.1: Generalized tectonic map of the western continental margin of India and the adjoining deep offshore regions, including the Laccadive-Chagos Ridge, along with global bathymetric grid of GEBCO_2020 in the background. LCP: Laccadive Plateau; MdR: Maldive Ridge; CB: Chagos Bank; CKE: Chain Kairali Escarpment; ATTC: Alleppey-Trivandrum Terrace Complex; LXB: Laxmi Basin; SMP: Seychelles-Mascarene Plateau; CR: Carlsberg Ridge; CIR: Central Indian Ridge; CMR: Comorin Ridge; LCB:Laccadive Basin.

possible accommodation of the Laccadive Plateau in the gap available between the conjugate reconstructed 2000 m bathymetric contours (Figure 5.2). However, several other studies dealing specifically with the Laccadive-Chagos Ridge (Verzhbitsky, 2003; Gupta et al., 2010) and those dealing with plate tectonic reconstruction of the Western Indian Ocean (Seton et al., 2012; Gibbons et al., 2013; Reeves et al., 2016; Siawal et al., 2019) continued to consider the hotspot origin for the entire Laccadive-Chagos Ridge, including the Laccadive Plateau, despite the proposition since 1980s to consider at least the Laccadive Plateau to have underlain by continental crust.

Bhattacharya and Yatheesh (2015) critically examined all the information available about the postulated microcontinents in the Western Indian Ocean, including the Laccadive Plateau, and accommodated them in their revised plate tectonic evolution model for the early opening of the Arabian Sea (Figure 5.2).

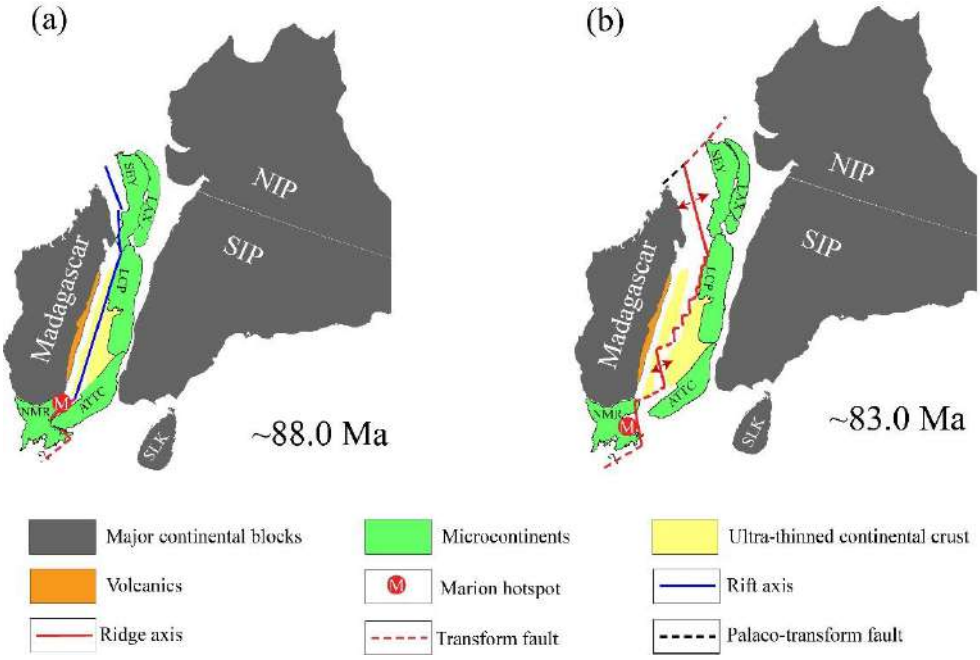

Figure 5.2: Revised plate tectonic reconstruction maps of the Western Indian Ocean at (a) ~ 88.0 Ma; (b) ~ 83.0 Ma (modified after Yatheesh, 2020), in fixed Madagascar reference frame. SIP: Southern Indian Protocontinent; NIP: Northern Indian Protocontinent; SEY: Seychelles Plateau; LAX: Laxmi Ridge; LCP: Laccadive Plateau; ATTC: Alleppey-Trivandrum Terrace Complex; NMR: Northern Madagascar Ridge; SLK: Sri Lanka

Although this reconstruction model strongly suggests the existence of these microcontinents, their crustal structure is yet to be confidently established. A careful analysis of the studies, which postulated the continental origin of the Laccadive Plateau, reveal that most of those studies have drawn their interpretation based on their stand-alone observations. Therefore, in the present study, an attempt is made to understand the morphotectonic signatures of the Laccadive Plateau and to evaluate its postulated continental nature based on an integrated analysis of multibeam bathymetry, seismic reflection and sea-surface gravity and magnetic data (Figure 5.3), complemented by the various geophysical observations used to propose the continental nature of the Laccadive Plateau.

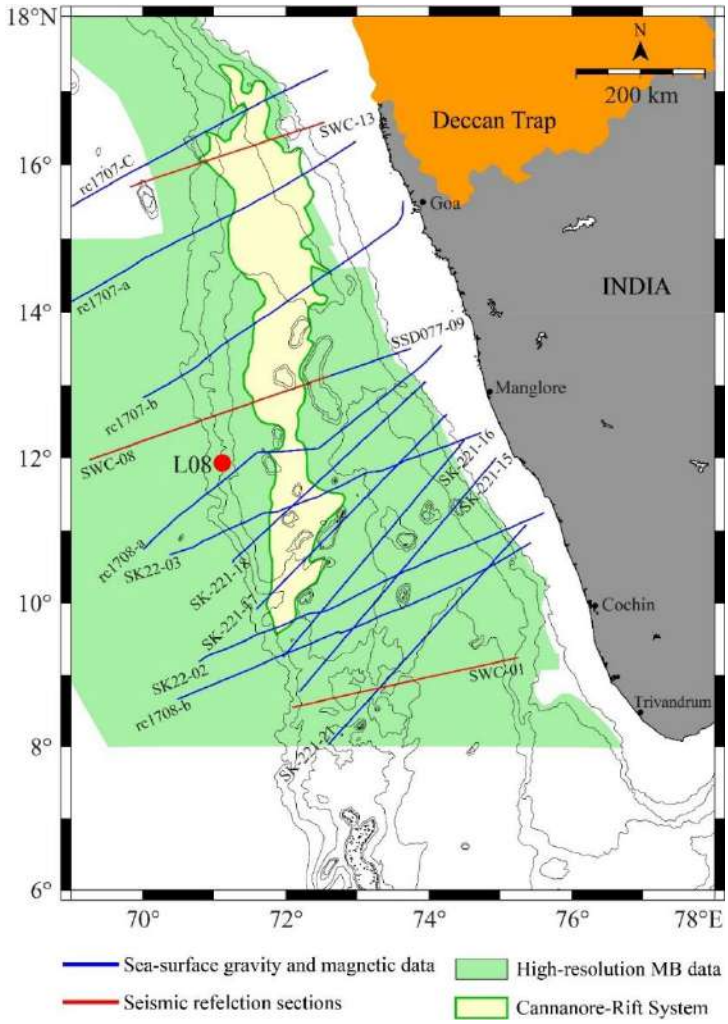

Figure 5.3: Map showing locations of sea-surface gravity, magnetic, and bathymetry profiles and seismic sections used in the present study. Black lines indicate the isobaths. Red circle represent the location of seismic refraction station.

5.2 Geophysical signatures of the Laccadive Plateau

5.2.1 Seafloor topography

The high-resolution bathymetric map of the Laccadive Plateau and the adjacent regions have been presented in the Figure 5.4. The Laccadive Plateau, which extends in N-S direction (along ~ 73°E) from ~ 8°N to ~ 17°N, exhibits an irregular topography. Several islands and banks are present between 8°N and 14°N over the crestal part and eastern flanks of the Laccadive Plateau. Among these, the slightly arcuate and nearly N-S trending Padua Bank represents the largest bank. The western flank of the Laccadive Plateau is steeper, while its eastern flank is gentle. The bathymetric map further suggests the presence of several isolated bathymetric highs over the central, eastern and western side of the Laccadive Plateau. There are several scour/depression like features observed in the central part of the Laccadive Plateau. The Laccadive Plateau is characterised by numerous westward dipping channels, which are observed prominently in its southern region. Two nearly parallel and E-W trending channels (along ~ 8.2°N and ~ 9°N latitudes), connecting the Laccadive Basin in the east and Arabian Basin in the west, are clearly distinguishable from the bathymetry map.

5.2.2 Basement topography

Three multichannel seismic reflection sections, SWC-01, SWC-08 and SWC-13, have been used to depict the basement configuration of the Laccadive Plateau and the adjoining Arabian Basin in the west and the Laccadive Basin in the east (Figure 5.5). These selected seismic sections, along SWC-01, SWC-08 and SWC-13, cut across the Laccadive Plateau in the southern, middle and northern parts, respectively. The SWC-08 spans through the Arabian Basin, Laccadive Plateau and the Laccadive Basin, showing four isolated highs situating over the Laccadive Plateau. The basement of the crestal region of the Laccadive Plateau, existing west of the Padua Bank, is characterized by the presence of a zone of disturbed basement consisting of block-faulting, coinciding with the Cannanore Rift System. Similar disturbed zone of basement is also seen along profile SWC-13, supporting the northward extension of the Cannanore Rift System at least up to ~ 16°N, in the triangular shaped region defined by 2000 m and 2500 m. isobaths immediately north of the Laccadive Plateau (defined by 2000 m. isobath).

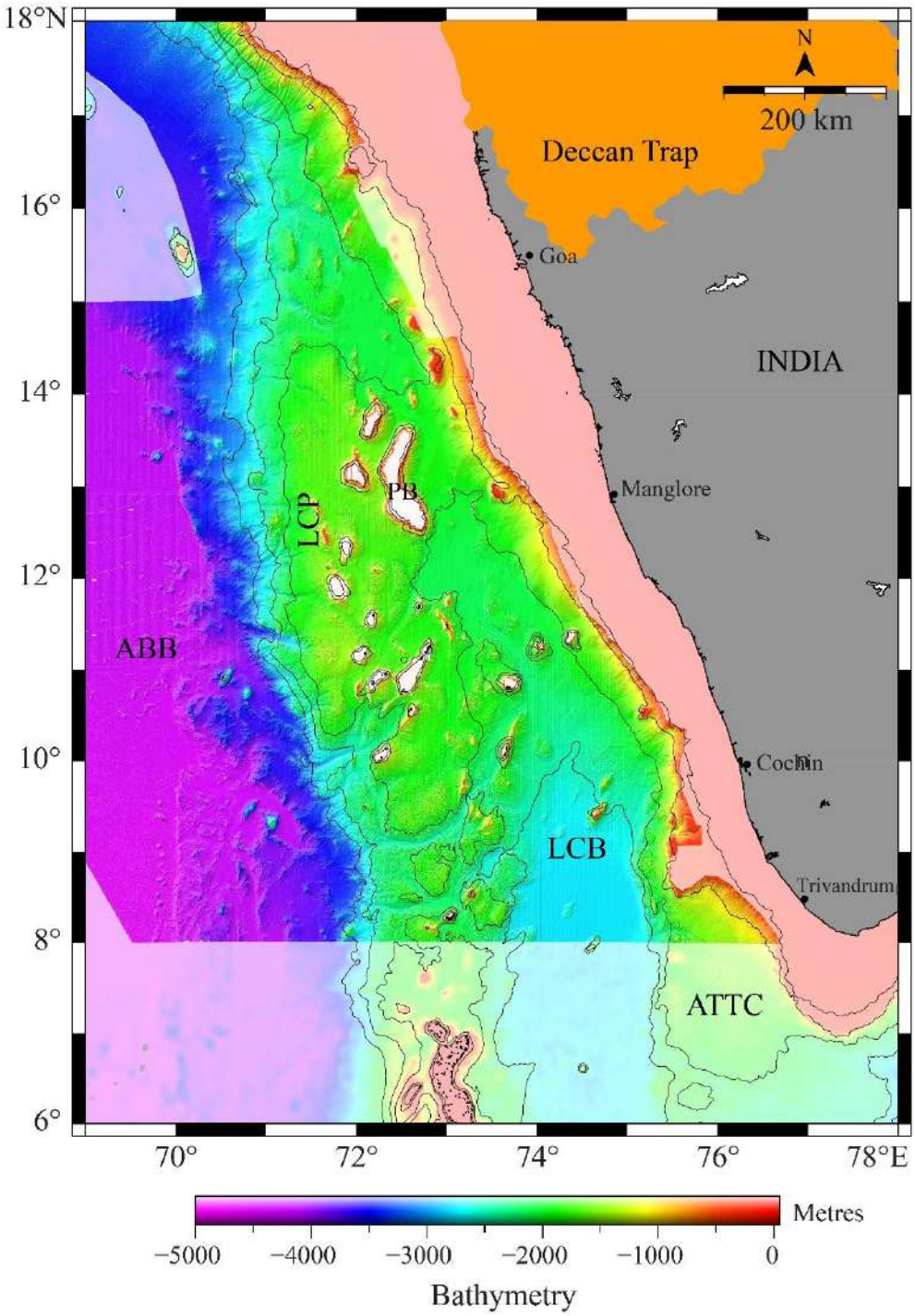

Figure 5.4: High-resolution bathymetric map of the southwestern continental margin of India prepared using multibeam bathymetry data, presented along with the GEBCO 2020 grid in the background. ABB: Arabian Basin; LCB: Laccadive Basin; PB: Padua Bank. Other details are as in Figure 5.1 and 5.3.

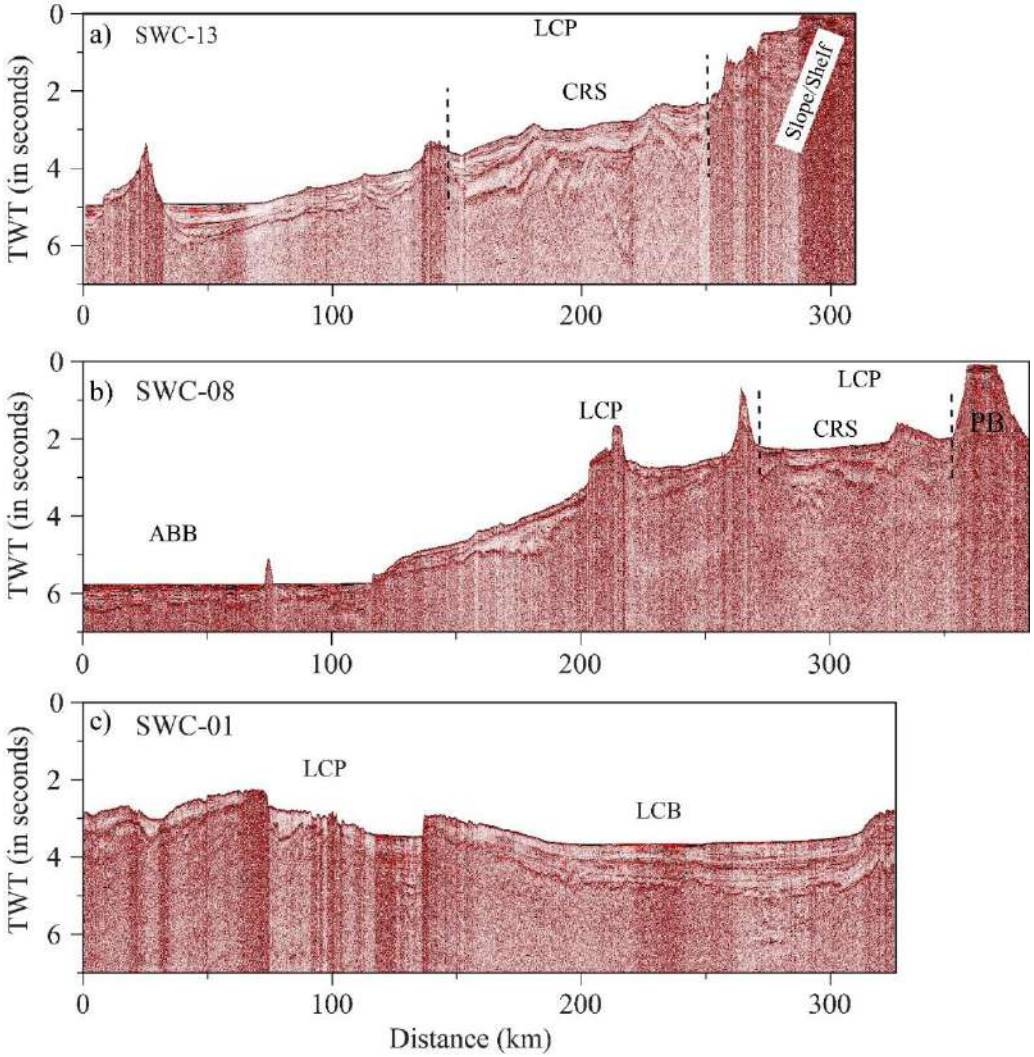

Figure 5.5: Seismic reflection sections along the profiles (a) SWC-13, (b) SWC-08 and (c) SWC-01. Locations of these sections are given in figure 5.2. LCP: Laccadive Plateau; LCB: Laccadive Basin; CRS: Cannanore-Rift System; ABB: Arabian Basin; PB: Padua Bank.

The westernmost part of the SWC-13 shows the presence of a basement/seafloor high representing the northward extension of the Wadia Guyot, and the basement/seafloor high in the eastern part of the seismic section represents the Angria Bank. The seismic section along the profile SWC-01 spans through the Arabian Basin, Laccadive Plateau and the Laccadive Basin, where the sharp vertical cuttings in the seafloor as seen from this seismic section represents breaches in the seafloor. There is no indication suggesting the presence of disturbed block-faulted basement zone representing Cannanore Rift System along this profile. Further east,

the Laccadive Basin is associated with relatively smoother basement and seafloor topography, with a distinct basement/seafloor high located over the Chain-Kairali Escarpment.

5.2.3 Gravity and magnetic signatures

The sea-surface gravity anomalies associated with the Laccadive Plateau and the adjacent regions have been presented as track-along wiggles overlain on the satellite-derived free-air gravity anomaly image (Figure 5.6) to understand the gravity signatures associated with these regions. The continental shelf region is associated with a linear belt of prominent gravity high anomaly, bounded in the west by the shelf break. The Laccadive Basin, in general, is associated with negative regional free-air gravity anomalies, with superimposed relative positive and negative residual anomalies. The Laccadive Plateau is associated with a belt of relatively positive anomalies bounded by relatively negative anomalies associated with the Laccadive Basin and the Arabian Basin in the east and west, respectively. Some of these relatively positive and high-amplitude free-air gravity anomalies are characterized by their correspondence with isolated bathymetry highs while others have no correspondence with the seafloor features.

The sea-surface magnetic anomalies associated with the Laccadive Plateau and the adjacent regions have been presented as track-along wiggles (Figure 5.7) to understand the magnetic signatures associated with these regions. The magnetic anomaly map shows that the continental shelf of India is associated with high-amplitude magnetic anomalies, coinciding with the location of the observed linear belt of prominent gravity high anomalies. The Laccadive Basin is associated with relatively low amplitude magnetic anomalies correlatable from profile-to-profile. The Laccadive Plateau is associated with broad wavelength and high amplitude magnetic anomalies with superimposed secondary high-frequency magnetic anomalies at places. Most of these high-amplitude magnetic anomalies observed over the Laccadive Plateau region are correlatable with the gravity and bathymetric signatures.

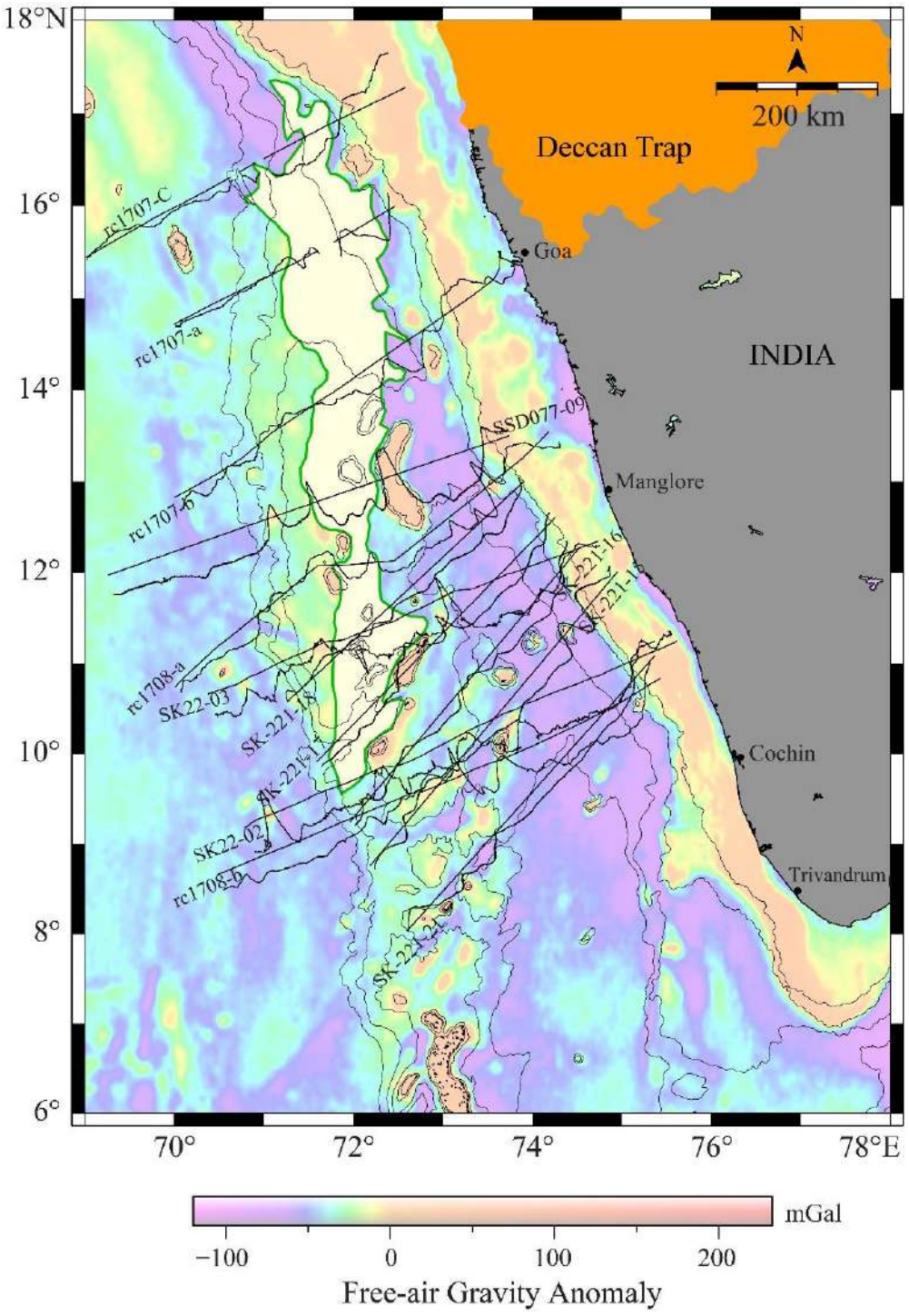

Figure 5.6: Satellite-derived free-air gravity anomaly map with sea-surface gravity anomaly data plotted perpendicular to the track over the Laccadive Plateau and adjacent regions. Other details are as in Figure 5.3.

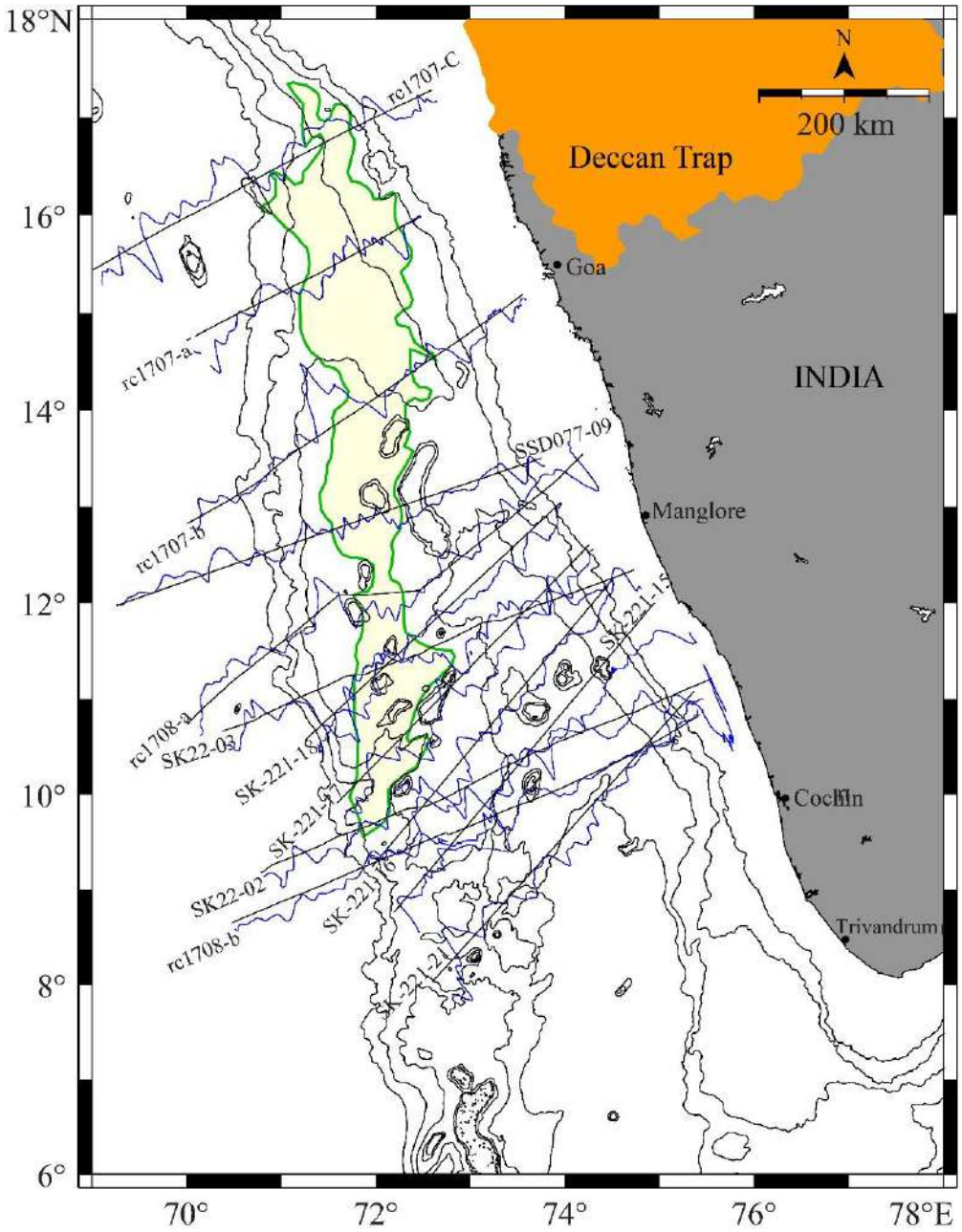

Figure 5.7: Sea-surface magnetic anomaly data plotted perpendicular to the track over the Laccadive Plateau and adjacent regions. Other details are as in Figure 5.3.

5.3 Crustal configuration of the Laccadive Plateau and the adjoining regions

The crustal configuration of the Laccadive Plateau and the adjoining regions has been derived based on integrated forward modelling of the gravity and magnetic anomalies, constrained by the seismic and geological information. For this purpose, a representative gravity and magnetic profile SSD077-09 that cut across the Arabian Basin, Laccadive Plateau, and the western continental shelf/slope of India have been selected (Figure 5.2). To start with, an initial crustal model has been generated using the various constraints available from this region (Table 5.1). The seafloor has been constrained using the shipborne multibeam bathymetry data used in the present study. The sea-surface gravity-magnetic profile SSD077-09 coincides with the seismic profile SWC-08, and therefore the sediment thickness and depth to the basement information in the model has been constrained from those available from seismic section along the profile SWC-08. The velocity-depth information corresponding to the deeper layers over the Arabian Basin and the Laccadive Plateau were obtained from the velocity-depth information derived from sonobuoy seismic refraction stations (Naini, 1980; Naini and Talwani, 1982). For the shelf-slope region, the velocity-depth information for the deeper layers have been constrained from those available (Kaila and Bhatia, 1981) from Deep Seismic Sounding studies from southern part of India. As will be shown later, the Laccadive Plateau and the continental shelf-slope regions are characterized by the presence of a volcanic flow layer in shallower region and a high velocity underplated layer in deeper region as evidenced from seismic refraction results. The constraints for these layers also have been obtained from the velocity-depth information derived from sonobuoy seismic refraction stations (Naini, 1980; Naini and Talwani, 1982). The velocity information constrained for each layer has been converted to the corresponding density using the velocity-density relationship of Brocher (2005). Keeping these density values, bathymetry and basement constraints unchanged, and by slightly changing the Moho depth and thickness of the deep layers, the model is refined to get a reasonably good fit between observed and computed gravity anomalies. Having obtained a reasonably good fit of gravity anomalies, attempt has been made to derive the magnetic structure of the crust underlying this region by accommodating the magnetic source bodies in the crustal model derived based on

forward modelling of gravity data. The forward modelling of magnetic anomalies has been performed based on Talwani and Heirtzler (1964) considering presence of volcanic intrusives in light of the tectonic framework of this region. Since genesis of these volcanic intrusives are assumed to have caused by Réunion hotspot volcanism, the published (Radhakrishna and Joseph, 2012) information of magnetic parameters representing Réunion hotspot related volcanics derived from paleomagnetic data have been adopted while carrying out magnetic modelling. Further, the extents of the magnetic bodies were refined to get a reasonably good fit between the observed and computed magnetic anomalies.

Table 5.1: Details of the velocity-density information used for the integrated forward modelling of gravity-magnetic profiles

Layer	ABB		LCP		Shelf/Slope	
	Velocity (km/s)	Density (g/cc)	Velocity (km/s)	Density (g/cc)	Velocity (km/s)	Density (g/cc)
Water	1.5	1.03	1.5	1.05	1.5	1.05
Sediments	3.00	2.20	3.00	2.20	3.00	2.00
Volcanic flow	-	-	4.4	2.45	-	-
Upper Crust	5.77	2.68	5.4	2.6	6	2.71
Lower Crust	6.4	2.88	6.3	2.78	6.5	2.82
Underplating	-	-	7.25	3.02	7.25	3.02
Mantle	8.10	3.3	8.10	3.3	8.1	3.3

The derived crustal model (Figure 5.8) suggests that the Arabian Basin consists of ~ 6 km thick two-layered (layer-2 with density 2.68 g/cc and layer-3 with 2.88 g/cc) oceanic crust buried under the sediments with density 2.20 g/cc. The continental shelf/slope region is underlain by two-layered (upper crust with density 2.71 g/cc and lower crust with 2.82 g/cc) continental crust, with an underlying high-density (3.02 g/cc) layer of underplating. The derived crustal model further suggests that the Laccadive Plateau can be reasonably explained in terms of two-layered continental crust (consisting of upper crust with density 2.60 g/cc and lower crust with density 2.78 g/cc) intermingled with volcanic intrusives (with density 2.88

g/cc). In the continental shelf/slope region, Moho is at a depth of ~ 21 km, suggesting a crustal thickness of about 18-19 km.

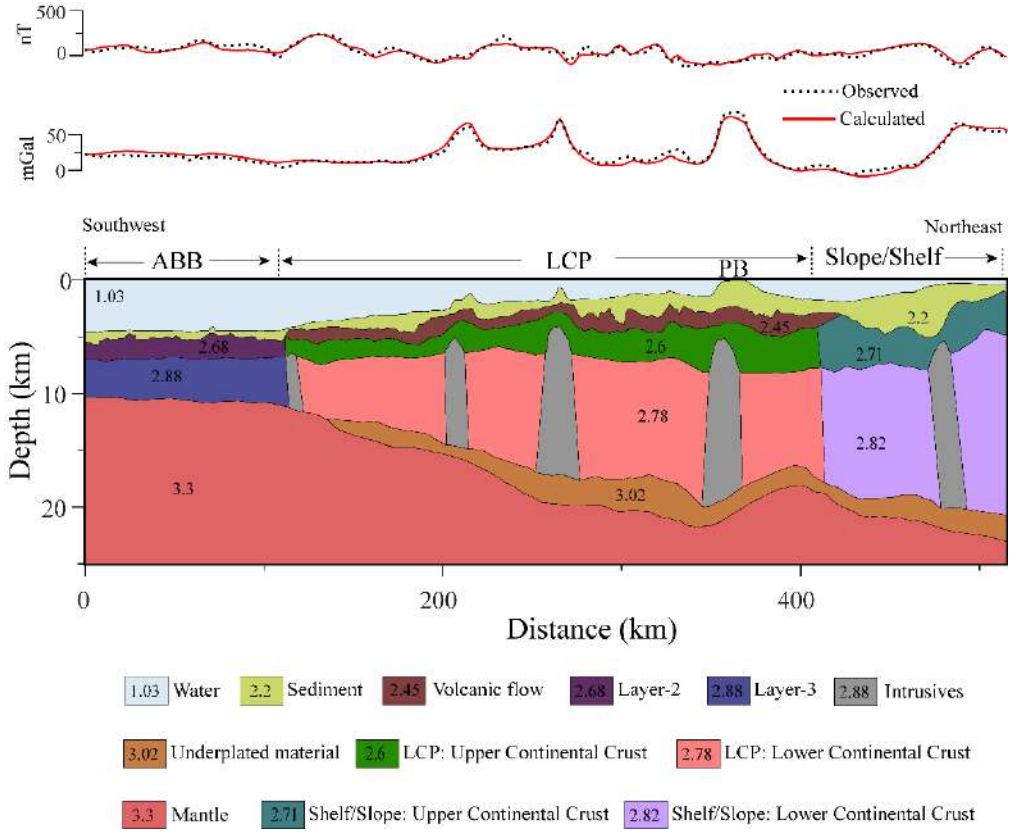

Figure 5.8: Crustal model derived based on integrated forward modelling of gravity and magnetic anomalies along the profile SSD077-09, the location of which is shown in figure 5.3. The decimal numbers given in each layers of the model represent density in g/cc. Other details are as in Figures 5.1 and 5.3. PB: Padua Bank. Magnetic anomalies are modelled with two-dimensional magnetic bodies of intrusive dykes and sills (For normally magnetized blocks: Remnant Inclination = -53.68°, Remnant Declination =328.66°; For reversely magnetized blocks: Remnant Inclination = 51.78°, Remnant Declination =154.5°).

Towards west, the Moho gradually shallows down and reaches to a level of ~ 11 km at the western extent of the Laccadive Plateau. However, there exists a deepening of Moho in a limited extent of the Laccadive Plateau under the Padua Bank, resulting a crustal thickness of ~ 20 km under the Padua Bank. Therefore, the crustal thickness underlying the Laccadive Plateau ranges between ~ 20 km in the

eastern side to ~ 11 km in the western side, suggesting a gradual crustal thinning from its easternmost extent to the western most extent along the modelled profile SSD077-09. The derived crustal model also suggests the existence of a high-density underplated layer sandwiched between the lower continental crust and mantle under the continental shelf/slope as well as the entire extent of the Laccadive Plateau. The presence of a high velocity/density layer of underplated material below the Indian mainland was recently reported by Saikia et al. (2017) and therefore consideration of an underplated layer in the thinned continental crust of these regions of India appears to be reasonable. The derived crustal model further depicts the presence of a layer of volcanic flow with a density of 2.45 g/cc sandwiched between the sediment layer and the upper crust, extending through the entire extent of the Laccadive Plateau. The postulated offshore extension of the Deccan flood basalt in the northwestern continental margin of India (Kumar and Chaubey, 2019) as evidenced from the seismic refraction results and the drill well information supports the interpretation of presence of volcanic flows in the Laccadive Plateau region. Therefore, the nature of the crust underlying the Laccadive Plateau can reasonably be interpreted as thinned continental crust intermingled with volcanic intrusives.

5.4 Discussion on nature of the crust underlying the Laccadive Plateau – continental vs hotspot genesis

The integrated forward modelling of the gravity and magnetic anomalies, constrained by the seismic and geological information suggests that the Laccadive Plateau can surely be explained in terms of thinned continental crust intermingled with volcanic intrusives. Such an inference is compatible with the tectonic framework of the Arabian Sea since the Réunion hotspot volcanism has imprinted several volcanic intrusives as well as volcanic flows in the western part of India and its conjugate regions of Seychelles (Courtlllot et al., 1986; Vandamme et al., 1991; Plummer and Belle, 1995; Hooper, 1999; Sen, 2001, Pande et al., 2007; Ganerod et al., 2011; Shellnut et al., 2017).

The main point that was considered as the evidence of hotspot origin for the entire Laccadive-Chagos Ridge was the north-to-south age progression (Whitmarsh, 1974; Morgan, 1981; Duncan, 1981, 1990), which was inferred from the basement age determinations at the DSDP site 219 and ODP sites 713 and 715

(Figure 5.1). Out of these three sites, the basement ages for sites 713 and 715 are radiometric ages of the basement basalts (Duncan and Hargraves, 1990) and for site 219, it is an estimate from the biostratigraphic age (Whitmarsh et al., 1974) of the oldest sediment overlying the basement. Even though the radiometric ages for sites 713 and 715 were qualified as imprecise by a later study (Baksi, 2005), still the ages of the three sites together do appear to suggest a pattern of increasing age of basement northward along the Laccadive-Chagos Ridge. However, it is important to note that the inferred age progression do not rule out the possibility that the Laccadive Plateau is underlain by continental crust. There are two reasons for believing so, the first one is that none of three sites are located over the Laccadive Plateau and the second one is that mere existence of age progression volcanics along parts of Laccadive-Chagos Ridge do not indicate anything unequivocal about the nature of the country rock, because the volcanics along the trail of a hotspot are expected to show evidence of age progression, irrespective of whether those volcanics are intrusives / extrusives over continental blocks or are manifested as volcanic islands in the oceanic areas.

Existence of rotated basement fault blocks and graben structures, which are characteristic of stretched continental crust, were reported in several areas of the Laccadive Plateau. Based on the analysis of seismic reflection data, Murty et al. (1999) reported the presence of clearly identifiable rotated fault blocks on either side of the Padua Bank, which represents a shallow carbonate bank atop the northern part of the Laccadive Plateau. Such a basement configuration is clearly identifiable from the published multichannel seismic reflection section along SK12-07 (Chaubey et al., 2002b), WC2K2-06 (DGH, 2018), and SWC-08 and SWC-13 (present study). Since such basement configurations are characteristic of stretched continental crust, the Padua Bank and its vicinity surely represents a stretched continental crust overlain by basaltic rocks. If the Laccadive Plateau is a continental block, then the western limit of the Laccadive Plateau should represent the continent ocean boundary between the Laccadive Plateau and the oceanic crust of the Arabian Basin. Interestingly, the presence of Seaward Dipping Reflectors (SDRs) have been identified by Ajay et al. (2010) from this region, corroborating the proposed continental origin for the Laccadive Plateau. The intermediate crustal thickness inferred based on seismic refraction studies (Naini, 1980; Babenko et al., 1981;

Naini and Talwani, 1982) and forward modelling of gravity / magnetic anomalies (Chaubey et al., 2002b; Ajay et al., 2010; Nair et al., 2013; Anand et al., 2014; Mishra et al., 2020) also is in agreement with crustal thickness usually seen in the continental crust that has undergone crustal thinning processes.

5.5 Summary

A detailed geophysical investigation was carried out over the Laccadive Plateau to understand its morphotectonic signatures and evaluate the postulated continental nature of the Laccadive Plateau, using an up-to-date compilation of the available geophysical data. The high-resolution bathymetric map suggests that the Laccadive Plateau is associated with irregular topography, with the presence of several islands, banks, isolated bathymetric highs and scour/depression like features. The multichannel seismic reflection suggests the presence of a region of faulted basement and graben structures suggesting a rift system in the crestal part of the Laccadive Plateau. The gravity anomalies of the Laccadive Plateau are associated with a belt of relatively positive anomalies bounded by relatively negative anomalies in the east and west, some of these high-amplitude free-air gravity anomalies are characterized by their correspondence with isolated bathymetry highs while others have no correspondence with the seafloor features. The Laccadive Plateau is associated with broad wavelength and high amplitude magnetic anomalies with superimposed secondary high-frequency magnetic anomalies at places, most of these high-amplitude magnetic anomalies are correlatable with the gravity and bathymetric signatures. The integrated forward modelling of the gravity and magnetic anomalies shows that the Laccadive Plateau can be explained as ~ 18-19 km thick two-layered continental crust, with magnetized intrusive bodies causing the magnetic anomalies. This derived crustal structure, in conjunction with the other geophysical signatures supporting the continental origin of the Laccadive Plateau, it is inferred that the Laccadive Plateau can surely be explained in terms of a thinned continental crust intermingled with volcanic intrusives.

Chapter 6

Sagar Kanya Bathymetric High Complex: An extinct giant submarine volcanic caldera in the Eastern Arabian Sea?

6.1 Introduction

The Sagar Kanya Seamount is an anomalous seafloor feature located southwest of the Laccadive Plateau in the Eastern Arabian Sea (Figure 6.1a). This seamount, centred around 9°19.5'N, 71°04.0'E, was discovered by Bhattacharya and Subrahmanyam (1991), based on bathymetry and geophysical data collected along one transect. They collected single beam bathymetry, gravity and magnetic profiles along this transect in order to attempt to understand the geomorphology, geophysical characteristics and the probable genesis of the Sagar Kanya Seamount. The bathymetry data revealed that the Sagar Kanya Seamount rises from an average water depth of 4150 m to a peak with least depth of 1686 m, indicating a bathymetric high feature with a maximum height of 2464 m and a basal width of 33 km. The seamount was found to be associated with a positive free-air gravity anomaly (~ +70 mGal) flanked by negative gravity anomalies (~ -10 mGal) and a well-developed magnetic anomaly pattern with an amplitude of the order of 200 nT. Based on the forward modelling of the gravity and magnetic anomalies, constrained by the geological and tectonic information from the region, Bhattacharya and Subrahmanyam (1991) attributed the genesis of the Sagar Kanya Seamount to the Réunion hotspot volcanism. Bhattacharya and Subrahmanyam (1991) provided important insights on the morphology, geophysical signatures and the probable genesis of this anomalous feature, however, they could not provide a detailed information on the entire spatial extent of this seamount since the data was available only along one transect. Therefore, an attempt has been made to understand the detailed morphology and geophysical characteristics of the entire Sagar Kanya Seamount and its adjacent regions, using newly acquired high-resolution multibeam bathymetry data along with sea surface magnetic and gravity data.

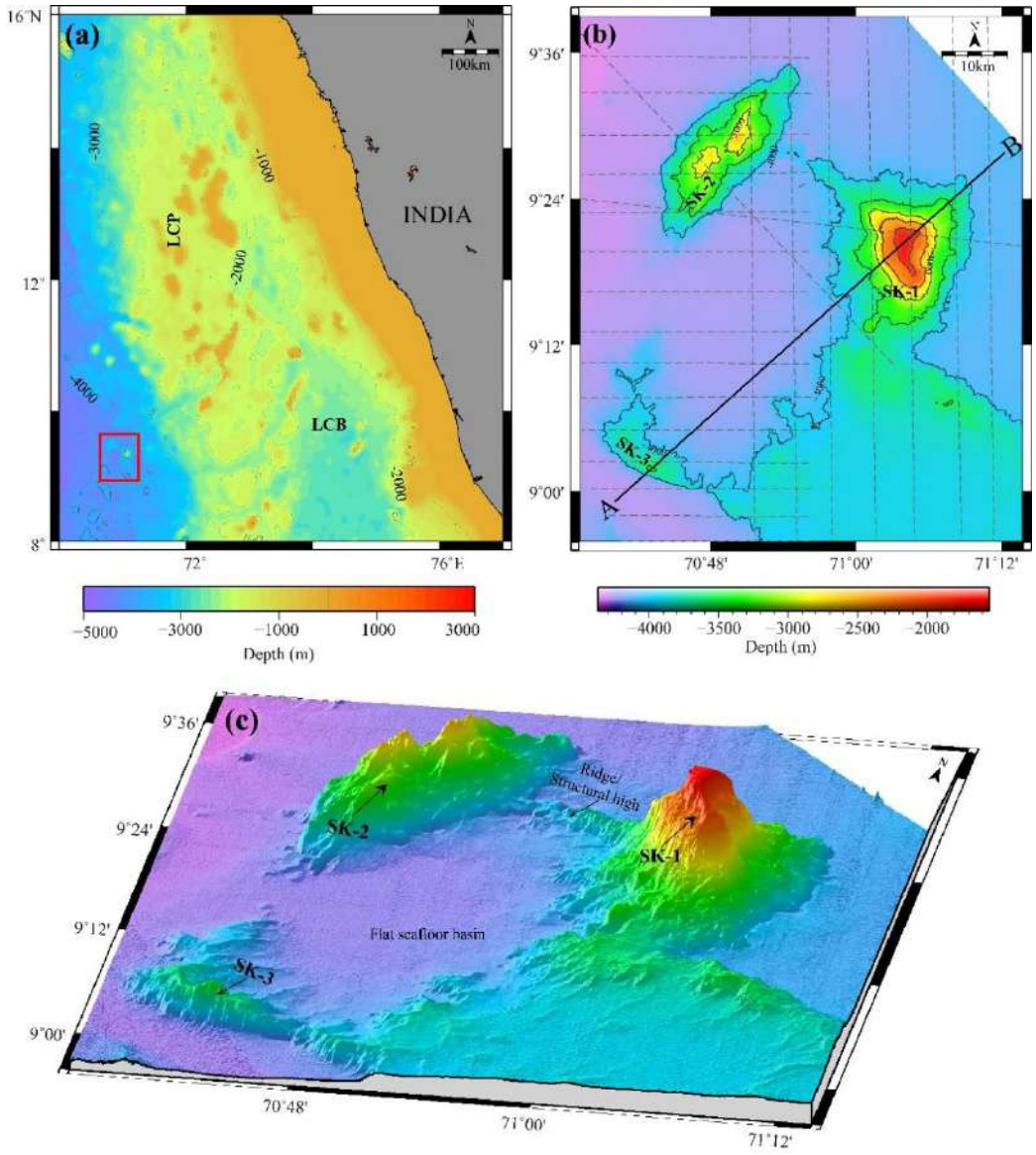

Figure 6.1: (a) Satellite-derived topographic map of the southwestern continental margin of India and the adjacent ocean basins showing the location of the study area as a square in red colour; (b) High-resolution multibeam bathymetry map of the study area shown as filled contour map; and (c) three-dimensional bathymetry image with major bathymetric features labelled. Black line AB represent profile location over which the forward modelling has been carried out and presented in Figure 6.7. SK-1: Sagar Kanya-1 Seamount; SK-2: Sagar Kanya-2 Seamount; SK-3: Sagar Kanya-3 Seamount; LCP: Laccadive Plateau; LCB: Laccadive Basin.

6.2 Geophysical signatures

6.2.1 Seafloor morphology

The high-resolution multibeam bathymetric maps of the study area (Figure 6.1b, c), which covers an areal extent of ~ 6500 km^2, reveals the presence of several bathymetric high features with different dimensions. These features mainly consist of three prominent elliptical bathymetric high complex surrounding a region of nearly flat seafloor measuring ~ 50 km x 30 km, at water depth 4200-4300 m. For the ease of further discussion in this study, these seamounts are referred as Sagar Kanya-1 (SK-1), Sagar Kanya-2 (SK-2), and Sagar Kanya-3 (SK-3) seamounts and the whole bathymetry high complex as the Sagar Kanya Bathymetric High Complex (SKBHC). Among these, the SK-1 Seamount represents the "Sagar Kanya Seamount" discovered by Bhattacharya and Subrahmanyam (1991).

The Sagar Kanya-1 (SK-1) Seamount is a nearly conical-shaped seamount, which is centred at 9°20.1'N, 71°04.0'E (Figures 6.1 and 6.2). This seamount is surrounded by a flat seafloor with a water depth range of 4150-4200 m, rising to a height of ~ 2500 m to summit at a depth of ~ 1665 m. The base of the SK-1 Seamount is nearly circular in shape with a basal areal extent of ~ 630 km^2 and its summit area is flat-topped with an areal extent of ~ 9 km^2. The SK-1 Seamount is characterized by the presence of several morphological features consisting of a lava terrace, a scarp face and a cluster of volcanic edifices. The NNW-SSE trending, well-developed, flat-topped and steep-sided lava terrace (~ 2300 m seafloor depth) identified (Figure 6.2b) on the western flank of the summit area of this seamount suggests a post-eruptive slope modification of this seamount. An ~ 8 km long and two-stepped scarp face / embayment with a moderately steep slope is identified (Figure 6.2c) on the eastern flank of the summit area of the SK-1 Seamount. Such sharpness of the embayment at the summit edge of a seamount and the relatively smooth flanks of the seamount below them are suggestive of representing a slope failure event. A close examination of the SK-1 Seamount further reveals the presence of numerous smaller discrete secondary volcanic cones (Figure 6.2d), most of which are clustered on the southeast and southwest corners of the seamount. In addition, the SK-1 Seamount is also characterized by the presence of an extensive pattern of gully-like features along its flanks.

The Sagar Kanya-2 (SK-2) Seamount, identified and mapped by the present study, is centred at 9°28.4'N, 70°50.2'E (Figures 6.1 and 6.3a). This NE-SW trending large elliptical-shaped seamount, located ~ 35 km (summit-to-summit distance) northwest of the SK-1 Seamount, has a basal area of ~ 350 km^2. The SK-2 Seamount is surrounded by a flat seafloor with a depth range of 4150-4200 m and the summit area is marked by two isolated domes at water depths of ~ 2500 m and ~ 2800 m. The elongated plateau-shaped SK-3 Seamount possesses a height of 815 m, with its centre location at 9.032°N, 70.714°E (Figures 6.1 and 6.3b). Compared to the SK-1 and SK-2 seamounts, the basal area of the SK-3 seamount is limited and it exhibits irregularly shaped summit area. The southwestern flank of the SK-3 Seamount is sharp while its northeastern flank is gentle in nature (Figure 6.3).

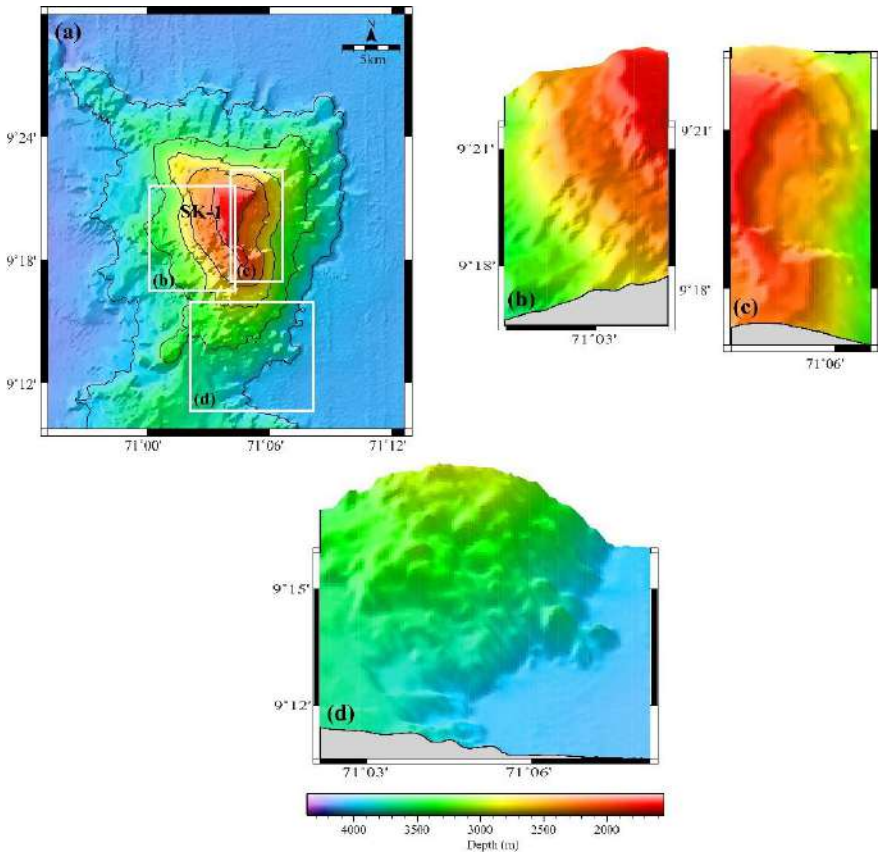

Figure 6.2: Bathymetric map of the (a) Sagar Kanya-1 (SK-1) Seamount, (b) steep-sided lava terrace, (c) scarp face / embayment, and (d) secondary volcanic cones.

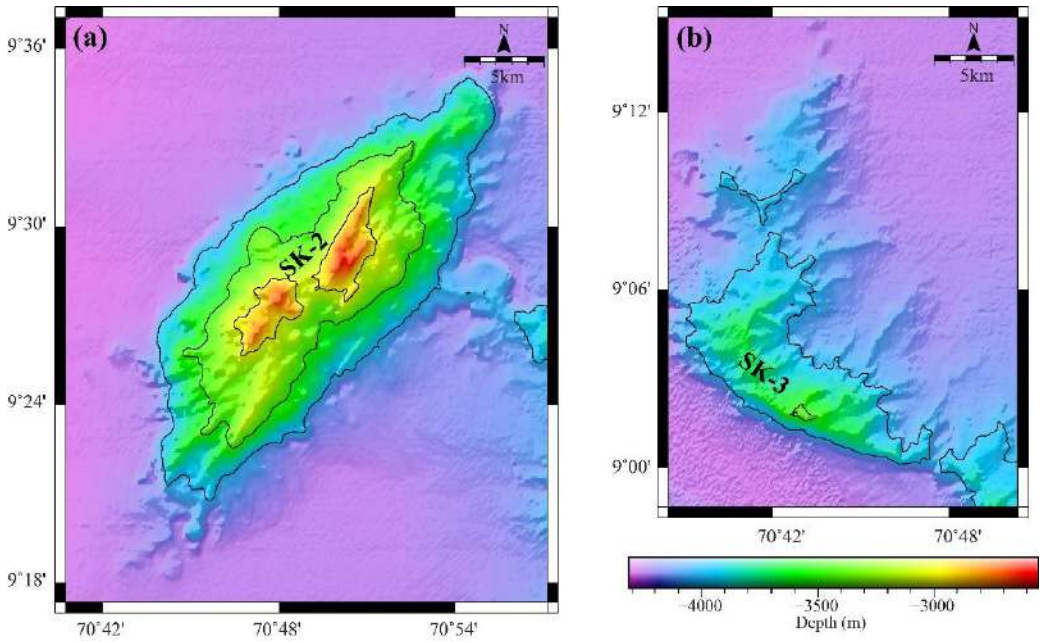

Figure 6.3: Bathymetric map of the (a) Sagar Kanya-2 (SK-2) Seamount, and (b) Sagar Kanya-3 (SK-3) Seamount.

Bathymetry data of the Sagar Kanya Bathymetric High Complex has also been analyzed in the perspective of morphological slope distribution (Figure 6.4). The major part of the study area is associated with slopes ranging from 0° to 10°, which represents the regions of sub-horizontal morphological characteristics. The slope distribution map suggests the presence of several regions with very-high slopes (> 25°) over different parts of the SKBHC, some of which are continuously banded while others are discontinuously banded in nature. This map clearly shows the presence of two concentric continuously banded zones with very-high slope (> 25°) that are centred over the flat summit region of the SK-1 Seamount. Among these, the inner band is marked by the steeply dipping flanks of the summit peak, while the outer band is marked by the steeply dipping flanks bordering the lava terraces. The SK-1 Seamount is also associated with several discontinuous bands of very-high slope (> 25°), which are mostly concentrated on its outer boundary. In contrary to this, the discontinuous bands of very-high slope are distributed randomly at several locations on the SK-2 Seamount, including at their outer boundary. A continuous band of very-high slope region is also observed on the outer limit of the SK-3 Seamount on the southwestern part of the study region.

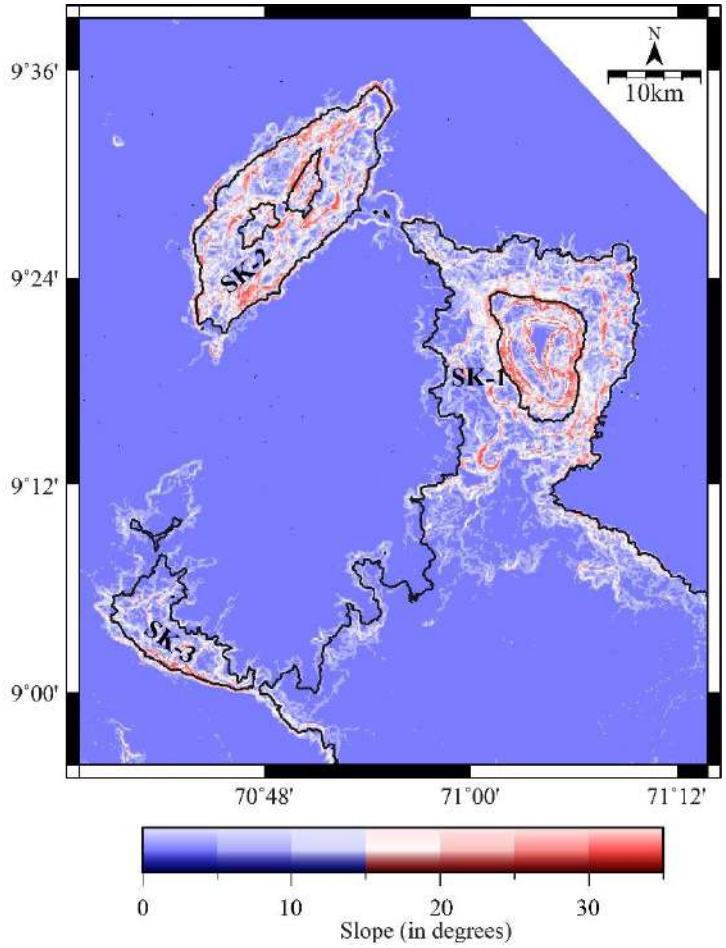

Figure 6.4: Slope map of the study area derived from the multibeam bathymetry data. The black contours represent the isobaths with 500 m contour interval, used to depict the extent of the seamounts and the other bathymetric features. Other details are as in Figure 6.1.

6.2.2 Gravity and magnetic signatures

The free-air and complete Bouguer gravity anomalies (Figure 6.5) of the study area have been presented along with the selected bathymetry contours, which defines the extent of the seafloor features, to describe the characteristic gravity signatures of these features in the study area. The free-air gravity anomalies of the Sagar Kanya Bathymetric High Complex are correlated with topography in general, with their maximum corresponding to the locations of the summit of the seafloor features (Figure 6.5a). However, the free-air gravity anomalies corresponding to the shallower seafloor features appear to get masked by the long-wavelength gravity anomalies caused by the deeper regional features, and therefore, a high-pass filtered map generated with cut-off wavelength 40 km (Figure 6.5b) to enhance the effect of the shallower features and diminish the effect of deeper features. The nearly

elliptical-shaped gravity high that surrounds a gravity low as observed from this high-pass filtered gravity anomalies (Figure 6.5b) suggests the presence of a nearly elliptical-shaped surface/subsurface high feature that surrounds a depression. In the case of SK-1 Seamount, the maximum slope region of the gravity anomalies that normally define the subsurface lateral extent of the feature buried under the sediments appears to be located very close to the extent of the SK-1 Seamount defined by the bathymetry contours. These nearly coinciding surface and subsurface lateral extents of the feature suggest nearly vertical flanks for the SK-1 Seamount. Unlike the SK-1 Seamount, the maximum slope region of the gravity anomalies that define the subsurface lateral extent of the SK-2 Seamount is wider than the extent of the seamount defined by the bathymetric contours. Such an observation suggests that the flanks of the SK-2 Seamount is gentle compared to the SK-1 Seamount and the base of the seamount is buried under sediments. Further computed complete Bouguer anomaly (CBA) to understand the variations in the crustal thickness or heterogeneity in the subsurface density of the material. This is achieved from the free-air gravity anomaly by subtracting the attraction of bathymetric relief considering the water-crust interface based on Parker (1972) method. For water and crust, used density values of 1.03 g/cc and 2.85 g/cc, respectively. The complete Bouguer anomaly map of the study area (Figure 6.5c) is characterized by the presence of moderate to long wavelength positive anomaly ranging from 180 to 290 mGal. The high amplitude anomalies are present in the region surrounding the northwestern part of Sagar Kanya Bathymetric High Complex. From the northwestern part to the southeastern part of the study area, the complete Bouguer anomaly shows a gentle decrease in general, with their minimum coinciding with the peaks of SK-1 (~ 190 mGal), SK-2 (~ 240 mGal) and SK-3 (220 mGal) seamounts (Figure 6.5c). As in the case of the free-air gravity anomaly, a high-pass filtered (with cut-off wavelengh 40 km) complete Bouguer anomaly map generated, which further enhances the residual Bouguer anomaly signatures corresponding to shallower features (Figure 6.5d). The high pass filtered complete Bouguer anomaly map also reveals the presence of distinct circular to elliptical shaped anomaly connecting the SK-1, SK-2 and SK-3 seamounts. Further, the surrounding flat seafloor region as well as the depression in the central region of the Sagar Kanya Bathymetric High Complex exhibits subdued anomaly within the range of 0 - +20 mGal (Figure 6.5d).

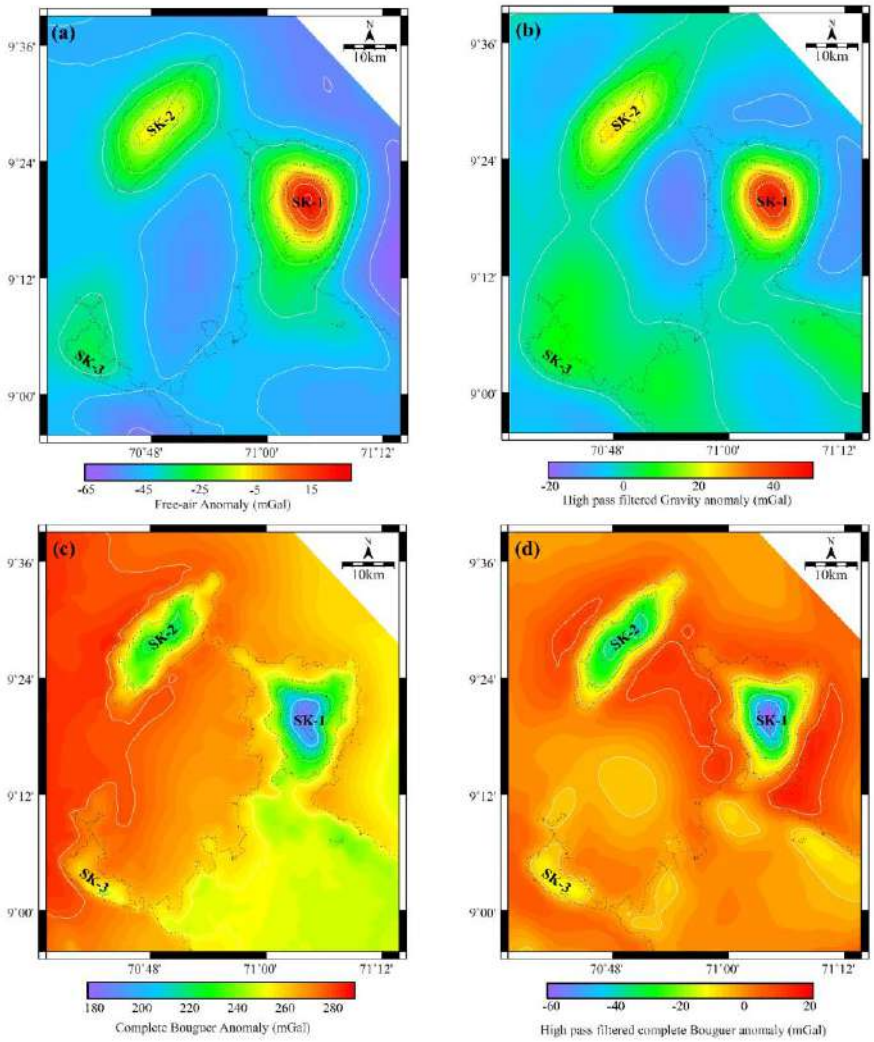

Figure 6.5: Images of the (a) free-air gravity anomaly; (b) high pass filtered (cut-off wave length of 40 km) free-air gravity anomaly; (c) Complete Bouguer anomaly; (d) high pass filtered (cut-off wave length of 40 km) complete Bouguer anomaly of the study area. Other details are as in Figure 6.4.

The magnetic anomalies (Figure 6.6a) of the study area have been presented along with the selected bathymetry contours, which defines the extent of the seafloor features, to describe the characteristic magnetic signatures of these features. As in the case of gravity anomalies, the residual magnetic anomalies of the

SKBHC also appears to have got masked by the long-wavelength magnetic anomalies. Therefore, a high-pass filtered (cut-off wavelength 40 km) magnetic anomaly map (Figure 6.6b) also has been generated to enhance the effect of the shallow features and diminish the effect of deeper features. The magnetic anomalies over the study area are complex, consisting of several positive and negative magnetic anomalies, representing the dipole magnetic field caused by the associated causative magnetic bodies. The central part of the SK-1 Seamount is associated with a negative magnetic anomaly, while that of the SK-2 Seamount is associated with a positive magnetic anomaly. The flat seafloor enclosed within the bathymetric high complex is associated with ~ WNW-ESE trending high amplitude positive and negative bands of magnetic anomalies, suggestive of the existence of causative magnetic bodies buried under the sediments.

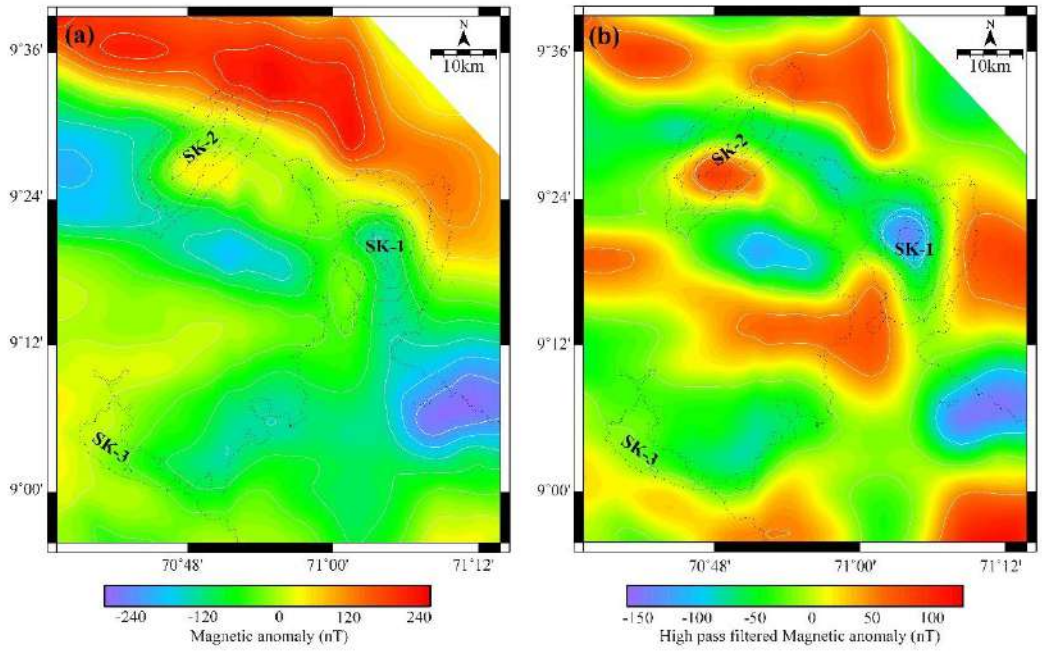

Figure 6.5: Images of the (a) magnetic anomaly and (b) high pass filtered (cut-off wave length of 40 km) magnetic anomaly of the study area. Other details are as in Figure 6.5.

6.2.3 Crustal architecture of the SKBHC

Integrated forward modelling of gravity and magnetic data carried out to understand the crustal configuration of the Sagar Kanya Bathymetric High Complex. For this, a representative profile AB (Figure 6.1b) that cut across the SKBHC through the SK-1 and SK-3 seamounts has been selected. The first step to carry out forward modelling of gravity anomalies based on the method of Talwani et al. (1959) is the construction of an initial crustal model constrained by geophysical and geological information available from those regions. Since the constraints are not too many, it is assumed a simple crustal model with two-layered oceanic crust around the SKBHC and a single layer intrusive structure for the SKBHC. In the shallower regions, the constraints available from bathymetry data of the present study and the sediment velocities available from the published results (Naini and Talwani, 1982) from the nearby area were used. For deeper layers, in the absence of velocity-depth information available from seismic refraction results, used the published information of velocity (Naini, 1980; Naini and Talwani, 1982) and velocities of layers available for a standard oceanic crust (Fowler, 2005). The above velocity information was converted to density using the velocity-density relationship of Ludwig et al. (1970). Accordingly, density values were assigned as 2.35 g/cc, 2.63 g/cc, 2.88 g/cc and 3.3 g/cc for the sediments, layer-2, layer-3, and mantle, respectively. Keeping those density constraints fixed, attempt has been made to derive a crustal model by refining the thicknesses and extents of the layers to get a reasonably good fit with computed and observed gravity anomalies. Having obtained a reasonable gravity model, attempt has been made to incorporate magnetic bodies into this model to get an integrated gravity-magnetic model that can satisfy both the gravity and magnetic signatures. For computing the magnetic anomalies across these assumed two-dimensional bodies, used the method of Talwani and Heirtzler (1964). In the absence of the paleomagnetic studies available from the rocks collected from SKBHC, it is considered the paleomagnetic results of volcanic rocks available from DSDP Site 220, which is located in the neighbouring area (Whitmarsh et al., 1974). Accordingly, assigned remnant inclination (RI) of 12° and remnant declination (RD) of 315° with magnetization (M) ranging 1.0 – 2.0 A/m for the magnetized bodies. The derived crustal model (Figure 6.7) suggests that the SKBHC can be reasonably interpreted in terms of a

volcanic intrusion within the existing oceanic crust. The excess masses corresponding to the SK-1 and SK-2 seamounts are compensated by deepening of the Moho to ~ 25.0 km under the SK-1 Seamount and ~ 13 km, under SK-3 Seamount. As a result, the SK-1 and SK-3 seamounts yield crustal thicknesses of ~ 20 km and ~ 7 km, respectively. The derived model further suggests that the SK-1 and SK-3 seamounts are underlain by normally and reversely magnetized crust, formed during a normal and a reverse polarity interval of the Earth's magnetic field, respectively.

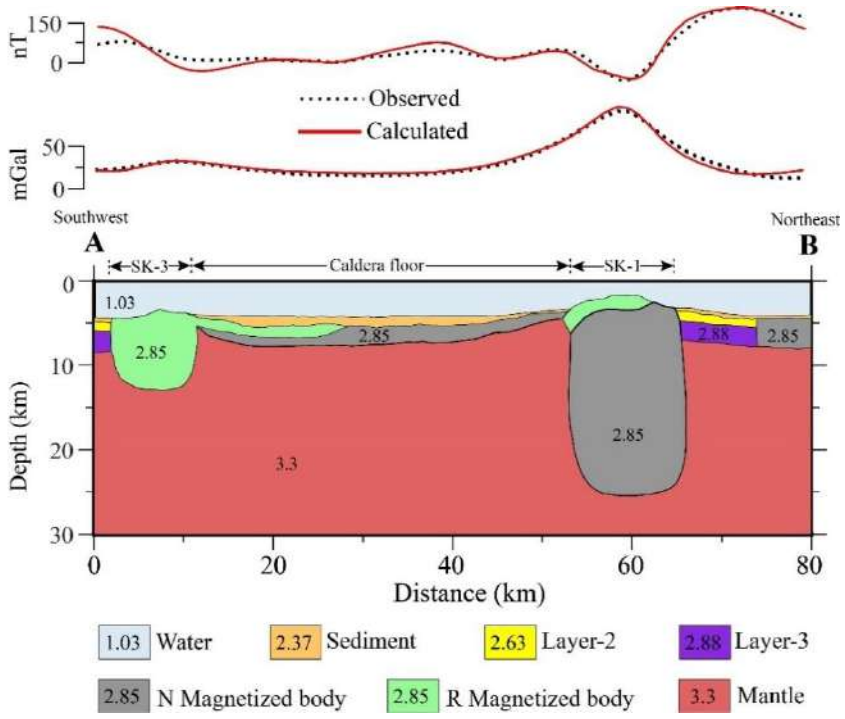

Figure 6.6: Crustal model derived based on integrated forward modelling of gravity and magnetic anomalies along the profile AB, the location of which is shown in Figure 6.1b. The decimal numbers given in the each layers of the model represent density in g/cc. Magnetic anomalies are modelled with two-dimensional magnetic bodies of intrusive dykes and sills (For normally magnetized blocks: Remnant magnetization = 1.0-2.0 A/m; Remnant Inclination = -40°, Remnant Declination =300°; For reversely magnetized blocks: Remnant magnetization = 1.0-2.0 A/m; Remnant Inclination = 12°, Remnant Declination =315°).

6.3 Sagar Kanya Bathymetric High Complex - A possible submarine volcanic caldera?

The multibeam bathymetric map (Figure 6.1) clearly shows the presence of three prominent seamounts and several linear ridge-like features, together representing a large, elliptical bathymetric high complex surrounding a region of nearly flat seafloor, elongated in NNE-SSW direction. This configuration of seafloor resembles with the shape of a volcanic caldera, which is defined as a volcanic structure, generally large, which is principally the result of collapse or subsidence into the top of a magma chamber during or immediately following eruptive activity (Cole et al., 2005). Therefore, this elliptical-shaped bathymetric high complex (SKBHC) appears to qualify to be considered as the rim surrounding the summit caldera of a large extinct submarine volcano, referred to as the Sagar Kanya Volcano. The morphology of this postulated caldera rim in the Arabian Sea is very similar to the shape of presently active known calderas in other parts of the globe, such as the Nikko Submarine Volcanic Caldera (Global Volcanism Program, 1990), Brothers Seamount Caldera (Stagpoole et al., 2016) and the Santorini Caldera (Nomikou et al., 2012). The areal extent of this postulated volcanic caldera, hereafter referred to as the Sagar Kanya Volcanic Caldera, is ~ 1500 km^2 (with a dimension of ~ 50 x 30 km). This areal extent is nearly half of the area of the Yellowstone Caldera of ~2400 km^2, measuring 60 x 40 km (Tizzani et al., 2015), Toba Caldera of ~ 3000 km^2 measuring 100 x 30 km (Chesner, 2012) and Gakkel Caldera of ~ 3200 km^2 measuring 80 x 40 km (Piskarev and Elkina, 2017), created by super volcanic events. The rim structure of the Sagar Kanya Volcanic Caldera can be traced for about 320° of the summit of the volcano, but appears to be slightly buried in the central part of its western side (Figure 6.4). Such a configuration is a common style associated with the asymmetrical subsidence resulted by tilting of the magma chamber (Kennedy et al., 2004). Roche et al. (2000) suggested from their experiments that shallow magma chambers with large diameters lead to coherent single block collapse structures, while deep chambers with small diameters lead to a series of multiple nested blocks. Since the caldera of the Sagar Kanya Volcano represents a single block structure with ~ 50 x 30 km dimension and asymmetric in nature, postulates that the collapse of Sagar Kanya Volcano is associated with a shallow tilted magma chamber. The high-pass filtered gravity anomalies support

the presence of a nearly elliptical continuous gravity high feature surrounding a gravity low region, representing the rim and depressions of the postulated caldera, respectively. The probable presence of ring-fault system formed due to the collapse of Sagar Kanya Volcano might have acted as conduits to form the SK-1, SK-2 and SK-3 seamounts, which were created as a result of a post-collapse phase of volcanism. The derived complete Bouguer anomaly (Figure 6.5c, d) and the crustal structure (Figure 6.7) exhibits the variation of the crustal thickness resulted after the multiphases of volcanism that shaped the Sagar Kanya Bathymetric High Complex as a whole. The minimum amplitude of Bouguer anomaly is associated with the central part of SK-1 Seamount (where the thickness is maximum as inferred from the forward modelling of gravity and magnetic anomalies, see Figure 6.7) and the maximum amplitude of Bouguer anomaly is associated with the crust having minimum crustal thickness (as inferred from the forward modelling of gravity and magnetic anomalies, see Figure 6.7). These observations depict an inverse correlation of Bouguer anomaly with the crustal thickness over the Sagar Kanya Bathymetric High Complex. Similar inverse relationship between the Bouguer anomalies and crustal thickness is observed over various physiographic features, such as the Wreck Seamount (Tasman Sea, Richards et al., 2018), Maldive Ridge (Kunnummal et al., 2018) and the NW Iberian margin (Druet et al., 2019).

6.4 Probable genesis of the Sagar Kanya Bathymetric High Complex

The genesis of intraplate volcanoes is generally attributed to the hotspot volcanism and therefore, the genesis of the Sagar Kanya Volcano can be reasonably explained in terms of volcanism caused by the Réunion hotspot, considering the tectonic framework of the western continental margin of India and the adjacent deep ocean basins. The crustal model derived from the integrated gravity and magnetic forward modelling indicates that the magnetic anomaly pattern in the study area represent the presence of normally and reversely magnetized bodies, formed in the southern hemisphere. Comparison of the location of the Sagar Kanya Bathymetric High Complex with the magnetic lineations in the Arabian Basin suggests that the oceanic crust over which this anomalous bathymetric high feature sits is much older than chron C24n3o (53.347 Ma, as per Cande and Kent, 1995). This observation,

along with the locations of the computed Réunion hotspot track (Müller et al., 1993) as shown in Figure 4.11, suggests ~ 56-57 Ma timing for the formation of the Sagar Kanya Bathymetric High Complex. Therefore, to understand the relationship of the formation of this feature with the evolution of the conjugate Arabian and Eastern Somali basins through the Carlsberg Ridge, and with the formation of the Laccadive-Chagos Ridge, it is provided the latest published reconstruction map (Yatheesh et al., 2020) of the Western Indian Ocean at 56.4 Ma- (Figure 6.8). This suggests that the Réunion hotspot was very close to the location of the SKBHC at 56.4 Ma and by this time, the Réunion hotspot has already reached to the southernmost part of the Laccadive Plateau. Therefore, it is quite reasonable to postulate that the major part of the SKBHC was formed due to the Réunion hotspot volcanism, at around 56-57 Ma, which consists of normal as well as reverse polarities. However, some secondary volcanism also might have occurred in these regions during subsequent periods since the effect of the hotspots can go over several hundreds of kilometres distance (Tolan et al., 1989; Storey et al., 1995).

It is further postulated that the formation of the Sagar Kanya Volcano as well as the SK-1 and SK-2 seamounts can be explained in terms of multiphase volcanism, considering the presence of randomly distributed seamounts over the postulated caldera rim structure. The western part of the SK-1 Seamount is characterized by the presence of a NNW-SSE trending, well-developed, flat-topped and steep-sided lava terrace, suggestive of post-eruptive slope modification. This seamount is also associated with numerous smaller discrete secondary volcanic cones, representing post multiphase volcanism. Similarly, the SK-2 Seamount is associated with multiple secondary peaks suggesting multiphase volcanism in this region. The opposite sense of magnetic signatures associated with these features suggest that the SK-1 and SK-3 seamounts were not formed contemporaneously, but during different phases of volcanism occurred during normal and reverse polarity intervals. The prominent high amplitude magnetic anomalies observed within the flat caldera floor also indicate the presence of large subsurface intrusive bodies, formed by these later phases of volcanism.

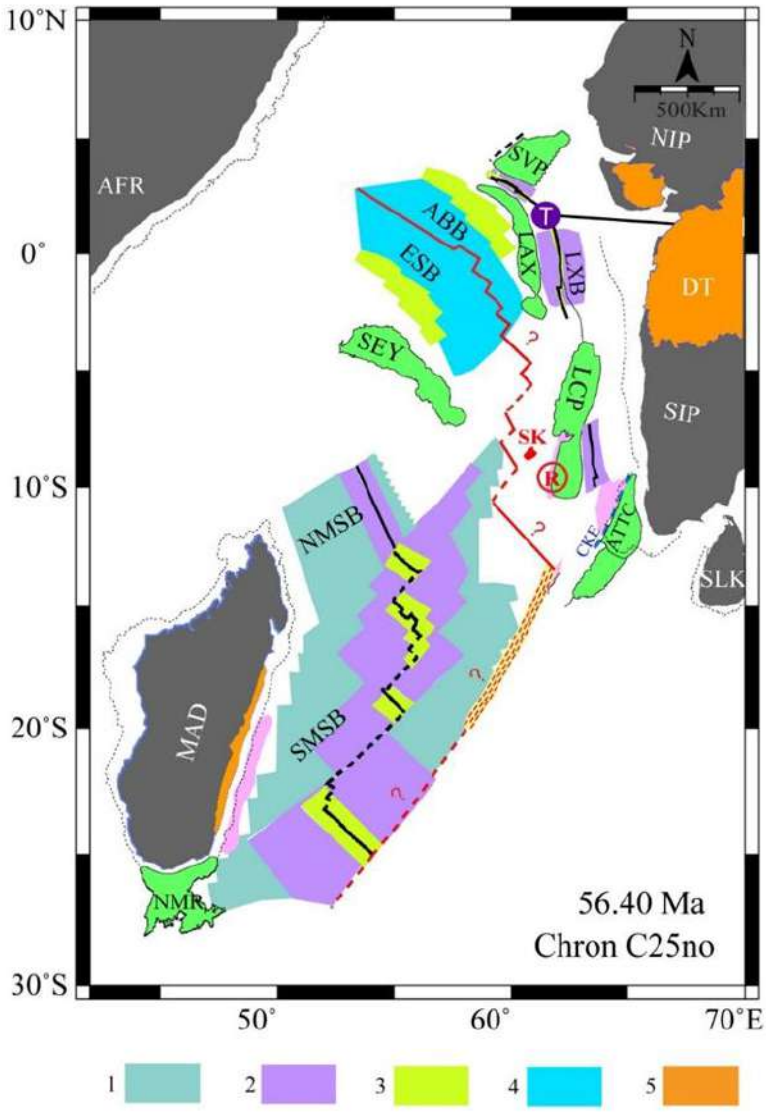

Figure 6.8: Simplified plate tectonic reconstruction map of the Western Indian Ocean region in fixed Africa reference frame, at 56.4 Ma (after Yatheesh et al., 2020), along with location of the Sagar Kanya Bathymetric High Complex. R: Location of the Réunion hotspot; SK: Location and extent of the Sagar Kanya Bathymetric High Complex; AFR: Africa; MAD: Madagascar; DT: Deccan Trap; SIP: Southern Indian Protocontinent; NIP: Northern Indian Protocontinent. Explanation of items of the legend - [1] Oceanic crust formed during 83.0–68.5 Ma; [2] Oceanic crust formed during 68.5–62.5 Ma; [3] Oceanic crust formed during 62.5–60.92 Ma; [4] Oceanic crust formed during 60.92–56.4 Ma; [5] Extent of volcanics.

6.5 Summary

A detailed marine geophysical investigation was carried out over the Sagar Kanya Seamount and its adjacent regions to understand the detailed geomorphology and geophysical characteristics over the entire spatial extent of this anomalous feature. The high-resolution multibeam bathymetric map reveals the presence of a nearly elliptical bathymetric high complex consisting of three seamounts and several linear ridge-like features surrounding a region of nearly flat seafloor measuring ~ 50 km x 30 km. This bathymetric high complex is referred to as the Sagar Kanya Bathymetric High Complex (SKBHC) and the above-mentioned three seamounts are referred to as the Sagar Kanya-1 (SK-1), Sagar Kanya-2 (SK-2) and Sagar Kanya-3 (SK-3) seamounts. The conical shaped SK-1 Seamount has ~ 2000 m height and is associated with well-developed and steep-sided lava terrace, a two-stepped scarp face and numerous secondary volcanic cones. The elliptical-shaped SK-2 Seamount has ~ 815 m height and its summit area is marked by two isolated domes. Compared to these SK-1 and SK-2 seamounts, the SK-3 Seamount exhibits irregularly shaped summit area. The free-air gravity anomalies of the Sagar Kanya Bathymetric High Complex are correlated with topography in general, with their maximum corresponding to the locations of the summit of the seafloor features. The Bouguer gravity anomalies show an inverse correlation with the topography, with their minimum over the summit of the SK-1, SK-2 and SK-3 seamounts. The nearly elliptical-shaped gravity high that surrounds a gravity low as observed from this high-pass filtered free-air gravity anomalies suggests the presence of a nearly elliptical-shaped surface/subsurface high feature that surrounds a depression. These gravity signatures suggest that the SK-1 Seamount is associated with nearly vertical flanks, while the SK-2 Seamount is associated with gently dipping flanks. The magnetic anomalies over the study area are complex, consisting of several positive and negative magnetic anomalies. The central parts of the SK-1 and SK-2 seamounts are associated with negative and positive magnetic anomalies, respectively, and the flat seafloor region enclosed within the SKBHC is associated with ~WNW-ESE trending high amplitude positive and negative bands of magnetic anomalies.

The morphology of the Sagar Kanya Bathymetric High Complex (SKBHC) appears to qualify to be considered as the rim surrounding the summit caldera of a

large extinct submarine volcano, referred to as the Sagar Kanya Volcano. The shape of SKBHC is comparable with the shape of presently active known calderas in other parts of the globe. Therefore, it is interpreted that the flat seafloor enclosed within the SKBHC as volcanic caldera and the bathymetric high features surrounding this flat seafloor as the caldera rim of the postulated Sagar Kanya Volcano. Since this caldera represents a single block structure with ~ 50 x 30 km dimension and asymmetric in nature, the collapse of the volcano is considered to have associated with a shallow tilted magma chamber. The SK-1, SK-2 and SK-3 seamounts might have formed through the ring-fault system, as a result of the post-collapse phase of volcanism. These phases of volcanism during normal and reverse polarity timing might have emplaced the SK-1 and SK-3 seamounts through the caldera rim structure as well as the volcanic flows within the collapsed caldera. Considering the tectonic framework of the western continental margin of India and the adjacent deep ocean basins, the genesis of these phases of volcanism can be attributed to the Réunion hotspot.

Chapter 7

Conjugate nature of the Alleppey-Trivandrum Terrace Complex with the Northern Madagascar Ridge in the early opening model of the Arabian Sea: Evaluation based on an integrated geophysical investigation

7.1 Introduction

The bathymetric map of the southwestern continental margin of India reveals the presence of an anomalous bathymetric high feature in the mid-continental slope region off Trivandrum (Figures 7.1a, b). Based on the analysis of limited single beam bathymetry transects available over this feature, and the isobaths available from GEBCO database (IOC-IHO-BODC, 2003), Yatheesh et al. (2006) inferred this feature to represent a "terrace" defined by a conspicuously wide low gradient zone between the 1000 and 2000 m isobaths, and referred it to as the 'Terrace Off Trivandrum (TOT)'. Using the available paleogeographic reconstruction models depicting the evolution of the Western Indian Ocean and updated compilation of identified offshore tectonic elements, Yatheesh et al. (2006) further inferred that the southern part of the TOT fits well in shape and size with bathymetric notch on the Northern Madagascar Ridge (NMR), implying the conjugate nature of TOT with NMR. Subsequently, Yatheesh et al. (2013) carried out detailed investigation on the TOT region using a new set of sea-surface gravity, magnetic and single beam bathymetry data, and inferred that the above anomalous topography feature consists of two contiguous terraces (Figure 7.1b), the Alleppey Terrace (defined by 300 m and 400 m isobaths) and the Trivandrum Terrace (defined by 1500 m and 1900 m isobaths), together referred to as the Alleppey-Trivandrum Terrace Complex (ATTC). They further provided gravity and magnetic characteristics of the ATTC and derived detailed crustal configuration model for the Alleppey Terrace and Trivandrum Terrace, based on forward modelling of gravity and magnetic profiles. Based on all these constraints from the southwestern continental margin of India, complemented with the magnetic anomaly interpretations in the Mascarene Basin, Bhattacharya and Yatheesh (2015) provided a revised plate tectonic evolution model for the Western Indian Ocean, where the anomalous feature defined by 2000 and 2500 m isobath from the southwestern

continental margin of India was found to fit with the bathymetric notch in the Northern Madagascar Ridge. Therefore, this feature also is considered to form a part of the Alleppey-Trivandrum Terrace Complex (Figure 7.1b), which is believed to have broken away from the Northern Madagascar Ridge. Even though the conjugate nature of the Northern Madagascar Ridge with ATTC is inferred from the plate tectonic reconstruction model and the detailed crustal structure of the ATTC was derived based on forward modelling, the comparison of geophysical signatures and the crustal architecture of these two postulated conjugate features are yet to be examined. Therefore, in the present paper, an attempt is made to derive the crustal configuration of the Northern Madagascar Ridge and compare this with crustal configuration of the ATTC, using an up-to-date compilation of the marine geophysical data available from the southeastern continental margin of Madagascar and its conjugate southwestern continental margin of India.

7.2 Geophysical signatures over NMR and ATTC

7.2.1 Seafloor and sub-seafloor topography

(a) Northern Madagascar Ridge

The Madagascar Ridge represents an elongated bathymetric high feature that extends southward from the Madagascar Island (Figure 7.1). This feature existing between 26°S and 36°S is defined by ~ 3000 m isobath, separating the Mozambique Basin in the west and the Mascarene and Madagascar basins in the east, abutting its south on the Southwest Indian Ridge. The Madagascar Ridge appears to consist of two domains – a southern domain (between 31°S and 36°S) consisting of a relatively flat area, and a northern domain (between 31°S and 26°S) consisting of complex and irregular topography (Goslin et al. 1980). Since the ATTC fits with the Northern Madagascar Ridge, it is analyzed the bathymetric signatures of the northern domain using the latest available GEBCO global bathymetric data (GEBCO Compilation Group, 2020). The bathymetric map of the NMR (Figure 7.2a) clearly exhibits a bathymetric notch (labelled as BN in Figure 7.2a) defined by 2000 m isobath in its northeastern part, adjacent to the Mascarene Basin. The central part of the NMR is characterized by the presence of several secondary bathymetric peaks within the 2000 m water depth, between 26°S and 28°S (Figure 7.2a). The NMR also exhibits an arcuate shaped saddle-like feature

(labelled as SLF in Figure 7.2a) along 28°S latitude, between 44°E and 48°E longitudes.

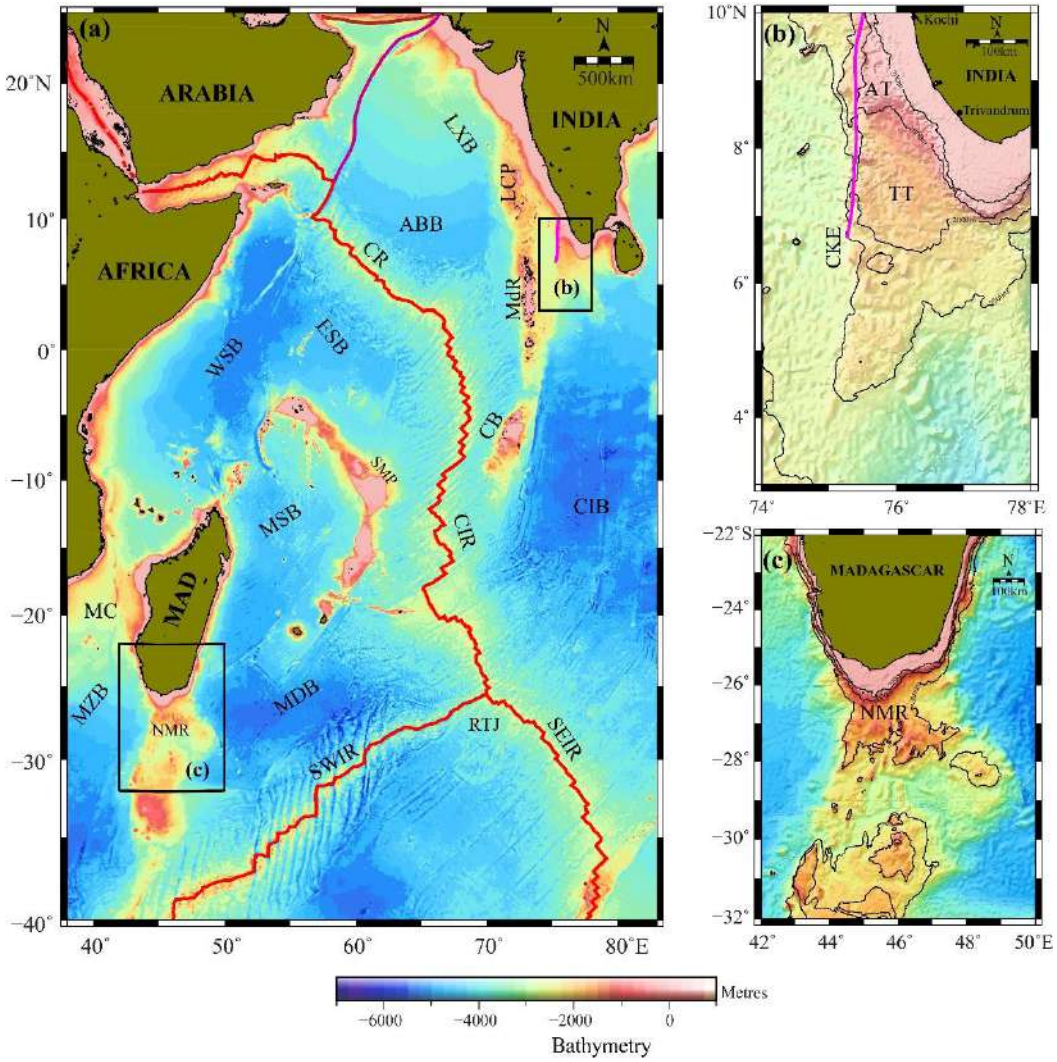

Figure 7.1: (a) Bathymetric map of the Western Indian Ocean prepared using GEBCO 2020 global bathymetric grid showing major tectonic elements. The study areas are marked as black solid boxes. Enlarged bathymetric map of the southwestern continental margin of India (b) and southeastern continental margin of Madagascar (c), along with selected GEBCO isobaths overlaid.

(b) Alleppey-Trivandrum Terrace Complex

The morphology of the Alleppey-Trivandrum Terrace Complex was originally defined (Yatheesh et al. 2006) based on the bathymetric contours (1000 m and 2000 m) available from GEBCO digital database (IOC-IHO-BODC, 2003). Subsequently, Yatheesh et al. (2013) published an updated bathymetric contour map of the Alleppey-Trivandrum Terrace Complex, based on a new set of single beam bathymetry profiles. With an aim to carryout detailed bathymetric imaging of this region, multibeam bathymetry data acquired for the first time over the northern part of the Alleppey-Trivandrum Terrace Complex falling between 400 m and 2000 m water depth. The updated bathymetric map (Figure 7.2b) generated using this high-resolution multibeam bathymetry data (complemented by the global GEBCO bathymetry data in the nearby regions) clearly depicts the morphology qualifying to consider the ATTC as a terrace defined by low gradient zones. The map further defines the sharp drop in the depth to the seafloor defining the location of the nearly N-S trending Chain-Kairali Escarpment (CKE) that defines the western boundary of the ATTC, and the ENE-WSW trending Quilon Escarpment (QE) south of the Alleppey Terrace. Small scale features representing slope failure events and submarine channels are also observed in the shelf/slope regions of the Alleppey and Trivandrum terraces. Trivandrum Terrace is a large feature that exists between the shelf edge in the east, CKE in the west and QE in the north, while the southern boundary of TT appears to continue towards south as the feature defined by the 2500 m isobath. As noticed by Yatheesh et al. (2013), north of 7°45'N, continental shelf-slope transition is gentle, while south of 7°45'N, this is comparatively steeper. The region in the vicinity of the CKE is characterized by the presence of several isolated bathymetric high features (Bijesh et al. 2018). Further, significant scouring/depression-like features are observed close to the CKE and in the central part of the TT that appears to have resulted due to the underwater current activity and its erosive-depositional process.

For understanding the sub-seafloor information of the ATTC, five multichannel seismic reflection sections (Figure 7.3). In the seismic sections, the CKE is marked by a steep gradient basement topography (Figures 7.3a, b). Seafloor / sub-seafloor bulging and block faulting are prominent underneath the TT region (Figures 7.3b-d). The basement corresponding to the QE shows a sharp drop in the

basement topography as seen from the seismic section along SWC-24 (Figure 7.3e). Yatheesh et al. (2013) divided the TT into the western and eastern basins (TT-WB and TT-EB) based on the central basement high flanked by thick sediment-filled basins with block-faulted basement on either sides (Figures 7.3b-d).

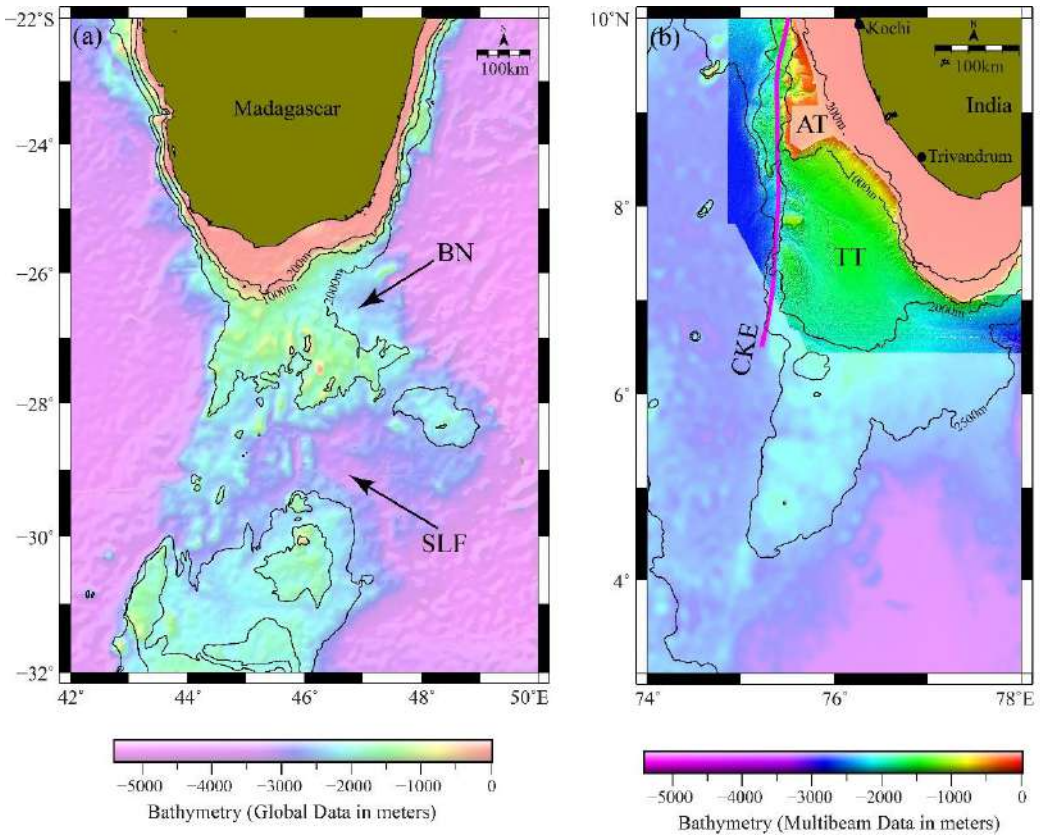

Figure 7. 2: (a) Bathymetric map prepared using GEBCO 2020 grid over the NMR. (b) High-resolution bathymetric map of the ATTC region prepared using multibeam bathymetry data, presented along with the GEBCO 2020 grid in the background. Other details are as in Figure 7.1.

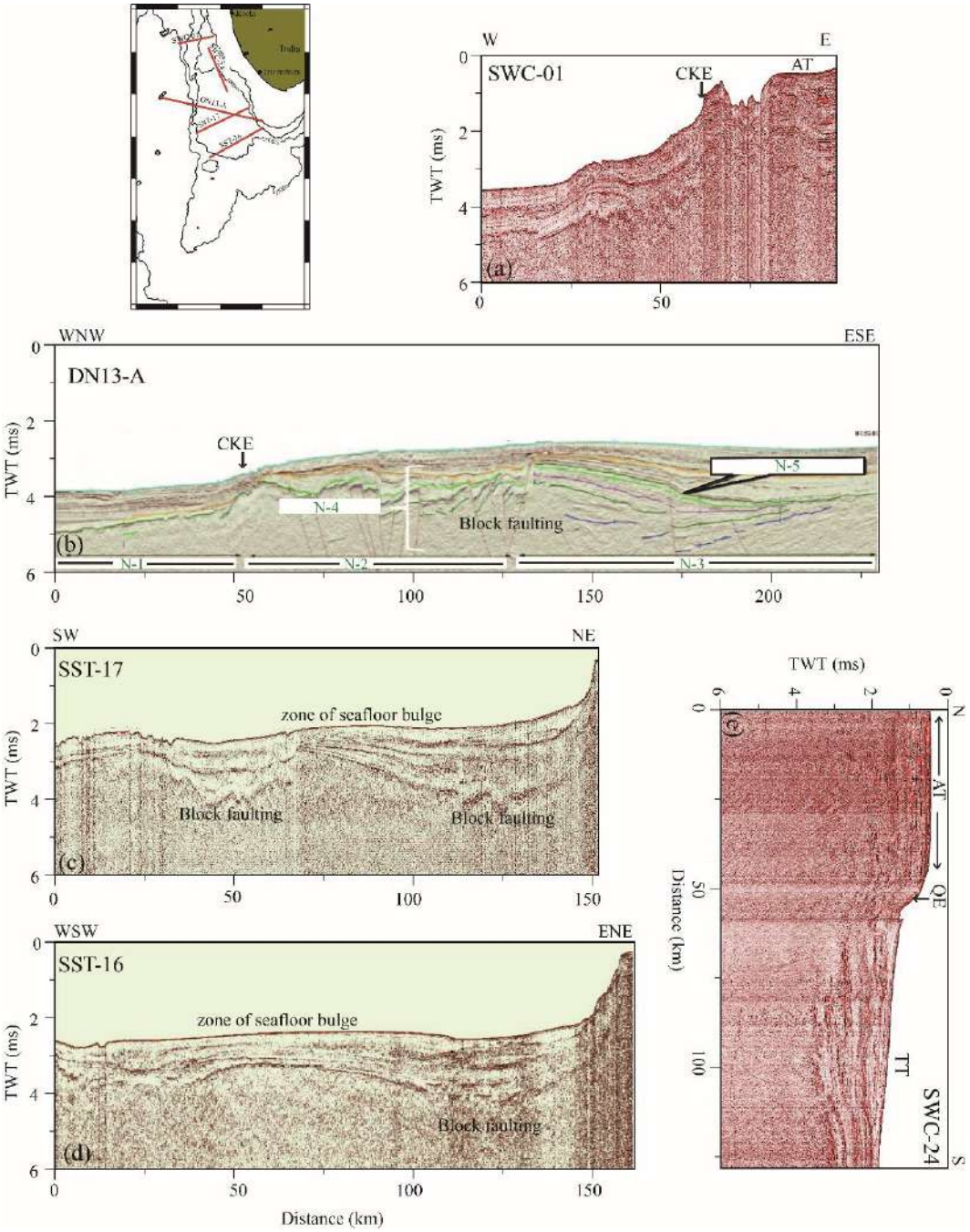

Figure 7.3: Seismic reflection sections along the profiles (a) SWC-01, (b) DN13-A (modified after Nathaniel 2013; Shuhail et al. 2018), (c) SST-17 (after Yatheesh et al. 2013), (d) SST-16 (after Yatheesh et al. 2013) and (e) SWC-24. Inset Figure shows the locations of these profiles. N1: oceanic / transition; N-2: Vishnu FZ; N-3: Inverted graben; N-4: Mesozoics; N-5: KT Boundary.

7.2.2 Gravity Signatures

(a) Northern Madagascar Ridge

The shipborne free-air gravity anomaly data available over the Northern Madagascar Ridge is sparse. Therefore, satellite-derived free-air gravity anomalies (Sandwell et al. 2014) also used to understand the broader gravity anomaly signature of the NMR. For this purpose, it is presented the satellite-derived free-air gravity anomaly image superimposed with the available sea-surface free-air gravity anomaly profiles. The 2-dimensional free-air gravity anomaly image and the track-along profiles (Figure 7.4a) exhibit several secondary positive and negative gravity anomalies superimposed over a broader dominant positive anomaly, which is correlatable with the topographic signature of the Northern Madagascar Ridge at its entire width. The boundary between the Mozambique Basin and the NMR is well defined by a sharp gradient in free-air gravity anomaly, while its eastern boundary with the Mascarene Basin is not delineable from the free-air gravity anomaly.

(b) Alleppey-Trivandrum Terrace Complex

The free-air gravity anomaly map (Figure 7.4b) of the ATTC region using the satellite-derived free-air gravity anomaly grid superimposed with the sea-surface gravity grid and selected track-along profiles. A distinct belt of gravity high is observed on the continental shelf lying immediately east of the ATTC. A linear gravity high region is observed with an ~ N-S trend in the central part of TT. This gravity high anomaly, which is wider in the south and narrower in the north, is superimposed over a high amplitude negative gravity anomaly. In addition, there exists several isolated gravity highs, which are associated with the bathymetric highs identified within the TT region and along-strike of CKE.

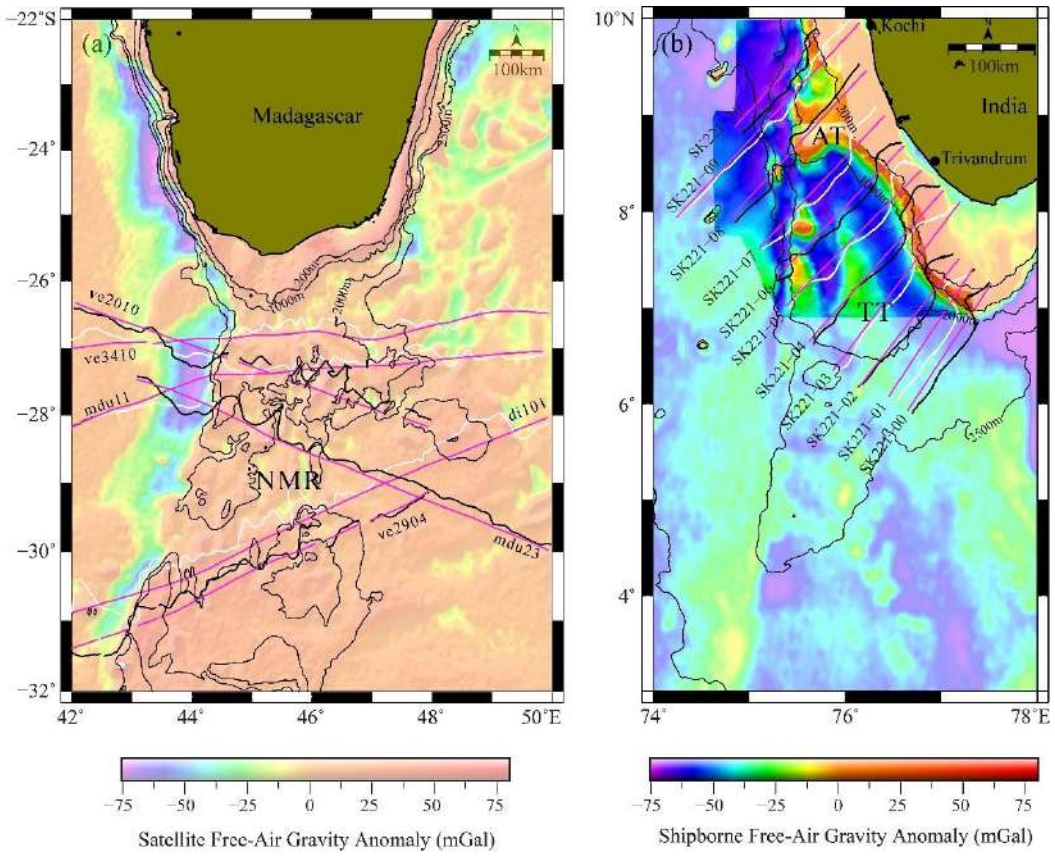

Figure 7.4: (a) Satellite-derived free-air gravity anomaly map with sea-surface gravity anomaly data plotted perpendicular to the track over NMR; (b) Shipborne free-air gravity anomaly image over the ATTC region plotted with the background of satellite-derived free-air gravity anomaly. Also plotted the selected shipborne free-air gravity anomaly profiles perpendicular to the track. Other details are as in Figure 7.1.

7.2.3 Magnetic signatures

(a) Northern Madagascar Ridge

The shipborne magnetic data available over the Northern Madagascar Ridge is limited and therefore to have a broader picture of the magnetic signature of the NMR, used EMAG2 magnetic anomaly grid (Maus et al. 2009) used along with the available sea-surface magnetic data. The 2-dimensional magnetic anomaly image and the track-along profiles (Figure 7.5a) exhibit complex magnetic anomaly pattern over the NMR that do not show any correlation from profile-to-profile. Some of these high-amplitude and short wavelength anomalies correspond to the bathymetric highs while others are not correlatable to any bathymetric features. The amplitude of the magnetic anomalies over NMR are higher compared to those in the adjacent Mozambique Basin in the west and the Mascarene Basin in the east. The amplitude of the magnetic anomalies also varies along the strike of the NMR, with highest amplitude north of 29°S.

(b) Alleppey-Trivandrum Terrace Complex

The magnetic anomaly map (Figure 7.5b) of the ATTC region presented using the EMAG2 magnetic anomaly grid (Maus et al. 2009) along with the up-to-date compiled sea-surface magnetic data. The magnetic anomaly map depicts the presence of complex magnetic anomalies with variable amplitudes on the ATTC and the adjoining Laccadive Basin in the west and the continental shelf in the east. The continental shelf is associated with relatively high amplitude and high frequency anomalies while the Laccadive Basin is associated with lower amplitude anomalies. The magnetic anomaly map shows the presence of several prominent high amplitude magnetic anomalies over the ATTC region and the Chain-Kairali Escarpment. In some areas of CKE, there is obvious correspondence for these magnetic anomalies with bathymetric highs.

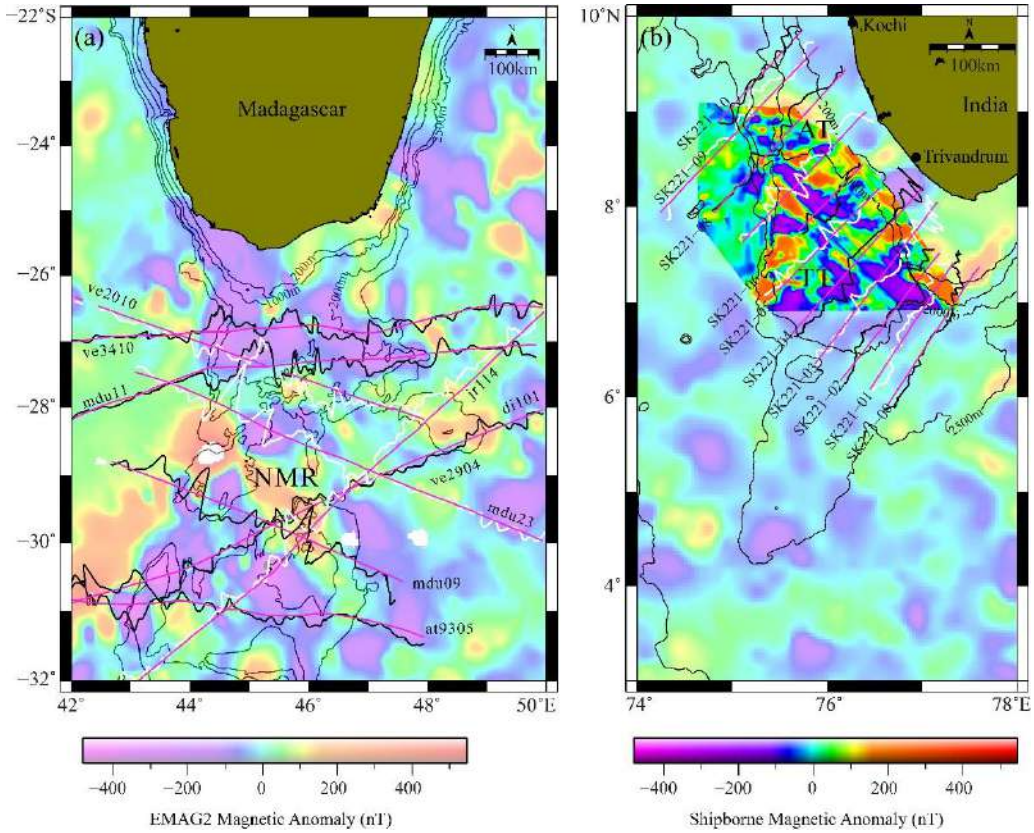

Figure 7.5: (a) EMAG2 magnetic anomaly map with sea-surface magnetic anomaly data plotted perpendicular to the track over NMR, (b) Shipborne magnetic anomaly image over the ATTC region plotted with the background of EMAG2 magnetic anomaly grid. Also plotted the selected shipborne magnetic anomaly profiles perpendicular to the track. Other details are as in Figure 7.1.

7.3 Crustal configurations of NMR and ATTC

7.3.1 Crustal configuration of the Northern Madagascar Ridge

To derive the crustal configuration of the Northern Madagascar Ridge, carried out integrated forward modelling of gravity and magnetic data along a representative profile, di-101 that cut across the Mozambique Basin, Northern Madagascar Ridge and the Mascarene Basin. As a first step, forward modelling of gravity anomalies has been performed based on the method of Talwani et al. (1959). An initial model constructed by considering all the geological and geophysical constraints available from different domains within the study area. The seafloor depth has been obtained from the sea-surface bathymetry data available along the

profile. Since there is no basement information available along the profile or its nearby areas, the sediment thickness information from the global 5-arc-minute total sediment thickness grid (Straume et al. 2019) used to constrain the basement. While constructing the initial model, the published velocity-depth information derived based on the seismic refraction studies carried out in the Mozambique Basin (Leinweber et al. 2013) and NMR (Goslin et al. 1981) for getting the constraints in deeper layers has been used. Since no seismic information is available for the Mascarene Basin, the velocity-depth information for a standard oceanic crust (Fowler, 2005) utilised. Based on the geophysical and geological framework of the study area, it is considered two-layered oceanic crust for Mozambique and Mascarene basins and two-layered continental crust under NMR. Seismic velocity information is converted into density values using the velocity-density relationship (Brocher, 2005). The model is refined further keeping these density values and seafloor depth unchanged, and by changing the Moho depth and thickness of different layers slightly to get a reasonably good fit with computed and observed gravity anomalies.

Once a reasonably good fit for the gravity model is obtained, attempt has been made to derive the magnetic source bodies fitting within the crustal configuration derived from the gravity anomalies. This is achieved by carrying out the forward modelling of magnetic data based on Talwani and Heitzler (1964) method. For this, considered the magnetic anomalies are resulted due to the presence of volcanic intrusives present in the crust, in light of the understanding on tectonic framework of the study area. The paleomagnetic studies (Storey et al. 1995; Torsvik et al. 1998) carried out in the Madagascar mainland and coastal regions revealed the wide-spread volcanism during the Late Cretaceous. Based on the radiometric age determination (~ 84-90 Ma), the genesis of these volcanics has been attributed to the Marion hotspot volcanism (Storey et al. 1995; Torsvik et al. 1998). Since this timing falls within the Cretaceous normal superchron, the volcanic intrusives are of normal polarity (Torsvik et al. 1998). Average values of inclination and declination (Average Remnant Inclination = -65°; Average Remnant Declination = 358°) have taken from the paleomagnetic data (Torsvik et al. 1998). The magnetic susceptibility values are considered within the range of 2.5-4.0 A/m. Once these parameters are fixed, the shape and extent of the intrusive bodies are

adjusted to obtain a good fit between observed and calculated magnetic anomalies through several iterations. The derived crustal model (Figure 7.6) suggests that the crust underlying the Mozambique and Mascarene Basin can be explained in terms of two-layered oceanic crust with an average thickness of 6-7 km. The model suggests a crustal thickness of ~ 16-17 km for the Northern Madagascar Ridge, with its Moho located at ~ 22 km. The magnetic anomalies over the Northern Madagascar Ridge can be explained in terms of volcanic intrusions occurred during a normal polarity. Therefore, considering the density and magnetic structures and the thickness of the crustal layers, it is inferred that the crust underlying the Northern Madagascar Ridge can reasonably be explained in terms of thinned continental crust intermingled with volcanic intrusives.

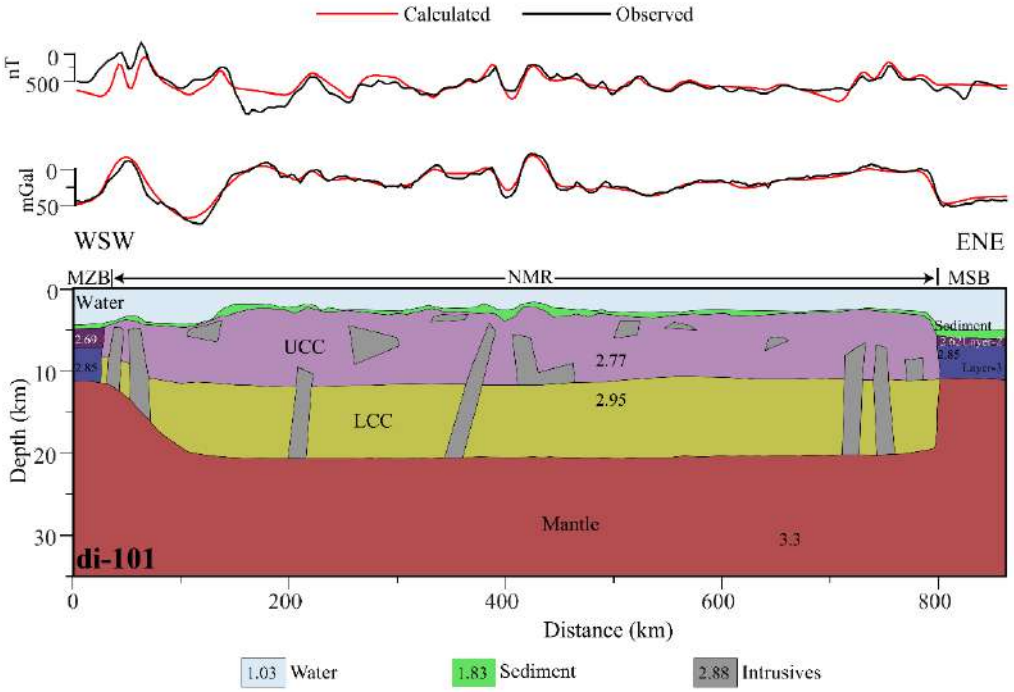

Figure 7.6: Crustal model of the NMR derived based on integrated gravity-magnetic modelling along the profile di-101. The constraints used have been discussed in the text. UCC: Upper continental crust; LCC: Lower continental crust.

7.3.2 Crustal configuration of the ATTC

To derive the crustal configuration of the ATTC, a profile ABC (profile AB extracted from satellite-derived free air gravity anomalies / global bathymetry and profile BC representing shipborne data along SK221-03) has been selected that cut

across a portion of the Laccadive Basin, ATTC and continental shelf. While constructing the initial model along this profile, it has adopted all the constraints from the crustal model derived for ATTC and the adjacent regions along SK221-05 from Yatheesh et al. (2013). As in the case of Northern Madagascar Ridge, as first step, carried out forward modelling of gravity data and then incorporated the magnetic source bodies based on forward modelling of magnetic data. The prominent magnetic anomalies along the profile SK221-03 can be considered to have caused by volcanic intrusives within the ATTC region since a large number of volcanic rocks formed by Marion hotspot volcanism have been identified within the proximity of this region. This constraint is adopted from the paleomagnetic studies carried out in the Indian mainland (Radhakrishna and Joseph, 2012) as well as the St. Mary Island (Torsvik et al. 2000), which revealed the normal magnetization characteristics of the volcanic intrusives. The volcanic intrusives are included as dykes and sills, in which dyke is extended to the Moho derived through modelling. Besides, the magnetic properties of the intrusives are limited to a depth of ~ 22 km, based on the Curie point temperature of ~ 580°C. All intrusive bodies are considered with an average remanent inclination of -56° and declination of 315°, by averaging of all normally magnetized bodies.

The derived crustal model (Figure 7.7) suggests that, in the continental shelf region, Moho is at a depth of 33 km and it shallows down to ~ 22 km in the boundary between ATTC and the Laccadive Basin. Therefore, the derived model suggests a crustal thickness of ~ 30 km under the continental shelf region thinning to ~ 16-17 km in the westernmost extent of the ATTC. Therefore, considering the density and magnetic structures and the thickness of the crustal layers, it is inferred that the crust underlying the Alleppey-Trivandrum Terrace Complex can reasonably be explained in terms of thinned continental crust intermingled with volcanic intrusives.

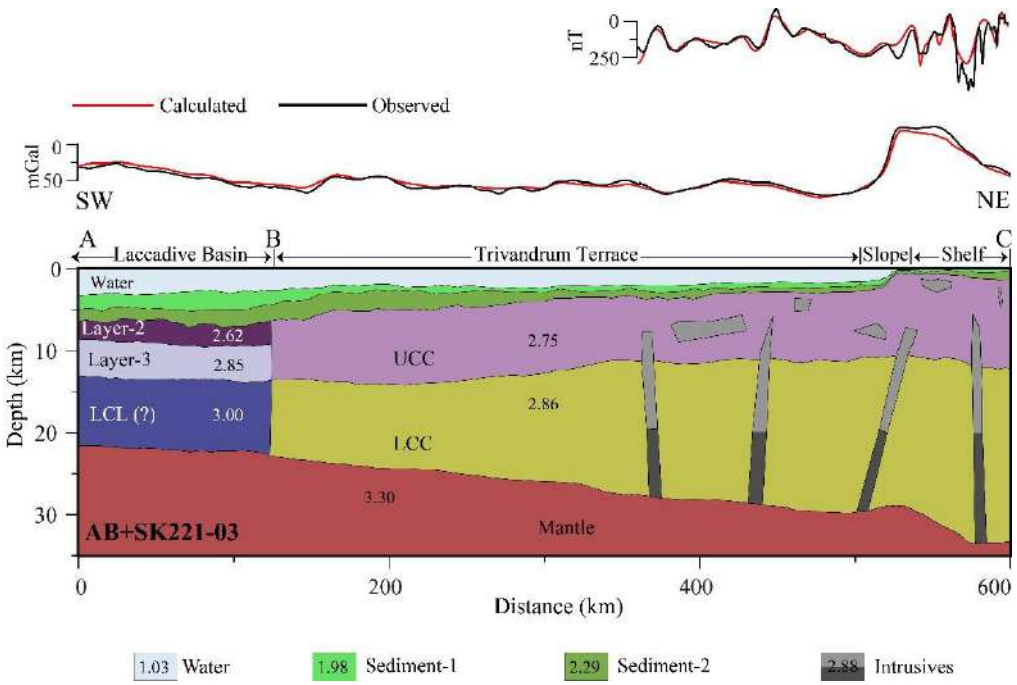

Figure 7.7: Crustal model of the ATTC derived based on integrated gravity-magnetic modelling along the profile ABC (AB+SK221-03). UCC: Upper continental crust; LCC: Lower continental crust; LCL: High velocity lower crustal layer.

7.4 Comparison of crustal structure of NMR and ATTC

The revised plate tectonic reconstruction model shows that the Alleppey-Trivandrum Terrace Complex fits well in a bathymetric notch on the Northern Madagascar Ridge in the immediate pre-drift scenario, at ~ 88.0 Ma (Figure 7.8a). This implies that geometries of both these features were formed after ~ 88 Ma, and prior to this period, both these features form a single unit of a crustal block. If the postulated juxtaposition of these features based on plate tectonic reconstruction is correct, then both these features should show a very similar crustal structure, even though some modifications might occur due to the geodynamic events occurred after their separation.

The exercise to derive the crustal configuration of these postulated conjugate features reveals that both these features can be explained in terms of thinned continental crust intermingled with volcanics. The derived crustal model for the Northern Madagascar Ridge suggests a two-layered continental crust with a total thickness of ~ 16-17 km in the eastern side at the continent-ocean boundary between

the NMR and the Mascarene Basin (Figure 7.8b). Similarly, the derived crustal model for the Alleppey-Trivandrum Terrace Complex suggests a two-layered continental crust with a total thickness of ~ 16-17 km in the continent-ocean boundary between ATTC and the Laccadive Basin (Figure 7.8c). The derived model for NMR further shows that the magnetic anomalies over the Northern Madagascar Ridge can be explained in terms of volcanic intrusion within the thinned continental crust. Similarly, the derived crustal model for ATTC suggests that the magnetic anomalies over this feature also can reasonably be explained in terms of volcanic intrusion within the thinned continental crust. Therefore, the above observations, complemented by the postulated juxtaposition observed from the plate tectonic reconstruction, strongly support that both these features existed as a single unit prior to ~ 88.0 Ma and this feature fragmented and broke away soon after ~ 88.0 Ma, possibly by the Marion hotspot activity. This age constraint comes from the age of the volcanic rocks identified from Madagascar side (Storey et al. 1995; Torsvik et al. 1998; Torsvik et al. 2000) and Indian side (Valsangkar et al. 1981; Radhakrishna et al. 1994; Radhakrishna et al. 1999; Anilkumar et al. 2001; Pande et al. 2001; Melluso et al. 2009; Radhakrishna and Joseph, 2012; Mohan et al. 2016; Sheth et al. 2017).

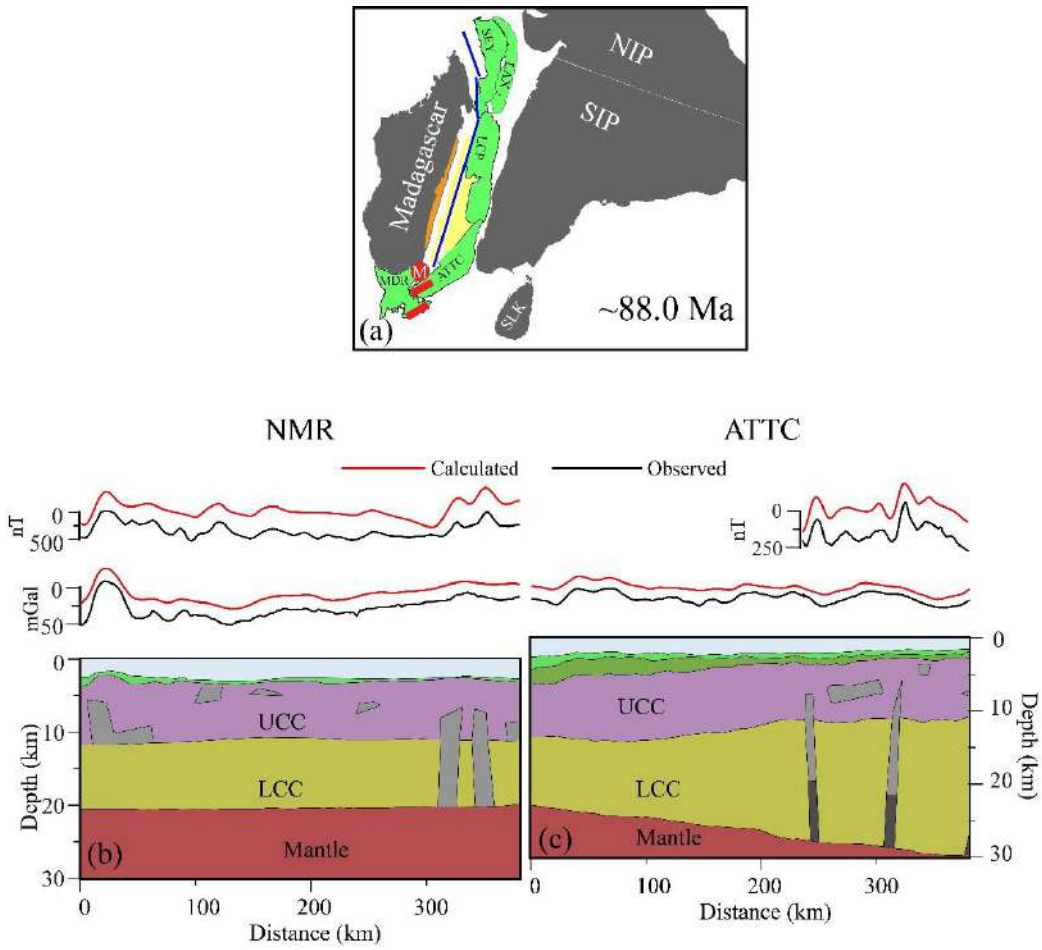

Figure 7.8: (a) Plate tectonic reconstruction map (in fixed Madagascar reference frame, modified after Yatheesh, 2020) showing relative configuration of India and Madagascar in their pre-break up scenario (~ 88 Ma) with location of the profiles (shown as thick lines) along which the section of the crustal model presented as (b) and (c); (b) Selected portion of the crustal model derived in the eastern side of NMR near inferred continent-ocean boundary; (c) Selected portion of the crustal model derived in the southern end of ATTC near inferred continent-ocean boundary. Other details are as in Figures 7.6 and 7.7.

7.5 Early opening of the Arabian Sea from pre-drift to 56.4 Ma

The revised plate tectonic reconstruction model shows that the Alleppey-Trivandrum Terrace Complex fits well in a bathymetric notch on the Northern Madagascar Ridge in the immediate pre-drift scenario, at ~ 88.0 Ma (Figure 7.8a). To understand the subsequent evolution of these major continental blocks and the intervening continental slivers, plate tectonic reconstruction maps have been generated using the rotation parameters that constrain the relative motion among the various pairs of continental blocks (Table 7.1) with the help of GPlates software. All the additional tectonic elements identified in the present study such as the locations of the identified isolated bathymetry highs and the Sagar Kanya bathymetric high complex also have been included in the reconstruction models.

Table 7.1: Finite rotation parameters describing relative motions among various plates used for making plate-tectonic reconstruction maps in the present study. Ages are after Cande and Kent (1995). CST: Cessation of spreading / rifting; INT: Initiation of spreading / rifting.

Chron	Age (Ma)	Finite rotation parameters			Reference
		Lat. (deg.)	Long. (deg.)	Angle (deg.)	
a) Seychelles block to Laxmi Ridge (Fixed LAX)					
C26ny	57.55	19.61	25.62	30.73	Royer et al. (2002)
C27ny	60.92	18.83	24.86	35.41	Royer et al. (2002)
C28ny	62.50	22.08	7.93	28.04	Shuhail et al. (2018)
Close-fit	65.00	20.75	-47.00	24.75	Shuhail et al. (2018)
b) Laxmi Ridge to Southern Indian Protocontinent (Fixed SIP)					
CST	56.40	-8.95	78.79	0.00	Bhattacharya and Yatheesh (2015)
C26no	57.91	-8.95	78.79	-0.10	Bhattacharya and Yatheesh (2015)
C28ny	62.50	-8.95	78.79	-0.46	Bhattacharya and Yatheesh (2015)
C28no	63.63	-8.95	78.79	-1.00	Bhattacharya and Yatheesh (2015)
C29ny	63.98	-8.95	78.79	-1.74	Bhattacharya and Yatheesh (2015)
C29no	64.75	-8.95	78.79	-2.70	Bhattacharya and Yatheesh (2015)
C30ny	65.58	-8.95	78.79	-3.02	Bhattacharya and Yatheesh (2015)
C30no	67.61	-8.95	78.79	-4.20	Bhattacharya and Yatheesh (2015)
INT	68.50	-8.95	78.79	-8.50	Bhattacharya and Yatheesh (2015)
c) Saurashtra Volcanic Platform to Laxmi Ridge (Fixed SVP)					
CST	56.40	20.68	56.77	0.00	Bhattacharya and Yatheesh (2015)
C28ny	62.50	20.68	56.77	-1.28	Bhattacharya and Yatheesh (2015)
C29no	64.75	20.42	60.79	-9.76	Bhattacharya and Yatheesh (2015)
INT	68.50	19.22	70.28	11.11	Bhattacharya and Yatheesh (2015)

Table 7.1 Contd.

Chron	Age (Ma)	Finite rotation parameters			Reference
		Lat. (deg.)	Long. (deg.)	Angle (deg.)	
d)	**Laccadive Plateau to Southern Indian Protocontinent (Fixed SIP)**				
EXT	62.50	90.0	0.0	0.0	Shuhail (2018)
C28no	63.63	11.51	72.99	2.840	Shuhail (2018)
C29no	64.75	12.33	71.67	4.484	Shuhail (2018)
C30ny	65.58	14.10	69.87	4.599	Shuhail (2018)
C31no	68.74	14.14	68.99	8.010	Shuhail (2018)
INT	88.00	15.26	68.32	20.00	Shuhail (2018)
e)	**Northern to Southern Indian Protocontinent (Fixes SIP)**				
CST	56.40	26.00	94.00	0.00	Bhattacharya and Yatheesh (2015)
INT	68.50	26.00	94.00	0.50	Bhattacharya and Yatheesh (2015)
f)	**Greater Mascarene-India to Madagascar (Fixed MAD)**				
CST	60.25	-15.91	-163.75	0.00	Eagles and Wibisono (2013)
C27ny	60.92	-15.99	-163.66	0.57	Eagles and Wibisono (2013)
C28ny	62.50	-18.09	-160.76	2.06	Eagles and Wibisono (2013)
C28no	63.63	-17.26	-161.82	3.05	Eagles and Wibisono (2013)
C29no	64.75	-17.11	-162.41	5.06	Eagles and Wibisono (2013)
C30ny	65.56	-15.06	-158.30	6.94	Eagles and Wibisono (2013)
C30no	67.61	-16.73	-158.93	9.59	Eagles and Wibisono (2013)
C31no	68.74	-18.51	-160.06	10.27	Eagles and Wibisono (2013)
C32n1y	71.07	-20.29	-160.67	11.96	Eagles and Wibisono (2013)
C33ny	73.62	-22.42	-162.39	13.12	Eagles and Wibisono (2013)
C33no	79.08	-31.59	-171.23	13.58	Eagles and Wibisono (2013)
C34ny	83.00	-28.54	-163.35	15.68	Shuhail et al. (2018)
INIT	88.00	-31.21	-163.68	16.97	Shuhail et al. (2018)
CST	60.25	-15.91	-163.75	0.00	Eagles and Wibisono (2013)

Based on this revised plate tectonic reconstruction model (Bhattacharya and Yatheesh, 2015; Shuhail et al., 2018; Shuhail, 2018), the early opening of the Arabian Sea can be explained in terms of rifting and drifting among Southern Indian Protocontinent (SIP), Northern Indian Protocontinent (NIP), Madagascar (MAD) and Seychelles (SEY), along with the microcontinental slivers of the Laxmi Ridge (LAX), Laccadive Plateau (LCP) and the Saurashtra Volcanic Platform (SVP), starting from 88.0 Ma to 56.4 Ma. At around 88 Ma, rifting was initiated between Madagascar and SIP-NIP-LAX-LCP-SEY block (Figure 7.9a) and followed by this, a strike-slip motion occurred between southeast coast of Madagascar and southwest coast of India, resulting in the formation of the Chain-Kairali Escarpment (CKE). This motion also resulted in a configuration where the Alleppey-Trivandrum Terrace Complex (ATTC) broke away from Madagascar side forming a bathymetric notch in the Northern Madagascar Ridge (NMR). The bathymetric high features

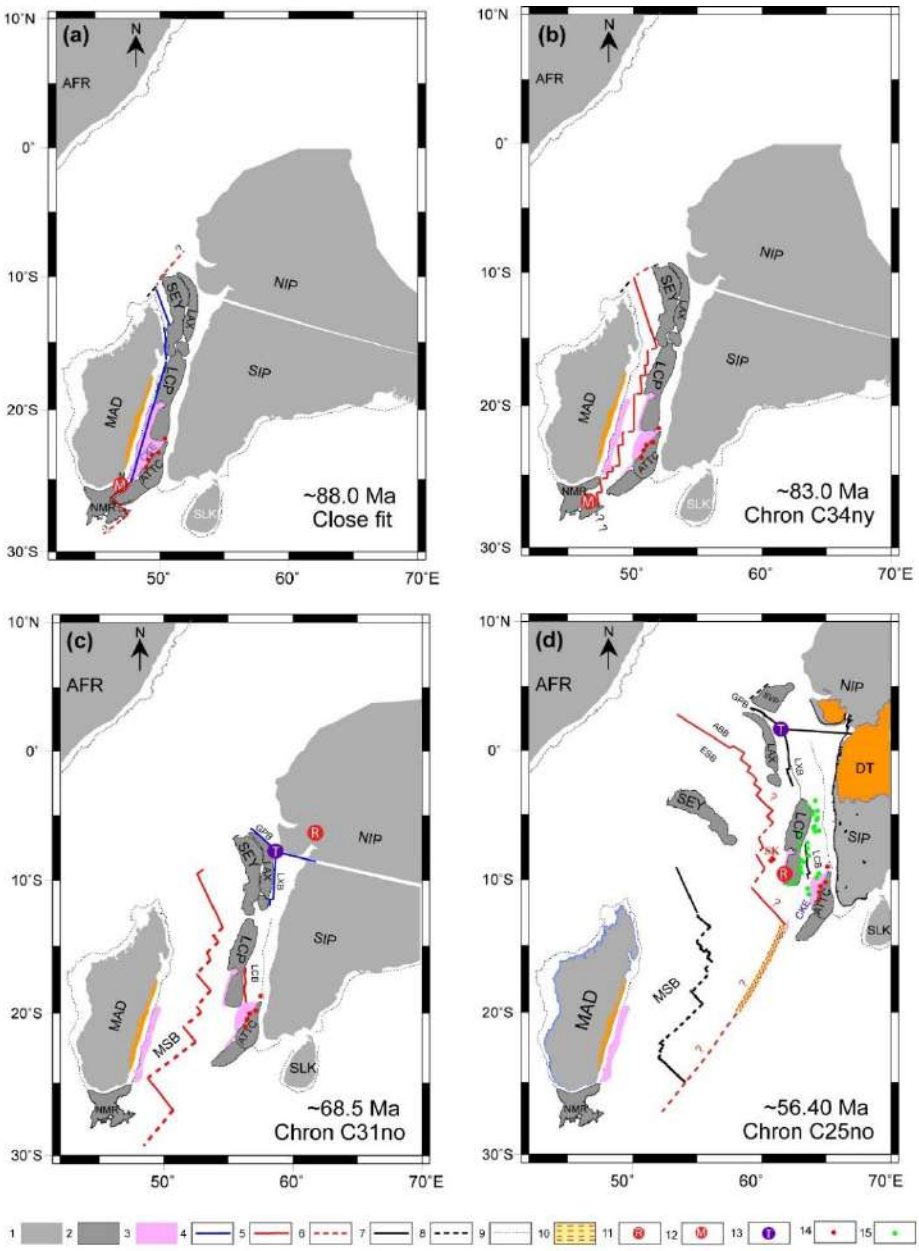

Figure 7.9: Simplified plate tectonic reconstruction maps in fixed Africa reference frame, depicting evolution of the ocean basins and associated tectonic features during early opening period of the Arabian Sea (compiled from Bhattacharya and Yatheesh, 2015; Shuhail et al., 2018; Shuhail, 2018; Yatheesh, 2020). (a) at ~ 88.0 Ma; (b) at ~ 83.0 Ma; (c) at ~ 68.5 Ma; (d) at ~ 56.4 Ma. Explanation of items of the legend – [1] Continental blocks; [2] Microcontinents; [3] Ultra-thinned continental crust; [4] Rift axis; [5] Ridge axis; [6] Transform fault; [7] Extinct spreading centre; [8] Paleo Transform fault; [9] 2000 m isobath; [10] En-echelon Fault System; [11] Réunion hotspot location for the time of the

presented reconstruction. [12] Marion hotspot location for the time of the presented reconstruction; [13] Postulated Gop-Narmada-Laxmi (GNL) fossil triple junction off Saurashtra peninsula; [14] location of bathymetric high features proposed to have linkage with Marion hotspot volcanism; [15] location of bathymetric high features proposed to have linkage with Réunion hotspot volcanism. [AFR] Africa; [DT] Deccan Trap.

near the continental shelf-slope regions are considered to have generated during this period as rift related volcanism caused by the Marion hotspot activity. This was followed by seafloor spreading in the Mascarene Basin, between Madagascar and SIP-NIP-LAX-LCP-SEY block (Figure 7.9b). Subsequently, shortly before 68.7 Ma, rifting was initiated between southwestern part of India and the Laccadive Plateau, and at around 68.5 Ma, rifting was initiated along three arms of the Gop-Narmada-Laxmi (GNL) Triple Junction off Saurashtra (Figure 7.9c). The divergences along these axes later created the Laccadive Basin (LCB), Laxmi Basin (LXB), Gop Basin (GPB) and the Narmada Aulacogen. Rift-drift transition occurred in the Laccadive, Laxmi and Gop basins at chrons C31n (~ 68.7 Ma), C30n (~ 67.6 Ma) and C29r (~ 64.7 Ma), respectively, and at around this time, the spreading ceased in the Northern Mascarene Basin. At around 62.5 Ma, a new spreading axis was initiated between Seychelles and the Laxmi Ridge, creating the conjugate Arabian (ABB) and Eastern Somali (ESB) basins. However, the spreading scenario in the Laxmi, Gop, Laccadive and Southern Mascarene basins continued further and sometime around 60.25 Ma, the spreading in the Southern Mascarene and Laccadive basins ceased. As a result, the Laccadive Plateau and the Laccadive Basin got attached with the Indian Plate, while the Southern Mascarene Basin got welded with the African Plate. Subsequently, at around 56.4 Ma (Figure 7.9d), the axes of divergence in the Gop Basin, Laxmi Basin and the Narmada Rift also became extinct and all these basins got welded to the Indian Plate. During this period, all the bathymetric highs with proposed linkage with Réunion hotspot volcanism were emplaced in the Laccadive Basin and the Laccadive Plateau, including the Sagar Kanya Bathymetric High Complex. Followed by this, seafloor spreading continued along the Carlsberg Ridge accreting oceanic crust in the conjugate Arabian and Eastern Somali basins.

7.6 Summary

The present study is aimed to compare the crustal configurations of the Northern Madagascar Ridge and the Alleppey-Trivandrum Terrace Complex to evaluate their postulated conjugate nature. For this, multibeam bathymetry, gravity and magnetic data were analysed and forward modelling of gravity and magnetic profiles were carried out. The derived crustal model for the NMR suggests that the Moho is nearly flat at a level of ~ 22 km with a crustal thickness of ~ 16-17 km and the magnetic anomalies can be explained in terms of volcanic intrusives. Similarly, the derived crustal configuration of the ATTC suggests that the Moho is at a level of ~ 32 km in the landward side of ATTC, shallowing to a level of ~ 22 km (with a thickness of ~ 16-17 km) at the boundary where the continental-oceanic crustal transition occurs between ATTC and the Laccadive Basin. The magnetic anomalies over the ATTC also have been interpreted in terms of volcanic intrusions. Comparison of the crustal configuration derived for these features reveal that both these features can be explained in terms of ~ 16-17 km thick thinned continental crust intermingled with volcanic intrusives. Therefore, based on these observations derived from the integrated interpretation of geophysical data, complemented by the postulated juxtaposition observed from the plate tectonic reconstruction, it support the earlier interpretation (Yatheesh et al., 2006; Yatheesh et al., 2013a; Bhattacharya and Yatheesh, 2015) that the NMR and ATTC represent conjugate features that was proposed based on the fitting of shape and size of the bathymetric notch observed in the southeastern continental margin of Madagascar with a bathymetric protrusion observed in the southwestern continental margin of India in the India-Madagascar pre-drift scenario. These features remained as a single unit prior to ~ 88 Ma and subsequently got separated during the India-Madagascar breakup. The bathymetric highs in the continental slope regions were considered to have formed during the breakup and moving away of the Alleppey-Trivandrum Terrace Complex and the Northern Madagascar Ridge, as rift related volcanics caused by the Marion hotspot shortly after 83.0 Ma. This moving away was further continued and shortly before 56.4 Ma, the location of the Réunion hotspot reached to the proximity of the Laccadive Basin and Laccadive Plateau and resulted the formation of the bathymetric highs in the Laccadive Basin and the Laccadive Plateau, including the Sagar Kanya Bathymetric High Complex.

Chapter 8

Summary and Conclusions

8.1 Introduction

The present study deals with the detailed understanding of the geomorphological signatures and morphotectonic architecture of the postulated continental slivers in the southwestern continental margin of India and its conjugate region of Madagascar. The data used for this study mainly consists of high-resolution multibeam bathymetry data, sea-surface gravity, magnetic and bathymetry profiles; satellite-derived gravity data; multichannel seismic sections; published seismic reflection and refraction results; and the geographic extent of the offshore and onshore tectonic elements.

8.2 Summary

The formation of the Indian Ocean and its adjacent continental margins were resulted by the breakup and spreading of the eastern sector of the Gondwanaland. The rifting followed by drifting of the continental blocks (Africa, Madagascar, Antarctica, India, Australia and Arabia) caused formation of various ocean basins in the Indian Ocean. Most of the Indian Ocean regions were studied through the geo-scientific investigations during the International Indian Ocean Expedition (IIOE) in the 1960s. Contemporarily, the concept of seafloor spreading was getting accepted into the theory of plate tectonics. Based on this concept and preliminary geophysical data collected during IIOE, researchers proposed a broad plate tectonic evolutionary history for the Indian Ocean by providing large-scale plate reconstruction models. Subsequent studies improved the identifications of magnetic anomalies in different ocean basins, and provided improved models for describing the sectoral plate tectonic evolution.

In the revised plate tectonic evolution model published by Bhattacharya and Yatheesh (2015), several postulated continental blocks (Northern Madagascar Ridge, Alleppey-Trivandrum Terrace Complex, Laccadive Plateau, Laxmi Ridge, and the Saurashtra Volcanic Platform) were accommodated as intervening continental slivers between India and Madagascar in their pre-breakup scenario. This proposal is mainly based on the existing information, the shape and fitting of

these features in the tectonic evolutionary model. The detailed understanding of the crustal architecture of these postulated microcontinental blocks are yet to be confidently established. In addition, the southwestern continental margin of India and its adjacent regions have experienced various geodynamic events that might have created imprints over the onshore as well as offshore regions, and the detailed morphological study on this aspect is awaiting. Therefore, present study aims the detailed understanding of the geomorphological signatures and morphotectonic architecture of the postulated continental slivers in the southwestern continental margin of India, associated deep offshore regions and its conjugate region of Madagascar.

The high-resolution bathymetric map of the southwestern continental margin of India and the adjacent deep offshore regions highlights 33 bathymetric high features, consisting of 14 seamounts, 8 hills, 3 knolls, 2 guyots and 6 plateaus. The inferred basement configuration suggests that some of the bathymetric features might represent volcanic extrusives while others might represent basement highs associated with bulging of sediment layers over the subsurface volcanic intrusive. The sea-surface gravity signatures of the selected features suggest a characteristic relatively high gravity anomaly superimposed over a regional negative anomaly. The magnetic anomalies over the bathymetric high features exhibits complex behaviour and it is difficult to correlate this only with the topography. Both negative and positive magnetic anomalies are observed over the features, superimposed over the regional magnetic signatures. Based on the proximity to the St. Mary Islands and the Ezhimala Igneous Complex, which are considered to be a product of the Marion hotspot volcanism, it is considered that the bathymetric highs located in the southwestern continental slope of India and along-strike of Chain-Kairali Escarpment were formed by the Marion hotspot volcanism. The bathymetric features in the Laccadive Basin and eastern part of the Laccadive Plateau are in the proximity of the Réunion hotspot track and therefore the genesis of these features are attributed to the Réunion hotspot volcanism.

The high-resolution bathymetric map suggests that the Laccadive Plateau is associated with irregular topography, with the presence of several islands, banks, isolated bathymetric highs and scour/depression like features. The multichannel seismic reflection suggests the presence of a region of faulted basement and graben

structures suggesting a rift system in the crestal part of the Laccadive Plateau. The gravity anomalies of the Laccadive Plateau are associated with a belt of relatively positive anomalies bounded by relatively negative anomalies in the east and west, some of these high-amplitude free-air gravity anomalies are characterized by their correspondence with isolated bathymetry highs while others have no correspondence with the seafloor features. The Laccadive Plateau is associated with broad wavelength and high amplitude magnetic anomalies with superimposed secondary high-frequency magnetic anomalies at places, most of these high-amplitude magnetic anomalies are correlatable with the gravity and bathymetric signatures. The integrated forward modelling of the gravity and magnetic anomalies shows that the Laccadive Plateau can be explained as ~ 18-19 km thick two-layered continental crust, with magnetized intrusive bodies causing the magnetic anomalies. This derived crustal structure, in conjunction with the other geophysical signatures supporting the continental origin of the Laccadive Plateau, suggests that the Laccadive Plateau can surely be explained in terms of a thinned continental crust intermingled with volcanic intrusives.

The high-resolution multibeam bathymetric map of the Arabian Basin (southwest of Laccadive Plateau) suggests the presence of a nearly elliptical bathymetric high complex consisting of three seamounts and several linear ridge-like features surrounding a region of nearly flat seafloor measuring ~ 50 km x 30 km. This bathymetric high complex is referred to as the Sagar Kanya Bathymetric High Complex (SKBHC), constituting Sagar Kanya-1 (SK-1), Sagar Kanya-2 (SK-2) and Sagar Kanya-3 (SK-3) seamounts. The free-air gravity anomalies of the Sagar Kanya Bathymetric High Complex are correlated with topography in general, with their maximum corresponding to the locations of the summit of the seafloor features. The magnetic anomalies over the study area are complex, consisting of several positive and negative magnetic anomalies. The morphology of the Sagar Kanya Bathymetric High Complex appears to qualify to be considered as the rim surrounding the summit caldera of a large extinct submarine volcano, referred to as the Sagar Kanya Volcano. Considering the tectonic framework of the western continental margin of India and the adjacent deep ocean basins, the genesis of these phases of volcanism has been attributed to the Réunion hotspot.

The proposed conjugate nature of Northern Madagascar Ridge and Alleppey-Trivandrum Terrace Complex is analysed in terms of geophysical signatures and the derived crustal model. Comparison of the crustal configuration derived for these features reveal that both these features can be explained in terms of thinned continental crust intermingled with volcanic intrusives. Therefore, based on these observations derived from the integrated interpretation of geophysical data, complemented by the postulated juxtaposition observed from the plate tectonic reconstruction, it support the earlier interpretation (Yatheesh et al., 2006; Yatheesh et al., 2013b; Bhattacharya and Yatheesh, 2015) that the Northern Madagascar Ridge and Alleppey-Trivandrum Terrace Complex represent conjugate features that was proposed based on the fitting of shape and size of the bathymetric notch observed in the southeastern continental margin of Madagascar with a bathymetric protrusion observed in the southwestern continental margin of India in the India-Madagascar pre-drift scenario. These features remained as a single unit prior to ~ 88 Ma and subsequently got separated during the India-Madagascar breakup. The bathymetric high features located close to the continental slope of Indian appears to have formed during this period as a result of the Marion hotspot volcanism and the bathymetric highs observed in the Laccadive Basin and Laccadive Plateau, including the Sagar Kanya Bathymetric High Complex were emplaced during subsequent period of evolution of the Arabian Sea.

8.3 Salient inferences from the study

1. The updated high-resolution bathymetric map of the Laccadive Basin and the adjoining regions have been generated and identified 33 individual bathymetric high features.
2. The entire spatial extent of the Sagar Kanya Seamount and its adjacent regions are mapped for the first time. The morphology of the Sagar Kanya Bathymetric High Complex can be considered as the rim surrounding the summit caldera of a large extinct submarine volcano, referred to as the Sagar Kanya Volcano.
3. The genesis of these bathymetric high features are discussed in terms of the geodynamic evolution and tectonic settings of the southwestern continental margin of India. The genesis of bathymetric highs near the continental slope of India is attributed to the Marion hotspot volcanism while those present in

the Laccadive Basin and Laccadive Plateau is attributed to the Réunion hotspot volcanism.

4. The crustal configuration of the Laccadive Plateau can be explained as thinned continental crust intermingled with volcanic intrusives, with crustal thickness gradually increasing from the western end towards the Padua Bank.
5. The proposed conjugate nature of the Northern Madagascar Ridge and the Alleppey-Trivandrum Terrace Complex were analysed and demonstrated that both these features can be explained as conjugate features containing thinned continental crust intermingled with volcanic intrusives, exhibiting crustal thickness of ~ 17 km at their conjugate continent-ocean boundaries.
6. Detailed plate tectonic evolution model for the southwestern continental margin of India and its adjoining regions have prepared incorporating the major results from the present study.

8.4 Scope for Further Studies

The present study provided important evidences on the submarine geomorphology and morphotectonic architecture of the postulated continental slivers in the southwestern continental margin of India and its conjugate region of Madagascar. However, more studies and selected ground truth data will be required to enhance the confidence in these inferences derived from geophysical interpretations. Following are some suggested geophysical studies, which may be pursued further.

1. The genesis of bathymetric high features located in the Laccadive Basin and the adjoining regions have been proposed considering the plate tectonic evolution framework of the western continental margin of India. Geochronological, paleomagnetic and geochemical investigations of the volcanic rocks collected from these identified features may provide information on age of formation of these features as well as validation to the postulations made in the present study on their genesis.

2. The postulation of Sagar Kanya Bathymetric High Complex as a submarine volcanic caldera is mainly based on the seafloor morphology of this

anomalous feature and its resemblance to the geometry of a volcanic caldera. Analysis of multichannel seismic reflection data acquired across the SKBHC in different radial directions will help to provide the detailed information on the morphological elements such as the topographic rim, inner caldera walls, caldera-bounding faults, intra-caldera fill and the flanks of the Sagar Kanya Volcano.

3. Existence of a nearly N-S trending rift system has been proposed along the crestal region of the Laccadive Plateau. A detailed investigation based on the closely-spaced multichannel seismic reflection, gravity and magnetic data will help to evaluate the existence and extent of this postulated rift system.

References

1. Agrawal, P.K., Pandey, O.P., Negi, J.G., 1992. Madagascar: A continental fragment of the paleo-super Dharwar craton of India. Geology, 20, 543-546.
2. Ajay, K. K., Chaubey, A. K., Krishna, K. S., Rao, D. G., Sar, D., 2010. Seaward dipping reflectors along the SW continental margin of India: Evidence for volcanic passive margin. Journal of Earth System Science, 119(6), 803–813.
3. Anand, S.P., Nair, N., Rajaram, M., 2014. Structure and evolution of the Laccadive Ridge from the analysis of free air gravity anomalies. Journal of Geophysics, 35, 97-102.
4. Anil Kumar, Pande, K., Venkatesan, T.R., Bhaskar Rao, Y.J., 2001. The Karnataka Late Cretaceous dykes as products of the Marion hotspot at the Madagascar-India breakup event: evidence from $^{40}Ar/^{39}Ar$ geochronology and geochemistry. Geophysical Research Letters, 28 (14), 2715-2718.
5. Armistead, S. E., Collins, A. S., Redaa, A., Jepson, G., Gillespie, J., Gilbert, S., Razakamanana, T., 2020. Structural evolution and medium-temperature thermochronology of central Madagascar: implications for Gondwana amalgamation. Journal of the Geological Society, 177(4), 784–798.
6. Ashalatha, B., Subrahmanyam, C., Singh, R.N., 1991. Origin and compensation of Chagos-Laccadive Ridge, Indian Ocean, from admittance analysis of gravity and bathymetry data. Earth and Planetary Science Letters, 105, 47-54.
7. Avraham, Z.B., Bunce, E.T., 1977. Geological study of the Chagos-Laccadive Ridge, Indian Ocean. Journal of Geophysical Research, 82, 1295-1305.
8. Babenko, K.M., Panaev, V.A., Svistunov, Y.I., Schlezinger, A.Y., 1981. Tectonics of the eastern margin of the Arabian Sea according to seismic data. Geotectonics 18, 37-62.
9. Baker, B. H., Miller, J. A., 1963. Geology and Geochronology of the Seychelles Islands and Structure of the Floor of the Arabian Sea. Nature, 199(4891), 346–348.
10. Baksi, A. K., 2005. Evaluation of radiometric ages pertaining to rocks hypothesized to have been derived by hotspot activity, in and around the Atlantic, Indian, and Pacific Oceans. In G. R. Foulger, J. H. Natland, D. C. Presnall, & D. L. Anderson (Eds.), Plates, plumes and paradigms (Vol. 388). Geological Society of America.
11. Bansal, A. R., Fairhead, J. D., Green, C. M., Fletcher, K. M. U. 2005., Revised gravity for offshore India and the isostatic compensation of submarine features. Tectonophysics, 404(1), 1–22.
12. Barron, E. J., 1987. Cretaceous plate tectonic reconstructions. Palaeogeography, Palaeoclimatology, Palaeoecology, 59, 3–29.

13. Basu, A. R., Renne, P. R., DasGupta, D. K., Teichmann, F., Poreda, R. J., 1993. Early and late alkali igneous pulses and a high-3He plume origin for the Deccan flood basalts. Science, 261(5123), 902–906.
14. Bernard, A., Munschy, M., 2000. Were the Mascarene and Laxmi Basins (western Indian Ocean) formed at the same spreading centre? Comptes Rendus De L Academie Des Sciences Serie Ii Fascicule a-Sciences De La Terre Et Des Planetes, 330, 777-783.
15. Besse, J., Courtillot, V., 1988. Paleogeographic Maps of the Continents Bordering the Indian-Ocean since the Early Jurassic. Journal of Geophysical Research-Solid Earth and Planets, 93, 11791-11808.
16. Bhattacharya, G. C., Chaubey, A. K., Murty, G. P. S., Srinivas, K., Sarma, K. V. L. N. S., Subrahmanyam, V., Krishna, K. S., 1994a. Evidence for seafloor spreading in the Laxmi Basin, northeastern Arabian Sea. Earth and Planetary Science Letters, 125(1), 211–220.
17. Bhattacharya, G. C., Subrahmanyam, V., 1986. Extension of the Narmada - Son lineament on the continental margin off Saurashtra, Western India as obtained from magnetic measurements. Marine Geophysical Researches, 8(4), 329–344.
18. Bhattacharya, G. C., Subrahmanyam, V., 1991. Geophysical study of a seamount located on the continental margin of India. Geo-Marine Letters, 11(2), 71–78.
19. Bhattacharya, G.C., Chaubey, A.K., 2001. Western Indian Ocean - A glimpse of the tectonic scenario. In: Sengupta R., Desa E. (Eds.) The Indian Ocean - A Perspective, Vol 2. Oxford & IBH, pp. 691-729.
20. Bhattacharya, G.C., Murty, G.P.S, Srinivas, K., Chaubey, A.K., Sudhakar, T., Nair, R.R., 1994b. Swath bathymetric investigation of the seamounts located in Laxmi Basin, Eastern Arabian Sea. Marine Geodesy, 17, 169-182.
21. Bhattacharya, G.C., Yatheesh, V., 2015. Plate-tectonic evolution of the deep ocean basins adjoining the western continental margin of India - a proposed model for the early opening scenario, In: Mukherjee, S. (Ed.), Petroleum Geoscience: Indian Contexts. Springer, pp. 1-61.
22. Bhowmik, S. K., Bernhardt, H.-J., Dasgupta, S., 2010. Grenvillian age high-pressure upper amphibolite-granulite metamorphism in the Aravalli-Delhi Mobile Belt, Northwestern India: New evidence from monazite chemical age and its implication. Precambrian Research, 178(1), 168–184.
23. Bijesh, C.M., John Kurian, P., Yatheesh, V., Tyagi, A., Twinkle, D., 2018. Morphotectonic characteristics, distribution and probable genesis of bathymetric highs off southwest coast of India. Geomorphology, 315, 33-44.
24. Biju-Sekhar, S., Yokoyama, K., Pandit, M. K., Okudaira, T., Yoshida, M., Santosh, M., 2003. Late Paleoproterozoic magmatism in Delhi Fold Belt, NW India and its implication: evidence from EPMA chemical ages of zircons. Journal of Asian Earth Sciences, 22(2), 189–207.
25. Biswas, S. K., 1987. Regional tectonic framework, structure and evolution of the western marginal basins of India. Tectonophysics, 135(4), 307–327.

26. Biswas, S.K., 1982. Rift basins in western margin of India and their hydrocarbon prospects with special reference to Kutch Basin. AAPG Bulletin 66, 1497-1513.
27. Biswas, S.K., 1989. Hydrocarbon exploration in western offshore basins of India. In: Recent Geoscientific Studies in the Arabian Sea off India, Geological Survey of India, Special Publication 24, 185-194.
28. Biswas, S.K., Singh, N.K., S. K. Biswas, N.K.S., 1988. Western continental margin of India and hydrocarbon potential of deep-sea basins, 7th Offshore South East Asia Conference. OSEA 88119, Singapore.
29. Boyden, J.A., Müller, R.D., Gurnis, M., Torsvik, T.H., Clark, J.A., Turner, M., Ivey-Law, H., Watson, R.J., Cannon, J.J., 2011. Next-generation platetectonic reconstructions using Plates, in: Keller, G.R., Baru, C. (Eds.), Geoinformatics: Cyberinfrastructure for the Solid Earth Sciences. Cambridge University Press, pp. 95-114.
30. Braun, I., Kriegsman, L. M., 2003. Proterozoic crustal evolution of southernmost India and Sri Lanka. M. Yoshida, B.F. Windley, S. Dasgupta (Eds.), Proterozoic East Gondwana: Supercontinent Assembly and Breakup, 206, Geological Society of London Special Publication, pp. 169-202.
31. Brocher T.M., 2005. Empirical relations between elastic wavespeeds and density in the Earth's crust. Bulletin of the Seismological Society of America, 95(6), 2081-2092.
32. Buck, W. R., 1986. Small scale convection induced by passive rifting: the cause for uplift of rift shoulders. Earth and Planetary Science Letters, 77, 362–372.
33. Calvès, G., Schwab, A. M., Huuse, M., Clift, P. D., Gaina, C., Jolley, D., Inam, A., 2011. Seismic volcanostratigraphy of the western Indian rifted margin: The pre-Deccan igneous province. Journal of Geophysical Research: Solid Earth, 116, B01101, doi:10.1029/2010JB000862.
34. Cande, S.C., Kent, D.V., 1995. Revised calibration of the geomagnetic polarity time scale for the Late Cretaceous and Cenozoic. Journal of Geophysical Research, 100, 6093-6095.
35. Cande, S.C., Patriat, P., 2015. The anticorrelated velocities of Africa and India in the Late Cretaceous and early Cenozoic. Geophysical Journal International, 200, 227-243.
36. Cande, S.C., Patriat, P., Dyment, J., 2010. Motion between the Indian ,Antarctic and African plates in the early Cenozoic. Geophysical Journal International, 183, 127-149.
37. Chakraborty, C., Ghosh, S. K., 2005. Pull-apart origin of the Satpura Gondwana basin, central India. Journal of Earth System Science, 114(3), 259–273.
38. Chaubey, A. K., Bhattacharya, G. C., Murty, G. P. S., Srinivas, K., Ramprasad, T., Rao, D. G., 1998. Early Tertiary seafloor spreading magnetic

anomalies and paleo-propagators in the northern Arabian Sea. Earth and Planetary Science Letters, 154(1), 41–52.

39. Chaubey, A.K., Dyment, J., Bhattacharya, G.C., Royer, J.Y., Srinivas, K., Yatheesh, V., 2002a. Paleogene magnetic isochrons and palaeo-propagators in the Arabian and Eastern Somali basins, NW Indian Ocean. In:Clift, P.D., Croon, D., Gaedicke, C., Craig, J. (Eds.), The Tectonic and Climatic Evolution of the Arabian Sea Region, Geological Society, London, Special Publication 195, 71-85.
40. Chaubey, A. K., Rao, D. G., Srinivas, K., Ramprasad, T., Ramana, M. V, Subrahmanyam, V., 2002b. Analyses of multichannel seismic reflection, gravity and magnetic data along a regional profile across the central-western continental margin of India. Marine Geology, 182, 303-323.
41. Chaubey, A.K., Srinivas, K., Ashalatha, B., Gopala Rao, D., 2008. Isostatic response of the Laccadive Ridge from admittance analysis of gravity and bathymetry data. Journal of Geodynamics, 46, 10-20.
42. Chesner, C.A., 2012. The Toba Caldera Complex. Quaternary International, 258, 5-18.
43. Chetty T. R. K., 2017. Proterozoic orogens of India. A critical window to Gondwana, Elsevier Inc 426 pp.
44. Chetty, T. R. K., 2021. Multiple thrust systems from the Southern Granulite Terrane, India: Insights on Precambrian convergent margin tectonics. Journal of Asian Earth Sciences, 208, 104674.
45. Clague, D. A., Reynolds, J. R., Davis, A. S., 2000. Near-ridge seamount chains in the northeastern Pacific Ocean. Journal of Geophysical Research-Solid Earth, 105, 16541–16561.
46. Clift, P. D., Calvès, G., Jonell, T. N., 2020. Evidence for simple volcanic rifting not complex subduction initiation in the Laxmi Basin. Nature Communications, 11(1), 2733.
47. Clouard, V., Bonneville, A., Gillot, P.-Y., 2003. The Tarava Seamounts: a newly characterized hotspot chain on the South Pacific Superswell. Earth and Planetary Science Letters 207, 117–130.
48. Cole, J.W., Milner, D.M., Spinks, K.D., 2005. Calderas and caldera structures: a review. Earth-Science Reviews, 69(1), 1-26.
49. Collier, J. S., Minshull, T. A., Hammond, J. O. S., Whitmarsh, R. B., Kendall, J.-M., Sansom, V., Rumpker, G., 2009. Factors influencing magmatism during continental breakup: New insights from a wide-angle seismic experiment across the conjugate Seychelles-Indian margins. Journal of Geophysical Research, 114, B03101, doi:10.1029/2008JB005898.
50. Collier, J. S., Minshull, T. A., Kendall, J.-M., Whitmarsh, R. B., Rümpker, G., Joseph, P., Dean, S. M., 2004. Rapid continental breakup and microcontinent formation in the western Indian Ocean. Eos, Transactions American Geophysical Union, 85(46), 481–487.

51. Collier, J. S., Sansom, V., Ishizuka, O., Taylor, R. N., Minshull, T. A., Whitmarsh, R. B., 2008. Age of Seychelles–India break-up. Earth and Planetary Science Letters, 272(1), 264–277.
52. Collins, A. S., Clark, C., Plavsa, D., 2014. Peninsular India in Gondwana: The tectonothermal evolution of the Southern Granulite Terrain and its Gondwanan counterparts. Gondwana Research, 25(1), 190–203.
53. Collins, A. S., Windley, B. F., 2002. The Tectonic Evolution of Central and Northern Madagascar and Its Place in the Final Assembly of Gondwana. The Journal of Geology, 110(3), 325–339.
54. Corfield, R. I., Carmichael, S., Bennett, J., Akhter, S., Fatimi, M., Craig, T., 2010. Variability in the crustal structure of the West Indian Continental Margin in the Northern Arabian Sea. Petroleum Geoscience, 16(3), 257–265.
55. Courtillot, V., Besse, J., Vandamme, D., Montigny, R., Jaeger, J.-J., Cappetta, H., 1986. Deccan flood basalts at the Cretaceous/Tertiary boundary? Earth and Planetary Science Letters, 80(3), 361–374.
56. Courtillot, V., Feraud, G., Maluski, H., Vandamme, D., Moreau, M.G., Besse, J., 1988. Deccan flood basalts and the Cretaceous/ Tertiary boundary. Nature, 333, 843-846.
57. Curray, J.R., Munasinghe, T., 1991. Origin of the Rajmahal Traps and the 85°E Ridge: Preliminary reconstructions of the trace of the Crozet hotspot. Geology, 19, 1237-1240.
58. Das, P., Iyer, S. D., Kodagali, V. N., 2007. Morphological characteristics and emplacement mechanism of the seamounts in the Central Indian Ocean Basin. Tectonophysics, 443(1–2), 1–18.
59. Das, P., Iyer, S. D., Kodagali, V. N., Krishna, K. S., 2005. Distribution and Origin of Seamounts in the Central Indian Ocean Basin. Marine Geodesy, 28(3), 259–269.
60. Devey, C. W., Lightfoot, P. C., 1986. Volcanological and tectonic control of stratigraphy and structure in the western Deccan traps. Bulletin of Volcanology, 48(4), 195–207.
61. DGH, 2014. Directorate General of Hydrocarbons (DGH), Noida, India web page: Kerala Konkan Basin (accessed 29.10.14), http://www.dghindia.org/15.aspx.
62. DGH, 2019. Directorate General of Hydrocarbons (DGH), Noida, India, web page: Kerala Konkan Basin. https://www.ndrdgh.gov.in/NDR/?page_id=814 [Accessed on 02nd November 2019].
63. Druet, M., Muñoz-Martín, A., Granja-Bruña, J.L., Carbó-Gorosabel, A., Llanes, P., Catalán, M., Maestro, A., Bohoyo, F., Martín-Dávila, J., 2019. Bouguer anomalies of the NW Iberian continental margin and the adjacent abyssal plains. Journal of Maps, 15, 635–641.
64. Dubey, C. P., Tiwari, V. M., 2018. Gravity anomalies and crustal thickness variations over the Western Ghats. Journal of the Geological Society of India, 92(5), 517–522.

65. Duncan, R., Pyle, D., 1988. Rapid eruption of the Deccan flood basalts at the Cretaceous/Tertiary boundary. Nature 333, 841–843.
66. Duncan, R.A., 1981. Hotspots in the Southern Oceans - an absolute frame of reference for the motion of the Gondwana continents. Tectonophysics, 74, 29-42.
67. Duncan, R.A., 1990. The volcanic record of the Réunion hotspot. In: R.A. Duncan, Backman, J., Peterson, L.C., et al. (Ed.), Proceedings of ODP Scientific Results. Ocean Drilling Programme, College Station, TX, pp. 3-10.
68. Duncan, R.A., Clague, D.A., 1985. Pacific plate motion recorded by linear volcanic chains. In: Nairn, A.E.M., Stehli, F.G.,Uyeda, S. (Eds.), The Ocean Basins and Margins, Vol. 7A. Plenum, New York, 89–112.
69. Duncan, R.A., Hargraves, R.B., 1990. $^{40}Ar/^{39}Ar$ Geochronology of basement rocks from the Mascarene Plateau, the Chagos Bank, and the Maldives Ridge, in: Backman J., Duncan, R. et al. (Eds.), Proceedings of the Ocean Drilling Program, 115 Scientific Results. Ocean Drilling Program, pp. 43-51.
70. Dyment, J., 1991. Structure et évolution de la lithosphère océanique dans l'océan Indien: apport des anomalies magnétiques. Doctoral Thesis, Université Louis Pasteur, Strasbourg.
71. Dyment, J., 1998. Evolution of the Carlsberg Ridge between 60 and 45 Ma: Ridge propagation, spreading asymmetry, and the Deccan-Reunion hotspot. Journal of Geophysical Research: Solid Earth, 103(10), 24067–24084.
72. Eagles, G., Wibisono, A.D., 2013. Ridge push, mantle plumes and the speed of the Indian plate. Geophysical Journal International 194, 670-677.
73. Faruque, B.M., Ramachandran, K. V, 2014. The continental shelf of western India, in: Chiocci, F.L., Chivas, A.R. (Eds.), The Continental Shelves of the World, Their Evolution during the Last Glacio-Eustatic Cycle. Geological Society of London, London, pp. 213-220.
74. Fisher, R. L., Sclater, J. G., McKenzie, D. P., 1971. Evolution of the Central Indian Ridge, Western Indian Ocean. Geological Society of America Bulletin, 82, 553-562.
75. Fornari, D.J., Perfit, M.R., Allen, J.F., Batiza, R., Haymon, R., Ryan, W.B.F., Smith, T., Simkin, T., Luckman, M.A., 1988. Seamounts as windows into the mantle process: structural and geochemical studies of the Lamont seamounts. Earth and Planetary Science Letters, 89, 63–83.
76. Fornari, D.J., Ryan, W.B.F., Fox, P.J., 1984. The evolution of craters and calderas on young seamounts: insight from sea MARC 1 and Sea Beam sonar surveys of a small seamount group near the axis of the East Pacific Rise at ∼10° N. Journal of Geophysical Research, 89, 11069–11083.
77. Fournier, M., Chamot-Rooke, N., Petit, C., Huchon, P., Al-Kathiri, A., Audin, L., Beslier, M.O., D'Acremont, E., Fabbri, O., Fleury, J.M., Khanbari, K., Lepvrier, C., Leroy, S., Maillot, B., Merkouriev, S., 2010. Arabia-Somalia plate kinematics, evolution of the Aden-Owen Carlsberg

triple junction, and opening of the Gulf of Aden. Journal of Geophysical Research, 115, B04102, doi:10.1029/2008JB006257.
78. Fowler, C.M.R., 2005. The Solid Earth: an Introduction to Global Geophysics. Cambridge University Press, Cambridge.
79. Francis, T.J.G., Shor, G.G., 1966. Seismic refraction measurements in the Northwest Indian Ocean. Journal of Geophysical Research, 71, 427-449.
80. Friend, C. R. L., Nutman, A. P., 1991. SHRIMP U-Pb Geochronology of the Closepet Granite and Peninsular Gneiss, Karnataka, South India. Journal of the Geological Society of India, 38, 357–368.
81. Ganerød, M., Torsvik, T. H., van Hinsbergen, D. J. J., Gaina, C., Corfu, F., Werner, S., Hendriks, B. W. H., 2011. Palaeoposition of the Seychelles microcontinent in relation to the Deccan traps and the plume generation zone in late Cretaceous-early Palaeogene time. Geological Society Special Publication, 357(1), 229–252.
82. GEBCO Compilation Group (2020) GEBCO 2020 Grid, doi:10.5285/a29c5465-b138-234d-e053-6c86abc040b9.
83. Ghatak, A., Basu, A. R., 2011. Vestiges of the Kerguelen plume in the Sylhet Traps, northeastern India. Earth and Planetary Science Letters, 308(1), 52–64.
84. Gibbons, A.D., Whittaker, J.M., Müller, R.D., 2013. The breakup of East Gondwana: Assimilating constraints from Cretaceous ocean basins around India into a best-fit tectonic model. Journal of Geophysical Research-Solid Earth, 118, 808-822.
85. Global Volcanism Program, 1990. Report on Nikko (Japan). In: L. McClelland (Ed.), Bulletin of the Global Volcanism Network. Smithsonian Institution.
86. Gombos, A. M., Powell, W. G., Norton, I. O., 1995. The tectonic evolution of western India and its impact on hydrocarbon occurrences: an overview. Sedimentary Geology, 96(1), 119–129.
87. Goslin J., Recq M., Schlich R.. 1981. Structure profonde du plateau de Madagascar: relations avec le plateau de crozet. Tectonophysics 76, 75-97.
88. Goslin J., Segoufin J., Schlich R., Fisher R.L., 1980. Submarine topography and shallow structure of the Madagascar Ridge, Western Indian Ocean. Geological Society of America Bulletin, 91 (12), 741–753.
89. Gunnell, Y, Fleitout, L., 2000. Morphotectonic evolution of the Western Ghats, India. In Geomorphology and Global Tectonics, pp. 321–339.
90. Gunnell, Y., Harbor, D., 2008. Structural underprint and tectonic overprint in the Angavo (Madagascar) and Western Ghats (India)-Implications for understanding scarp evolution at passive margins. Journal of Geological Society of India, 71, 763-779.
91. Harris, P. T., Macmillan-Lawler, M., Rupp, J., Baker, E. K., 2014. Geomorphology of the oceans. Marine Geology, 352, 4–24.
92. Hooper, P., Widdowson, M., Kelley, S., 2010. Tectonic setting and timing of the final Deccan flood basalt eruptions. Geology, 38(9), 839–842.

93. Hooper, P.R., 1999. The winds of change, The Deccan Traps: A personal perspective, in: Subbarao, K.V. (Ed.), Deccan Volcanic Province. Geological Society of India Memoir, pp. 153-165.
94. IOC-IHO, 2013. Standardization of undersea feature names. Publication B-6, Edition 4.1.0, 18p.
95. IOC-IHO-BODC, 2003. Centenary Edition of the GEBCO Digital Atlas. CD-ROM on Behalf of the Intergovernmental Oceanographic Commission and the International Hydrographic Organization as Part of the General Bathymetric Chart of the Oceans, British Oceanographic Data Centre, Liverpool, UK.
96. Ishwar-Kumar, C., Windley, B. F., Horie, K., Kato, T., Hokada, T., Itaya, T., Sajeev, K., 2013. A Rodinian suture in western India: New insights on India-Madagascar correlations. Precambrian Research, 236, 227–251.
97. Iyer, S.D., 2009. Seamounts- their formation, mineral deposits, biodiversity and atmospheric oxygen. Geo-Spectrum Interface, 4, 33-36.
98. Iyer, S.D., Mehta, C.M., Das, P., Kalangutkar, N.G., 2012. Seamounts - characteristics, formation, mineral deposits and biodiversity. Geologica Acta, 10(3), 295-308.
99. Janardhan, A. S., 1999. Southern Granulite Terrain, South of the Palghat-Cauvery Shear Zone: Implications for India-Madagascar Connection. Gondwana Research, 2(3), 463–469.
100. Kaila, K.L., Bhatia, S.C., 1981. Gravity study along the Kavali-Udipi deep seismic sounding profile in the indian peninsular shield: Some inferences about the origin of anorthosites and the eastern ghats orogeny. Tectonophysics, 79, 129-143.
101. Kale, V. S., 2009. The Western Ghat: The Great Escarpment of India. In: Migon P. (eds) Geomorphological Landscapes of the World. Springer, Dordrecht.
102. Katz, M.B., Premoli, C., 1979. India and Madagascar in Gondwanaland based on matching Precambrian lineaments. Nature, 279, 312-315.
103. Kennedy, B., Stix, J., Vallance, J.W., Lavallée, Y., Longpré, M.-A., 2004. Controls on caldera structure: Results from analogue sandbox modeling. GSA Bulletin, 116(5-6), 515-524.
104. Kodagali V N., 1989. Morphometric Studies on a part of Central Indian Ocean. Journal of Geological Society of India, 33, 547-555.
105. Kodagali, V. N., 1992. Morphologic investigation of uncharted seamount from central Indian Basin revisited with multibeam sonar system. Marine Geodesy, 15, 47–56.
106. Kodagali, V.N., 1998. A pair of seamount chains in the Central Indian Basin, identified from multibeam mapping. Marine Geodesy, 21(2), 147-158.
107. Kolla, V., Coumes, 1990. Extension of structural and tectonic trends from the Indian subcontinent into the Eastern Arabian Sea. Marine and Petroleum Geology, 7(2), 188–196.

108. Krishna, K. S., Gopala Rao, D., Sar, D., 2006. Nature of the crust in the Laxmi Basin (14°–20°N), western continental margin of India. Tectonics, 25, TC1006, doi:10.1029/2004TC001747.
109. Kroener, A., Hegner, E., Collins, A. S., Windley, B. F., Brewer, T. S., Razakamanana, T., Pidgeon, R. T., 2000. Age and magmatic history of the Antananarivo Block, central Madagascar, as derived from zircon geochronology and Nd isotopic systematics. American Journal of Science, 300 (4), 251-288
110. Kumar, A., Pande, K., Venkatesan, T.R., Rao, Y.J.B., 2001.The Karnataka Late Cretaceous Dykes as products of the Marion Hot Spot at the Madagascar–India Breakup Event: Evidence from 40Ar-39Ar geochronology and geochemistry. Geophysical Research Letters, 28, 2715-2718.
111. Kumar, P., Chaubey, A.K., 2019. Extension of flood basalt on the northwestern continental margin of India. Journal of Earth System Science, 128, 81.
112. Kumar, U., Narayan, S., Pal, S. K., 2020. Structural and tectonic interpretation of EGM2008 gravity data around the Laccadive ridge in the Western Indian Ocean: an implication to continental crust. Geocarto International, 1–20.
113. Kunnummal, P., Anand, S. P., 2022. Crustal structure and tectonic evolution of Greater Maldive Ridge, Western Indian Ocean, in the context of plume-ridge interaction. Gondwana Research, 106, 142-163.
114. Kunnummal, P., Anand, S.P., Haritha, C., Rama Rao, P., 2018. Moho depth variations over the Maldive Ridge and adjoining Arabian and Central Indian Basins, Western Indian Ocean, from three dimensional inversion of gravity anomalies. Jornal of Asian Earth Sciences, 156, 316–330.
115. Lawver, L. A., Gahagan, L. M., Dalziel, I., 1998. A Tight fit-Early Mesozoic Gondwana, a Plate Reconstruction Perspective. Memoirs of National Institute of Polar Research. Special Issue, 53, 214–229.
116. Leinweber, V. T., Klingelhoefer, F., Neben, S., Reichert, C., Aslanian, D., Matias, L., Jokat, W., 2013. The crustal structure of the Central Mozambique continental margin — Wide-angle seismic, gravity and magnetic study in the Mozambique Channel, Eastern Africa. Tectonophysics, 599, 170–196.
117. Ludwig, J.W., Nafe, J.E., Drake, C.L., 1970. Seismic refraction. In: A.E. Maxwell (Ed.), The Sea. Wiley, New York, pp. 53-84.
118. Malod, J. A., Droz, L., Kemal, B. M., Patriat, P., 1997. Early spreading and continental to oceanic basement transition beneath the Indus deep-sea fan: northeastern Arabian Sea. Marine Geology, 141(1), 221–235.
119. Mandal, B., Vijaya Rao, V., Karuppannan, P., Raju, S., Ganguli, S. S., 2021. Thick-skinned tectonics of the Achankovil Shear Zone, southern India, inferred from new deep seismic reflection image: Constraints on the East African Orogen. Precambrian Research, 356, 106110.

120. Mart, Y., 1988. The tectonic setting of the Seychelles, Mascarene and Amirante plateaus in the western equatorial Indian Ocean. Marine Geology, 79(3), 261–274.
121. Matthews, H.D., 1966. The Owen Fracture Zone and the Northern End of the Carlsberg Ridge. Philosophical Transactions of The Royal Society B: Biological Sciences, 259, 172-186.
122. Maus S., Barckhausen U., Berkenbosch H., et al., 2009. EMAG2: A 2–arc min resolution Earth Magnetic Anomaly Grid compiled from satellite, airborne, and marine magnetic measurements. Geochemistry, Geophys Geosystems, 10, Q08005, doi:10.1029/2009GC002471.
123. McKenzie, D., Sclater, J.G., 1971. The Evolution of the Indian Ocean since the Late Cretaceous. Geophysical Journal of the Royal Astronomical Society, 24, 437-528.
124. Melluso, L., Sheth, H.C., Mahoney, J.J., Morra, V., Petrone, C.M., Storey, M., 2009. Correlations between silicic volcanic rocks of the St. Mary's Islands (southwestern India) and eastern Madagascar: implications for Late Cretaceous India Madagascar reconstructions. Journal of Geological Society, London 166, 283-294.
125. Menard, H.W., 1964. Marine Geology of the Pacific. New York. McGraw-Hill Book Company, 271p.
126. Menon, R.D., Santosh, M., 1995. A Pan-African gemstone province of East Gondwana, in: Yoshida, M., Santosh, M. (Eds.), India and Antarctica during the Precambrian. Geological Society of India, Bangalore, pp. 357-371.
127. Merkouriev, S., DeMets, C., 2006. Constraints on Indian plate motion since 20 Ma from dense Russian magnetic data: Implications for Indian plate dynamics. Geochemistry, Geophysics, Geosystems, 7, Q02002, doi:10.1029/2005GC001079.
128. Miles P.R., Roest, W.R., 1993. Earliest seafloor spreading magnetic anomalies in the north Arabian Sea and the ocean-continent transition. Geophysical Journal International 115 (3), 1025-1031.
129. Minshull, T. A., Lane, C. I., Collier, J. S., Whitmarsh, R. B., 2008. The relationship between rifting and magmatism in the northeastern Arabian Sea. Nature Geoscience, 1(7), 463–467.
130. Mishra, A., Kumar Chaubey, A., Kumar, S., Vinay Kumar, P., Kumar, P., Mani Dubey, K., 2020. Does the Laxmi Ridge continue towards the Laccadive Ridge? New insights from an integrated geophysical study. Journal of Asian Earth Sciences, 104491.
131. Misra, A. A., Sinha, N., Mukherjee, S., 2015. Repeat ridge jumps and microcontinent separation: Insights from NE Arabian Sea. Marine and Petroleum Geology, 59, 406–428.
132. Mittal, T., Richards, M. A., Fendley, I. M., 2021. The Magmatic Architecture of Continental Flood Basalts: 2. A New Conceptual Model. Journal of Geophysical Research: Solid Earth, 126(12), e2021JB021807.

133. Mohan, M. R., Shaji, E., Satyanarayanan, M., Santosh, M., Tsunogae, T., Yang, Q. Y., Dhanil Dev, S. G., 2016. The Ezhimala Igneous Complex, southern India: Possible imprint of Late Cretaceous magmatism within rift setting associated with India-Madagascar separation. Journal of Asian Earth Sciences, 121, 56–71.
134. Morgan, W. J., 1972. Deep mantle convection plumes and plate motions. AAPG Bulletin, 56(2), 203–213.
135. Morgan, W.J., 1981. Hotspot tracks and the opening of the Atlantic and Indian Oceans, in: Emiliani (Ed.), The Sea. Wiley Inter science New York, pp. 443-487.
136. Mukhopadhyay, R., Batiza, R., 1994. Basinal seamounts and seamount chains of the Central Indian Ocean: Probable near-axis origin from a fast-spreading Ridge. Marine Geophysical Researches, 16, 303-314.
137. Mukhopadhyay, R., Khadge, N.H., 1990. Seamounts in the Central Indian Ocean Basin: indicators of the Indian plate movement. Proceedings of the Indian Academy of Sciences (Earth and Planetary Sciences), 99, 357-365.
138. Mukhopadhyay, R., Rajesh, M., De, S., Chakraborty, B., Jauhari, P., 2008. Structural highs on the western continental slope of India: Implications for regional tectonics. Geomorphology, 96 (1–2), 48–61.
139. Müller, D. R., Royer. J.-Y., Lawver, A. L., 1993. Revised plate motions relative to the hotspots from combined Atlantic and Indian Ocean hotspot tracks. Geology, 21, 275-278.
140. Murty A.V.S., Arasu R.T., Dhanawat B.S., Subrahmanyam V.S.R., 1999. Some aspects of deepwater exploration in the light of new evidences in the western Indian offshore. In: Third international petroleum conference and exhibition. PETROTECH, pp 457–462.
141. Naini, B.R., 1980. Geological and Geophysical study of the continental margin of Western India, and the adjoining Arabian Sea including the Indus conePh.D. Thesis, Columbia University, 173 pp.
142. Naini, B.R., Talwani, M., 1982. Structural framework and the evolutionary history of the continental margin of Western India. In: J.S. Watkins, C.L. Drake (Eds.), Studies in continental margin geology. American Association of Petroleum Geologists, pp. 167-191.
143. Nair, N., Anand, S. P., Rajaram, M., 2013. Tectonic framework of Laccadive Ridge in Western Continental Margin of India. Marine Geology, 346, 79–90.
144. Naqvi, S.M., 2005. Geology and evolution of the Indian Plate, 1st ed. Capital Publishing Company, New Delhi. 450 p.
145. Narain, H., Kaila, K. L., Verma, R. K., 1968. Continental margins of India. Canadian Journal of Earth Sciences, 5(4), 1051–1065.
146. Nathaniel, D.M., 2013. Hydrocarbon Potential of Sub-Basalt Mesozoics of Deepwater Kerala Basin, Southwestern Continental Margin of India. Ph.D Thesis, Andhra University.
147. Nomikou, P., Carey, S., Papanikolaou, D., Croff Bell, K., Sakellariou, D., Alexandri, M., Bejelou, K., 2012. Submarine volcanoes of the Kolumbo

volcanic zone NE of Santorini Caldera, Greece. Global and Planetary Change, 90-91, 135-151.
148. Norton, Sclater, 1979. A modelfor the evolution of the Indian Ocean and the breakup of Gondwanaland. Journal of Geophysical Research, 84, 6803-6830.
149. Pande K., Sheth, H.C., Bhutani, R., 2001. ^{40}Ar - ^{39}Ar age of the St. Mary's Islands volcanics, southern India: record of India - Madagascar break-up on the Indian subcontinent. Earth and Planetary Science Letters, 193, 39-46.
150. Pande, K., 2002. Age and duration of the Deccan Traps, India: A review of radiometric and paleomagnetic constraints. Proceedings of the Indian Academy of Sciences - Earth and Planetary Sciences, 111, 115, https://doi.org/10.1007/BF02981139.
151. Pande, K., Yatheesh, V., Sheth, H., 2017. ^{40}Ar/^{39}Ar dating of the Mumbai tholeiites and Panvel flexure: intense 62.5 Ma onshore-offshore Deccan magmatism during India-Laxmi Ridge-Seychelles breakup. Geophysical Journal International, 210, 1160-1170.
152. Pandey, D. K., Pandey, A., Whattam, S. A., 2019. Relict subduction initiation along a passive margin in the northwest Indian Ocean. Nature Communications, 10(1), 1–10.
153. Parker, R.L., 1972. The rapid calculation of potential anomalies. Geophysical Journal of the Royal Astronomical Society, 31, 447–455.
154. Patriat, P., 1987. Reconstitution de l'évolution du systeme de dorsales de l'Ocean Indien par les methodes de la Cinématique des Plaques. Territore des terres australes et Antartiques Francaises, Mission de recherche, Paris.
155. Patro, B.P.K., Sarma, S.V.S., 2007. Trap thickness and the subtrappean structures related to mode of eruption in the Deccan Plateau of India: results from magnetotellurics. Earth Planets Space, 59, 75-81.
156. Pepper, J.F., Everhart, G.M., 1963. The Indian Ocean: The geology of its bordering lands and the configuration of its floor, in: Miscellaneous Geologic Investigations. U.S. Geological Survey, pp. 1-33.
157. Piskarev, A., Elkina, D., 2017. Giant caldera in the Arctic Ocean: Evidence of the catastrophic eruptive event. Scientific Reports, 7, 46248.
158. Plummer, P. S., Belle, E. R., 1995. Mesozoic tectono-stratigraphic evolution of the Seychelles microcontinent. Sedimentary Geology, 96(1–2), 73–91.
159. Praharaj, P., Rekha, S., Bhattacharya, A., 2021. Structure and chronology across the Achankovil terrain boundary shear zone system (South India), and its Madagascar connection in the Gondwanaland. International Journal of Earth Sciences, 110(5), 1545–1573.
160. Radhakrishna, T., Bansal, B. K., Ramakrishna, C., 2021. Geodynamic events leading to formation of passive western continental margin of India. Journal of Geodynamics, 148, 101878.
161. Radhakrishna, T., Dallmeyer, R.D., Joseph, M., 1994. Paleomagnetism and 36Ar/40Ar vs 39Ar/40Ar isotope correlation ages of dyke swarms in Central

Kerala, India: tectonic implications. Earth and Planetary Science Letters, 121, 213-226.

162. Radhakrishna, T., Joseph, M., 2012. Geochemistry and paleomagnetism of Late Cretaceous mafic dikes in Kerala, southwest coast of India in relation to large igneous provinces and mantle plumes in the Indian Ocean region. Geological Society of America Bulletin, 124 (1/2), 240-255.
163. Radhakrishna, T., Maluski, H., Mitchell, J.G., Joseph, M., 1999. $^{40}Ar^{39}Ar$ and K/Ar geochronology of the dykes from the south Indian granulite terrain. Tectonophysics, 304, 109-129.
164. Radhakrishna, T., Mohamed, A. R., Venkateshwarlu, M., Soumya, G. S., Prachiti, P. K., 2019. Mechanism of rift flank uplift and escarpment formation evidenced by Western Ghats, India. Scientific Reports, 9(1), 1–7.
165. Raharimahefa, T., Kusky, T. M., Toraman, E., Rasoazanamparany, C., Rasaonina, I., 2013. Geometry and kinematics of the late Proterozoic Angavo Shear Zone, Central Madagascar: Implications for Gondwana Assembly. Tectonophysics, 592, 113–129.
166. Ramana, M. V., Desa, M. A., Ramprasad, T., 2015. Re-examination of geophysical data off Northwest India: Implications to the Late Cretaceous plate tectonics between India and Africa. Marine Geology, 365, 36–51.
167. Ramana, M. V., Rajendraprasad, B., Hansen, R.D., 1987. Geophysical and geological surveys along the northeastern flank of Mount Error, northwestern Indian Ocean. Marine Geology, 76, 153-162.
168. Rao, D. G., Paropkari, A. L., Krishna, K. S., Chaubey, A. K., Ajay, K. K., Kodagali, V. N., 2010. Bathymetric highs in the mid-slope region of the western continental margin of India-Structure and mode of origin. Marine Geology 276(1–4), 58–70.
169. Rao, G. S., Kumar, M., Radhakrishna, M., 2018. Structure, mechanical properties and evolution of the lithosphere below the northwest continental margin of India. International Journal of Earth Sciences, 107(6), 2191–2207.
170. Ratheesh-Kumar, R. T., Ishwar-Kumar, C., Windley, B. F., Razakamanana, T., Nair, R. R., Sajeev, K., 2015. India–Madagascar paleo-fit based on flexural isostasy of their rifted margins. Gondwana Research, 28(2), 581–600.
171. Ratheesh-Kumar, R.T., Santosh, M., Yang, Q.-Y., Ishwar-Kumar, C., Chen, N.-S., Sajeev, K., 2016. Archean tectonics and crustal evolution of the Biligiri Rangan Block, southern India. Precambrian Research 275, 406-428.
172. Reeves, C.V., Teasdale, J.P., Mahanjane, E.S., 2016. Insight into the Eastern Margin of Africa from a new tectonic model of the Indian Ocean, In: Nemčok, M., Rybár, S., Sinha, S.T., Hermeston, S.A., Ledvényiová, L. (Eds.), Transform Margins: Development, Controls and Petroleum Systems. Geological Society, London, Special Publications, 431, London, pp. 299-322.
173. Richards, F.D., Kalnins, L.M., Watts, A.B., Cohen, B.E., Beaman, R.J., 2018. The Morphology of the Tasmantid Seamounts: Interactions between

Tectonic Inheritance and Magmatic Evolution. Geochemistry, Geophys. Geosystems 19, 3870–389.
174. Roche, O., Druitt, T.H., Merle, O., 2000. Experimental study of caldera formation. Journal of Geophysical Research: Solid Earth, 105, 395-416.
175. Rogers, J.J.W., Miller, J.S., Clements, A.S., 1995. A Pan African zone linking East and West Gondwana, in: Yoshida, M., Santosh, M. (Eds.), India and Antarctica during the Precambrian. Geological Society of India Memoir 34, Bangalore, pp. 11–23.
176. Royer, J.-Y., Chaubey, A. K., Dyment, J., Bhattacharya, G. C., Srinivas, K., Yatheesh, V., Ramprasad, T., 2002. Paleogene plate tectonic evolution of the Arabian and Eastern Somali basins. Geological Society, London, Special Publications, 195(1), 7– 23.
177. Sahabi, M., 1993. Un Modele generele de d'evolution de l'ocean Indien. Doctoral Thesis, Universite de Bretagne Occidentale.
178. Saikia, U., Das, R., Rai, S. S., 2017. Possible magmatic underplating beneath the west coast of India and adjoining Dharwar craton: Imprint from Archean crustal evolution to breakup of India and Madagascar. Earth and Planetary Science Letters, 462, 1–14.
179. Sandwell, D.T., Müller, R.D., Smith, W.H.F., Garcia, E., Francis, R., 2014. New global marine gravity model from CryoSat-2 and Jason-1 reveals buried tectonic structure. Science, 346, 65-67.
180. Santosh, M., Yang, Q.-Y., Shaji, E., Tsunogae, T., Mohan, M. R., Satyanarayanan, M., 2015. An exotic Mesoarchean microcontinent: The Coorg Block, southern India. Gondwana Research, 27(1), 165–195.
181. Sato, T., Nogi, Y., Sato, H., Fujii, M., 2022. A New Tectonic Model between the Madagascar Ridge and Del Cano Rise in the Indian Ocean. Journal of Geophysical Research: Solid Earth, 127(1), e2021JB021743.
182. Savio, J. J., Yatheesh, V., Sheldon, R., Kallathian, M., Kessarkar, P., Kumar, K., Verma, S., 2022. Caldera-like features located over the Panikkar Seamount and adjacent regions in the Laxmi Basin, eastern Arabian Sea. Journal of Earth System Science, 131(1), 44.
183. Schlich, R., 1982. The Indian Ocean: Aseismic Ridges, Spreading Centers, and Oceanic Basins, in: Nairn A.E.M., Stehli F.G. (Eds.), The Ocean Basins and Margins: The Indian Ocean. Springer US, Boston, MA, pp. 51-147.
184. Schreurs, G., Giese, J., Berger, A., Gnos, E., 2010. A new perspective on the significance of the Ranotsara shear zone in Madagascar. International Journal of Earth Sciences, 99(8), 1827–1847.
185. Sclater, J. G., Fisher, R. L., 1974. The evolution of the east central Indian Ocean. Geological Society of America Bulletin 85, 683-702.
186. Scotese, C.R., Gahagan, L.M., Larson, R.L., 1988. Plate tectonic reconstructions of the Cretaceous and Cenozoic ocean basins. Tectonophysics, 155, 27-48.
187. Sen, G., 2001. Generation of Deccan Trap magmas. Journal of Earth System Science 110, 409-431.

188. Seton, M., Müller, R.D., Zahirovic, S., Gaina, C., Torsvik, T.H., Shephard, G., Talsma, A., Gurnis, M., Turner, M., Maus, S., Chandler, M., 2012. Global continental and ocean basin reconstructions since 200 Ma. Earth-Science Reviews, 113, 212-270.
189. Sharma, R.S., 2009. Cratons and Fold Belts of India, Lecture Notes in Earth Sciences. Springer-Verlag, Berlin, Heidelberg. 304 p.
190. Shellnutt, J. G., Yeh, M.-W., Suga, K., Lee, T.-Y., Lee, H.-Y., Lin, T.-H., 2017. Temporal and structural evolution of the Early Palæogene rocks of the Seychelles microcontinent. Scientific Reports, 7(1), 179.
191. Shen, Y., Scheirer, D.S., Forsyth, D.W., Macdonald, K.C., 1993. Two forms of volcanism: implications for mantle flow and off-axis crustal production on the west flank of the southern East Pacific Rise. Journal of Geophysical Research, 98, 17875–17889.
192. Sheth, H., Pande, K., Vijayan, A., Sharma, K.K., Cucciniello, C., 2017. Recurrent Early Cretaceous, Indo-Madagascar (89–86 Ma) and Deccan (66 Ma) alkaline magmatism in the Sarnu-Dandali complex, Rajasthan: 40Ar/39Ar age evidence and geodynamic significance. Lithos, 284–285, 512-524.
193. Sheth, H.C., 2005. From Deccan to Reunion: No trace of a mantle plume. In: Foulger, G.R., Natland, J.H., Presnall, D.C., Anderson, D.L. (Eds.) Plates, Plumes, and Paradigms, Special Paper 388. Geological Society of America, pp. 477-501.
194. Shuhail, M., 2018. Study of the deep offshore regions off the southwestern continental margin of India and its conjugate regions to understand their pre-breakup juxtapositions and subsequent plate tectonic evolution. Ph.D. Thesis, Goa University.
195. Shuhail, M., Yatheesh, V., Bhattacharya, G.C., Müller, R.D., Kamesh Raju, K.A., Mahender, K., 2018. Formation and evolution of the Chain-Kairali Escarpment and the Vishnu Fracture Zone in the Western Indian Ocean. Journal of Asian Earth Sciences, 164, 307-321.
196. Siawal, A., Dash, P.P., Srivastava, H.C., 2019. Evolution of west coast of India - A plate tectonic approach. ONGC Bullettin 54, 147-164.
197. Siawal, A., Samal, D. J., Kaul, A., 2014. A note on identification of SDR's in Laxmi Basin of Arabian Sea Region. ONGC Bulletin: A Bi Annual Journal of an International E&P Company, 49, 45–50.
198. Sinha, M. C., and Louden, K. E., 1981. The crustal structure of the Madagascar Ridge. Geophysical Journal International 66 (2), 351-377.
199. Smith, D.K., Jordan, T.H., 1988. Seamount statistics in the Pacific Ocean. Journal of Geophysical Research, 93, 2899-2918.
200. Sreejith, K.M., Unnikrishnan, P., Radhakrishna, M., 2019. Isostasy and crustal structure of the Chagos–Laccadive Ridge, Western Indian Ocean: Geodynamic implications. Journal of Earth System Science, 128, 157.
201. Stagpoole, V., Schenke, H.W., Ohara, Y., 2016. A name directory for the ocean floor. EOS Transactions American Geophysical Union, 97.

202. Storey, M., Mahoney, J.J., Saunders, A.D., Duncan, R.A., Kelley, S.P., Coffin, M.F., 1995. Timing of hotspot related volcanism and the breakup of Madagascar and India. Science, 267(5199), 852-855.
203. Straume E.O., Gaina C., Medvedev S., et al., 2019. GlobSed: Updated total sediment thickness in the World's Oceans. Geochemistry, Geophys Geosystems 20, 1756–1772.
204. Talwani, M., Heitzler, J.R., 1964. Computation of Magnetic anomalies caused by two dimensional structures of arbitrary shape. In: G.A. Parks (Ed.), Computers in the Mineral Industries. Stanford University, pp. 464-480.
205. Talwani, M., Worzel, J.L., Landisman, M., 1959. Rapid gravity computations for two-dimensional bodies with application to the Mendocino Submarine Fracture Zone. Journal of Geophysical Research, 64(1), 49-59.
206. Tewari, H. C., Prasad, B., Kumar, P., 2018. Structure and Tectonics of the Indian Continental Crust and Its Adjoining Region: Deep Seismic Studies: Second Edition. Structure and Tectonics of the Indian Continental Crust and Its Adjoining Region: Deep Seismic Studies: Second Edition.
207. Tewari, V.M., Rao, V.V., 2003. Structure and tectonics of the Proterozoic Aravalli-Delhi Geological Province, NW Indian Peninsular Shield. In: Mahadevan, T.M., Arora, B.R., Gupta, K.R. (Eds.). Indian Continental Lithosphere, Geological Society of India, Memoir 53, 57-78.
208. Tizzani, P., Battaglia, M., Castaldo, R., Pepe, A., Zeni, G., Lanari, R., 2015. Magma and fluid migration at Yellowstone Caldera in the last three decades inferred from InSAR, leveling, and gravity measurements. Journal of Geophysical Research: Solid Earth, 120(4), 2627-2647.
209. Todal, A., Eldholm, O., 1998. Continental margin off western India and Deccan Large Igneous Province. Marine Geophysical Researches, 20, 273-291.
210. Tolan, T.L., Reidel, S.P., Beeson, M.H., Anderson, J.L., Fecht, K.R., Swanson, D.A., 1989. Revisions to the estimates of the areal extent and volume of the Columbia River Basalt Group, In: Reidel, S.P., Hooper, P.R. (Eds.), Volcanism and Tectonism in the Columbia River Flood-Basalt Province. Geological Society of America Special Paper 239, pp. 1-20.
211. Torsvik, T. H., Amundsen, H., Hartz, E. H., Corfu, F., Kusznir, N., Gaina, C., Jamtveit, B., 2013. A Precambrian microcontinent in the Indian Ocean. Nature Geoscience, 6(3), 223–227.
212. Torsvik, T. H., Tucker, R. D., Ashwal, L. D., Eide, E. A., Rakotosolofo, N. A., de Wit, M. J., 1998. Late Cretaceous magmatism in Madagascar: palaeomagnetic evidence for a stationary Marion hotspot. Earth and Planetary Science Letters, 164(1), 221–232.
213. Torsvik, T.H., Tucker, R.D., Ashwal, L.D., Carter, L.M., Jamtveit, V., Vidyadharan, K.T., Venkataramana, P., 2000. Late cretaceous India - Madagascar fit and timing of breakup related magmatism. Terra Nova, 12, 220-224.

214. Tucker, R. D., Roig, J. Y., Macey, P. H., Delor, C., Amelin, Y., Armstrong, R. A., Ralison, A. V., 2011. A new geological framework for south-central Madagascar, and its relevance to the "out-of-Africa" hypothesis. Precambrian Research, 185(3), 109–130.
215. Udintsev, G.B., Fisher, R.L., Kanaev, F. V, Laughton, S.A., Simpson, W.E.S., Zhiv, I.D., 1975. Geological-geophysical atlas of the Indian Ocean. Academy of Sciences of the U.S.S.R, Moscow.
216. Valsangkar, A.B., Radhakrishnamurthy, C., Subbarao, K.V., Beckinsale, R.D., 1981. Paleomagnetism and Potassium-Argon age studies of acid igneous rocks from the St. Mary Islands. Geological Society of India, pp. 265-275.
217. Vandamme, D., Courtillot, V., Besse, J., Montigny, R., 1991. Paleomagnetism and age determinations of the Deccan Traps (India): Results of a Nagpur-Bombay Traverse and review of earlier work. Reviews of Geophysics, 29(2), 159–190.
218. Venkatesan, T. R., Pande, K., Gopalan, K., 1986. 40Ar-39Ar dating of Deccan basalts. Journal of the Geological Society of India, 27(1), 102–109.
219. Verzhbitsky, E.V., 2003. Geothermal regime and genesis of the Ninety-East and Chagos-Laccadive Ridges. Journal of Geodynamics, 35, 289-302.
220. Weatherall, P., Marks, K.M., Jakobsson, M., Schmitt, T., Tani, S., Arndt, J.E., Rovere, M., Chayes, D., Ferrini, V., Wigley, R., 2015. A new digital bathymetric model of the world's oceans. Earth and Space Science, 2, 331-345.
221. Wessel, P., 2001. Global distribution of seamounts inferred from gridded Geosat/ERS-1 altimetry. Journal of Geophysical Research 106, 19431-19441.
222. Wessel, P., Sandwell, D.T., Kim, S.S., 2010. The global seamount census. Oceanography 23, 24-33.
223. Wessel, P., Smith, W.H.F., Scharroo, R., Luis, J., Wobbe, F., 2013. Generic Mapping Tools: Improved version released. EOS Transactions American Geophysical Union, 94(45), 409-410.
224. White, R. S., McKenzie, D., 1995. Mantle plumes and flood basalts. Journal of Geophysical Research: Solid Earth, 100(B9), 17543–17585.
225. Whitmarsh, R.B., 1974. Some aspects of plate tectonics in the Arabian Sea, Initial Reports of the Deep Sea Drilling Project. US Government Printing Office, Washington, pp. 527-535.
226. Windley, B. F., Razafiniparany, A., Razakamanana, T., Ackermand, D., 1994. Tectonic framework of the Precambrian of Madagascar and its Gondwana connections: a review and reappraisal. Geologische Rundschau, 83(3), 642–659.
227. Yatheesh, V., 2007. A study of tectonic elements of the western continental margin of India and adjoining ocean basins to understand the early opening of the Arabian Sea. Ph.D. Thesis, Goa University.

228. Yatheesh, V., 2020. Structure and tectonics of the continental margins of India and the adjacent deep ocean basins: Current status of knowledge and some unresolved problems. Episodes, 43(1), 586-608.
229. Yatheesh, V., Bhattacharya, G.C., Dyment, J., 2009. Early oceanic opening off Western India–Pakistan margin: The Gop Basin revisited. Earth and Planetary Science Letters, 284(3), 399–408.
230. Yatheesh, V., Bhattacharya, G.C., Mahender, K., 2006. The terrace like feature in the mid-continental slope region off Trivandrum and a plausible model for India–Madagascar juxtaposition in immediate pre-drift scenario. Gondwana Research, 10, 179-185.
231. Yatheesh, V., Bhattacharya, G.C., Shuhail, M., 2020. Revised plate tectonic reconstruction model for the early opening of the Arabian Sea, In: Rossi, P., François, C., Miles, P. (Eds.), The Indian Ocean and its Margins. Commission for the Geological Map of the World, France, pp. 11-12.
232. Yatheesh, V., Dyment, J., Bhattacharya, G.C., Müller, R.D., 2013a. Deciphering detailed plate kinematics of the Indian Ocean and developing a unified model for East Gondwanaland reconstruction: An Indian-Australian French initiative. Deep Continental Studies in India Newsletter, 23, 2-9.
233. Yatheesh, V., Kurian, P.J., Bhattacharya, G. C., Rajan, S., 2013b. Morphotectonic architecture of an India-Madagascar breakup related anomalous submarine terrace complex on the southwest continental margin of India. Marine and Petroleum Geology, 46, 304–318.
234. Yatheesh, V., Dyment, J., Bhattacharya, G.C., Royer, J. Y., Kamesh Raju, K. A., Ramprasad, T., A. K. Chaubey, A. K., Patriat, P., Srinivas, K., Choi, Y., 2019. Detailed structure and plate reconstructions of the Central Indian Ocean between 83.0 and 42.5 Ma (Chrons 34 and 20). Journal of Geophysical Research: Solid Earth, 124, 4305– 4322.
235. Yoshida, M., Rajesh, H.M., Santosh, M., 1999. Juxtaposition of India and Madagascar: A Perspective. Gondwana Research, 2(3), 449–462.

Annexures

Publications from thesis

1. **Bijesh C.M.,** John Kurian P., Yatheesh V., Abhishek Tyagi, Twinkle D., (2018). Morphotectonic characteristics, distribution and probable genesis of bathymetric highs off southwest coast of India. Geomorphology, 315, 33-44.
2. **Bijesh, C.M.,** Yatheesh, V., Twinkle, D., Tyagi, A., Kurian, P.J., (2021). Sagar Kanya Bathymetric High Complex: An extinct giant submarine volcanic caldera in the Eastern Arabian Sea? Geomorphology, 373, 107488.
3. **Bijesh, C.M.,** Yatheesh,V., John Kurian, P., John Savio, J., Vasudev Mahale, Abhishek Shet, Gautham, S., (2022). Conjugate nature of the Alleppey-Trivandrum Terrace Complex with the Northern Madagascar Ridge in the early opening model of the Arabian Sea: Evaluation based on an integrated geophysical investigation. Marine Geophysical Research, 43, 14.

Conferences in which the findings from the thesis research were presented

1. **Bijesh C.M.,** Yatheesh V., Twinkle D., Tyagi A, John Kurian, P. Identification, distribution and geophysical characteristics of bathymetric highs off southwest coast of India. 54thAnnual Convention of Indian Geophysical Union (IGU), CSIR-NGRI, Hyderabad, December 2017.
2. **C.M. Bijesh,** D. Twinkle, N. Mahesh, P. John Kurian, V. Yatheesh. Geophysical Mapping of the Sagar Kanya Seamount, Arabian Sea. SCORInterRidge workshop, CSIR-NIO, Goa, 14-16 November 2018.
3. **C.M. Bijesh,** V. Yatheesh, P. John Kurian, D. Twinkle, A. Tyagi. Morphotectonics of the southwestern continental margin of India and the adjacent deep offshore regions. International Indian Ocean Science Conference (IIOSC-2022), Goa, 14-18 March 2022.

Geomorphology 315 (2018) 33–44

Contents lists available at ScienceDirect

Geomorphology

journal homepage: www.elsevier.com/locate/geomorph

Morphotectonic characteristics, distribution and probable genesis of bathymetric highs off southwest coast of India

C.M. Bijesh [a,b], P. John Kurian [a,*], V. Yatheesh [c], Abhishek Tyagi [a], D. Twinkle [a]

[a] National Centre for Antarctic and Ocean Research, Vasco da Gama, Goa 403804, India
[b] Department of Marine Sciences, Goa University, Taleigao Plateau, Goa 403206, India
[c] CSIR - National Institute of Oceanography, Dona Paula, Goa 403004, India

ARTICLE INFO

Article history:
Received 15 January 2018
Received in revised form 10 April 2018
Accepted 29 April 2018
Available online 3 May 2018

Keywords:
Seafloor morphology
Hotspot volcanism
Laccadive Basin
Laccadive Plateau

ABSTRACT

The western continental margin of India and the adjacent deep ocean basins were formed by break-up and separation among India, Seychelles and Madagascar since the Late Cretaceous. The initial India-Madagascar separation and the subsequent India-Seychelles separation are believed to have been caused by the Marion hotspot at ~90 Ma and the Réunion hotspot at ~68.5 Ma, respectively. These geodynamic events resulted in the formation of several bathymetric highs that probably represent imprints of these volcanic events. In the present study these bathymetric high features were mapped comprehensively to understand their morphotectonic characteristics, using a fresh set of multibeam bathymetry, sea-surface gravity and magnetic anomalies, complemented by the available multichannel seismic reflection sections. A high-resolution bathymetric map of the southwestern continental margin of India and the adjoining deep offshore regions has been generated to decipher detailed morphological configuration and distribution of prominent undersea bathymetric features. We also carried out detailed morphometric analysis of these features to deduce the morphological parameters. A total of 33 individual bathymetric high features were identified and classified as seamounts, hills, knolls, guyots and plateaus based on the standardization of undersea feature names published by Intergovernmental Oceanographic Commission (IOC) and International Hydrographic Organization (IHO) in 2013. Multichannel seismic reflection, sea-surface gravity and magnetic data were used to describe the sub-seafloor configuration and qualitative interpretation of the geophysical signatures associated with the bathymetric highs. Interpretation of the multichannel seismic reflection sections suggest that some of these identified features are extrusive in nature, while others are intrusive. These features are associated with characteristic gravity highs superimposed over regional negative anomalies and complex negative and positive magnetic anomalies. The study results suggest that the genesis of the bathymetric highs mapped in the study area could be attributed to the hotspot volcanism, caused by the Marion or Réunion hotspots. We infer that the features in the southwestern continental margin of India closer to the Alleppey-Trivandrum Terrace Complex might have been created by the Marion hotspot volcanism, while those in the Laccadive Basin and eastern sector of the Laccadive Plateau might have been formed by Réunion hotspot volcanism.

1. Introduction

Bathymetric high features are important submarine physiographic features, which have been a subject of interest in geophysical, geological, oceanographic and biological aspects. Detailed investigations of the bathymetric features are important because such studies can provide vital clues for understanding the evolution of deep ocean basins and the adjacent continental margins as well as identification of economically important mineral deposits. Research focused on the morphological and geophysical aspects of the bathymetric high features were widely conducted in the world ocean (Menard, 1964; Smith and Jordan, 1988; Wessel, 2001; Wessel et al., 2010; Harris et al., 2014). Various hypotheses were proposed for the formation of these bathymetric high features, mainly, hotspot activity, ridge-hotspot interaction, ridge parallel faulting, off axis volcanism and propagating fracture (Fornari et al., 1984; Duncan and Clague, 1985; Fornari et al., 1988; Shen et al., 1993; Clague et al., 2000; Clouard et al., 2003; Das et al., 2007).

In the Indian Ocean, extensive studies of geomorphologic features were carried out in the Central Indian Basin (Kodagali, 1989, 1992, 1998; Mukhopadhyay and Khadge, 1990; Mukhopadhyay and Batiza, 1994; Das et al., 2005, 2007; Iyer, 2009; Iyer et al., 2012), however, such studies of morphological features are comparatively sparse in the Western Indian Ocean except a few in the Arabian Sea (Bhattacharya

* Corresponding author.
E-mail address: john@ncaor.gov.in (P. John Kurian).

https://doi.org/10.1016/j.geomorph.2018.04.015
0169-555X/

and Subrahmanyam, 1991; Bhattacharya et al., 1994; Mukhopadhyay et al., 2008; Rao et al., 2010). Bhattacharya and Subrahmanyam (1991) carried out detailed geophysical study over the Sagar Kanya Seamount (Fig. 1) in the Arabian Basin and provided crustal configuration and probable genesis for this seamount. Bhattacharya et al. (1994) mapped a seamount chain in the Laxmi Basin, consisting of the Raman Seamount, Panikkar Seamount and Wadia Guyot (Fig. 1). Subsequently, Mukhopadhyay et al. (2008) and Rao et al. (2010) studied bathymetric highs in the mid continental slope region of the southwestern continental margin of India (SWCMI). However, such detailed geomorphologic studies were not undertaken in the Laccadive Basin and the adjacent areas (Fig. 1), which consists of several prominent bathymetric highs. In the present study, we attempt first to map these bathymetric features in the Laccadive Basin, eastern part of the Laccadive Plateau and the southwestern continental margin of India and then to discuss their distribution and probable mode of emplacement.

2. Tectonic framework

The study area (Fig. 1) mainly consists of the southwestern continental margin of India, the Laccadive Basin and the eastern part of the Laccadive Plateau, located between 6°N and 16°N latitudes. The southwestern continental margin of India clearly shows the presence of an anomalous terrace like feature in the mid continental slope region off Trivandrum. Yatheesh et al. (2013) referred this feature as the Alleppey-Trivandrum Terrace Complex, which mainly consists a smaller northerly terrace, the Alleppey Terrace, and a larger southerly terrace, the Trivandrum Terrace (Yatheesh et al., 2006). The western boundary of the Alleppey-Trivandrum Terrace Complex is marked by an escarpment, the Chain-Kairali Escarpment, which is defined by a ~500 km-long feature with a sharp drop in the bathymetry (Yatheesh et al., 2013). The region located west of the Chain-Kairali Escarpment and east of the Laccadive Plateau is the Laccadive Basin, which is a triangular shaped basin created due to divergence between India and the Laccadive Plateau (Bhattacharya and Chaubey, 2001; Bhattacharya and Yatheesh, 2015). The nature of crust underlying the Laccadive Basin is still equivocal. Based on the presence of rotated fault blocks representing half grabens, Chaubey et al. (2002a) suggested that the Laccadive Basin represents a failed rift consisting of stretched continental crust intermingled with volcanics. Considering the presence of seaward dipping reflectors (SDRs) west of the Laccadive Plateau and based on gravity modeling, Ajay et al. (2010) inferred that the Laccadive Basin is underlain by thinned continental crust. Yatheesh et al. (2013), based on gravity modeling, demonstrated that the Laccadive Basin region could be underlain either by a much thinned continental crust or by an anomalously thick oceanic crust. The Laccadive Plateau is the northernmost segment of the Laccadive-Chagos Ridge, which is slightly arcuate, elongated feature extending about 2500 km between 14°N and 9°S latitudes. Various views exist for the genesis of the Laccadive-Chagos Ridge, such as, a leaky transform fault (Fisher et al., 1971; Sclater and Fisher, 1974), hotspot trail (Whitmarsh, 1974a; Duncan, 1981; Morgan, 1981), a composite structural elements of various origin (Avraham and Bunce, 1977) and crack propagation (Sheth, 2005). Though the hotspot trail genesis appears to have broader acceptance for the genesis of the Laccadive-Chagos Ridge as a whole, there are several observations, which strongly suggest that the Laccadive Plateau is a continental sliver (Bhattacharya and Yatheesh, 2015 and references therein). The Laccadive Plateau area has a complex block-faulted basement structure, constituting system of grabens, half grabens and single normal faults, which are grouped into a rift system, referred as the Cannanore Rift System (DGH, 2014).

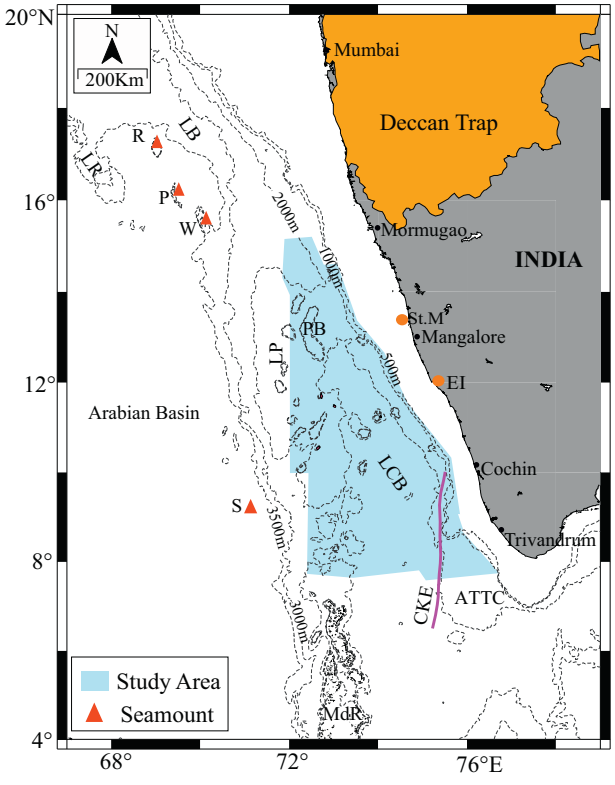

Fig. 1. Generalized map of the southwestern continental margin of India and the adjoining deep offshore regions showing the major tectonic features and geographic extent of the study area. Black dotted lines are selected (500, 1000, 2000, 3000 and 3500 m) isobaths from GEBCO digital data set (IOC-IHO-BODC, 2003). R: Raman Seamount; P: Panikkar Seamount; W: Wadia Guyot; S: Sagar Kanya Seamount; LP: Laccadive Plateau; PB: Padua Bank; MdR: Maldive Ridge; CKE: Chain Kairali Escarpment; ATTC: Alleppey-Trivandrum Terrace Complex; LR: Laxmi Ridge; LB: Laxmi Basin; StM: St. Mary Islands; EI: Ezhimala Igneous Complex.

3. Data and methodology

The main data used in the present study comprise of sea-surface magnetic, gravity and multibeam bathymetry data, acquired by National Centre for Antarctic and Ocean Research (NCAOR), Goa, India, during 2007 to 2016 onboard various research vessels (Table 1). The multibeam bathymetry data was collected using Atlas Hydrosweep DS System (onboard *MV Akademic Boris Petrov*), SeaBeam 3012 Multibeam System (onboard *ORV Sagar Kanya*) and Reson SeaBat 7150 (onboard *MV MGS Sagar*). The Atlas Hydrosweep DS System was operated at a frequency of 15.5 kHz with maximum angular coverage of 120°. The

Table 1
Details of cruises from which marine geophysical data have compiled for the present study.

Cruise ID	Vessel	Year	Bathymetry	Gravity	Magnetic
ABP-27	Akademic Boris Petrov	2007	✓	×	×
SK-249	O R V Sagar Kanya	2008	✓	×	×
SK-250	O R V Sagar Kanya	2008	✓	×	×
ABP-33	Akademic Boris Petrov	2008	✓	×	×
SK-257	O R V Sagar Kanya	2009	✓	×	×
SK-275	O R V Sagar Kanya	2010	✓	×	×
ABP-44	Akademic Boris Petrov	2010	✓	×	×
SK-292	O R V Sagar Kanya	2012	✓	×	×
SK-316	O R V Sagar Kanya	2014	✓	×	×
SK-322	O R V Sagar Kanya	2015	✓	×	×
MGS-01	MGS Sagar	2015	✓	✓	×
MGS-02	MGS Sagar	2015	✓	✓	✓
MGS-03	MGS Sagar	2016	✓	✓	✓
MGS-04	MGS Sagar	2016	✓	✓	✓
MGS-06	MGS Sagar	2016	✓	✓	✓
MGS-07	MGS Sagar	2016	✓	✓	✓

SeaBeam 3012, with a maximum angular coverage of 140°, was operated at a frequency of 12 kHz. The Reson SeaBat 7150 was operated in dual-frequency (12 kHz and 24 kHz), depending on the depth range. The measured depth values are corrected for variation of sound velocity in seawater by collecting sound velocity profiles in real time. This raw multibeam dataset was processed using Caris Hips & Sips software package in which all the datasets were merged together. Finally, manual de-spiking and qualitative filtering were applied to minimize the erroneous depth soundings. The processed data was then extracted in ASCII format and prepared a bathymetric grid with 250 m spatial resolution using Generic Mapping Tools (GMT). Mobile Gravimeter Chekan - AM was used to acquire the sea-surface gravity data and was reduced to gravity anomalies by applying normal and Eötvös corrections. The total field magnetic data was collected using Marine Magneto

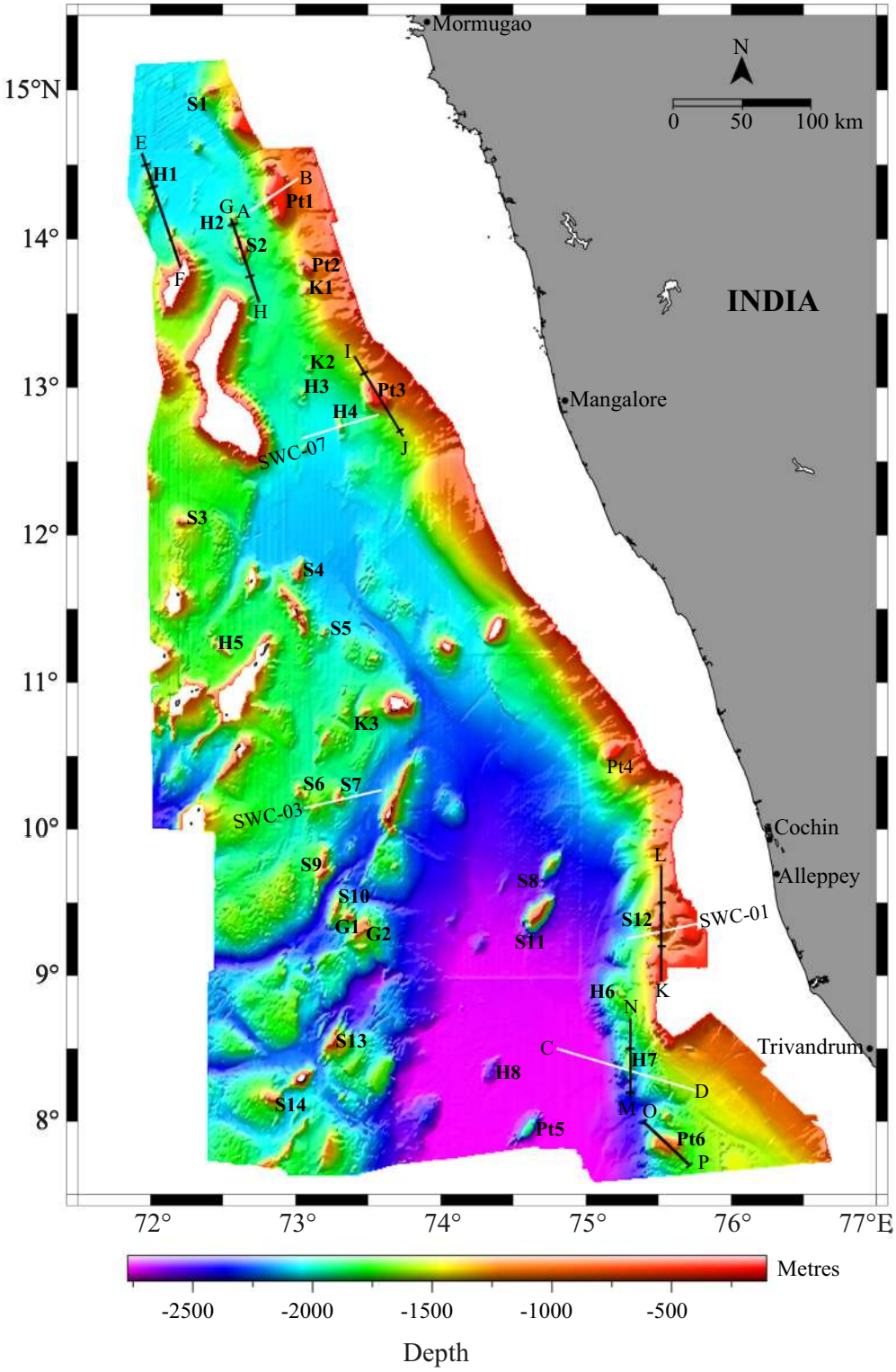

Fig. 2. The updated high resolution bathymetric map of the study area, showing the locations of the bathymetric high features identified in the present study. White lines represent locations of the seismic reflection sections presented in Fig. 8. Black lines represent locations of sea-surface bathymetry, gravity and magnetic profiles presented in Fig. 9 (profile plots). Black cross marks on these lines represent the extent of the profiles shown in Fig. 9. Labels to the bathymetric high features are as in Table 2.

Explorer Pro magnetometer. These data were reduced to residual magnetic anomalies by applying International Geomagnetic Reference Field (IGRF) for the corresponding epoch. Both gravity and magnetic data were acquired with ~30 m spatial resolution along the track and using these data, 1 × 1 km grids were generated for the preparation of 2D gravity and magnetic anomaly maps. To understand the sub-seafloor characteristics of the various features, we used multichannel seismic reflection data (along the profiles SWC-01, SWC-03 and SWC-07), collected by Directorate General of Hydrocarbon (DGH), India, as well as two published (Whitmarsh, 1974b; Rao et al., 2010) seismic sections. The locations of sea-surface gravity, magnetic and seismic reflection profiles used to characterize various bathymetric features in the present study are given in Fig. 2 and Supplementary Fig. S1.

4. Results and discussion

4.1. Seafloor morphology from multibeam bathymetry data

The updated bathymetric maps (Fig. 2 and Supplementary Fig. S1) of the study region covers an area of ~234,000 km^2. This high resolution bathymetric map shows the presence of 33 distinct bathymetric highs with varying size and height. We classify these seafloor features into different categories such as seamounts, hills, knolls, guyots and plateaus, following the classification scheme of International Hydrographic Organization (IOC-IHO, 2013). We inferred the morphological characteristics of these features and derived their morphometric parameters. Locations of the identified features and their morphometric characteristics are shown in Fig. 2 and Fig. 3, respectively. The derived morphometric parameters, which mainly consist of height, basal area, basal width, slope angle, flatness and height-width ratio, are detailed in Table 2. In this section, we provide a detailed description of geomorphology of the identified bathymetric features and their morphometric characteristics.

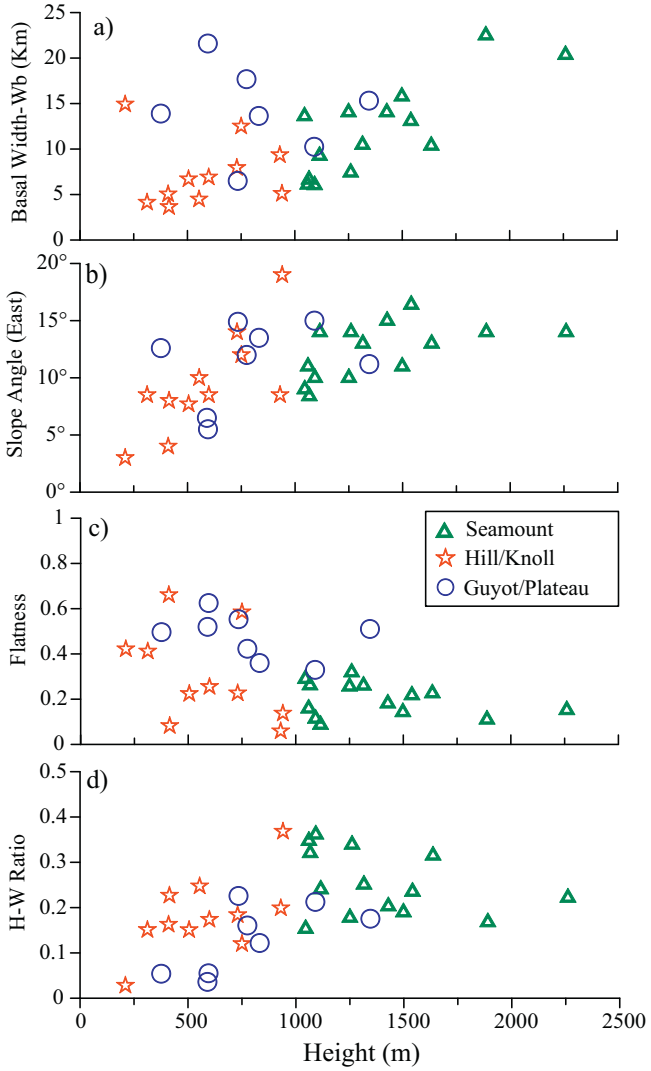

Fig. 3. Plots of (a) height versus basal width (Wb), (b) height versus slope angle, (c) height versus flatness and (d) height versus H-W ratio of identified bathymetric high features. Morphometric details are given in Table 2.

4.1.1. Seamounts

Seamounts are distinct generally equi-dimensional elevation greater than 1000 m above the surrounding relief as measured from the deepest isobath that surrounds most of the feature (IOC-IHO, 2013). From the updated bathymetric map of the study area, 14 seamounts (S1 to S14, as shown in Fig. 2 and Table 2), with varying height of 1045–2260 m from the surrounding seafloor, were identified. Among these, 12 seamounts (S2 to S11 and S13 to S14) are located in the eastern sector of the Laccadive Plateau and the adjacent region of the Laccadive Basin, while two seamounts (S1 and S12) are located close to the south-western continental slope of India. Most of these features are with single peak along the summit, but seamounts S9, S12 and S14 are characterized by four, two and three peaks, respectively. Seamount S5, a conical feature, has least basal extent (~55 km^2) and seamount S11 has maximum basal extent (~694 km^2). The 3D bathymetric images and corresponding contour maps of two representative seamounts, S2 and S11 are presented in Fig. 4. (See Supplementary Fig. S2 for bathymetric image of all the other seamounts). Seamount S11, which has maximum height (2260 m), shows (Fig. 3) significantly large slope angle and basal width but less flatness. The plot of basal width against height for the seamounts shows that height increases (1000 to 1500 m) roughly with increasing basal width (7 to 17 km) for the seamounts (Fig. 3).

4.1.2. Hills and knolls

Hills are distinct elevations generally of irregular shape, less than 1000 m above the surrounding relief as measured from the deepest isobath that surrounds most of the feature (IOC-IHO, 2013). On the other hand, Knolls are distinct elevations with a rounded profile less than 1000 m above the surrounding relief, as measured from the deepest isobath that surrounds most of the feature (IOC-IHO, 2013). The bathymetric map reveals the presence of clearly distinguishable 8 hills (H1 to H8) and 3 knolls (K1 to K3). These identified features are presented in Fig. 2 and their morphometric details are given in Table 2. Most of the hills and knolls are characterized by an increase in basal width and slope angle against increasing height (Fig. 3). The hills H1 to H5 and H8 are situated in relatively flat seafloor. The basal depth of hills H1 to H5 ranges between 1800–2000 m, while the basal depth of H8 is about 2750 m. These hills exhibit basal extents varying between 20.65 km^2 (H3) and 350 km^2 (H8), with varying height-width (H-W) ratio between 0.028 and 0.247. Three knolls, with basal depth ranging 1400–1800 m, were identified in the Laccadive Basin, with varying heights (310–940 m) and areal extents (25–100 km^2). The 3D bathymetric image of a representative hill (H1) and knoll (K1) along with the contour maps are presented in Fig. 5 to describe the characteristic signatures of hills and knolls mapped in the study area. The bathymetric images of other hills and knolls are given in Supplementary Figs. S3 and S4, respectively.

4.1.3. Guyots and plateaus

Guyots are seamounts with comparatively smooth flat top and plateaus are large, relatively flat elevations that are higher than the

Table 2
Morphometric details of the bathymetric high features identified in the study area. Locations of the features are shown in Fig. 2.

Feature	Centre location (DD)	Depth (m)		Height (m) H	Length (km)		Width (km)		Area (sq. km)		H-W ratio (2H/Wb)	Flatness (Ws/Wb)	Average slope along flanks in degrees	
		Summit	Basal		Summit	Basal	Summit	Basal (Wb)	Summit	Basal			East	West
Seamount-1 (S1)	72.433°E, 15.001°N	464	1530	1066	5.26	11.54	1.74	6.65	9.15	76.74	0.321	0.262	8.4	13
Seamount-2 (S2)	72.629°E, 13.943°N	340	1880	1540	5.30	26.70	2.85	13.09	15.11	349.50	0.235	0.218	16.4	18.5
Seamount-3 (S3)	72.212°E, 12.087°N	440	1500	1060	3.82	8.73	0.97	6.10	3.71	53.25	0.348	0.159	11	17
Seamount-4 (S4)	73.022°E, 11.736°N	392	1890	1498	5.48	23.36	2.26	15.79	12.38	368.85	0.190	0.143	11	14
Seamount-5 (S5)	73.201°'E, 11.335°N	848	1940	1092	1.30	9.25	0.69	6.04	0.90	55.87	0.362	0.114	10	16
Seamount-6 (S6)	73.023°E, 10.271°N	540	1800	1260	8.40	16.38	2.37	7.43	19.91	121.70	0.339	0.319	14	15
Seamount-7 (S7)	73.294°E, 10.214°N	710	1825	1115	5.20	15.80	0.81	9.27	4.21	146.46	0.241	0.087	14	12
Seamount-8 (S8)	74.763°E, 9.762°N	1265	2310	1045	9.22	27.56	3.95	13.62	36.42	375.36	0.153	0.290	9	10
Seamount-9 (S9)	73.199°E, 9.732°N	300	1935	1635	15.27	40.20	2.35	10.38	35.88	417.27	0.315	0.226	13	19
Seamount-10 (S10)	73.281°E, 9.452°N	895	2210	1315	11.87	34.20	2.73	10.48	32.41	358.41	0.251	0.260	13	17
Seamount-11 (S11)	74.684°E, 9.427°N	240	2500	2260	15.25	34.10	3.1	20.36	47.28	694.27	0.222	0.152	14	12.6
Seamount-12 (S12)	75.504°E, 9.357°N	410	1660	1250	14.34	28.40	3.6	14.05	51.62	399.02	0.178	0.256	10	7.7
Seamount-13 (S13)	73.255E, 8.531°N	208	2097	1889	6.80	40.20	2.48	22.5	16.86	904.50	0.168	0.110	14	17
Seamount-14 (S14)	72.836°E, 8.152°N	362	1790	1428	7.85	17.75	2.55	14.05	20.02	249.38	0.203	0.181	15	5
Hill-1 (H1)	71.985°E, 14.421°N	1290	2020	730	3.58	10.44	1.80	7.94	6.44	82.89	0.184	0.227	14	8.4
Hill-2 (H2)	72.572°E, 14.13°N	1271	1870	599	5.30	10.52	1.76	6.90	9.33	72.59	0.174	0.255	8.5	7.5
Hill-3 (H3)	73.057°E, 12.965°N	1491	1905	414	1.10	5.66	0.30	3.65	0.33	20.65	0.227	0.082	8	4.5
Hill-4 (H4)	73.308E, 12.740°N	1335	1889	554	1.23	14.83	0.28	4.48	0.34	66.44	0.247	0.063	10	11
Hill-5 (H5)	72.495°E, 11.225°	1010	1760	750	11.20	21.20	7.31	12.50	81.87	265.00	0.120	0.585	12	10
Hill-6 (H6)	75.229°E, 8.888°N	1500	1910	410	7.96	12.50	3.33	5.04	26.51	63.00	0.163	0.661	4	8
Hill-7 (H7)	75.301°E, 8.405°N	1505	2010	505	10.10	18.50	1.50	6.70	151.50	123.95	0.151	0.224	7.7	4.1
Hill-8 (H8)	74.355°E, 8.360°N	2540	2750	210	10.42	23.50	6.29	14.92	65.54	350.62	0.028	0.422	3	2
Knoll-1 (K1)	73.074°E, 13.654°N	490	1430	940	1.70	6.50	0.70	5.10	1.19	33.15	0.368	0.137	19	10
Knoll-2 (K2)	73.098°E, 13.126°N	1508	1820	312	2.60	6.10	1.70	4.13	4.42	25.19	0.151	0.412	8.5	7.5
Knoll-3 (K3)	73.485°E, 10.800°N	810	1740	930	2.02	10.70	0.55	9.35	1.11	100.05	0.199	0.059	8.5	10.5
Guyot-1 (G1)	73.364°E, 9.401°N	720	1810	1090	2.50	9.41	3.38	10.25	8.45	96.45	0.213	0.330	15	11.5
Guyot-2 (G2)	73.462°E, 9.332°N	525	1870	1345	11.2	21.60	7.82	15.32	87.58	330.91	0.176	0.510	11.2	16
Plateau-1 (Pt1)	72.893°E, 14.331°N	325	920	595	35.40	54.30	13.5	21.6	477.90	1172.80	0.055	0.625	5.5	6.5
Plateau-2 (Pt2)	73.088°E, 13.811°N	376	1110	734	11.60	19.00	3.60	6.50	41.76	123.50	0.226	0.553	14.9	10.3
Plateau-3 (Pt3)	73.563°E, 12.938°N	265	1040	775	20.00	31.30	7.48	17.68	149.60	553.38	0.161	0.423	12	11.3
Plateau-4 (Pt4)	75.202°E, 10.537°N	370	746	376	11.65	18.00	6.90	13.90	80.39	250.20	0.054	0.496	12.6	11.8
Plateau-5 (Pt5)	74.609°E, 7.955°N	1888	2720	832	13.40	32.60	4.91	13.64	65.79	444.66	0.122	0.360	13.5	9.5
Plateau-6 (Pt6)	75.511°E, 7.844°N	1080	1670	590	7.10	21.30	17.00	32.70	120.70	696.51	0.036	0.520	6.5	7.7

surrounding relief with one or more relatively steep sides (IOC-IHO, 2013). The study area contains two guyots, which are located in relatively flat seafloor close to the eastern flank of the Laccadive Plateau (Fig. 2). These guyots G1 and G2, whose basal depths are about 1800 m, show basal extent of 96 km^2 and 330 km^2, with flatness of 0.330 to 0.510, respectively (Fig. 3 and Table 2). The 3D bathymetric and the contour maps of guyots G1 and G2 are presented in Fig. 6. From the bathymetric map, we also identify six plateaus, Pt1 to Pt6 in the study area (Fig. 2). All the plateaus, except Pt6 are situated in the southwestern continental slope of India, while the plateau Pt5 is located in the Laccadive Basin. The plateaus in the continental slope exhibit different basal depths in the landward and seaward sides of these features. The basal depths for plateaus given in Table 2 represent those measured in the landward direction. These plateaus possess basal extent ranging from 123-1172 km^2 and flatness varying from 0.350 to 0.625 (Table 2). All plateaus exhibit moderate to steep sloping flanks, showing gully patterns over both the flanks. The 3D bathymetric images as well as contour maps of two representative plateaus, Pt1 and Pt2 are presented in Fig. 7 and the other plateaus are shown in Supplementary Fig. S5.

4.2. Sub-seafloor configuration from seismic reflection data

We used three multichannel and two single channel seismic sections (Fig. 8) to depict sub-seafloor configuration of the selected bathymetric features considered in the present study. The seismic sections SWC-01, SWC-03, SWC-07, AB and CD (Fig. 2) cut across the bathymetric high features S12, S7, H4, Pt1, and H7, respectively. Some of these features (Pt1, H7 and S12) are located in the continental slope region, while others (H4 and S7) are located in the deep sea basin. The multichannel seismic image of the hill H4 (Fig. 8a) and seamount S7 (Fig. 8b) show that the flanks of these features are steep and the sediments are nearly absent on top of them. This observation suggests that both these features might represent volcanic extrusives, with a basement high piercing through the sediment surface. On the other hand, the multichannel seismic image of the seamount S12 depict (Fig. 8c) a basement high associated with bulging of thick sediment layers (~2.5s TWT) on top of it, suggesting the presence of a subsurface intrusive. The single channel seismic section (Fig. 8d) across the plateau Pt1 shows that only a thin layer of the sediments (~0.4s TWT) exists on top of this ~20 km-wide bathymetric and basement highs. This feature, located in the continental slope region, was earlier identified by Rao et al. (2010) and they reported that the lower half of the flanks is covered mostly by slump sediments. The hill H7 represents a bathymetric feature with steep flanks (Fig. 8e), suggesting a volcanic extrusive. This feature represents the same bathymetric high identified by Yatheesh et al. (2013) in the Chain-Kairali Escarpment domain in the southwestern continental margin of India.

4.3. Gravity and magnetic signatures

The free-air gravity anomalies and magnetic anomalies of the selected representative bathymetric high features are presented in Fig. 9 as images, contours and profiles to analyze their characteristics. The free-air gravity anomalies corresponding to all the features (presented in Fig. 9) are highly correlated with the topography, with an observed maximum corresponding to their summit. These anomalies decrease along the flanks of the features and get superimposed on the gravity signature of the surrounding flat seafloor.

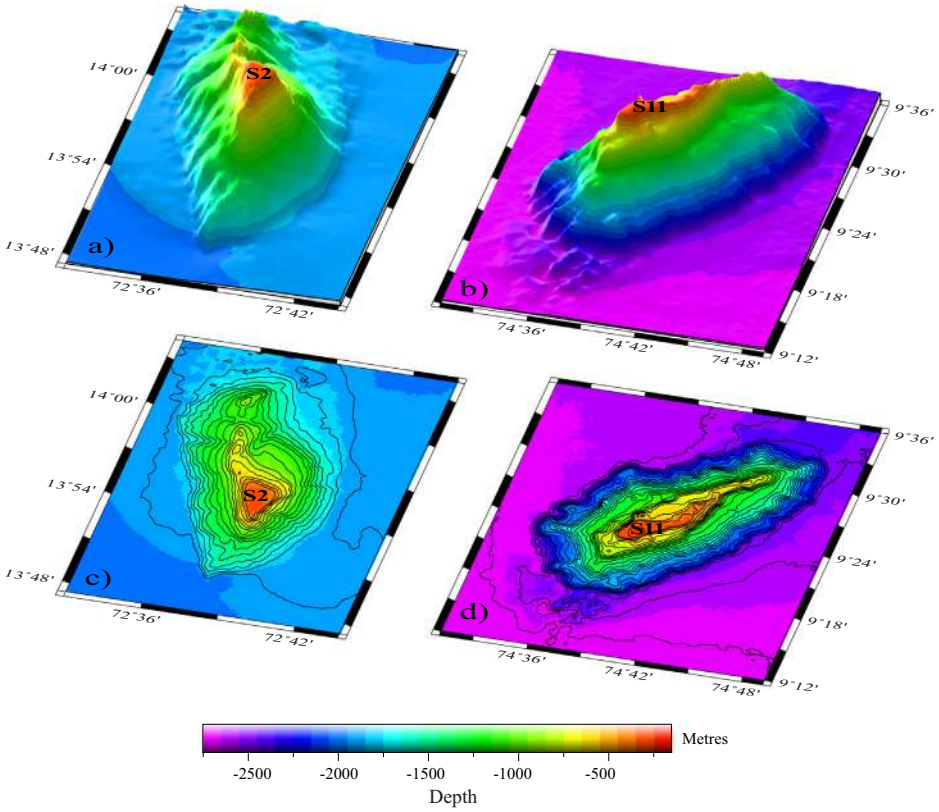

Fig. 4. Three-dimensional images (a and b) and the contour maps at 100 m interval (c and d) of the representative seamounts in the study area (Seamounts S2 and S11).

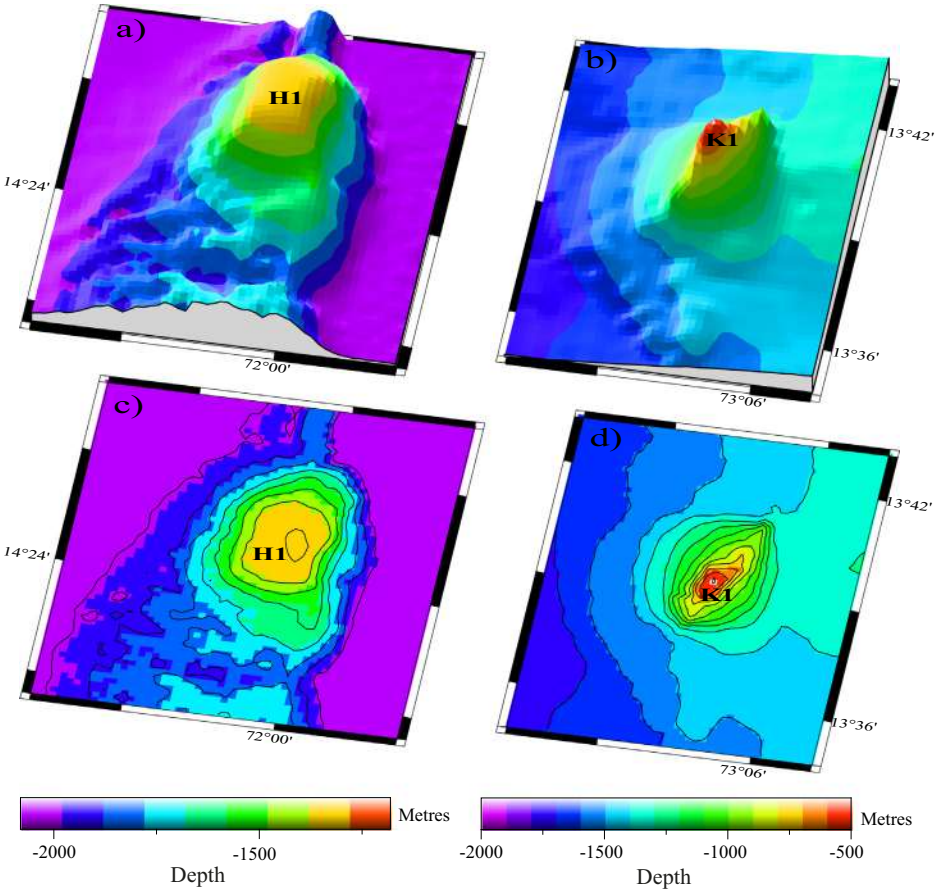

Fig. 5. Three-dimensional images (a and b) and the contour maps at 100 m interval (c and d) of the representative hills and knolls in the study area (Hill H1 and Knoll K1).

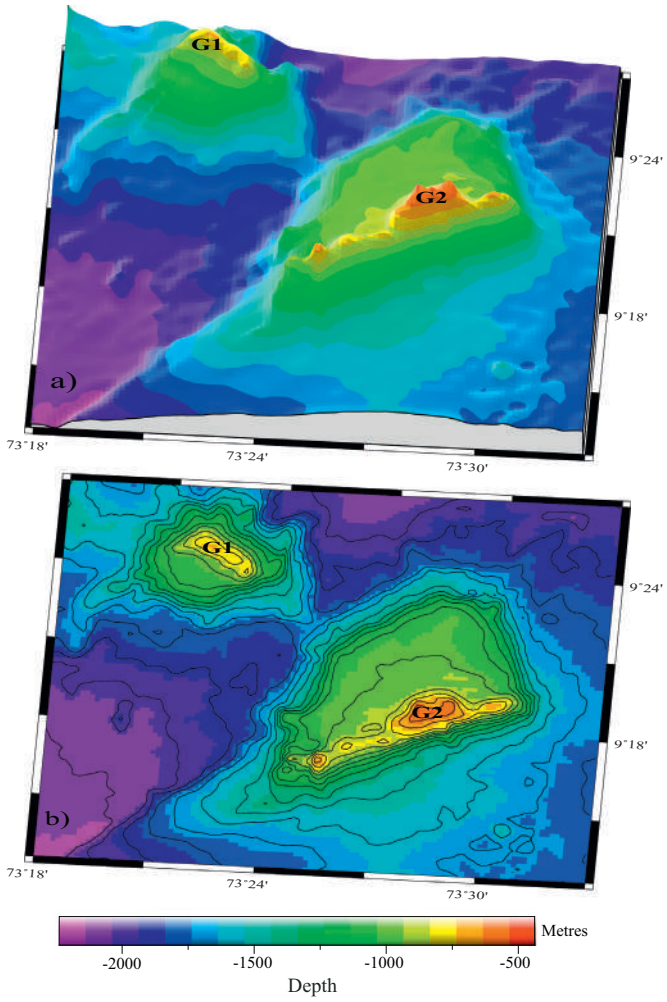

Fig. 6. Three-dimensional image (a) and the contour map at 100 m interval (b) of the representative Guyots G1 and G2 in the study area.

The hill H1 is characterized by a broader gravity anomaly with its maximum (~−25 mGal) over its summit (Fig. 9a). The gravity anomaly at the summit of seamount S2 is ~−5 mGal and its base is defined by the −50 mGal contour (Fig. 9b). The highest magnitude of free-air gravity anomaly, among all the features presented in Fig. 9, is observed over the central part of plateau Pt3, reaching up to ~20 mGal, with a magnitude of ~−70 mGal at the base of the feature (Fig. 9c). The seamount S12 is described by free-air gravity anomalies of ~−15 mGal for the summit and ~−40 mGal for its base (Fig. 9d). The hill H7 corresponds to a nearly N-S trending gravity high with free-air gravity anomaly magnitudes of ~−15 mGal over the summit and ~−35 mGal at the base (Fig. 9e). The plateau Pt6 is represented as an E-W trending gravity high with ~5 mGal at summit and ~−30 mGal at its base (Fig. 9f).

The northernmost region of Hill H1 is associated with an E-W trending negative magnetic anomaly with maximum intensity of −60 nT and the southernmost region of this feature is characterized by a N-S trending positive magnetic anomaly with a maximum intensity of 130 nT (Fig. 9a). The seamount S2 is characterized by a relatively broader magnetic anomaly with two peaks, one located closer to the northern flank and the other one located at the western flank of the seamount S2 (Fig. 9b). The intensity of this magnetic anomaly, trending nearly NNW-SSE, gradually decreases towards southern and eastern flanks of the seamount with a sharp change in magnetic intensity from 90 nT to 60 nT from the base of the seamount to the adjacent flat seafloor. The magnetic anomaly over plateau Pt3 exhibits a nearly circular pattern (Fig. 9c) with an observed maximum intensity corresponding to the foot of the western flank (~270 nT). The eastern part of the plateau Pt3 displays negative anomaly with an apparent intensity of ~−30 nT, which gradually increases westward and northward from the summit of the plateau. The seamount S12 exhibit a relatively flat signature of magnetic anomaly with an intensity of ~100 nT, with a gradual increase in intensity towards southwest and a decrease in intensity towards north in its southwestern and northern extremities, respectively (Fig. 9d). The northernmost flank of the hill H7 coincides with a positive magnetic anomaly peak of ~170 nT, with a gradual decrease in intensity towards the south (Fig. 9e). The Plateau Pt6 is characterized by two negative magnetic anomalies, located on the northern and southern parts of the seamount, with intensities up to ~−380 nT and ~−440 nT,

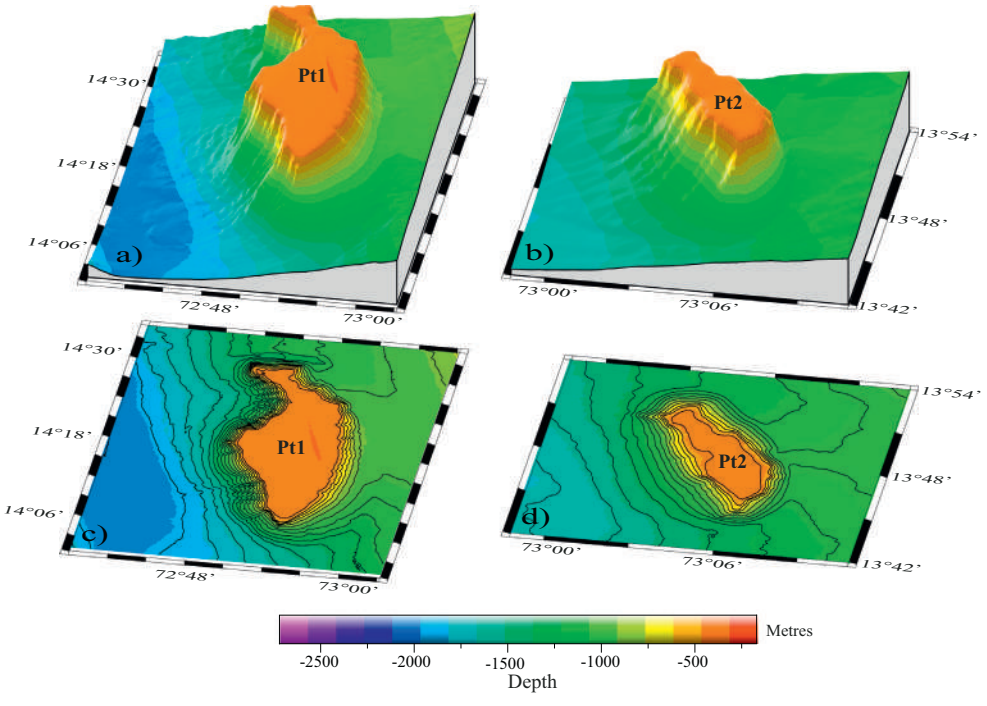

Fig. 7. Three-dimensional images (a and b) and the contour maps at 100 m interval (c and d) of the representative plateaus in the study area (Plateaus Pt1 and Pt2).

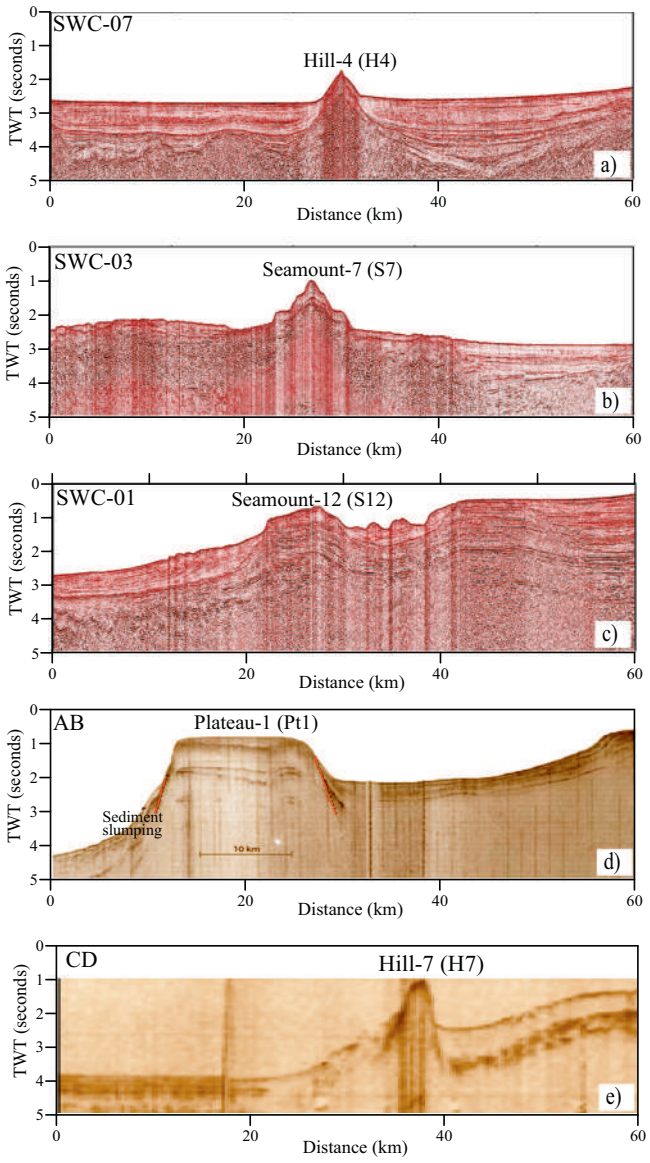

Fig. 8. Seismic reflection sections across (a) Hill H4; (b) Seamount S7; (c) Seamount S12; (d) Plateau Pt1; and (e) Hill H7. Locations of these sections are given in Fig. 2 as white lines and in Supplementary Fig. S1 as pink lines.

respectively (Fig. 9f). The negative magnetic anomaly in the south coincides with the southern flank of the plateau, while those in the north are located on the northernmost region of the plateau summit. These two negative magnetic anomalies, trending nearly WNW-ESE, are divided by a zone of magnetic anomalies with maximum intensity of ~−260 nT.

4.4. Probable genesis of bathymetric highs

The updated plate tectonic evolution model of the Arabian Sea (Bhattacharya and Yatheesh, 2015) suggests that the western continental margin of India was formed by the rifting and subsequent drifting among India, Seychelles and Madagascar, along with the adjacent microcontinental slivers of the Laxmi Ridge and the Laccadive Plateau. Among these, the first episode was separation of India-Laxmi Ridge-Seychelles block from Madagascar, believed to have been caused by the Marion hotspot. The evidence to this inference comes from the existence of ~85–92 Ma volcanics from the western side of India (Valsangkar et al., 1981; Radhakrishna et al., 1994, 1999; Torsvik et al., 2000; Anil Kumar et al., 2001; Pande et al., 2001; Melluso et al., 2009; Radhakrishna and Joseph, 2012; Ram Mohan et al., 2016) and the eastern side of Madagascar (Storey et al., 1995; Torsvik et al., 2000). The second episode was separation of Seychelles-Laxmi Ridge block from India, which is considered to have been initiated by oldest pulse of Réunion hotspot (at ~68.5 Ma) as evidenced from the existence of ~68.5 Ma old volcanics located north of the main Deccan Flood Basalt province (Basu et al., 1993). During this period, a break-up occurred also between the Laccadive Plateau and India. At around 65–66 Ma, the bulk of the Deccan Flood Basalt was emplaced on the Indian mainland with a large fraction of its activity during chron 29R (Courtillot et al., 1988), under the influence of the Réunion hotspot. Subsequently, the third episode of the break-up between Seychelles and Laxmi Ridge-India block occurred shortly before 62.5 Ma, coinciding with the formation of Ghatkopar-Powai tholeiitic basalt (Pande et al., 2017) and emplacement of Raman-Panikkar-Wadia seamount chain in the Laxmi Basin (Bhattacharya and Yatheesh, 2015; Pande et al., 2017). Evidence to this comes from the oldest magnetic anomalies (chron 28ny) inferred from the conjugate Arabian and Eastern Somali basins (Miles and Roest, 1993; Chaubey et al., 2002b), formed by seafloor spreading along the Carlsberg Ridge. The spreading along the Carlsberg Ridge continued with the northward motion of Indian plate over the Réunion hotspot and this motion caused the formation of the Laccadive-Chagos Ridge, which mainly consists of the Laccadive Plateau, Maldive Ridge and the Chagos Bank, along with the relatively deep saddle-like features.

The genesis of the bathymetric highs in the oceanic regions are generally explained in terms of hotspot activity, ridge-hotspot interaction, ridge parallel faulting, off-axis volcanism and propagating fracture, depending on the respective geological settings (Das et al., 2007 and references therein). The main geodynamic events occurred in the vicinity of our study area are the Marion and Réunion hotspots volcanism. Therefore, we attempt to provide a reasonable explanation for the genesis of the bathymetric highs in terms of hotspot volcanism. The bathymetric highs in the study area mainly falls in two domains, those located either in the continental slope of India or in the Laccadive Basin and the adjacent part of the Laccadive Plateau. The bathymetric features in the continental slope region are the plateaus Pt1, Pt2, Pt3, Pt4 and Pt6, hills H6 and H7, knoll K1, and seamount S12. The features, hills H6 and H7, seamount S12 and plateaus Pt4 and Pt6 are located over the Chain-Kairali Escarpment, which represents the western boundary of the thinned continental crust of the Alleppey-Trivandrum Terrace Complex. The Chain-Kairali Escarpment is interpreted (Yatheesh et al., 2013) to represent the transform boundary formed due to the gliding between India and Madagascar during the initial stages of India-Madagascar separation, caused by the Marion hotspot volcanism. Therefore, we believe that the bathymetric features located in the relatively southern region of Alleppey-Trivandrum Terrace Complex were created by the Marion hotspot volcanism (e.g. H-7, showing the characteristics of an extrusive body in Fig. 8e).

The plateaus Pt1, Pt2 and Pt3 and knoll K1 are located relatively north and some of these features (plateaus Pt1 and Pt3) were interpreted by Rao et al. (2010) to represent continental slivers and horst structures formed during stretching and faulting along the southwestern continental margin of India, implying India-Madagascar break-up. However, we observe that these features located in the relatively northern part of the study area are very close to the Réunion hotspot track (Fig. 10) and therefore one can equally argue the genesis of these features to Réunion hotspot volcanism as well as India-Madagascar rifting, caused by the Marion hotspot volcanism. Fig. 10 also shows that the Réunion hotspot track is very close to the eastern part of the Laccadive Plateau and therefore, we are tempted to attribute the genesis of these bathymetric highs in the Laccadive Basin and the Laccadive Plateau to the Réunion hotspot volcanism. Since the effect of the hotspot can go over several hundreds of kilometers distance (Tolan et al., 1989; Storey et al., 1995), such an interpretation is reasonable even if the referred features in the Laccadive Basin are located not over the hotspot track exactly. This suggestion on

the effect of hotspot to a larger area is valid in the case of Sagar Kanya Seamount (Bhattacharya and Subrahmanyam, 1991) in the Arabian Sea. This seamount, which is inferred to have been formed by Réunion hotspot, is nearly 200 km away from the Réunion hotspot track (Fig. 10).

5. Summary and conclusion

We carried out detailed geophysical investigations of bathymetric high features in the Laccadive Basin and the adjacent areas to understand their distribution, morphometry, geophysical characteristics and probable genesis. The updated bathymetric map of the study area highlights 33 bathymetric high features, consisting of 14 seamounts, 8 hills, 3 knolls, 2 guyots and 6 plateaus. Majority of the identified seamounts are located in the Laccadive Basin and the eastern sector of the Laccadive Plateau. Most of these seamounts are with single peak, but a few seamounts show multiple peaks. Morphometric analysis of these seamounts shows that height of the seamount increases roughly with increasing basal width. Morphology of the identified hills and knolls suggest a characteristic increase in basal width and slope angle against increasing height. We identified two adjacent guyots, located in relatively flat seafloor close to the eastern flank of the Laccadive Plateau. Most of the plateaus identified in the study area are located in the western continental slope of India and they exhibit moderate to

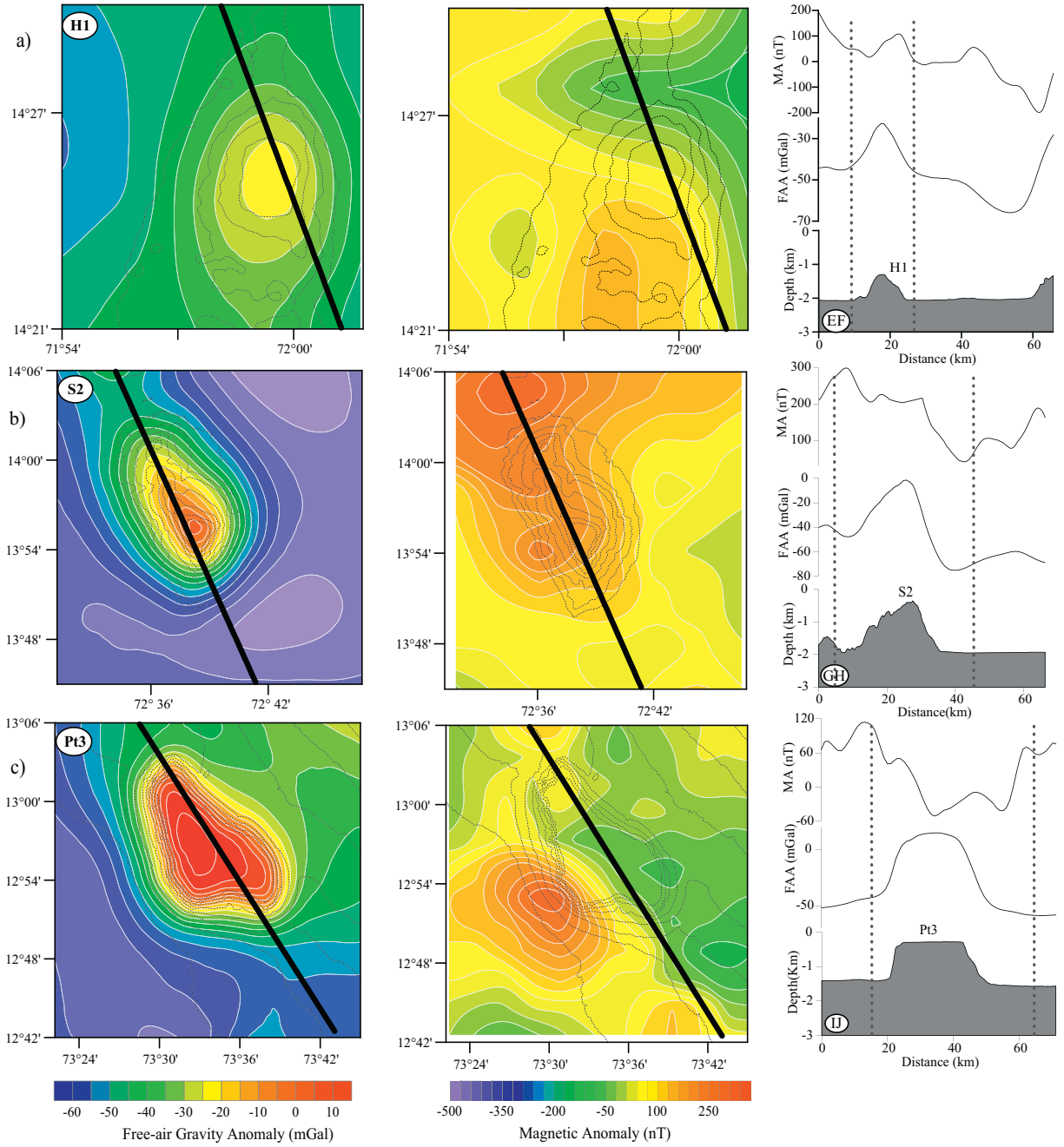

Fig. 9. Maps of the gravity and magnetic anomalies along with the stacked bathymetry, gravity and magnetic profiles across selected features (a) Hill H1; (b) Seamount S2; (c) Plateau Pt3; (d) Seamount S12; (e) Hill H7; (f) Plateau Pt6. The black contours represent the isobaths at 200 m interval, used to depict the extent of the bathymetric features. The white lines on the gravity image represents gravity anomaly contours in 5 mGal interval and those in the magnetic image represents magnetic anomaly contours in 30 nT interval. The locations of the stacked bathymetry, gravity and magnetic profiles segments within the grey dotted lines are shown as black thick lines in the gravity and magnetic images. FAA: Free-air gravity anomaly; MA: Magnetic anomaly.

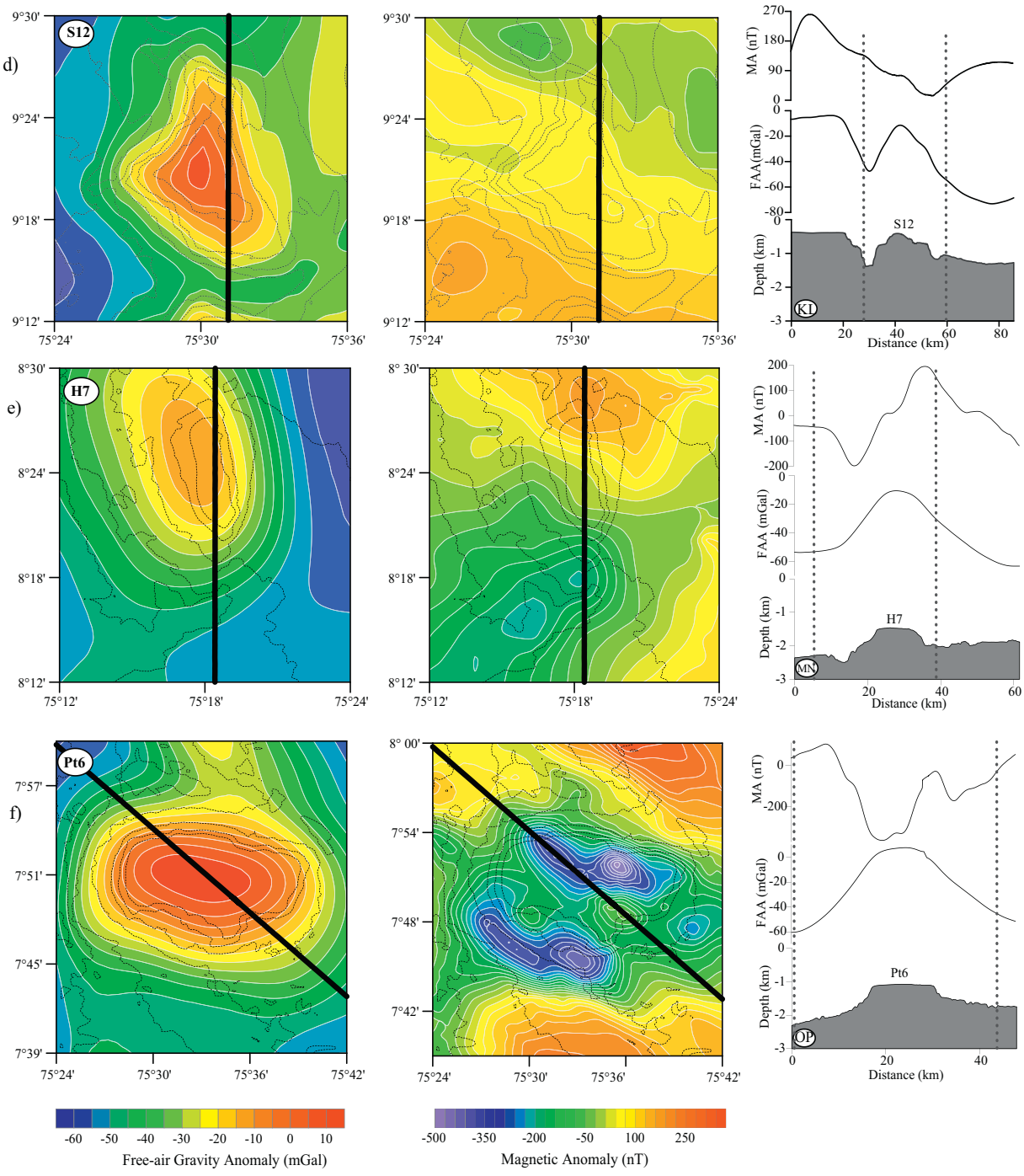

Fig. 9 (*continued*).

steep sloping flanks, showing gully pattern on both the flanks. We analyzed sub-seafloor configuration of the selected bathymetric features using seismic reflection sections. The inferred basement configuration suggests that some of the bathymetric features might represent volcanic extrusives while others might represent basement highs associated with bulging of sediment layers over the subsurface volcanic intrusive. The sea-surface gravity signatures of the selected features suggest a characteristic relatively high gravity anomaly superimposed over a regional negative anomaly. This relative gravity high corresponds to the summit area of the bathymetric high and this gravity anomaly reduces along its flanks. The magnetic anomalies over the bathymetric high features exhibit complex behavior. Both negative and positive magnetic anomalies are observed over the features, superimposed over the regional magnetic signatures.

The study area is located very close to the southwestern continental margin of India, which was formed by the India-Seychelles-Madagascar break-up. The updated plate tectonic evolution model for the Arabian Sea suggests that the break-up between India and Madagascar occurred at ~90 Ma, believed to have been caused by the Marion hotspot, and then Seychelles-India break-up occurred at ~68.5 Ma, possibly caused by the earliest pulse of the Réunion hotspot (Bhattacharya and Yatheesh, 2015). We attempted to provide a reasonable answer for the genesis of the bathymetric features in the study area, under the constraints of this tectonic setting. Majority of these features appears to have caused by the hotspot volcanism, however, at present it is not

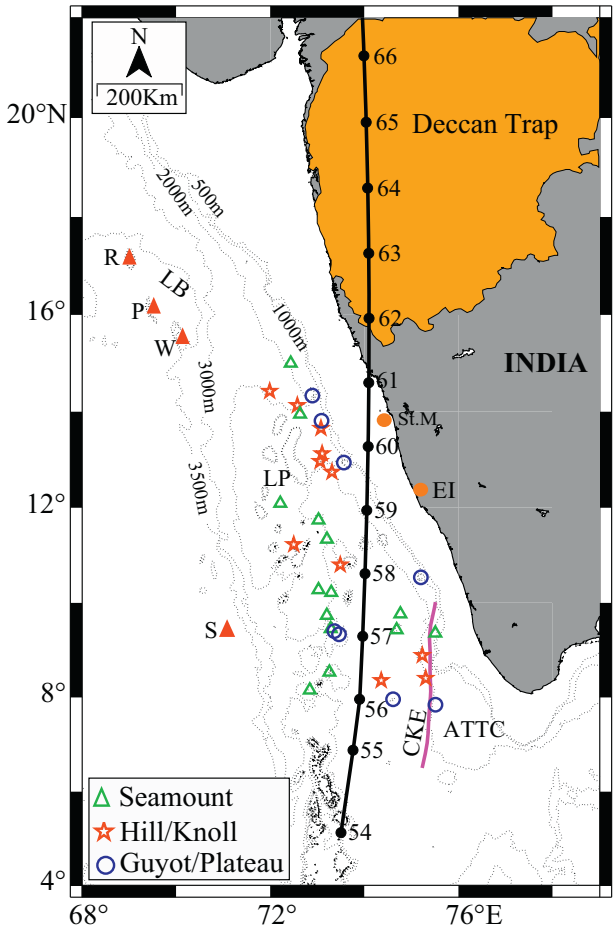

Fig. 10. Generalized bathymetric map (GEBCO isobaths) of the study area showing locations and distribution of the bathymetric features identified in the present study. The thick black line connecting the black solid circles represents the Réunion hotspot track computed based on Müller et al. (1993). The numbers given to the solid black circles represent the ages in million years (Ma). Other details are as in Fig. 1.

possible to conclude whether these bathymetric highs are related to the Marion hotspot volcanism or Réunion hotspot volcanism. Based on the proximity of this region to the St. Mary Islands and the Ezhimala Igneous Complex, which are considered to be a product of the Marion hotspot, we consider that the bathymetric highs located in the southwestern continental slope of India were formed by the Marion hotspot volcanism. But, the bathymetric features in the Laccadive Basin and eastern Laccadive Plateau are in the proximity of the Réunion hotspot track and therefore we attribute the genesis of these bathymetric features to the Réunion hotspot volcanism. However, detailed geochronological, paleomagnetic and geochemical investigations of the volcanic rocks collected from these identified features need to be carried out for the validation of the genesis proposed in the present study.

Supplementary data to this article can be found online at https://doi.org/10.1016/j.geomorph.2018.04.015.

Acknowledgement

The authors are grateful to the Director, National Centre for Antarctic and Ocean Research (NCAOR), Goa and Director, CSIR – National Institute of Oceanography (CSIR-NIO), Goa, for their encouragement and support to carry out this work. The authors are also thankful to Ministry of Earth Sciences (MoES/EC/EEZ/32/2012-PC-II), New Delhi for their financial support through the EEZ Programme and EEZ Advisory Committee for permission to publish this work. This study forms a part of the PhD work of CMB at Goa University. We are indebted to the two anonymous reviewers for their careful review of the manuscript and valuable comments. We are grateful to Prof. Andrew James Plater, Editor, for editorial handling of the manuscript. We gratefully acknowledge the support received from the shipboard scientific party, officers and crew members of all the cruises of the EEZ Programme conducted onboard *Akademic Boris Petrov*, *ORV Sagar Kanya* and *MGS Sagar*. Directorate General of Hydrocarbons, New Delhi is thanked for providing the multichannel seismic reflection sections used in the present study. Figures were drafted with GMT (Wessel and Smith, 1995) and *SURFER* (www.goldensoftware.com). This is NCAOR contribution number 16/2018 and NIO contribution number 6216.

References

Ajay, K.K., Chaubey, A.K., Krishna, K.S., Rao, D.G., Sar, D., 2010. Seaward dipping reflectors along the SW continental margin of India: Evidence for volcanic passive margin. Journal of Earth System Science 119 (6), 803–813.

Avraham, Z.B., Bunce, E.T., 1977. Geological study of the Chagos-Laccadive Ridge, Indian Ocean. J. Geophys. Res. 82, 1295–1305.

Basu, A.R., Renne, P.R., Dasgupta, D.K., Teichmann, F., Poreda, R.J., 1993. Early and late igneous pulses and high ^{3}He plume origin for the Deccan Flood Basalts. Science 261, 902–906.

Bhattacharya, G.C., Chaubey, A.K., 2001. Western Indian Ocean - a glimpse of the tectonic scenario. In: Sengupta, R., Desa, E. (Eds.), The Indian Ocean - A Perspective. Vol 2. Oxford & IBH, pp. 691–729.

Bhattacharya, G.C., Subrahmanyam, V., 1991. Geophysical study of a seamount located on the continental margin of India. Geo-Mar. Lett. 11 (2), 71–78.

Bhattacharya, G.C., Yatheesh, V., 2015. Plate-tectonic evolution of the deep ocean basins adjoining the western continental margin of India - a proposed model for the early opening scenario. In: Mukherjee, S. (Ed.), Petroleum Geoscience: Indian Contexts. Springer, pp. 1–61.

Bhattacharya, G.C., Murty, G.P.S., Srinivas, K., Chaubey, A.K., Sudhakar, T., Nair, R.R., 1994. Swath bathymetric investigation of the seamounts located in Laxmi Basin, Eastern Arabian Sea. Mar. Geod. 17, 169–182.

Chaubey, A.K., Rao, D.G., Srinivas, K., Ramprasad, T., Ramana, M.V., Subrahmanyam, V., 2002a. Analyses of multichannel seismic reflection, gravity and magnetic data along a regional profile across the central-western continental margin of India. Mar. Geol. 182, 303–323.

Chaubey, A.K., Dyment, J., Bhattacharya, G.C., Royer, J.Y., Srinivas, K., Yatheesh, V., 2002b. Paleogene magnetic isochrons and palaeo-propagators in the Arabian and Eastern Somali basins, NW Indian Ocean. In: Clift, P.D., Croon, D., Gaedicke, C., Craig, J. (Eds.), The Tectonic and Climatic Evolution of the Arabian Sea Region. 195. Geological Society, London, pp. 71–85 Special Publication.

Clague, D.A., Reynolds, J.R., Davis, A.S., 2000. Near-ridge seamount chains in the northeastern Pacific Ocean. J. Geophys. Res. 105, 16541–16561.

Clouard, V., Bonneville, A., Gillot, P.-Y., 2003. The Tarava Seamounts: a newly characterized hotspot chain on the South Pacific Superswell. Earth Planet. Sci. Lett. 207, 117–130.

Courtillot, V., Feraud, G., Maluski, H., Vandamme, D., Moreau, M.G., Besse, J., 1988. Deccan flood basalts and the Cretaceous/Tertiary boundary. Nature 333, 843–846.

Das, P., Iyer, S.D., Kodagali, V.N., Krishna, K.S., 2005. Distribution and Origin of Seamounts in the Central Indian Ocean Basin. Mar. Geod. 28 (3), 259–269.

Das, P., Iyer, S.D., Kodagali, V.N., 2007. Morphological characteristics and emplacement mechanism of the seamounts in the Central Indian Ocean Basin. Tectonophysics 443 (1–2), 1–18.

DGH, 2014. Directorate general of hydrocarbons (DGH), Noida. India Web Page: Kerala Konkan Basin accessed 29.10.14. http://www.dghindia.org/15.aspx.

Duncan, R.A., 1981. Hotspots in the Southern Oceans - an absolute frame of reference for the motion of the Gondwana continents. Tectonophysics 74, 29–42.

Duncan, R.A., Clague, D.A., 1985. Pacific plate motion recorded by linear volcanic chains. In: Nairn, A.E.M., Stehli, F.G., Uyeda, S. (Eds.), The Ocean Basins and Margins. Vol. 7A. Plenum, New York, pp. 89–112.

Fisher, R.L., Sclater, J.G., McKenzie, D.P., 1971. Evolution of the Central Indian Ridge, Western Indian Ocean. Geol. Soc. Am. Bull. 82, 553–562.

Fornari, D.J., Ryan, W.B.F., Fox, P.J., 1984. The evolution of craters and calderas on young seamounts: insight from sea MARC 1 and Sea Beam sonar surveys of a small seamount group near the axis of the East Pacific Rise at ~10° N. J. Geophys. Res. 89, 11069–11083.

Fornari, D.J., Perfit, M.R., Allen, J.F., Batiza, R., Haymon, R., Ryan, W.B.F., Smith, T., Simkin, T., Luckman, M.A., 1988. Seamounts as windows into the mantle process: structural and geochemical studies of the Lamont seamounts. Earth Planet. Sci. Lett. 89, 63–83.

Harris, P.T., Macmillan-Lawler, M., Rupp, J., Baker, E.K., 2014. Geomorphology of the oceans. Mar. Geol. 352, 4–24.

IOC-IHO, 2013. Standardization of undersea feature names. Publication B-6, Edition 4.1 0, p. 18.

IOC-IHO-BODC, 2003. Centenary Edition of the GEBCO Digital Atlas. CD-ROM on Behalf of the Intergovernmental Oceanographic Commission and the International Hydrographic Organization as Part of the General Bathymetric Chart of the Oceans. British Oceanographic Data Centre, Liverpool, UK.

Iyer, S.D., 2009. Seamounts- their formation, mineral deposits, biodiversity and atmospheric oxygen. Geo-Spectrum Interface 4, 33–36.

Iyer, S.D., Mehta, C.M., Das, P., Kalangutkar, N.G., 2012. Seamounts - characteristics, formation, mineral deposits and biodiversity. Geol. Acta 10 (3), 295–308.
Kodagali, V.N., 1989. Morphometric Studies on a part of Central Indian Ocean. J. Geol. Soc. India 33, 547–555.
Kodagali, V.N., 1992. Morphologic investigation of uncharted seamount from central Indian Basin revisited with multibeam sonar system. Mar. Geod. 15, 47–56.
Kodagali, V.N., 1998. A pair of seamount chains in the Central Indian Basin, identified from multibeam mapping. Mar. Geod. 21 (2), 147–158.
Kumar, Anil, Pande, K., Venkatesan, T.R., Bhaskar Rao, Y.J., 2001. The Karnataka Late Cretaceous dykes as products of the Marion hotspot at the Madagascar-India breakup event: evidence from $^{40}Ar/^{39}Ar$ geochronology and geochemistry. Geophys. Res. Lett. 28 (14), 2715–2718.
Melluso, L., Sheth, H.C., Mahoney, J.J., Morra, V., Petrone, C.M., Storey, M., 2009. Correlations between silicic volcanic rocks of the St. Mary's Islands (southwestern India) and eastern Madagascar: implications for Late Cretaceous India Madagascar reconstructions. J. Geol. Soc. Lond. 166, 283–294.
Menard, H.W., 1964. Marine Geology of the Pacific. McGraw-Hill Book Company, New York 271.
Miles, P.R., Roest, W.R., 1993. Earliest seafloor spreading magnetic anomalies in the north Arabian Sea and the ocean-continent transition. Geophys. J. Int. 115, 1025–1031.
Morgan, W.J., 1981. Hotspot tracks and the opening of the Atlantic and Indian Oceans. In: Emiliani (Ed.), The Sea. Vol 7. Wiley Interscience New York, pp. 443–487.
Mukhopadhyay, R., Batiza, R., 1994. Basinal seamounts and seamount chains of the Central Indian Ocean: Probable near-axis origin from a fast-spreading Ridge. Mar. Geophys. Res. 16, 303–314.
Mukhopadhyay, R., Khadge, N.H., 1990. Seamounts in the Central Indian Ocean Basin: indicators of the Indian plate movement. Proceedings of the Indian Academy of Sciences (Earth and Planetary Science) 99, 357–365.
Mukhopadhyay, R., Rajesh, M., De, S., Chakraborty, B., Jauhari, P., 2008. Structural highs on the western continental slope of India: implications for regional tectonics. Geomorphology 96 (1–2), 48–61.
Müller, D.R., Royer, J.-Y., Lawver, A.L., 1993. Revised plate motions relative to the hotspots from combined Atlantic and Indian Ocean hotspot tracks. Geology 21, 275–278.
Pande, K., Sheth, H.C., Bhutani, R., 2001. ^{40}Ar-^{39}Ar age of the St. Mary's Islands volcanics, southern India: record of India - Madagascar break-up on the Indian subcontinent. Earth Planet. Sci. Lett. 193, 39–46.
Pande, K., Yatheesh, V., Sheth, H., 2017. $^{40}Ar/^{39}Ar$ dating of the Mumbai tholeiites and Panvel flexure: intense 62.5 Ma onshore-offshore Deccan magmatism during India-Laxmi Ridge-Seychelles breakup. Geophys. J. Int. 210, 1160–1170.
Radhakrishna, T., Joseph, M., 2012. Geochemistry and paleomagnetism of Late Cretaceous mafic dikes in Kerala, southwest coast of India in relation to large igneous provinces and mantle plumes in the Indian Ocean region. Geol. Soc. Am. Bull. 124 (1/2), 240–255.
Radhakrishna, T., Dallmeyer, R.D., Joseph, M., 1994. Paleomagnetism and 36Ar/40Arvs 39Ar/40Ar isotope correlation ages of dyke swarms in Central Kerala, India: tectonic implications. Earth Planet. Sci. Lett. 121, 213–226.
Radhakrishna, T., Maluski, H., Mitchell, J.G., Joseph, M., 1999. $^{40}Ar^{39}Ar$ and K/Ar geochronology of the dykes from the south Indian granulite terrain. Tectonophysics 304, 109–129.
Ram Mohan, M., Shaji, E., Satyanarayanan, M., Santosh, M., Tsunogae, T., Yang, Q.Y., Dhanil Dev, S.G., 2016. The Ezhimala Igneous Complex, southern India: possible imprint of Late Cretaceous magmatism within rift setting associated with India-Madagascar separation. J. Asian Earth Sci. 121, 56–71.
Rao, D.G., Paropkari, A.L., Krishna, K.S., Chaubey, A.K., Ajay, K.K., Kodagali, V.N., 2010. Bathymetric highs in the mid-slope region of the western continental margin of India–structure and mode of origin. Mar. Geol. 276 (1–4), 58–70.
Sclater, J.G., Fisher, R.L., 1974. The evolution of the east central Indian Ocean. Geol. Soc. Am. Bull. 85, 683–702.
Shen, Y., Scheirer, D.S., Forsyth, D.W., Macdonald, K.C., 1993. Two forms of volcanism: implications for mantle flow and off-axis crustal production on the west flank of the southern East Pacific Rise. J. Geophys. Res. 98, 17875–17889.
Sheth, H.C., 2005. From Deccan to Reunion: No trace of a mantle plume. In: Foulger, G.R., Natland, J.H., Presnall, D.C., Anderson, D.L. (Eds.), Plates, Plumes, and Paradigms, Special Paper 388. Geological Society of America, pp. 477–501.
Smith, D.K., Jordan, T.H., 1988. Seamount statistics in the Pacific Ocean. J. Geophys. Res. 93, 2899–2918.
Storey, M., Mahoney, J.J., Saunders, A.D., Duncan, R.A., Kelley, S.P., Coffin, M.F., 1995. Timing of hotspot related volcanism and the breakup of Madagascar and India. Science 267 (5199), 852–855.
Tolan, T.L., Reidel, S.P., Beeson, M.H., Anderson, J.L., Fecht, K.R., Swanson, D.A., 1989. Revisions to the estimates of the areal extent and volume of the Columbia River Basalt Group. In: Reidel, S.P., Hooper, P.R. (Eds.), Volcanism and Tectonism in the Columbia River Flood-Basalt Province. 239. Geological Society of America, pp. 1–20 Special Paper.
Torsvik, T.H., Tucker, R.D., Ashwal, L.D., Carter, L.M., Jamtveit, V., Vidyadharan, K.T., Venkataramana, P., 2000. Late cretaceous India - Madagascar fit and timing of breakup related magmatism. Terra Nova 12, 220–224.
Valsangkar, A.B., Radhakrishnamurthy, C., Subbarao, K.V., Beckinsale, R.D., 1981. Paleomagnetism and Potassium-Argon age studies of acid igneous rocks from the St. Mary Islands. Geological Society of India 3, 265–275.
Wessel, P., 2001. Global distribution of seamounts inferred from gridded Geosat/ERS-1 altimetry. J. Geophys. Res. 106, 19431–19441.
Wessel, P., Smith, W.H.F., 1995. New version of the Generic Mapping Tools released. EOS Transactions. Am. Geophys. Union 329.
Wessel, P., Sandwell, D.T., Kim, S.S., 2010. The global seamount census. Oceanography 23, 24–33.
Whitmarsh, R.B., 1974a. Some aspects of plate tectonics in the Arabian Sea. Initial Reports of the Deep Sea Drilling Project, 23. US Govt. Printing Office, Washington, pp. 527–535.
Whitmarsh, R.B., 1974b. Appendix V. Geophysical Appendix. Initial Reports of the Deep Sea Drilling Project, 23. US Govt. Printing Office, Washington, pp. 1159–1171.
Yatheesh, V., Bhattacharya, G.C., Mahender, K., 2006. The terrace like feature in the mid-continental slope region off Trivandrum and a plausible model for India–Madagascar juxtaposition in immediate pre-drift scenario. Gondwana Res. 10, 179–185.
Yatheesh, V., Kurian, P.J., Bhattacharya, G.C., Rajan, S., 2013. Morphotectonic architecture of an India-Madagascar breakup related anomalous submarine terrace complex on the southwest continental margin of India. Mar. Pet. Geol. 46, 304–318.

Geomorphology 373 (2021) 107488

Annexure 2

Contents lists available at ScienceDirect

Geomorphology

journal homepage: www.elsevier.com/locate/geomorph

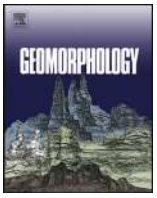

Sagar Kanya Bathymetric High Complex: An extinct giant submarine volcanic caldera in the Eastern Arabian Sea?

C.M. Bijesh [a,b], V. Yatheesh [c], D. Twinkle [a], Abhishek Tyagi [a], P. John Kurian [a,*]

[a] National Centre for Polar and Ocean Research, Ministry of Earth Sciences, Vasco-da-Gama, Goa 403 804, India
[b] School of Earth, Ocean and Atmospheric Sciences, Goa University, Taleigao Plateau, Goa 403206, India
[c] CSIR-National Institute of Oceanography, Dona Paula, Goa 403 004, India

ARTICLE INFO

Article history:
Received 27 April 2020
Received in revised form 12 October 2020
Accepted 2 November 2020
Available online 06 November 2020

Keywords:
Sagar Kanya Seamount
Morphology
Volcanic caldera
Eastern Arabian Sea

ABSTRACT

The marine geophysical investigations carried out in the Eastern Arabian Sea revealed the presence of a bathymetric high feature, referred to as the Sagar Kanya Seamount. The preliminary morphology and geophysical characteristics of this feature were studied along a single transect by earlier researchers, however, a detailed geophysical mapping over the entire extent of this feature is still awaited. The present study aims for such a detailed investigation on the Sagar Kanya Seamount and its adjacent regions using newly acquired high-resolution multibeam bathymetry data, complemented with sea surface magnetic and gravity data. Bathymetric map reveals the presence of well-defined bathymetric high features constituting three seamounts connected with structural high/ridge-like features, together representing a large nearly elliptical bathymetric high complex surrounding a region of nearly flat seafloor, referred to as the Sagar Kanya Bathymetric High Complex (SKBHC). The overall morphology of this feature closely resembles with the shape of a submarine volcanic caldera. The gravity anomalies over this feature are mostly correlatable with topography; elliptical-shaped gravity highs are associated with bathymetric highs and gravity lows are associated with the enclosed flat seafloor. Some magnetic anomalies observed over the SKBHC are correlatable with the topographic highs, while others are observed over the flat seafloor. The magnetic anomalies are interpreted as features of post-caldera volcanism. In view of the proximity of this feature to the Réunion hotspot track, and the tectonic framework of the region, the genesis of the SKBHC is attributed to the Réunion hotspot volcanism.

1. Introduction

The Sagar Kanya Seamount is an anomalous seafloor feature located southwest of the Laccadive Plateau in the Eastern Arabian Sea (Fig. 1). This seamount, centred around 9°19.5′N, 71°04.0′E, was discovered by Bhattacharya and Subrahmanyam (1991), based on bathymetry and geophysical data collected along one transect. They collected single beam bathymetry, gravity and magnetic data along this transect, in order to understand the geomorphology, geophysical characteristics and the probable genesis of the Sagar Kanya Seamount. The bathymetry data revealed that the Sagar Kanya Seamount rises from an average water depth of 4150 m to a peak with least depth of 1686 m, indicating a bathymetric high feature with a maximum height of 2464 m and a basal width of 33 km. The seamount was found to be associated with a positive free-air gravity anomaly (~+70 mGal) flanked by negative gravity anomalies (~−10 mGal) and a well-developed magnetic anomaly pattern with an amplitude of the order of 200 nT. Based on the forward modelling of the gravity and magnetic anomalies, constrained by the geological and tectonic information from the region, Bhattacharya and Subrahmanyam (1991) attributed the genesis of the Sagar Kanya Seamount to the Réunion hotspot volcanism. Bhattacharya and Subrahmanyam (1991) provided important insights on the morphology, geophysical signatures and the probable genesis of this anomalous feature, however, they could not provide a detailed information on the entire spatial extent of this seamount since the data was available only along one transect. Therefore, we made an attempt to understand the detailed morphology and geophysical characteristics of the entire Sagar Kanya Seamount and its adjacent regions, using newly acquired high-resolution multibeam bathymetry data along with sea surface magnetic and gravity data.

2. Tectonic framework

The revised plate reconstruction model (Bhattacharya and Yatheesh, 2015; Shuhail et al., 2018; Yatheesh, 2020; Yatheesh et al., 2020) for the evolution of the Western Indian Ocean suggests that the western continental margin of India and its adjacent deep offshore regions were evolved by the rifting and drifting among the Southern Indian Protocontinent (SIP), Northern Indian Protocontinent (NIP), Seychelles

* Corresponding author.
E-mail address: john@ncpor.res.in (P.J. Kurian).

https://doi.org/10.1016/j.geomorph.2020.107488
0169-555X/

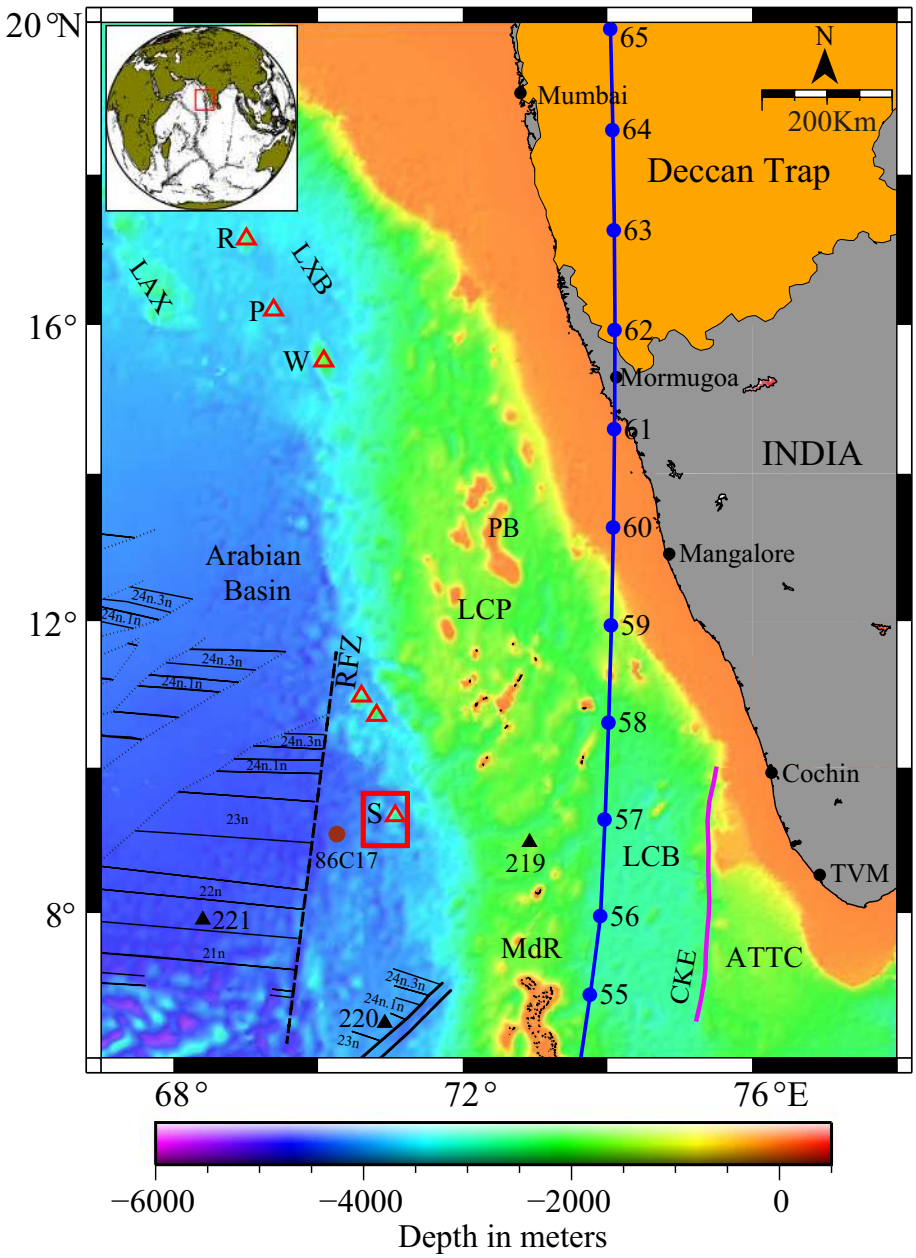

Fig. 1. Generalized tectonic map of the southwestern continental margin of India and the adjoining deep offshore regions, along with satellite derived topography of GEBCO_2014 (Weatherall et al., 2015) in the background. The thick blue line connecting the blue solid circles represents the Réunion hotspot track computed based on Müller et al. (1993). The numbers given to the solid blue circles represent the ages (in Ma). Black solid triangles are the DSDP sites and brown solid circle is the location of seismic refraction station (Naini, 1980). Thin black lines, dotted lines and dashed lines in the Arabian Basin are magnetic lineations, pseudofaults and fracture zones, respectively (Chaubey et al., 2002). Red triangles represent locations of the major seamounts in the Eastern Arabian Sea (Bhattacharya and Subrahmanyam, 1991; Bhattacharya et al., 1994; Bijesh and John Kurian, 2020) R: Raman Seamount; P: Panikkar Seamount; W: Wadia Guyot; S: Sagar Kanya Seamount; LCP: Laccadive Plateau; PB: Padua Bank; MdR: Maldive Ridge; CKE: Chain Kairali Escarpment; ATTC: Alleppey-Trivandrum Terrace Complex; LXB: Laxmi Basin; LCB: Laccadive Basin; LAX: Laxmi Ridge; RFZ: Rudra Fracture Zone; TVM: Trivandrum.

(SEY), Madagascar (MAD), Laxmi Ridge (LAX) and the Laccadive Plateau (LCP). The evolution of this entire region can be considered to have occurred in three stages (Fig. 2). The first stage was the rifting of the conjoint SIP-NIP-LAX-LCP-SEY block from Madagascar, initiated at ~88.0 Ma (Fig. 2a), followed by seafloor spreading at around 83.0 Ma, creating the Mascarene Basin (Fig. 2b). The second stage was the rifting and drifting among SIP, NIP and the conjoint SEY-LAX block through the Gop-Narmada-Laxmi Triple Junction, initiated at ~68.5 Ma, creating the Laxmi Basin, Gop Basin and the Narmada Rift Graben (Fig. 2c). Contemporaneously, another axis of divergence existed between SIP and LCP, creating the Laccadive Basin. The third stage was the breakup between LAX and SEY, initiated at ~62.5 Ma, creating the Arabian Basin in the Laxmi Ridge side and its conjugate Eastern Somali Basin in the Seychelles side (Fig. 2d).

The Marion and Réunion hotspot volcanisms are considered to have played a major role in the initiation of various episodes of the continental breakup and subsequent evolution of the deep offshore regions in the Western Indian Ocean. The first episode of separation between Madagascar and India (more specifically, the conjoint SIP-NIP-LAX-LCP-SEY block) is believed to have been caused by the Marion hotspot volcanism, and the second and third episodes of separation among SIP, NIP, LAX, LCP and SEY were considered to have been caused by different phases of the Réunion hotspot volcanism (Bhattacharya and Yatheesh, 2015; Shuhail et al., 2018; Yatheesh, 2020; Yatheesh et al., 2020). The

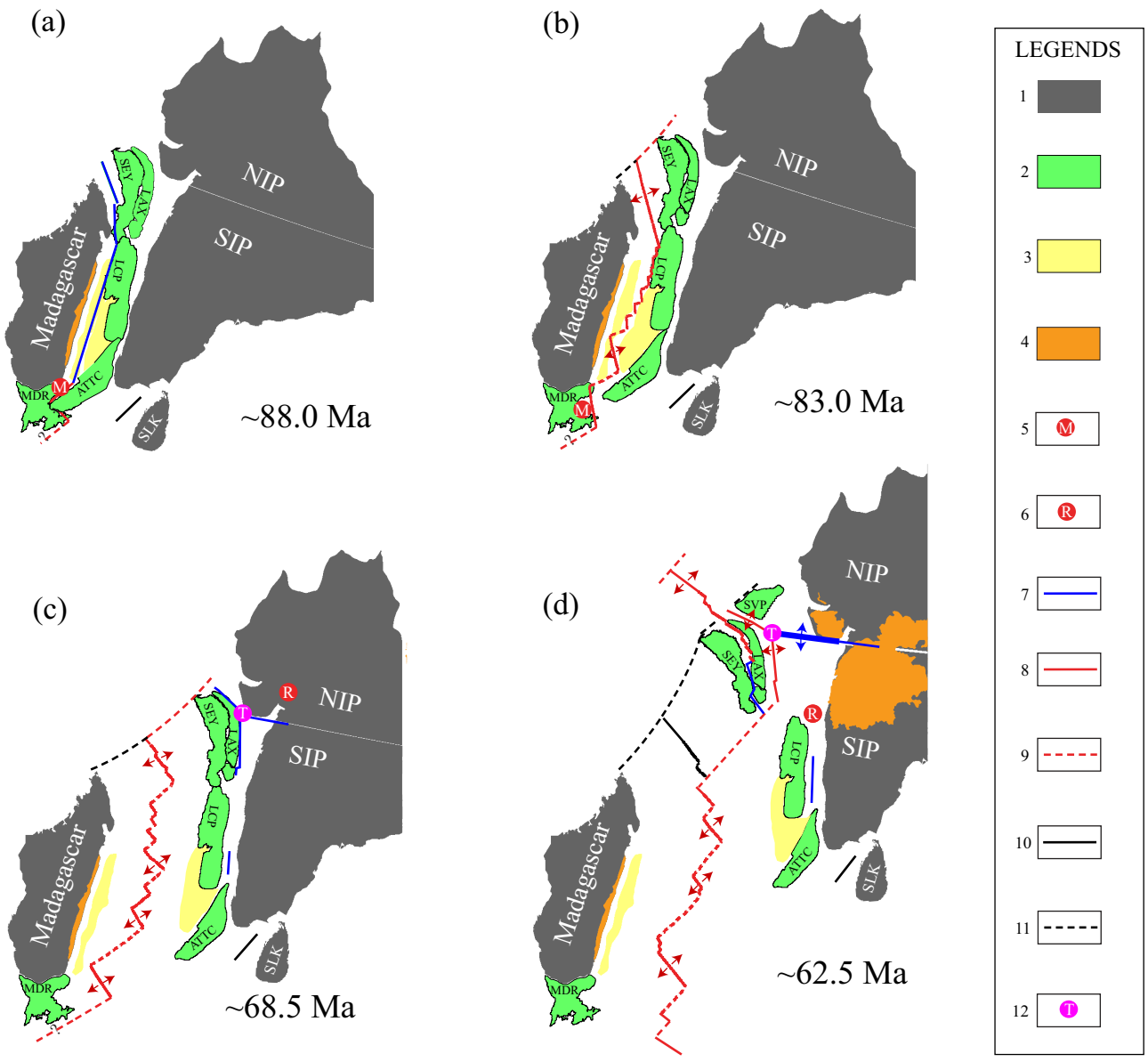

Fig. 2. Schematic diagram depicting the major stages of formation and evolution of the western continental margin of India and the adjacent deep ocean basins (modified after Yatheesh (2020)). (a) ~88.0 Ma; (b) ~83.0 Ma; (c) ~68.5 Ma; (d) ~62.5 Ma; Legends: [1] Major continental blocks, [2] Microcontinents, [3] Ultra-thinned continental crust, [4] Volcanics, [5] Location of the Marion Hotspot, [6] location of the Réunion Hotspot, [7] Rift axis, [8] Ridge axis, [9] Transform fault, [10] Extinct spreading centre/failed rift, [11] Palaeo-transform fault, [12] location of the Gop-Narmada-Laxmi fossil Triple Junction off the Saurashtra Peninsula. SIP: Southern Indian Protocontinent; NIP: Northern Indian Protocontinent; SLK: Sri Lanka. Other details are as in Fig. 1.

role of Marion hotspot for India-Madagascar breakup has been inferred from the existence of ~85–92 Ma old volcanics from the western side of India (Anilkumar et al., 2001; Melluso et al., 2009; Pande et al., 2001; Radhakrishna et al., 1994; Radhakrishna and Joseph, 2012; Radhakrishna et al., 1999; Ram Mohan et al., 2016; Sheth et al., 2017; Torsvik et al., 2000; Valsangkar et al., 1981) and the eastern side of Madagascar (Storey et al., 1995; Torsvik et al., 2000). The evidence to the timing of initiation of rifting through the arms of the Gop-Narmada-Laxmi Triple Junction comes from the existence of ~68.5 Ma old volcanics, representing the oldest pulse of the Réunion hotspot, located north of the main Deccan Flood Basalt Province (Basu et al., 1993). The timing of ~62.5 Ma for the third episode of the breakup between Seychelles and Laxmi Ridge comes from the oldest magnetic anomalies identified from the conjugate Arabian and Eastern Somali basins. This timing also coincides with the formations of Raman-Panikkar-Wadia seamount chain in the Laxmi Basin and the Ghatkopar-Powai tholeiitic basalt in the onshore region (Bhattacharya and Yatheesh, 2015; Pande et al., 2017). The seafloor spreading along the Carlsberg Ridge, separating the Laxmi Ridge and Seychelles, continued with the northward motion of the Indian plate over the Réunion hotspot, resulting in the formation of the major part of the Laccadive-Chagos Ridge (Duncan, 1990) and the several identified isolated bathymetric highs representing the seamounts, hills, knolls, plateaus and guyots in the Laccadive Basin and the adjacent regions off southwest coast of India (Bijesh et al., 2018).

3. Data and methodology

In the present study, we used high-resolution multibeam bathymetry data, and sea-surface magnetic and gravity profiles collected by National Centre for Polar and Ocean Research (NCPOR), Goa, India, onboard RV MGS Sagar in 2015. The multibeam bathymetry data was acquired along tracklines with ~5 km interval with 50% overlap, using Reson SeaBat 7150 multibeam echosounder operated at 12 kHz

frequency. Sound velocity profiles collected in the regular interval were applied to the multibeam data in real-time for compensating variation in sound velocity in the water column. Manual de-spiking was undertaken using Caris Hips & Sips software during the post-processing stage and finally, the processed data was used to create a bathymetric grid with a spatial resolution of 50 m for the interpretation. Simultaneous with the multibeam data acquisition, sea-surface gravity and magnetic data were acquired using the Mobile Gravimeter Chekan – AM and SeaSPY2 Marine magnetometer, respectively. The sea-surface gravity data has been reduced to the free-air gravity anomaly by applying normal and Eötvös corrections. The total field magnetic data has been reduced to the residual magnetic anomaly by applying the International Geomagnetic Reference Field for the year 2015. In addition, tie correction has been carried out by correlating the measured values by acquiring data along cross transects. These sea-surface gravity and magnetic anomalies were used for the integrated forward modelling, following the methods of Talwani et al. (1959) and Talwani and Heirtzler (1964), to understand the crustal architecture beneath the Sagar Kanya Seamount and the adjoining regions.

4. Results

4.1. Seafloor morphology

The high-resolution multibeam bathymetric maps of the study area (Fig. 3), which covers an areal extent of ~6500 km^2, reveals the presence of several bathymetric high features with different dimensions. These features mainly consist of three prominent seamounts and several linear ridge-like features, together representing a NNE-SSW trending large, nearly elliptical bathymetric high complex surrounding a region of nearly flat seafloor measuring ~50 km × 30 km, at water depth 4200–4300 m. For the ease of further discussion in this study, we refer these seamounts as Sagar Kanya-1 (SK-1), Sagar Kanya-2 (SK-2), and Sagar Kanya-3 (SK-3) seamounts and the whole bathymetry high complex as the Sagar Kanya Bathymetric High Complex (SKBHC). Among these, the SK-1 Seamount represents the "Sagar Kanya Seamount" discovered by Bhattacharya and Subrahmanyam (1991).

The Sagar Kanya-1 (SK-1) Seamount is a nearly conical-shaped seamount, which is centred at 9°20.1′N, 71°04.0′E (Figs. 3 and 4a). This seamount is surrounded by a flat seafloor with a water depth range of 4150–4200 m, rising to a height of ~2500 m to summit at a depth of ~1665 m. The base of the SK-1 Seamount is nearly circular in shape with a basal areal extent of ~630 km^2 and its summit area is flat-topped with an areal extent of ~9 km^2. The SK-1 Seamount is characterized by the presence of several morphological features consisting of a lava terrace, a scarp face and a cluster of volcanic edifices. The NNW-SSE trending, well-developed, flat-topped and steep-sided lava terrace (~2300 m seafloor depth) identified (Fig. 4b) on the western flank of the summit area of this seamount suggests a post-eruptive slope modification of this seamount. An ~8 km long and two-stepped scarp face/embayment with a moderately steep slope is identified (Fig. 4c) on the eastern flank of the summit area of the SK-1 Seamount. Such sharpness of the embayment at the summit edge of a seamount and the relatively smooth flanks of the seamount below them are suggestive of representing a slope failure event. A close examination of the SK-1 Seamount further reveals the presence of numerous smaller discrete secondary volcanic cones (Fig. 4d), most of which are clustered on the southeast and southwest corners of the seamount. In addition, the SK-1 Seamount is also characterized by the presence of an extensive pattern of gully-like features along its flanks.

The Sagar Kanya-2 (SK-2) Seamount, identified and mapped by the present study, is centred at 9°28.4′N, 70°50.2′E (Figs. 3 and 5a). This NE-SW trending large elliptical-shaped seamount, located ~35 km (summit-to-summit distance) northwest of the SK-1 Seamount, has a basal area of ~350 km^2. The SK-2 Seamount is surrounded by a flat seafloor with a depth range of 4150–4200 m and the summit area is marked by two isolated domes at water depths of ~2500 m and ~2800 m. The elongated plateau-shaped SK-3 Seamount possesses a height of 815 m, with its centre location at 9.032°N, 70.714°E (Figs. 3 and 5b). Compared to the SK-1 and SK-2 seamounts, the basal area of the SK-3 seamount is limited and it exhibits irregularly shaped summit area. The southwestern flank of the SK-3 Seamount is sharp while its northeastern flank is gentle in nature (Fig. 3).

We also analyzed bathymetry data of the Sagar Kanya Bathymetric High Complex in the perspective of morphological slope distribution (Fig. 6). The major part of the study area is associated with slopes ranging from 0° to 10°, which represents the regions of sub-horizontal morphological characteristics. The slope distribution map (Fig. 6) suggest the presence of several regions with very-high slopes (>25°) over different parts of the SKBHC, some of which are continuously banded while others are discontinuously banded in nature. This map clearly shows the presence of two concentric continuously banded zones with very-high slope (>25°) that are centred over the flat summit region of the SK-1 Seamount. Among these, the inner band is marked by the steeply dipping flanks of the summit peak, while the outer band is marked by the steeply dipping flanks bordering the lava terraces. The SK-1 Seamount is also associated with several discontinuous bands of very-high slope (>25°), which are mostly concentrated on its outer boundary. In contrary to this, the discontinuous bands of very-high slope are distributed randomly at several locations on the SK-2 Seamount, including at their outer boundary. A continuous band of very-high slope region is also observed on the outer limit of the SK-3 Seamount on the southwestern part of the study region.

4.2. Gravity and magnetic signatures

The free-air and complete Bouguer gravity anomalies (Fig. 7) of the study area have been presented along with the selected bathymetry contours, which defines the extent of the seafloor features, to describe the characteristic gravity signatures of these features in the study area. The free-air gravity anomalies of the Sagar Kanya Bathymetric High Complex are correlated with topography in general, with their maximum corresponding to the locations of the summit of the seafloor features (Fig. 7a). However, the free-air gravity anomalies corresponding to the shallower seafloor features appear to get masked by the long-wavelength gravity anomalies caused by the deeper regional features, and therefore, we have generated high-pass filtered map with cut-off wavelength 40 km (Fig. 7b) to enhance the effect of the shallower features and diminish the effect of deeper features. The nearly elliptical-shaped gravity high that surrounds a gravity low as observed from this high-pass filtered gravity anomalies (Fig. 7b) suggests the presence of a nearly elliptical-shaped surface/subsurface high feature that surrounds a depression. In the case of SK-1 Seamount, the maximum slope region of the gravity anomalies that normally define the subsurface lateral extent of the feature buried under the sediments appears to be located very close to the extent of the SK-1 Seamount defined by the bathymetry contours. These nearly coinciding surface and subsurface lateral extents of the feature suggest nearly vertical flanks for the SK-1 Seamount. Unlike the SK-1 Seamount, the maximum slope region of the gravity anomalies that define the subsurface lateral extent of the SK-2 Seamount is wider than the extent of the seamount defined by the bathymetric contours. Such an observation suggests that the flanks of the SK-2 Seamount is gentle compared to the SK-1 Seamount and the base of the seamount is buried under sediments. We further computed complete Bouguer anomaly (CBA) to understand the variations in the crustal thickness or heterogeneity in the subsurface density of the material. This is achieved from the free-air gravity anomaly by subtracting the attraction of bathymetric relief considering the water-crust interface based on Parker (1972) method. For water and crust, we used density values of 1.03 g/cc and 2.85 g/cc, respectively. The complete Bouguer anomaly map of the study area (Fig. 7c) is characterized by the presence of moderate to long wavelength positive anomaly ranging

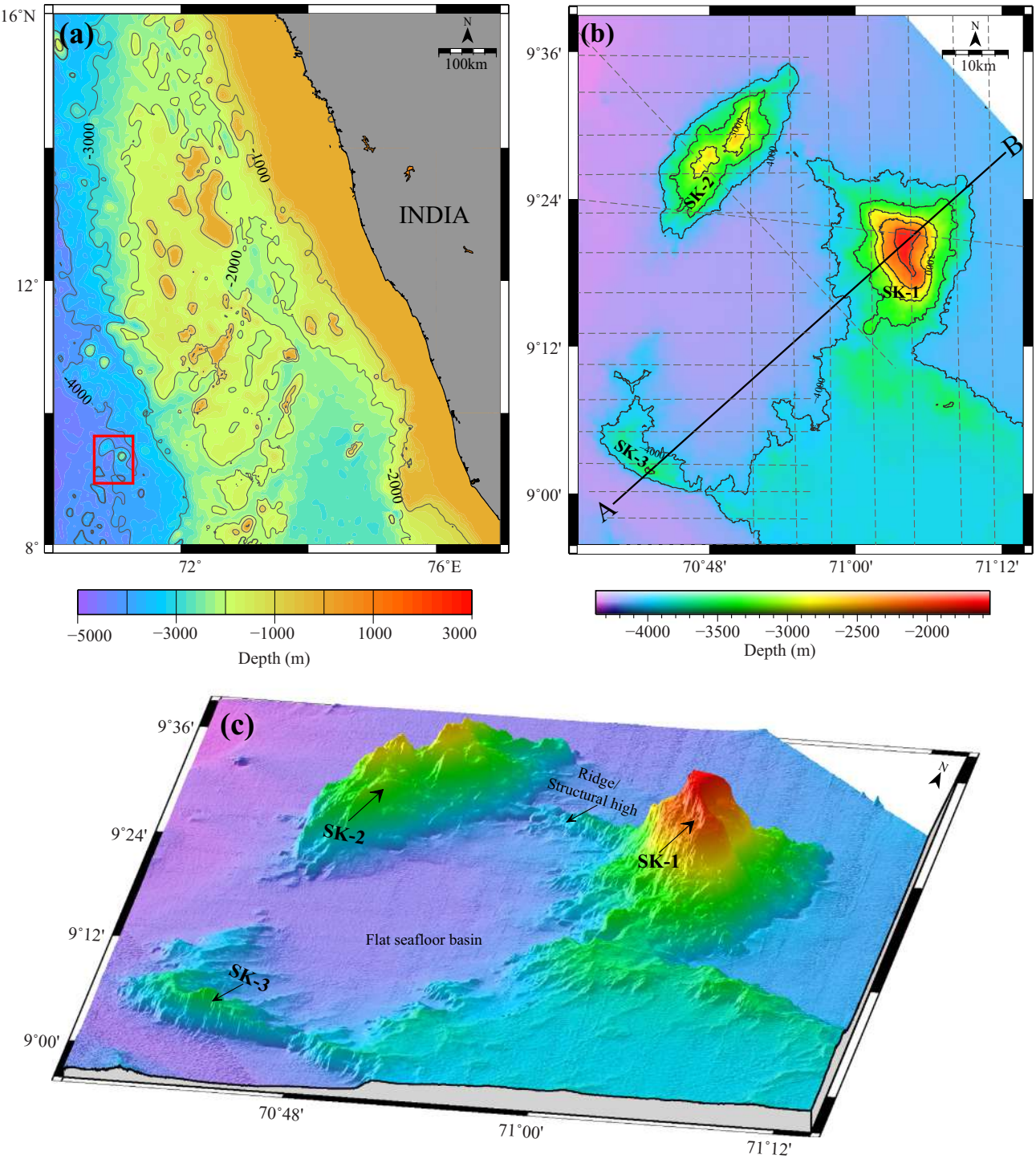

Fig. 3. (a) Satellite-derived topographic map of the southwestern continental margin of India and the adjacent ocean basins showing the location of the study area as a square in red colour; (b) High-resolution multibeam bathymetry map of the study area shown as filled contour map; and (c) three-dimensional bathymetry image with major bathymetric features labelled. Black line AB represent profile location over which the forward modelling has been carried out and presented in Fig. 9. SK-1: Sagar Kanya-1 Seamount; SK-2: Sagar Kanya-2 Seamount; SK-3: Sagar Kanya-3 Seamount.

from 180 to 290 mGal. The high amplitude anomalies are present in the region surrounding the northwestern part of Sagar Kanya Bathymetric High Complex. From the northwestern part to the southeastern part of the study area, the complete Bouguer anomaly shows a gentle decrease in general, with their minimum coinciding with the peaks of SK-1 (~190 mGal), SK-2 (~240 mGal) and SK-3 (220 mGal) seamounts (Fig. 7c). As in the case of the free-air gravity anomaly, we have generated a high-pass filtered (with cut-off wavelength 40 km) complete Bouguer anomaly map, which further enhances the residual Bouguer anomaly signatures corresponding to shallower features (Fig. 7d). The high pass filtered complete Bouguer anomaly map also reveals the presence of distinct circular to elliptical shaped anomaly connecting the SK-1, SK-2 and SK-3 seamounts. Further, the surrounding flat seafloor region as well as the depression in the central region of the Sagar Kanya Bathymetric High Complex exhibits subdued anomaly within the range of 0 to +20 mGal (Fig. 7d).

The magnetic anomalies (Fig. 8a) of the study area have been presented along with the selected bathymetry contours, which defines

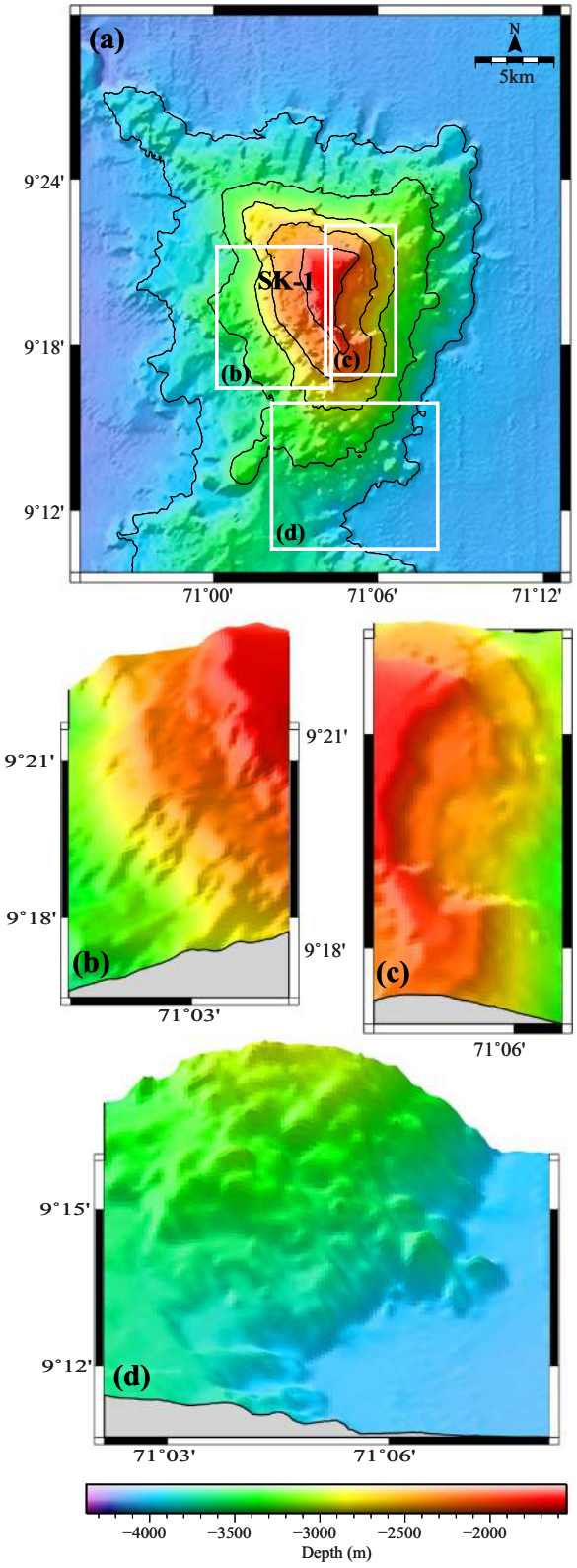

Fig. 4. Bathymetric map of the (a) Sagar Kanya-1 (SK-1) Seamount, (b) steep-sided lava terrace, (c) scarp face/embayment, and (d) secondary volcanic cones.

the extent of the seafloor features, to describe the characteristic magnetic signatures of these features. As in the case of gravity anomalies, the residual magnetic anomalies of the SKBHC also appears to have got masked by the long-wavelength magnetic anomalies. Therefore, we have also generated a high-pass filtered (cut-off wavelength 40 km) magnetic anomaly map (Fig. 8b) to enhance the effect of the shallow features and diminish the effect of deeper features. The magnetic anomalies over the study area are complex, consisting of several positive and negative magnetic anomalies, representing the dipole magnetic field caused by the associated causative magnetic bodies. The central part of the SK-1 Seamount is associated with a negative magnetic anomaly, while that of the SK-2 Seamount is associated with a positive magnetic anomaly. The flat seafloor enclosed within the bathymetric high complex is associated with ~WNW-ESE trending high amplitude positive and negative bands of magnetic anomalies, suggestive of the existence of causative magnetic bodies buried under the sediments.

4.3. Crustal architecture of the SKBHC

We carried out integrated forward modelling of gravity and magnetic data to understand the crustal configuration of the Sagar Kanya Bathymetric High Complex. For this, we selected a representative profile AB (Fig. 3b) that cut across the SKBHC through the SK-1 and SK-3 seamounts. The first step to carry out forward modelling of gravity anomalies based on the method of Talwani et al. (1959) is the construction of an initial crustal model constrained by geophysical and geological information available from those regions. Since the constraints are not too many, we assumed a simple crustal model with two-layered oceanic crust around the SKBHC and a single layer intrusive structure for the SKBHC. In the shallower regions, the constraints available from bathymetry data of the present study and the sediment velocities available from the published results (Naini and Talwani, 1982) from the nearby area were used. For deeper layers, in the absence of velocity-depth information available from seismic refraction results, we used the published information of velocity (Naini, 1980; Naini and Talwani, 1982) and velocities of layers available for a standard oceanic crust (Fowler, 2005). The above velocity information was converted to density using the velocity-density relationship of Ludwig et al. (1970). Accordingly, we assigned densities of 2.35 g/cc, 2.63 g/cc, 2.88 g/cc and 3.3 g/cc for the sediments, layer-2, layer-3, and mantle, respectively. Keeping those density constraints fixed, an attempt has been made to derive a crustal model by refining the thicknesses and extents of the layers to get a reasonably good fit with computed and observed gravity anomalies. Having obtained a reasonable gravity model, attempt has been made to incorporate magnetic bodies into this model to get an integrated gravity-magnetic model that can satisfy both the gravity and magnetic signatures. For computing the magnetic anomalies across these assumed two-dimensional bodies, we used the method of Talwani and Heirtzler (1964). In the absence of the paleomagnetic studies available from the rocks collected from SKBHC, we considered the paleomagnetic results of volcanic rocks available from DSDP Site 220, which is located in the neighbouring area (Whitmarsh et al., 1974). Accordingly, we assigned remnant inclination (RI) of 12° and remnant declination (RD) of 315° with magnetization (M) ranging 1.0–2.0 A/m for the reversely magnetized bodies. For normally magnetized bodies we assigned remnant inclination of -40° and remnant declination of 300° with magnetization ranges from 1.0-2.0 A/m following Bhattacharya and Subrahmanyam (1991). The derived crustal model (Fig. 9) suggests that the SKBHC can be reasonably interpreted in terms of a volcanic intrusion within the existing oceanic crust. The excess masses corresponding to the SK-1 and SK-2 seamounts are compensated by deepening of the Moho to ~25.0 km under the SK-1 Seamount and ~13 km, under SK-3 Seamount. As a result, the SK-1 and SK-3 seamounts yield crustal thicknesses of ~20 km and ~7 km, respectively. The derived model further suggests that the SK-1 and SK-3 seamounts are underlain by normally and reversely magnetized crust, formed during a normal and a reverse polarity interval of the Earth's magnetic field, respectively.

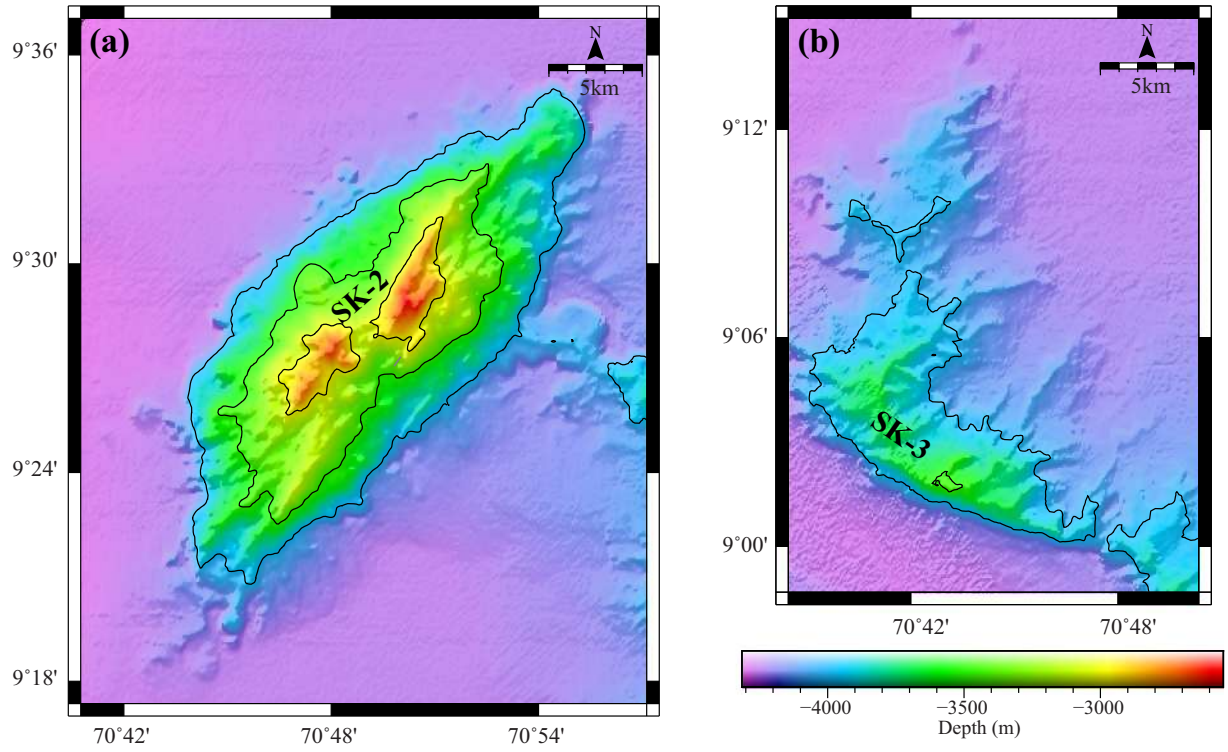

Fig. 5. Bathymetric map of the (a) Sagar Kanya-2 (SK-2) Seamount, and (b) Sagar Kanya-3 (SK-3) Seamount.

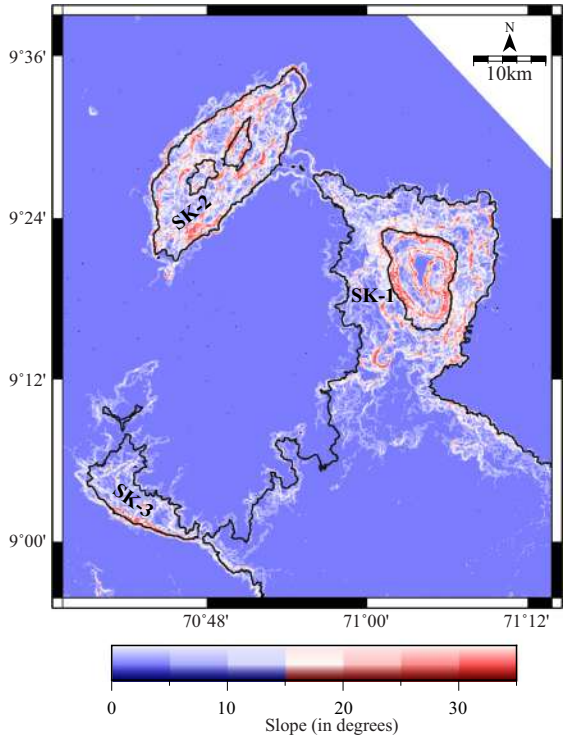

Fig. 6. Slope map of the study area derived from the multibeam bathymetry data. The black contours represent the isobaths with 500 m contour interval, used to depict the extent of the seamounts and the other bathymetric features.

5. Discussion

5.1. Sagar Kanya Bathymetric High Complex - a possible submarine volcanic caldera?

As explained in the Section 4.1, the multibeam bathymetric map (Fig. 3) clearly shows the presence of three prominent seamounts and several linear ridge-like features, together representing a large, elliptical bathymetric high complex surrounding a region of nearly flat seafloor, elongated in NNE-SSW direction. This configuration of seafloor resembles with the shape of a volcanic caldera, which is defined as a volcanic structure, generally large, which is principally the result of collapse or subsidence into the top of a magma chamber during or immediately following eruptive activity (Cole et al., 2005). Therefore, this elliptical-shaped bathymetric high complex (SKBHC) appears to qualify to be considered as the rim surrounding the summit caldera of a large extinct submarine volcano, referred to as the Sagar Kanya Volcano. The morphology of this postulated caldera rim in the Arabian Sea is very similar to the shape of presently active known calderas in other parts of the globe, such as the Nikko Submarine Volcanic Caldera (Global Volcanism Program, 1990), Brothers Seamount Caldera (Stagpoole et al., 2016) and the Santorini Caldera (Nomikou et al., 2012). The areal extent of this postulated volcanic caldera, hereafter referred to as the Sagar Kanya Volcanic Caldera, is ~1500 km^2 (with a dimension of ~50 × 30 km). This areal extent is nearly half of the area of the Yellowstone Caldera of ~2400 km^2, measuring 60 × 40 km (Tizzani et al., 2015), Toba Caldera of ~3000 km^2 measuring 100 × 30 km (Chesner, 2012) and Gakkel Caldera of ~3200 km^2 measuring 80 × 40 km (Piskarev and Elkina, 2017), created by super volcanic events. The rim structure of the Sagar Kanya Volcanic Caldera can be traced for about 320° of the summit of the volcano, but appears to be slightly buried in the central part of its western side (Fig. 3). Such a configuration is a common style associated with the asymmetrical subsidence resulted by tilting of the magma chamber (Kennedy et al., 2004). Roche et al. (2000) suggested from their experiments that shallow magma chambers with

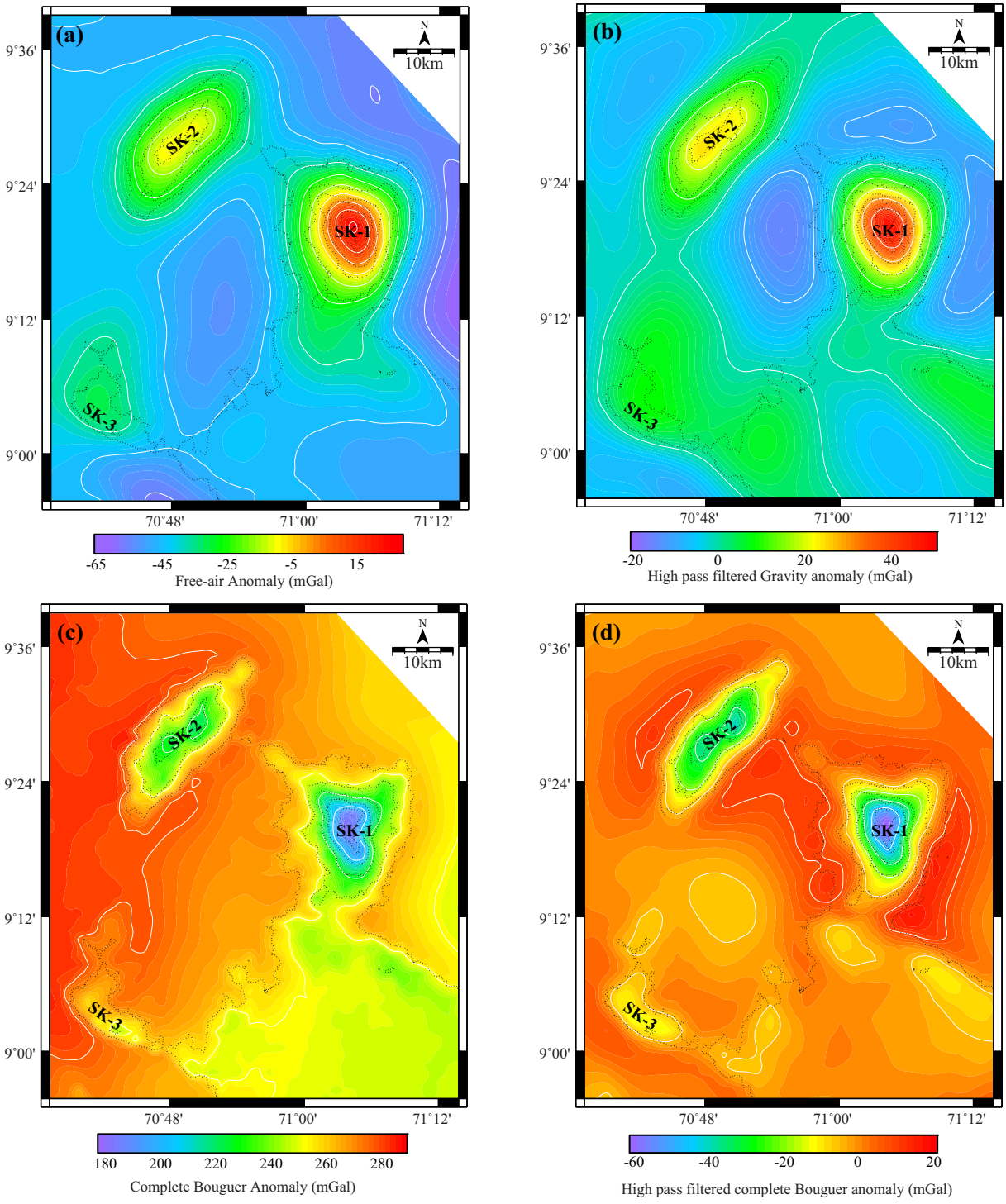

Fig. 7. Images of the (a) free-air gravity anomaly; (b) high pass filtered (cut-off wavelength of 40 km) free-air gravity anomaly; (c) Complete Bouguer anomaly; (d) high pass filtered (cut-off wavelength of 40 km) complete Bouguer anomaly of the study area. Other details are as in Fig. 6.

large diameters lead to coherent single block collapse structures, while deep chambers with small diameters lead to a series of multiple nested blocks. Since the caldera of the Sagar Kanya Volcano represents a single block structure with ~50 × 30 km dimension and asymmetric in nature, we postulate that the collapse of Sagar Kanya Volcano is associated with a shallow tilted magma chamber. The high-pass filtered gravity anomalies support the presence of a nearly elliptical continuous gravity high feature surrounding a gravity low region, representing the rim and depressions of the postulated caldera, respectively. The probable presence of ring-fault system formed due to the collapse of Sagar Kanya Volcano might have acted as conduits to form the SK-1, SK-2 and SK-3 seamounts, which were created as a result of a post-collapse phase of volcanism. The derived complete Bouguer anomaly (Fig. 7c, d) and the crustal structure (Fig. 9) exhibits the variation of the crustal thickness resulted after the multiphases of volcanism that shaped the Sagar Kanya Bathymetric High Complex as a whole. The minimum amplitude of Bouguer anomaly is associated with the central part of SK-1 Seamount (where the thickness is maximum as inferred from the forward modelling of gravity and magnetic anomalies, see Fig. 9) and the maximum amplitude of Bouguer anomaly is associated with the crust having

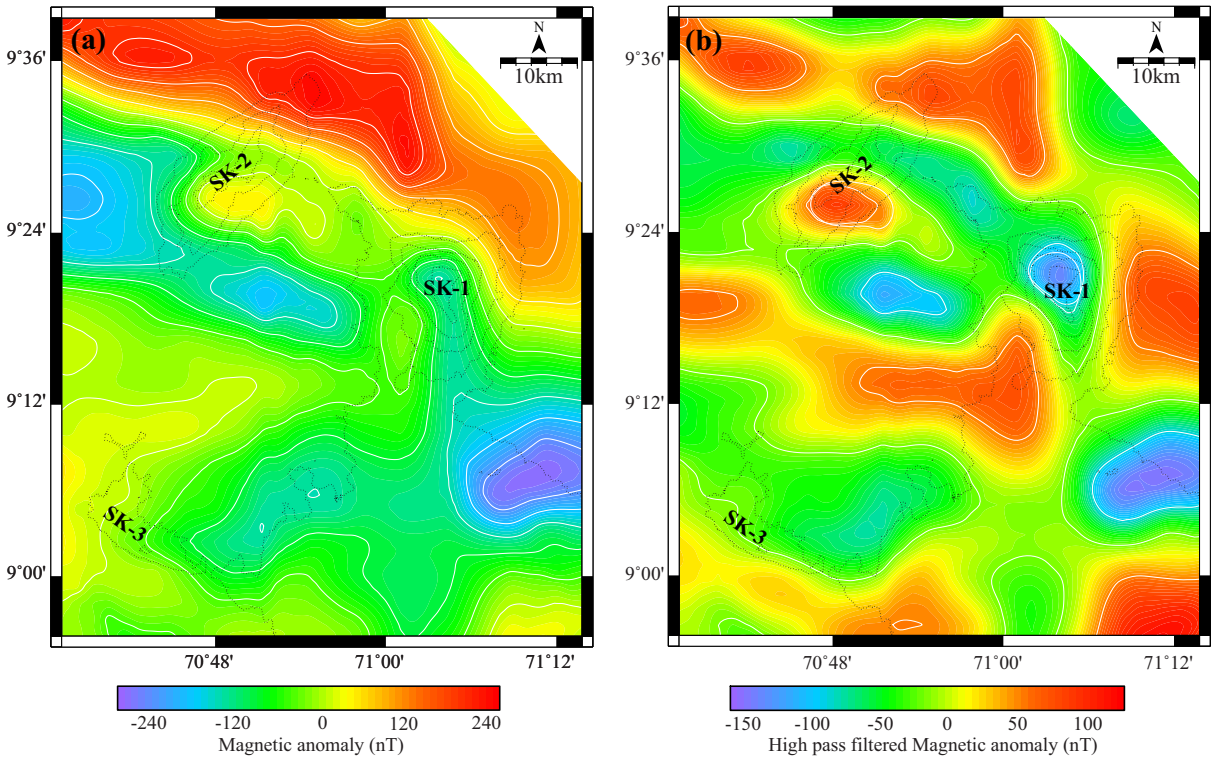

Fig. 8. Images of the (a) magnetic anomaly and (b) high pass filtered (cut-off wavelength of 40 km) magnetic anomaly of the study area. Other details are as in Fig. 6.

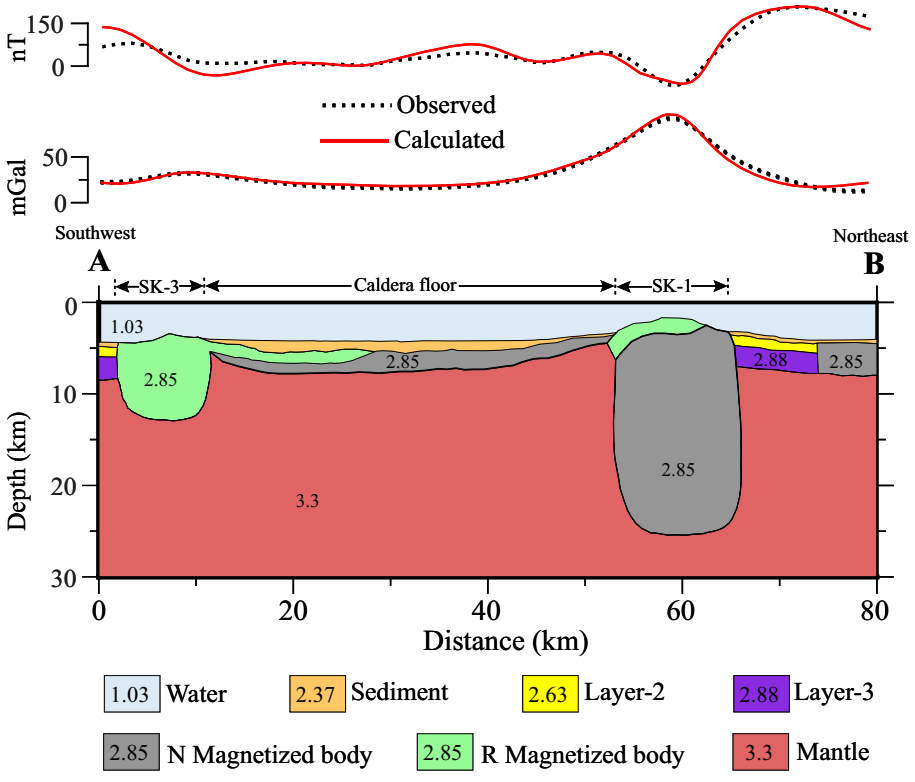

Fig. 9. Crustal model derived based on integrated forward modelling of gravity and magnetic anomalies along the profile AB, the location of which is shown in Fig. 3b. The decimal numbers given in the each layers of the model represent density in g/cc. Magnetic anomalies are modelled with two-dimensional magnetic bodies of intrusive dykes and sills (For normally magnetized blocks: Remnant magnetization = 1.0–2.0 A/m; Remnant Inclination = −40°, Remnant Declination = 300°; For reversely magnetized blocks: Remnant magnetization = 1.0–2.0 A/m; Remnant Inclination = 12°, Remnant Declination = 315°).

minimum crustal thickness (as inferred from the forward modelling of gravity and magnetic anomalies, see Fig. 9). These observations depict an inverse correlation of Bouguer anomaly with the crustal thickness over the Sagar Kanya Bathymetric High Complex. Similar inverse relationship between the Bouguer anomalies and crustal thickness is observed over various physiographic features, such as the Wreck Seamount (Tasman Sea, Richards et al., 2018), Maldive Ridge (Kunnummal et al., 2018) and the NW Iberian margin (Druet et al., 2019).

5.2. Probable genesis of the Sagar Kanya Bathymetric High Complex

The genesis of intraplate volcanoes is generally attributed to the hotspot volcanism and therefore, the genesis of the Sagar Kanya Volcano can be reasonably explained in terms of volcanism caused by the Réunion hotspot, considering the tectonic framework of the western continental margin of India and the adjacent deep ocean basins. The crustal model derived from the integrated gravity and magnetic forward modelling indicates that the magnetic anomaly pattern in the study area represent the presence of normally and reversely magnetized bodies, formed in the southern hemisphere. Comparison of the location of the Sagar Kanya Bathymetric High Complex with the magnetic lineations (see Fig. 1) in the Arabian Basin suggests that the oceanic crust over which this anomalous bathymetric high feature sits is much older than chron C24n3o (53.347 Ma, as per Cande and Kent, 1995). This observation, along with the locations of the computed Réunion hotspot track (Müller et al., 1993) as shown in Fig. 1, suggests ~56–57 Ma timing for the formation of the Sagar Kanya Bathymetric High Complex. Therefore, to understand the relationship of the formation of this feature with the evolution of the conjugate Arabian and Eastern Somali basins through the Carlsberg Ridge, and with the formation of the Laccadive-Chagos Ridge, we provide the latest published reconstruction map (Yatheesh et al., 2020) of the Western Indian Ocean at 56.4 Ma, incorporating the location of the SKBHC. This map (Fig. 10) suggests that the Réunion hotspot was very close to the location of the SKBHC at 56.4 Ma and by this time, the Réunion hotspot has already reached to the southernmost part of the Laccadive Plateau. Therefore, it is quite reasonable to postulate that the major part of the SKBHC was formed due to the Réunion hotspot volcanism, at around 56–57 Ma, which consists of normal as well as reverse polarities. However, some secondary volcanism also might have occurred in these regions during subsequent periods since the effect of the hotspots can go over several hundreds of kilometres distance (Tolan et al., 1989; Storey et al., 1995).

We postulate that the formation of the Sagar Kanya Volcano as well as the SK-1 and SK-2 seamounts can be explained in terms of multiphase volcanism, considering the presence of randomly distributed seamounts over the postulated caldera rim structure. The western part of the SK-1 Seamount is characterized by the presence of a NNW-SSE trending, well-developed, flat-topped and steep-sided lava terrace, suggestive of post-eruptive slope modification. This seamount is also associated with numerous smaller discrete secondary volcanic cones, representing post multiphase volcanism. Similarly, the SK-2 Seamount is associated with multiple secondary peaks suggesting multiphase volcanism in this region. The opposite sense of magnetic signatures associated with these features suggest that the SK-1 and SK-3 seamounts were not formed contemporaneously, but during different phases of volcanism occurred during normal and reverse polarity intervals. The prominent high amplitude magnetic anomalies observed within the flat caldera floor also indicate the presence of large subsurface intrusive bodies, formed by these later phases of volcanism.

6. Summary and conclusion

We carried out marine geophysical investigations over the Sagar Kanya Seamount and its adjacent regions to understand the detailed geomorphology and geophysical characteristics over the entire spatial

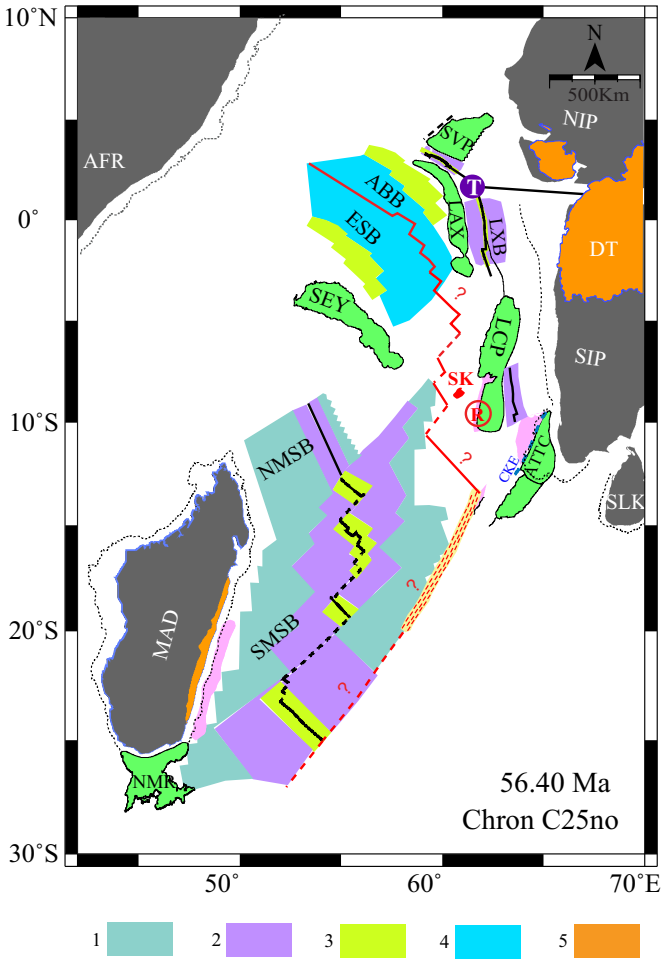

Fig. 10. Simplified plate tectonic reconstruction map of the Western Indian Ocean region in fixed Africa reference frame, at 56.4 Ma (after Yatheesh et al., 2020), along with location of the Sagar Kanya Bathymetric High Complex. R: Location of the Réunion hotspot; SK: Location and extent of the Sagar Kanya Bathymetric High Complex; AFR: Africa; MAD: Madagascar; DT: Deccan Trap. Explanation of items of the legend – [1] Oceanic crust formed during 83.0–68.5 Ma; [2] Oceanic crust formed during 68.5–62.5 Ma; [3] Oceanic crust formed during 62.5–60.92 Ma; [4] Oceanic crust formed during 60.92–56.4 Ma; [5] Extent of volcanics. Other details are as in Fig. 2.

extent of this anomalous feature. The high-resolution multibeam bathymetric map reveals the presence of a nearly elliptical bathymetric high complex consisting of three seamounts and several linear ridge-like features surrounding a region of nearly flat seafloor measuring ~50 km × 30 km. This bathymetric high complex is referred to as the Sagar Kanya Bathymetric High Complex (SKBHC) and the above-mentioned three seamounts are referred to as the Sagar Kanya-1 (SK-1), Sagar Kanya-2 (SK-2) and Sagar Kanya-3 (SK-3) seamounts. The conical shaped SK-1 Seamount has ~2000 m height and is associated with well-developed and steep-sided lava terrace, a two-stepped scarp face and numerous secondary volcanic cones. The elliptical-shaped SK-2 Seamount has ~815 m height and its summit area is marked by two isolated domes. Compared to these SK-1 and SK-2 seamounts, the SK-3 Seamount exhibits irregularly shaped summit area. The free-air gravity anomalies of the Sagar Kanya Bathymetric High Complex are correlated with topography in general, with their maximum corresponding to the locations of the summit of the seafloor features. The Bouguer gravity anomalies show an inverse correlation with the topography, with their minimum over the summit of the SK-1, SK-2 and SK-3 seamounts. The nearly elliptical-shaped gravity high that surrounds a gravity low as observed from these high-pass filtered free-air gravity anomalies suggests the presence of a nearly elliptical-shaped surface/subsurface

high feature that surrounds a depression. These gravity signatures suggest that the SK-1 Seamount is associated with nearly vertical flanks, while the SK-2 Seamount is associated with gently dipping flanks. The magnetic anomalies over the study area are complex, consisting of several positive and negative magnetic anomalies. The central parts of the SK-1 and SK-2 seamounts are associated with negative and positive magnetic anomalies, respectively, and the flat seafloor region enclosed within the SKBHC is associated with ~WNW-ESE trending high amplitude positive and negative bands of magnetic anomalies.

The morphology of the Sagar Kanya Bathymetric High Complex (SKBHC) appears to qualify to be considered as the rim surrounding the summit caldera of a large extinct submarine volcano, referred to as the Sagar Kanya Volcano. The shape of SKBHC is comparable with the shape of presently active known calderas in other parts of the globe. Therefore, we interpret the flat seafloor enclosed within the SKBHC as volcanic caldera and the bathymetric high features surrounding this flat seafloor as the caldera rim of the postulated Sagar Kanya Volcano. Since this caldera represents a single block structure with ~50 × 30 km dimension and asymmetric in nature, the collapse of the volcano is considered to have associated with a shallow tilted magma chamber. The SK-1, SK-2 and SK-3 seamounts might have formed through the ring-fault system, as a result of the post-collapse phase of volcanism. These phases of volcanism during normal and reverse polarity timing might have emplaced the SK-1 and SK-3 seamounts through the caldera rim structure as well as the volcanic flows within the collapsed caldera. Considering the tectonic framework of the western continental margin of India and the adjacent deep ocean basins, we attribute the genesis of these phases of volcanism to the Réunion hotspot.

The evidence for the existence of giant volcanic calderas has important consequences, not only in the understanding of the geodynamic events, but also in the economic point of view, since most of the submarine extinct calderas are associated with mineralizations. The present study is only based on the multibeam bathymetry data, complemented by the sea-surface gravity and magnetic anomalies and such studies can provide preliminary information on the shape and extent of these features. High-resolution multichannel seismic reflection investigations in these regions will help to map the extent of the flanks of the Sagar Kanya Volcano buried under the sediments and to understand its overall structure. Such seismic investigations complemented with the microbathymetric and magnetic surveys using an autonomous underwater vehicle will help to provide the detailed information on the morphological elements such as the topographic rim, inner caldera wall, caldera-bounding faults, structural caldera floor and intra-caldera fill. The study of intra-caldera fill using multichannel seismic reflection data will help to identify multistage post-caldera eruptions. Further, the geochronological investigations that could be carried out using the rock samples collected from the different locations of the SKBHC will provide important constraints on the age of formation of the Sagar Kanya Volcano.

Declaration of competing interest

The authors declare that they have no known competing financial interests or personal relationships that could have appeared to influence the work reported in this paper.

Acknowledgement

The authors are grateful to Dr. M. Ravichandran, Director, National Centre for Polar and Ocean Research (ESSO-NCPOR), Goa, and Prof. Sunil Kumar Singh, Director, CSIR-National Institute of Oceanography (CSIR-NIO), Goa, for their permission to publish the present work. We also thank Mr. Mahesh N. for helping in the computations. We are grateful to the Ministry of Earth Sciences (MoES/EC/EEZ/32/2012-PC-II), New Delhi, for the financial support through the "Geoscientific Studies of the Exclusive Economic Zone of India" Programme. This study forms a part of the PhD work of CMB at Goa University. We are indebted to Dr. Mathieu Rodriguez and two anonymous reviewers for their careful review of the manuscript and valuable comments. We thank Dr. Jérôme Dyment and Mr. G. C. Bhattacharya for their valuable inputs. We are grateful to Prof. Yongqiang Zong for editorial handling of the manuscript. We thank the shipboard scientific party, officers and crew members of the MGS-02 Expedition conducted onboard *MGS Sagar* for extending their support. For plotting the figures presented in this paper, we used Generic Mapping Tools (GMT) software (Wessel et al., 2013). This is NCPOR contribution J-75/2020-21 and NIO contribution 6627.

References

Anilkumar, Pande, K., Venkatesan, T.R., Bhaskar Rao, Y.J., 2001. The Karnataka Late Cretaceous dykes as products of the Marion hotspot at the Madagascar - India breakup event: evidence from $^{40}Ar/^{39}Ar$ geochronology and geochemistry. Geophys. Res. Lett. 28 (14), 2715–2718.

Basu, A.R., Renne, P.R., Dasgupta, D.K., Teichmann, F., Poreda, R.J., 1993. Early and late alkali igneous pulses and a high-^{3}He plume origin for the Deccan Flood Basalts. Science 261, 902–906.

Bhattacharya, G.C., Subrahmanyam, V., 1991. Geophysical study of a seamount located on the continental margin of India. Geo-Mar. Lett. 11, 71–78.

Bhattacharya, G.C., Yatheesh, V., 2015. Plate-tectonic evolution of the deep ocean basins adjoining the western continental margin of India - a proposed model for the early opening scenario. In: Mukherjee, S. (Ed.), Petroleum Geoscience: Indian Contexts. Springer International Publishing, Switzerland, pp. 1–61.

Bhattacharya, G.C., Murty, G.P.S., Srinivas, K., Chaubey, A.K., Sudhakar, T., Nair, R.R., 1994. Swath bathymetric investigation of the seamounts located in Laxmi Basin, Eastern Arabian Sea. Mar. Geod. 17, 169–182.

Bijesh, C.M., John Kurian, P., 2020. Morphology of the two unnamed seamounts in the Arabian Basin and their probable tectonic implications. Curr. Sci. 118 (7), 1118–1123.

Bijesh, C.M., John Kurian, P., Yatheesh, V., Tyagi, A., Twinkle, D., 2018. Morphotectonic characteristics, distribution and probable genesis of bathymetric highs off southwest coast of India. Geomorphology 315, 33–44.

Cande, S.C., Kent, D.V., 1995. Revised calibration of the geomagnetic polarity time scale for the Late Cretaceous and Cenozoic. J. Geophys. Res. 100, 6093–6095.

Chaubey, A.K., Dyment, J., Bhattacharya, G.C., Royer, J.Y., Srinivas, K., Yatheesh, V., 2002. Paleogene magnetic isochrons and palaeo-propagators in the Arabian and Eastern Somali basins, NW Indian Ocean. In: Clift, P.D., Croon, D., Gaedicke, C., Craig, J. (Eds.), The Tectonic and Climatic Evolution of the Arabian Sea Region. Geological Society, London, Special Publication vol. 195, pp. 71–85.

Chesner, C.A., 2012. The Toba Caldera Complex. Quat. Int. 258, 5–18.

Cole, J.W., Milner, D.M., Spinks, K.D., 2005. Calderas and caldera structures: a review. Earth Sci. Rev. 69 (1), 1–26.

Druet, M., Muñoz-Martín, A., Granja-Bruña, J.L., Carbó-Gorosabel, A., Llanes, P., Catalán, M., Maestro, A., Bohoyo, F., Martín-Dávila, J., 2019. Bouguer anomalies of the NW Iberian continental margin and the adjacent abyssal plains. J. Maps 15, 635–641.

Duncan, R.A., 1990. The volcanic record of the Réunion hotspot. In: Duncan, R.A., Backman, J., Peterson, L.C., et al. (Eds.), Proceedings of ODP Scientific Results. Ocean Drilling Programme, College Station, TX, pp. 3–10.

Fowler, C.M.R., 2005. The Solid Earth: An Introduction to Global Geophysics. Cambridge University Press, Cambridge.

Global Volcanism Program, 1990. Report on Nikko (Japan). In: McClelland, L. (Ed.), Bulletin of the Global Volcanism Network. Smithsonian Institution.

Kennedy, B., Stix, J., Vallance, J.W., Lavallée, Y., Longpré, M.-A., 2004. Controls on caldera structure: results from analogue sandbox modeling. GSA Bull. 116 (5–6), 515–524.

Kunnummal, P., Anand, S.P., Haritha, C., Rama Rao, P., 2018. Moho depth variations over the Maldive Ridge and adjoining Arabian and Central Indian Basins, Western Indian Ocean, from three dimensional inversion of gravity anomalies. J. Asian Earth Sci. 156, 316–330.

Ludwig, J.W., Nafe, J.E., Drake, C.L., 1970. Seismic refraction. In: Maxwell, A.E. (Ed.), The Sea. Wiley, New York, pp. 53–84.

Melluso, L., Sheth, H.C., Mahoney, J.J., Morra, V., Petrone, C.M., Storey, M., 2009. Correlations between silicic volcanic rocks of the St. Mary's Islands (southwestern India) and eastern Madagascar: implications for Late Cretaceous India-Madagascar reconstructions. J. Geol. Soc. Lond. 166, 283–294.

Müller, R.D., Royer, J.Y., Lawver, L.A., 1993. Revised plate motions relative to the hotspot from combined Atlantic and Indian Ocean hotspot tracks. Geology 21, 275–278.

Naini, B.R., 1980. Geological and Geophysical Study of the Continental Margin of Western India, and the Adjoining Arabian Sea Including the Indus Cone. Ph.D. Thesis. Columbia University (173 pp).

Naini, B.R., Talwani, M., 1982. Structural framework and the evolutionary history of the continental margin of Western India. In: Watkins, J.S., Drake, C.L. (Eds.), Studies in Continental Margin Geology. American Association of Petroleum Geologists, pp. 167–191.

Nomikou, P., Carey, S., Papanikolaou, D., Croff Bell, K., Sakellariou, D., Alexandri, M., Bejelou, K., 2012. Submarine volcanoes of the Kolumbo volcanic zone NE of Santorini Caldera, Greece. Glob. Planet. Chang. 90-91, 135–151.

Pande, K., Sheth, H.C., Bhutani, R., 2001. ^{40}Ar - ^{39}Ar age of the St. Mary's Islands volcanics, southern India: record of India - Madagascar break-up on the Indian subcontinent. Earth Planet. Sci. Lett. 193, 39–46.

Pande, K., Yatheesh, V., Sheth, H., 2017. 40Ar/39Ar dating of the Mumbai tholeiites and Panvel flexure: intense 62.5 Ma onshore–offshore Deccan magmatism during India-Laxmi Ridge–Seychelles breakup. Geophys. J. Int. 210 (2), 1160–1170.
Parker, R.L., 1972. The rapid calculation of potential anomalies. Geophys. J. R. Astron. Soc. 31, 447–455.
Piskarev, A., Elkina, D., 2017. Giant caldera in the Arctic Ocean: evidence of the catastrophic eruptive event. Sci. Rep. 7, 46248.
Radhakrishna, T., Joseph, M., 2012. Geochemistry and paleomagnetism of Late Cretaceous mafic dikes in Kerala, southwest coast of India in relation to large igneous provinces and mantle plumes in the Indian Ocean region. Geol. Soc. Am. Bull. 124 (1/2), 240–255.
Radhakrishna, T., Dallmeyer, R.D., Joseph, M., 1994. Paleomagnetism and 36Ar/40Ar vs 39Ar/40Ar isotope correlation ages of dyke swarms in Central Kerala, India: tectonic implications. Earth Planet. Sci. Lett. 121, 213–226.
Radhakrishna, T., Maluski, H., Mitchell, J.G., Joseph, M., 1999. 40Ar-39Ar and K/Ar geochronology of the dykes from the south Indian granulite terrain. Tectonophysics 304, 109–129.
Ram Mohan, M.R., Shaji, E., Satyanarayanan, M., Santosh, M., Tsunogae, T., Yang, Q.-Y., Dhanil Dev, S.G., 2016. The Ezhimala Igneous Complex, southern India: possible imprint of Late Cretaceous magmatism within rift setting associated with India–Madagascar separation. J. Asian Earth Sci. 121, 56–71.
Richards, F.D., Kalnins, L.M., Watts, A.B., Cohen, B.E., Beaman, R.J., 2018. The morphology of the Tasmantid Seamounts: interactions between tectonic inheritance and magmatic evolution. Geochem. Geophys. Geosyst. 19, 3870–3891.
Roche, O., Druitt, T.H., Merle, O., 2000. Experimental study of caldera formation. J. Geophys. Res. Solid Earth 105, 395–416.
Sheth, H., Pande, K., Vijayan, A., Sharma, K.K., Cucciniello, C., 2017. Recurrent Early Cretaceous, Indo-Madagascar (89–86 Ma) and Deccan (66 Ma) alkaline magmatism in the Sarnu-Dandali complex, Rajasthan: 40Ar/39Ar age evidence and geodynamic significance. Lithos 284–285, 512–524.
Shuhail, M., Yatheesh, V., Bhattacharya, G.C., Müller, R.D., Kamesh Raju, K.A., Mahender, K., 2018. Formation and evolution of the Chain-Kairali Escarpment and the Vishnu Fracture Zone in the Western Indian Ocean. J. Asian Earth Sci. 164, 307–321.
Stagpoole, V., Schenke, H.W., Ohara, Y., 2016. A name directory for the ocean floor. EOS Trans. Am. Geophys. Union 97.
Storey, M., Mahoney, J.J., Saunders, A.D., Duncan, R.A., Kelley, S.P., Coffin, M.F., 1995. Timing of hotspot related volcanism and the breakup of Madagascar and India. Science 267 (5199), 852–855.
Talwani, M., Heirtzler, J.R., 1964. Computation of magnetic anomalies caused by two dimensional structures of arbitrary shape. In: Parks, G.A. (Ed.), Computers in the Mineral Industries. Stanford University, pp. 464–480.
Talwani, M., Worzel, J.L., Landisman, M., 1959. Rapid gravity computations for two-dimensional bodies with application to the Mendocino Submarine Fracture Zone. J. Geophys. Res. 64 (1), 49–59.
Tizzani, P., Battaglia, M., Castaldo, R., Pepe, A., Zeni, G., Lanari, R., 2015. Magma and fluid migration at Yellowstone Caldera in the last three decades inferred from InSAR, leveling, and gravity measurements. J. Geophys. Res. Solid Earth 120 (4), 2627–2647.
Tolan, T.L., Reidel, S.P., Beeson, M.H., Anderson, J.L., Fecht, K.R., Swanson, D.A., 1989. Revisions to the estimates of the areal extent and volume of the Columbia River Basalt Group. In: Reidel, S.P., Hooper, P.R. (Eds.), Volcanism and Tectonism in the Columbia River Flood-Basalt Province. Geological Society of America Special Paper vol. 239, pp. 1–20.
Torsvik, T.H., Tucker, R.D., Ashwal, L.D., Carter, L.M., Jamtveit, V., Vidyadharan, K.T., Venkataramana, P., 2000. Late Cretaceous India - Madagascar fit and timing of breakup related magmatism. Terra Nova 12, 220–224.
Valsangkar, A.B., Radhakrishnamurthy, C., Subbarao, K.V., Beckinsale, R.D., 1981. Paleomagnetism and Potassium-Argon Age Studies of Acid Igneous Rocks From the St. Mary Islands. Geological Society of India, pp. 265–275.
Weatherall, P., Marks, K.M., Jakobsson, M., Schmitt, T., Tani, S., Arndt, J.E., Rovere, M., Chayes, D., Ferrini, V., Wigley, R., 2015. A new digital bathymetric model of the world's oceans. Earth and Space Science 2, 331–345.
Wessel, P., Smith, W.H.F., Scharroo, R., Luis, J., Wobbe, F., 2013. Generic mapping tools: improved version released. EOS Trans. Am. Geophys. Union 94 (45), 409–410.
Whitmarsh, R.B., Weser, O.E., et al., 1974. Site 219, 220, and 221. Initial Reports of the Deep Sea Drilling Project 23. U.S. Government Printing Office, Washington D.C., pp. 35–210.
Yatheesh, V., 2020. Structure and tectonics of the continental margins of India and the adjacent deep ocean basins: current status of knowledge and some unresolved problems. Episodes 43 (1), 586–608.
Yatheesh, V., Bhattacharya, G.C., Shuhail, M., 2020. Revised plate tectonic reconstruction model for the early opening of the Arabian Sea. In: Rossi, P., François, C., Miles, P. (Eds.), The Indian Ocean and its Margins. Commission for the Geological Map of the World, France, pp. 11–12.

Marine Geophysical Research (2022) 43:14
https://doi.org/10.1007/s11001-022-09469-x

Annexure 3

ORIGINAL RESEARCH PAPER

Conjugate nature of the Alleppey-Trivandrum Terrace Complex with the Northern Madagascar Ridge in the early opening model of the Arabian Sea: evaluation based on an integrated geophysical investigation

C. M. Bijesh[1,2] · V. Yatheesh[3] · P. John Kurian[1] · J. John Savio[3] · Vasudev Mahale[3] · Abhishek Shet[3] · S. Gautham[3]

Received: 25 September 2021 / Accepted: 21 February 2022

Abstract

The southwestern continental margin of India reveals the presence of an anomalous bathymetric high feature located in the mid-continental slope region off Trivandrum. Based on the analysis of the available geophysical data and plate tectonic reconstruction, this feature was interpreted as a scar of India-Madagascar separation, with its conjugate identified on the Northern Madagascar Ridge. Although the conjugate nature of the Alleppey-Trivandrum Terrace Complex and the Northern Madagascar Ridge was postulated, this inference has not yet been evaluated by comparing their geophysical signatures and crustal structure. The present study is aimed to derive and compare the crustal configuration of these two features using an up-to-date compilation of the bathymetry, gravity and magnetic data, and by employing integrated forward modelling of gravity and magnetic anomalies. Our derived crustal models for the Alleppey-Trivandrum Terrace Complex and the Northern Madagascar Ridge suggest that both these features can be explained in terms of thinned continental crust intermingled with volcanic intrusives. The crustal thicknesses of the Northern Madagascar Ridge and Alleppey-Trivandrum Terrace Complex at their conjugate continent-ocean boundaries are ~17 km and both these features are associated with high amplitude magnetic anomalies whose genesis is attributed to the volcanism caused by the Marion hotspot activity. Therefore, based on our integrated interpretation of the geophysical data, we support the earlier interpretation on conjugate nature of the Northern Madagascar Ridge and the Alleppey-Trivandrum Terrace Complex that was proposed based on the fitting of shape and size of the bathymetric notch observed in the southeastern continental margin of Madagascar with a bathymetric protrusion observed in the southwestern continental margin of India in the India-Madagascar pre-drift scenario. These features remained as a single unit prior to ~88 Ma and subsequently got separated during the India-Madagascar breakup.

Keywords Alleppey-Trivandrum Terrace Complex · Northern Madagascar Ridge · Crustal configuration · Gravity and magnetic anomalies · Marion hotspot

Introduction

The bathymetric map of the southwestern continental margin of India reveals the presence of an anomalous bathymetric high feature in the mid-continental slope region off Trivandrum (Fig. 1a, b). Based on the analysis of limited single beam bathymetry transects available over this feature, and the isobaths available from GEBCO database (IOC-IHO-BODC, 2003), Yatheesh et al. (2006) inferred this feature to represent a "terrace" defined by a conspicuously wide low gradient zone between the 1000 and 2000 m isobaths, and referred it to as the 'Terrace Off Trivandrum (TOT)'. Using the available paleogeographic reconstruction models depicting the evolution of the Western Indian

V. Yatheesh
yatheeshv@gmail.com; yatheesh@nio.org

[1] National Centre for Polar and Ocean Research, Ministry of Earth Sciences, 403804 Vasco-da-Gama, Goa, India

[2] School of Earth, Ocean and Atmospheric Sciences, Goa University, 403 206 Taleigao Plateau, Goa, India

[3] CSIR – National Institute of Oceanography, 403004 Dona Paula, Goa, India

Published online: 16 April 2022

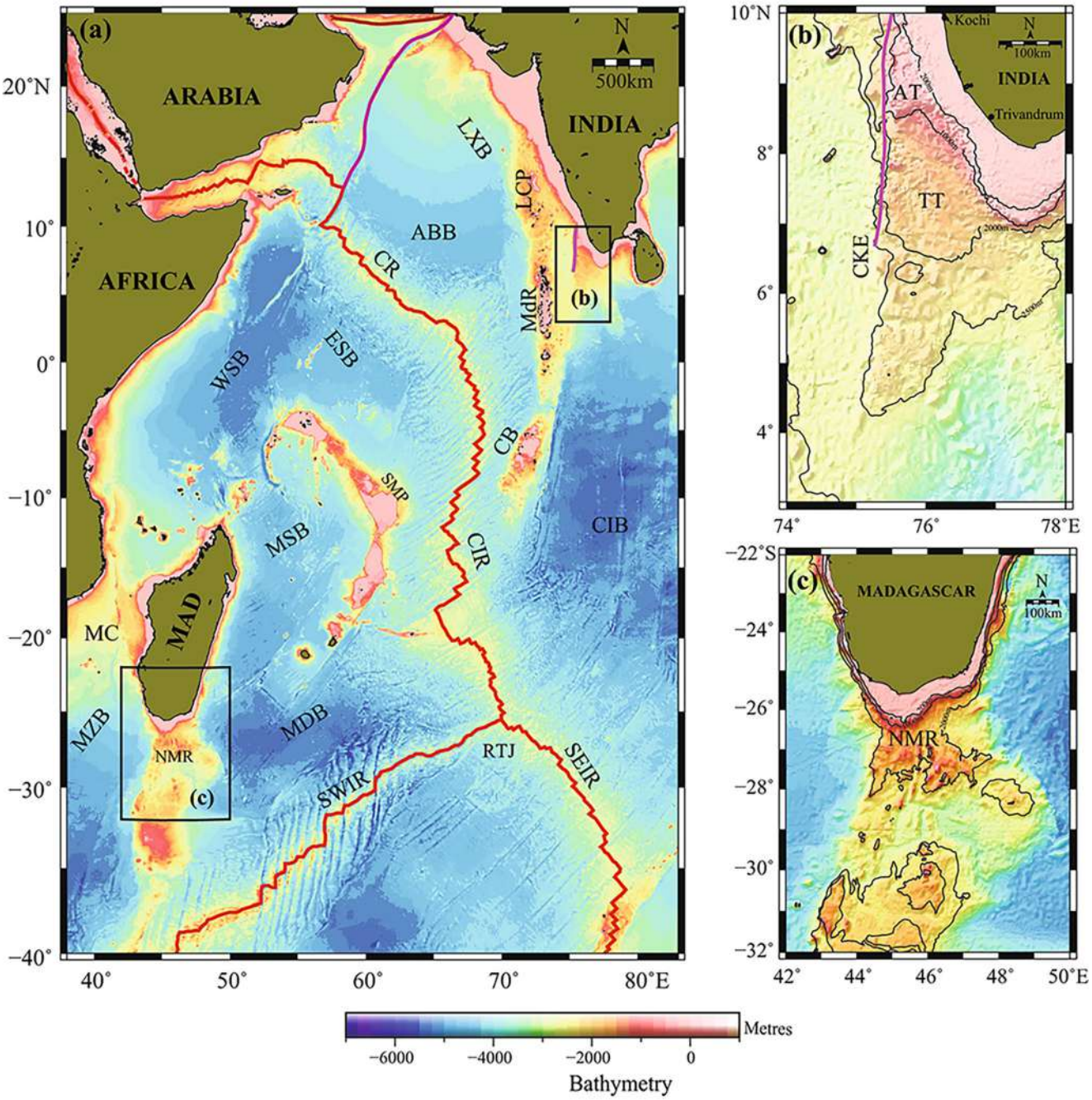

Fig. 1 (a) Bathymetric map of the Western Indian Ocean prepared using GEBCO 2020 global bathymetric grid showing major tectonic elements. The study areas are marked as black solid boxes. Enlarged bathymetric map of the southwestern continental margin of India (b) and southeastern continental margin of Madagascar (c), along with selected GEBCO isobaths overlaid. LCP: Laccadive Plateau; MdR: Maldive Ridge; CB: Chagos Bank; CKE: Chain Kairali Escarpment; AT: Alleppey Terrace; TT: Trivandrum Terrace; LXB: Laxmi Basin; ABB: Arabian Basin; ESB: Eastern Somali Basin; WSB: Western Somali Basin; CIB: Central Indian Basin; SMP: Seychelles-Mascarene Plateau; MZB; Mozambique Basin; MC: Mozambique Channel; MDB; Madagascar Basin; MSB: Mascarene Basin; CR: Carlsberg Ridge; CIR: Central Indian Ridge; SWIR: Southwest Indian Ridge; SEIR: Southeast Indian Ridge; RTJ: Rodrigues Triple Junction; MAD: Madagascar; NMR: Northern Madagascar Ridge

Ocean and updated compilation of identified offshore tectonic elements, Yatheesh et al. (2006) further inferred

that the southern part of the TOT fits well in shape and size with bathymetric notch on the Northern Madagascar Ridge (NMR, Fig. 1c), implying the conjugate nature of TOT with NMR. Subsequently, Yatheesh et al. (2013) carried out detailed investigation on the TOT region using a new set of sea-surface gravity, magnetic and single beam bathymetry data, and inferred that the above anomalous topography feature consists of two contiguous terraces (Fig. 1b), the Alleppey Terrace (defined by 300 and 400 m isobaths) and the Trivandrum Terrace (defined by 1500 and 1900 m isobaths), together referred to as the Alleppey-Trivandrum Terrace Complex (ATTC). They further provided gravity and magnetic characteristics of the ATTC and derived detailed crustal configuration model for the Alleppey Terrace and Trivandrum Terrace, based on forward modelling of gravity and magnetic profiles. Based on all these constraints from the southwestern continental margin of India, complemented with the magnetic anomaly interpretations in the Mascarene Basin, Bhattacharya and Yatheesh (2015) provided a revised plate tectonic evolution model for the Western Indian Ocean, where the anomalous feature defined by 2000 and 2500 m isobath from the southwestern continental margin of India was found to fit with the bathymetric notch in the Northern Madagascar Ridge. Therefore, this feature also is considered to form a part of the Alleppey-Trivandrum Terrace Complex (Fig. 1b), which is believed to have broken away from the Northern Madagascar Ridge. Even though the conjugate nature of the Northern Madagascar Ridge with ATTC is inferred from the plate tectonic reconstruction model and the detailed crustal structure of the ATTC was derived based on forward modelling, the comparison of geophysical signatures and the crustal architecture of these two postulated conjugate features are yet to be examined. Therefore, in the present paper, an attempt is made to derive the crustal configuration of the Northern Madagascar Ridge and compare this with crustal configuration of the ATTC, using an up-to-date compilation of the marine geophysical data available from the southeastern continental margin of Madagascar and its conjugate southwestern continental margin of India.

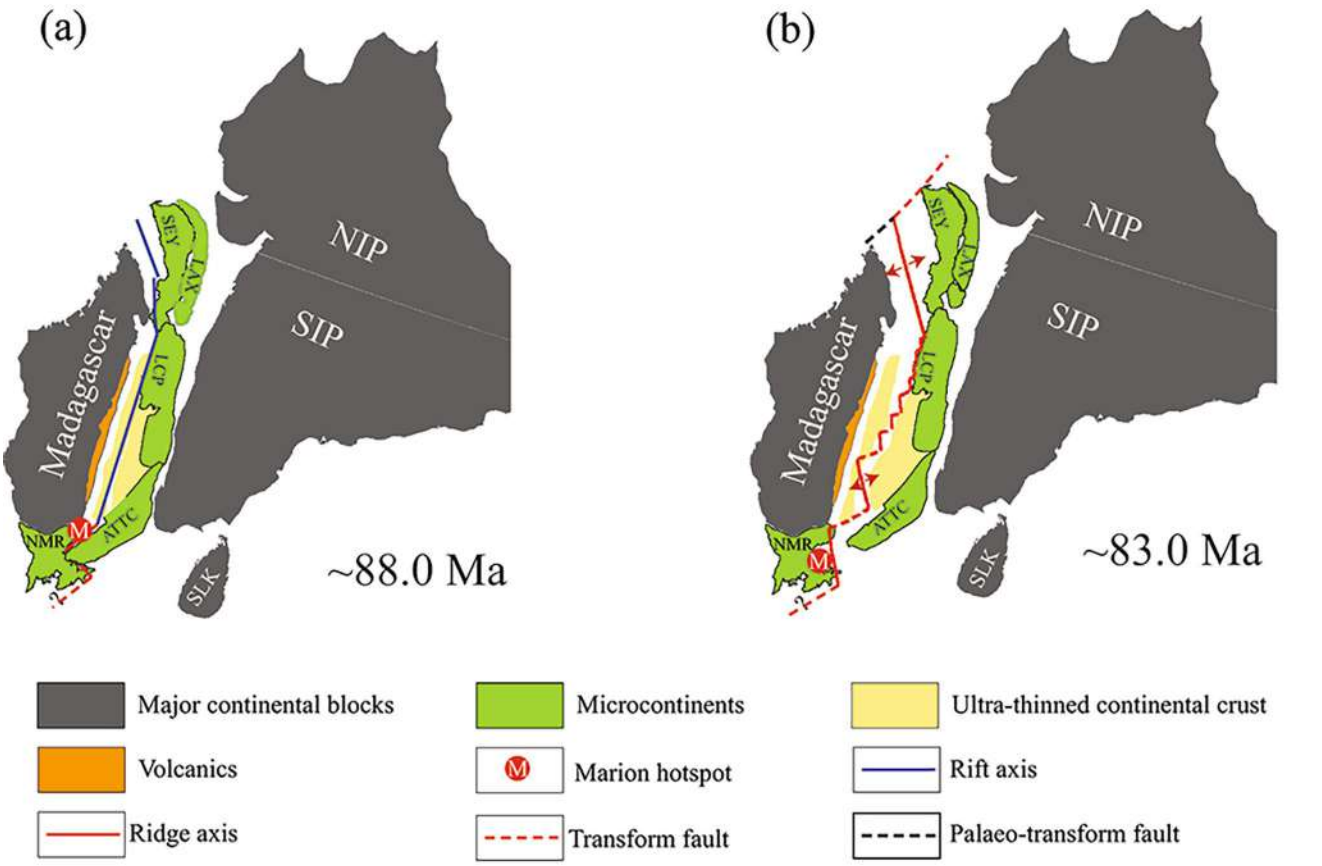

Fig. 2 Revised plate tectonic reconstruction maps of the Western Indian Ocean at (a) ~ 88.0 Ma; (b) ~ 83.0 Ma (modified after Yatheesh, 2020), in fixed Madagascar reference frame. SIP: Southern Indian Protocontinent; NIP: Northern Indian Protocontinent; SEY: Seychelles Plateau; LAX: Laxmi Ridge; LCP: Laccadive Plateau; ATTC: Alleppey-Trivandrum Terrace Complex; NMR: Northern Madagascar Ridge; SLK: Sri Lanka

Tectonic framework

The revised plate tectonic reconstruction model (Fig. 2) for the Western Indian Ocean (Bhattacharya and Yatheesh, 2015; Shuhail et al. 2018; Yatheesh, 2020; Yatheesh et al. 2020) suggests that the western continental margin of India and its conjugate regions were formed by the continental breakup among the Southern Indian Protocontinent (SIP), Northern Indian Protocontinent (NIP), Seychelles Plateau (SEY), Madagascar (MAD), Laxmi Ridge (LAX), and the Laccadive Plateau (LCP). In this context, the Alleppey-Trivandrum Terrace Complex and the Northern Madagascar Ridge were juxtaposed and existed as the intervening continental slivers between the major continental blocks of India and Madagascar in the south prior to 88.0 Ma. Followed by this, the rifting between Madagascar and conjoint SIP-NIP-LAX-LCP-SEY block has occurred due to the influence of Marion hotspot at around 88.0 Ma (Fig. 2a), followed by the initiation of seafloor spreading in the Mascarene Basin shortly before 83.0 Ma (Fig. 2b). The shapes of the ATTC as a protrusion on the Indian side and as a notch in the Madagascar side appear to have been created by the spreading and transform segments of the initial spreading geometry. As a result, the western limit of the Alleppey-Trivandrum Terrace Complex is defined by a ~ 500 km long steep linear escarpment, known as the Chain-Kairali Escarpment, coinciding with the transform boundary. The southern limit of the ATTC is marked by the feature defined by the 2500 m

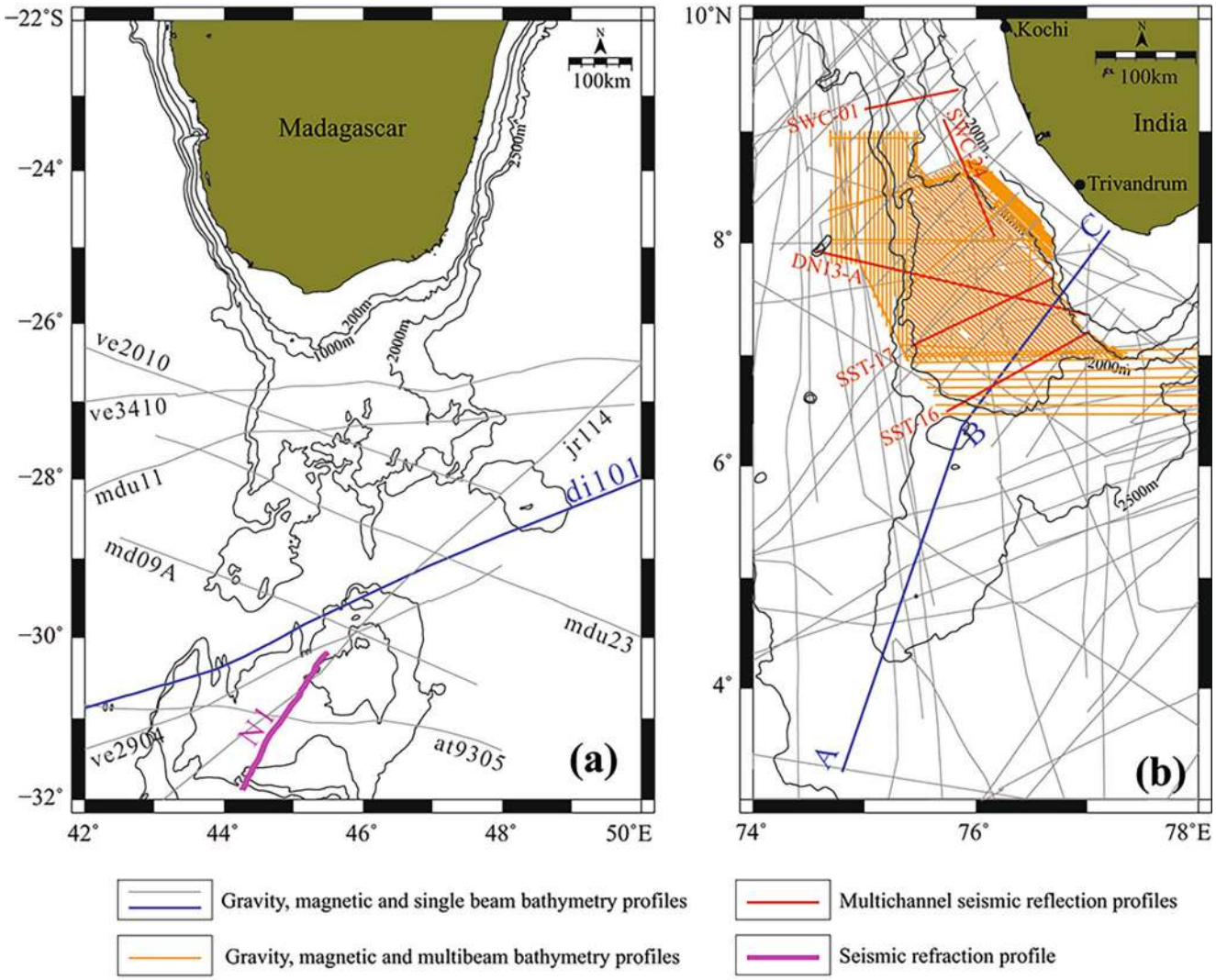

Fig. 3 Map showing locations of selected sea-surface gravity, magnetic, and bathymetry profiles and seismic sections used in the present study over (a) NMR and (b) ATTC. The gravity and magnetic anomalies along profiles di101 and ABC have been used for deriving the crustal models of NMR (in Fig. 6) and ATTC (in Fig. 7), respectively. The line labelled as N1 represents refraction profile over the Northern Madagascar Ridge (Goslin et al. 1981)

isobath, which is located immediately east of the southernmost spreading centre segment.

Data and Methodology

The main data used in the present study are sea-surface multibeam bathymetry, gravity and magnetic data collected by National Centre for Polar and Ocean Research (NCPOR), Goa, and CSIR - National Institute of Oceanography (CSIR-NIO), Goa, under the project "Geoscientific Studies of Exclusive Economic Zone of India", complemented with those available from Yatheesh et al. (2013) and National Centres for Environmental Information (https://www.ngdc.noaa.gov/ngdc.html). Multibeam bathymetry data over the ATTC region were acquired through four expeditions (MGS-03, MGS-04, MGS-08 and SSD-059) and are archived as grids in 100 m spatial resolution, after systematic post-processing. Sea-surface gravity and magnetic data were reduced to gravity and magnetic anomalies, after applying the respective corrections. For understanding the sub-seafloor characteristics of the ATTC, we used multichannel seismic reflection data (profiles SWC-01 and SWC-24) acquired by the Directorate General of Hydrocarbon

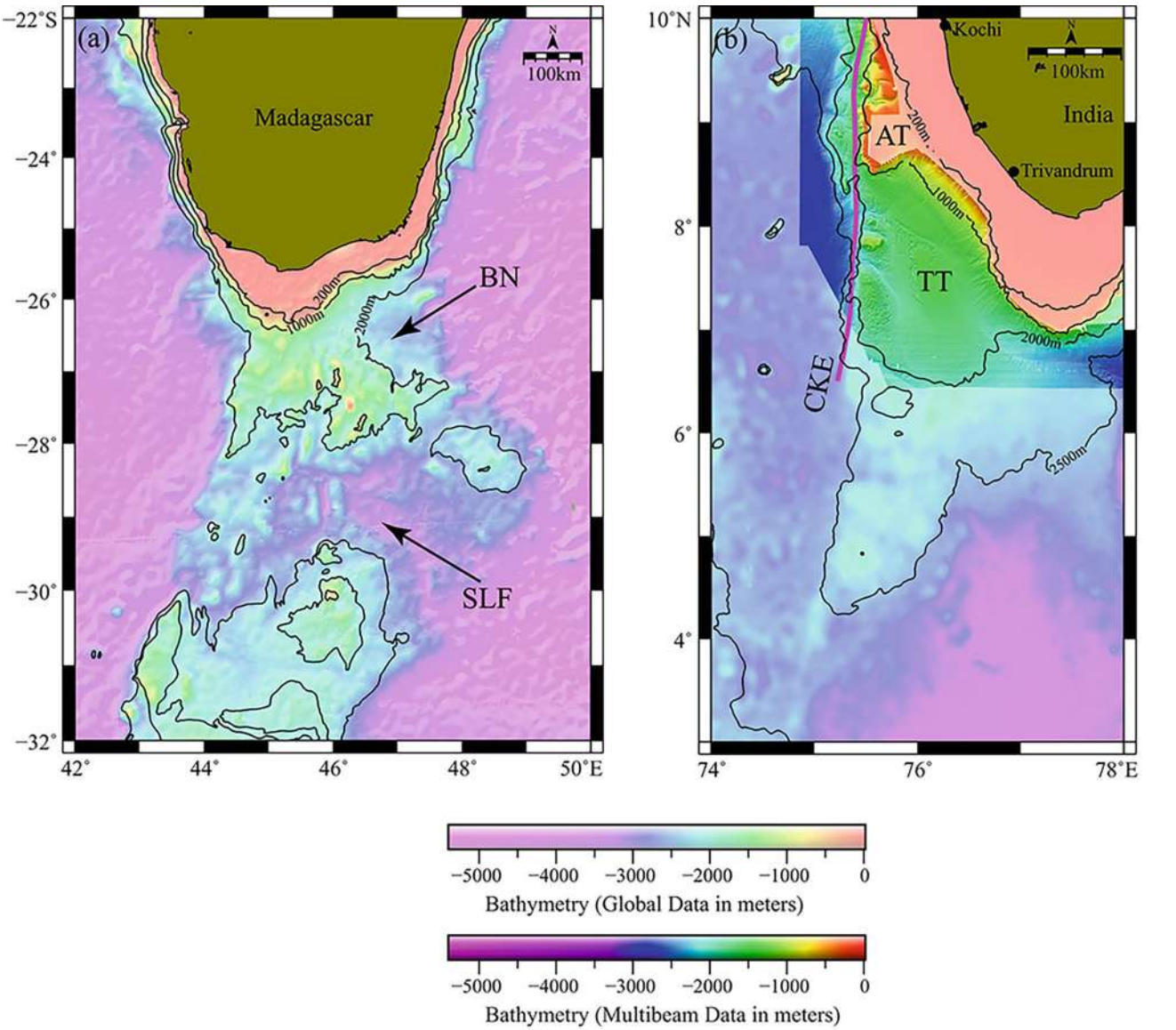

Fig. 4 (a) Bathymetric map prepared using GEBCO 2020 grid over the NMR. (b) High-resolution bathymetric map of the ATTC region prepared using multibeam bathymetry data, presented along with the GEBCO 2020 grid in the background. Other details are as in Fig. 1

(DGH), India, and published seismic sections (Nathaniel, 2013; Yatheesh et al. 2013; Shuhail et al. 2018). Further, to aid our analysis and interpretation, we used satellite derived free-air gravity anomalies (Sandwell et al. 2014), GEBCO global bathymetry grid (GEBCO Compilation Group, 2020), and EMAG2 magnetic anomaly grid (Maus et al. 2009), in the areas where sea-surface data is not available. The locations of sea-surface gravity, magnetic, multibeam and seismic reflection profiles used in the present study are shown in Fig. 3.

Geophysical signatures over NMR and ATTC

Seafloor and sub-seafloor topography

Northern Madagascar Ridge

The Madagascar Ridge represents an elongated bathymetric high feature that extends southward from the Madagascar Island (Fig. 1). This feature existing between 26°S and 36°S is defined by ~3000 m isobath, separating the Mozambique Basin in the west and the Mascarene and Madagascar basins in the east, abutting its south on the Southwest Indian Ridge. The Madagascar Ridge appears to consist of two domains – a southern domain (between 31°S and 36°S) consisting of a relatively flat area, and a northern domain (between 31°S and 26°S) consisting of complex and irregular topography (Goslin et al. 1980). Since the ATTC fits with the Northern Madagascar Ridge, we analyzed the bathymetric signatures of the northern domain using the latest available GEBCO global bathymetric data (GEBCO Compilation Group, 2020). The bathymetric map of the NMR (Fig. 4a) clearly exhibits a bathymetric notch (labelled as BN in Fig. 4a) defined by 2000 m isobath in its northeastern part, adjacent to the Mascarene Basin. The central part of the NMR is characterized by the presence of several secondary bathymetric peaks within the 2000 m water depth, between 26°S and 28°S (Fig. 4a). The NMR also exhibits an arcuate shaped saddle-like feature (labelled as SLF in Fig. 4a) along 28°S latitude, between 44°E and 48°E longitudes.

Alleppey-Trivandrum Terrace Complex

The morphology of the Alleppey-Trivandrum Terrace Complex was originally defined (Yatheesh et al. 2006) based on the bathymetric contours (1000 and 2000 m) available from GEBCO digital database (IOC-IHO-BODC, 2003). Subsequently, Yatheesh et al. (2013) published an updated bathymetric contour map of the Alleppey-Trivandrum Terrace Complex, based on a new set of single beam bathymetry profiles. With an aim to carryout detailed bathymetric imaging of this region, we acquired multibeam bathymetry data for the first time over the northern part of the Alleppey-Trivandrum Terrace Complex falling between 400 and 2000 m water depth. The updated bathymetric map (Fig. 4b) generated using this high-resolution multibeam bathymetry data (complemented by the global GEBCO bathymetry data in the nearby regions) clearly depicts the morphology qualifying to consider the ATTC as a terrace defined by low gradient zones. The map further defines the sharp drop in the depth to the seafloor defining the location of the nearly N-S trending Chain-Kairali Escarpment (CKE) that defines the western boundary of the ATTC, and the ENE-WSW trending Quilon Escarpment (QE) south of the Alleppey Terrace. Small scale features representing slope failure events and submarine channels are also observed in the shelf/slope regions of the Alleppey and Trivandrum terraces. Trivandrum Terrace is a large feature that exists between the shelf edge in the east, CKE in the west and QE in the north, while the southern boundary of TT appears to continue towards south as the feature defined by the 2500 m isobath. As noticed by Yatheesh et al. (2013), north of 7°45'N, continental shelf-slope transition is gentle, while south of 7°45'N, this is comparatively steeper. The region in the vicinity of the CKE is characterized by the presence of several isolated bathymetric high features (Bijesh et al. 2018). Further, significant scouring/depression-like features are observed close to the CKE and in the central part of the TT that appears to have resulted due to the underwater current activity and its erosive-depositional process.

For understanding the sub-seafloor information of the ATTC, we present five multichannel seismic reflection sections (Fig. 5). In the seismic sections, the CKE is marked by a steep gradient basement topography (Fig. 5a, b). Seafloor / sub-seafloor bulging and block faulting are prominent underneath the TT region (Fig. 5b-d). The basement corresponding to the QE shows a sharp drop in the basement topography as seen from the seismic section along SWC-24 (Fig. 5e). Yatheesh et al. (2013) divided the TT into the western and eastern basins (TT-WB and TT-EB) based on the central basement high flanked by thick sediment-filled basins with block-faulted basement on either sides (Fig. 5b-d).

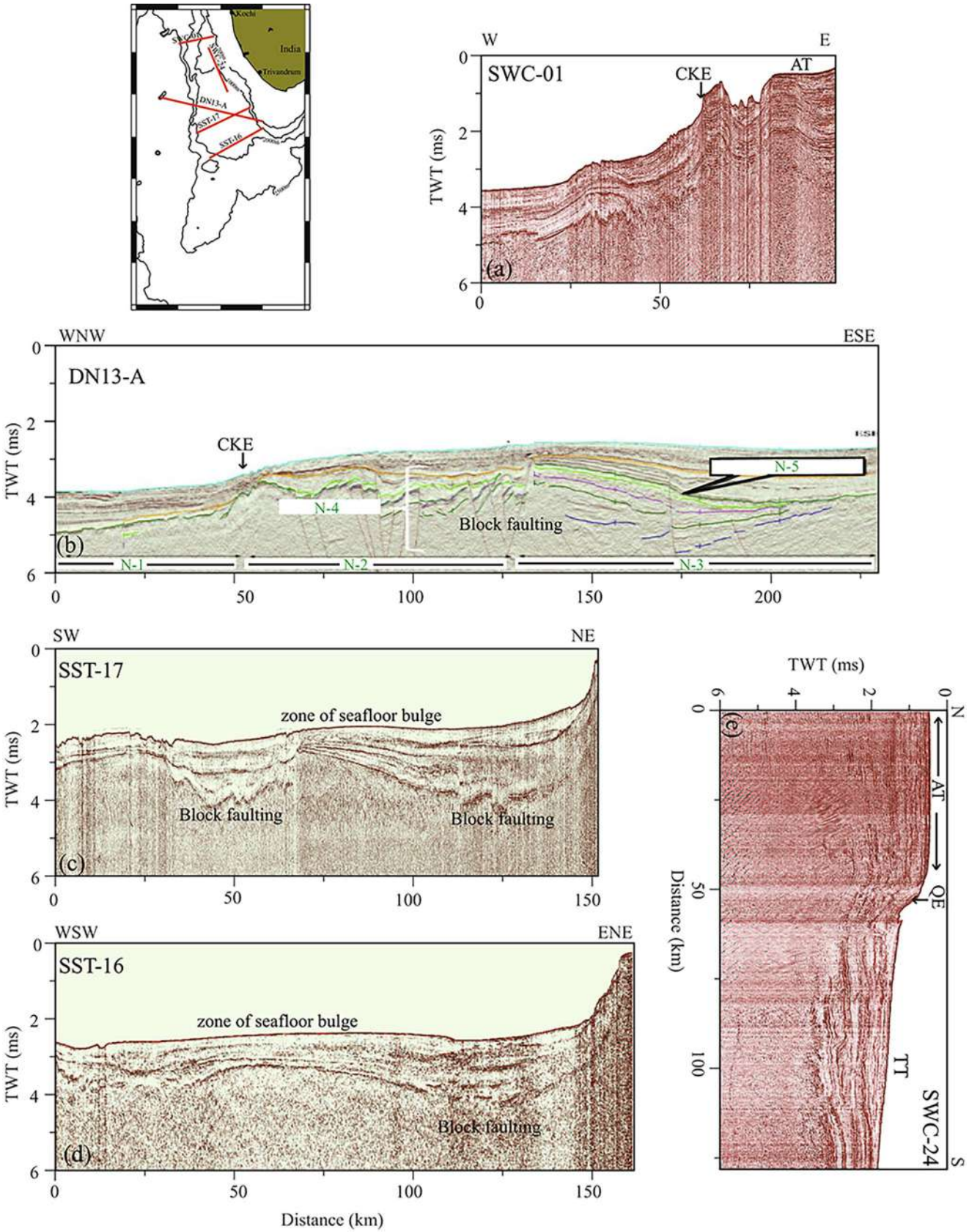

Fig. 5 Seismic reflection sections along the profiles (a) SWC-01, (b) DN13-A (modified after Nathaniel 2013; Shuhail et al. 2018, with permission from Elsevier), (c) SST-17 (after Yatheesh et al. 2013, with permission from Elsevier), (d) SST-16 (after Yatheesh et al. 2013, with permission from Elsevier) and (e) SWC-24. Inset figure shows the locations of these profiles. N1: oceanic / transition; N-2: Vishnu FZ; N-3: Inverted graben; N-4: Mesozoics; N-5: KT Boundary

Gravity Signatures

Northern Madagascar Ridge

The shipborne free-air gravity anomaly data available over the Northern Madagascar Ridge is sparse. Therefore, we also used satellite-derived free-air gravity anomalies (Sandwell et al. 2014) to understand the broader gravity anomaly signature of the NMR. For this purpose, we present the satellite-derived free-air gravity anomaly image superimposed with the available sea-surface free-air gravity anomaly profiles. The 2-dimensional free-air gravity anomaly image and the track-along profiles (Fig. 6a) exhibit several secondary positive and negative gravity anomalies superimposed over a broader dominant positive anomaly, which is correlatable with the topographic signature of the Northern Madagascar Ridge at its entire width. The boundary between the Mozambique Basin and the NMR is well defined by a sharp gradient in free-air gravity anomaly, while its eastern boundary with the Mascarene Basin is not delineable from the free-air gravity anomaly.

Alleppey-Trivandrum Terrace Complex

We present the free-air gravity anomaly map (Fig. 6b) of the ATTC region using the satellite-derived free-air gravity anomaly grid superimposed with the sea-surface gravity grid and selected track-along profiles. A distinct belt of gravity

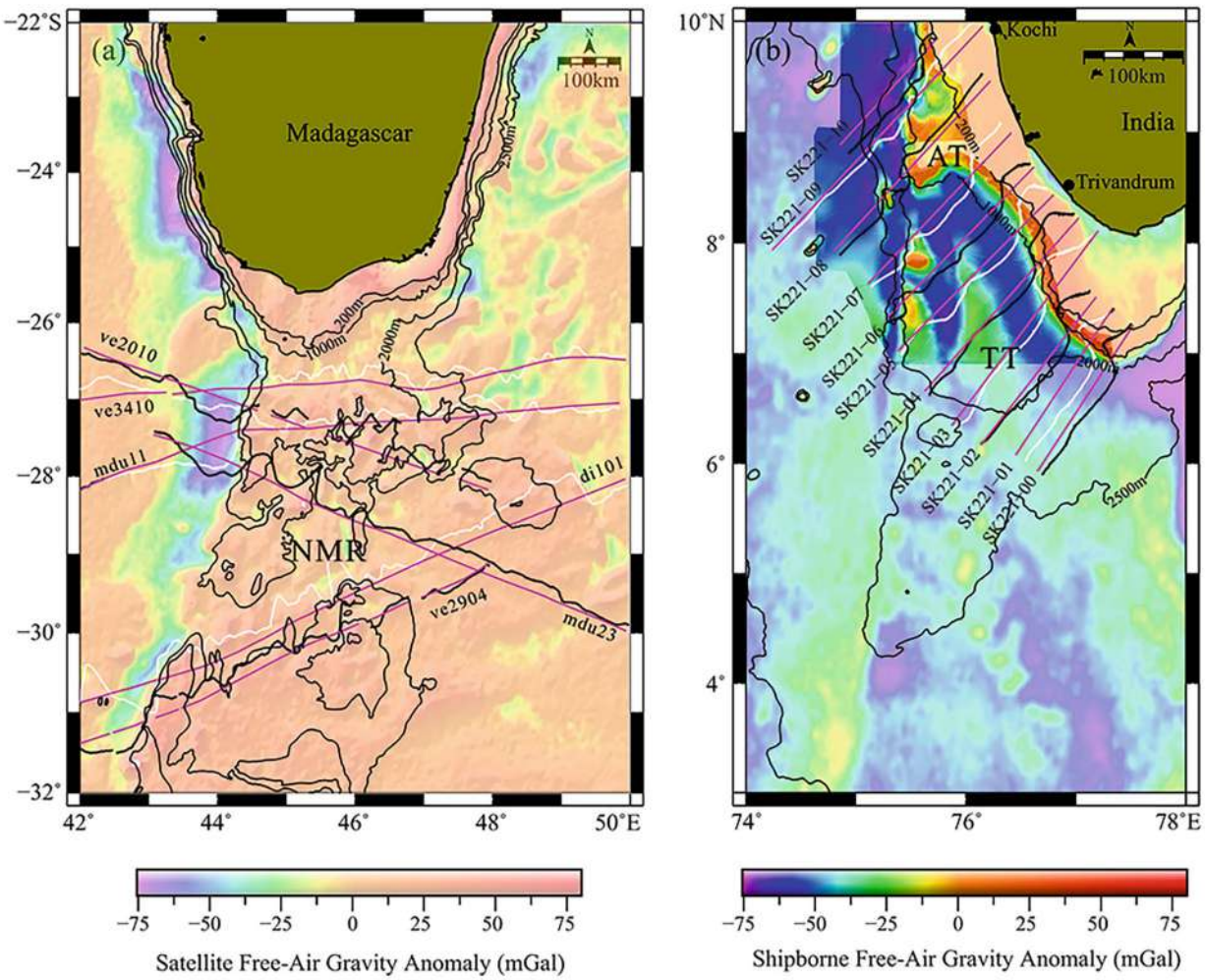

Fig. 6 (a) Satellite-derived free-air gravity anomaly map with sea-surface gravity anomaly data plotted perpendicular to the track over NMR; (b) Shipborne free-air gravity anomaly image over the ATTC region plotted with the background of satellite-derived free-air gravity anomaly. Also plotted the selected shipborne free-air gravity anomaly profiles perpendicular to the track. Other details are as in Fig. 1

high is observed on the continental shelf lying immediately east of the ATTC. A linear gravity high region is observed with an ~N-S trend in the central part of TT. This gravity high anomaly, which is wider in the south and narrower in the north, is superimposed over a high amplitude negative gravity anomaly. In addition, there exists several isolated gravity highs, which are associated with the bathymetric highs identified within the TT region and along-strike of CKE.

Magnetic signatures

Northern Madagascar Ridge

The shipborne magnetic data available over the Northern Madagascar Ridge is limited and therefore to have a broader picture of the magnetic signature of the NMR, we used EMAG2 magnetic anomaly grid (Maus et al. 2009) along with the available sea-surface magnetic data. The 2-dimensional magnetic anomaly image and the track-along profiles (Fig. 7a) exhibit complex magnetic anomaly pattern over the NMR that do not show any correlation from profile-to-profile. Some of these high-amplitude and short wavelength anomalies correspond to the bathymetric highs while

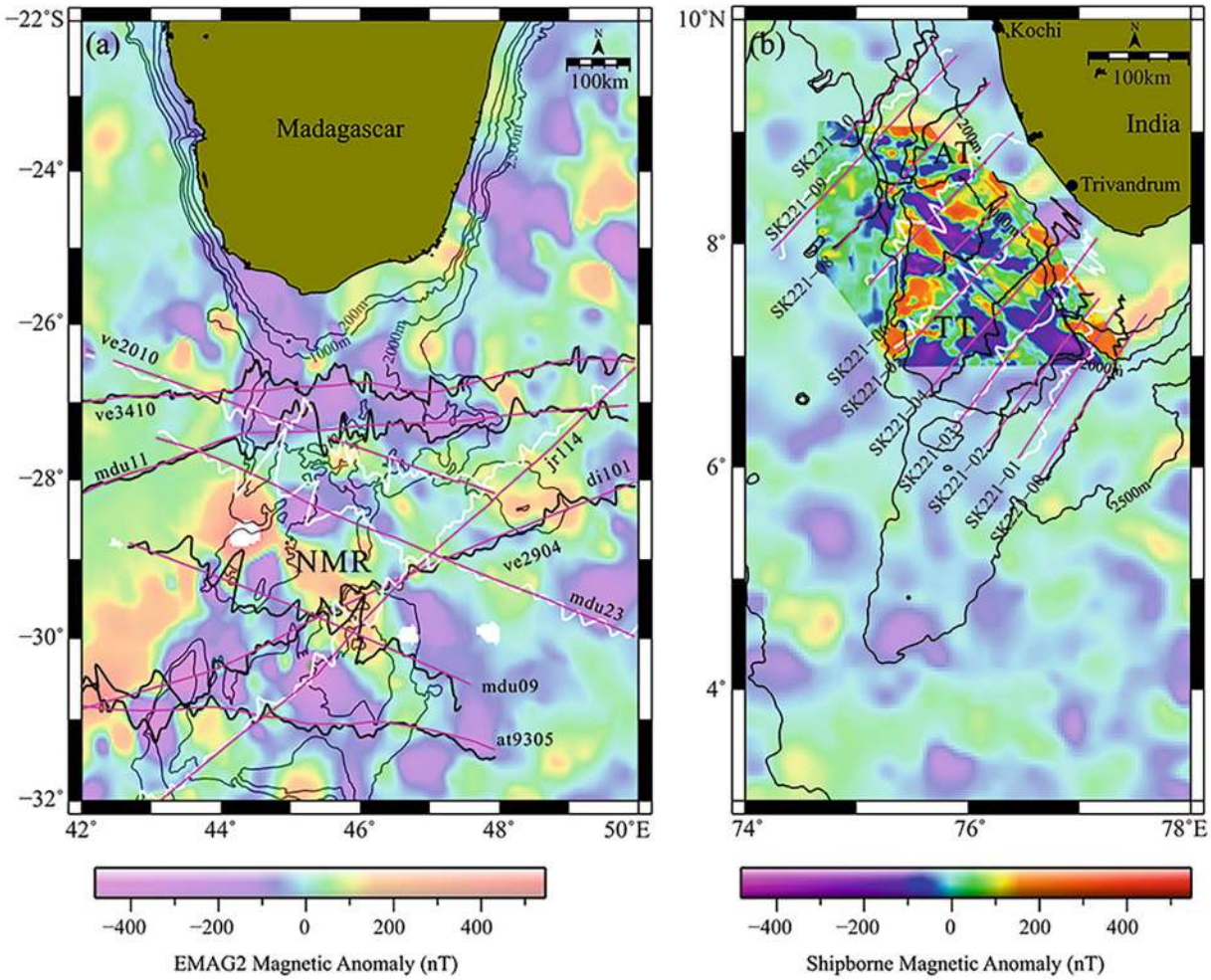

Fig. 7 (a) EMAG2 magnetic anomaly map with sea-surface magnetic anomaly data plotted perpendicular to the track over NMR, (b) Shipborne magnetic anomaly image over the ATTC region plotted with the background of EMAG2 magnetic anomaly grid. Also plotted the selected shipborne magnetic anomaly profiles perpendicular to the track. Other details are as in Fig. 1

others are not correlatable to any bathymetric features. The amplitude of the magnetic anomalies over NMR are higher compared to those in the adjacent Mozambique Basin in the west and the Mascarene Basin in the east. The amplitude of the magnetic anomalies also varies along the strike of the NMR, with highest amplitude north of 29°S.

Alleppey-Trivandrum Terrace Complex

We present the magnetic anomaly map (Fig. 7b) of the ATTC region using the EMAG2 magnetic anomaly grid (Maus et al. 2009) along with the up-to-date compiled sea-surface magnetic data. The magnetic anomaly map depicts the presence of complex magnetic anomalies with variable amplitudes on the ATTC and the adjoining Laccadive Basin in the west and the continental shelf in the east. The continental shelf is associated with relatively high amplitude and high frequency anomalies while the Laccadive Basin is associated with lower amplitude anomalies. The magnetic anomaly map shows the presence of several prominent high amplitude magnetic anomalies over the ATTC region and the Chain-Kairali Escarpment. In some areas of CKE, there is obvious correspondence for these magnetic anomalies with bathymetric highs.

Crustal configurations of NMR and ATTC

Crustal configuration of the Northern Madagascar Ridge

To derive the crustal configuration of the Northern Madagascar Ridge, we carried out integrated forward modelling of gravity and magnetic data along a representative profile, di-101 (profile location is shown in Fig. 3a) that cut across the Mozambique Basin, Northern Madagascar Ridge and the Mascarene Basin. As a first step, forward modelling of gravity anomalies has been performed based on the method of Talwani et al. (1959). We constructed an initial model by considering all the geological and geophysical constraints available from different domains within the study area. The seafloor depth has been obtained from the sea-surface

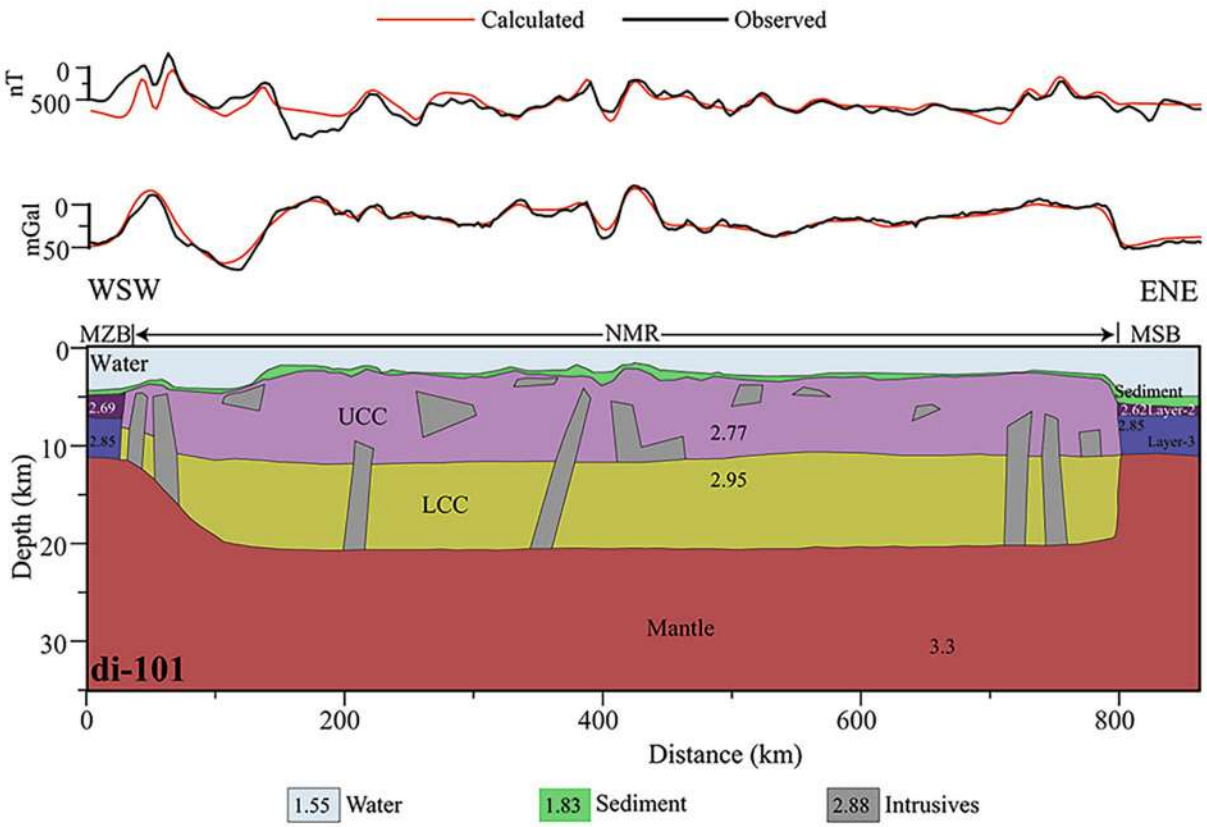

Fig. 8 Crustal model of the NMR derived based on integrated gravity-magnetic modelling along the profile di-101. The constraints used have been discussed in the text. UCC: Upper continental crust; LCC: Lower continental crust

bathymetry data available along the profile. Since there is no basement information available along the profile or its nearby areas, we used the sediment thickness information from the global 5-arc-minute total sediment thickness grid (Straume et al. 2019) to constrain the basement. While constructing the initial model, we used the published velocity-depth information derived based on the seismic refraction studies carried out in the Mozambique Basin (Leinweber et al. 2013) and NMR (Goslin et al. 1981) for getting the constraints in deeper layers. Since no seismic information is available for the Mascarene Basin, we used the velocity-depth information for a standard oceanic crust (Fowler, 2005). Based on the geophysical and geological framework of the study area, we considered two-layered oceanic crust for Mozambique and Mascarene basins and two-layered continental crust under NMR. Seismic velocity information is converted into density values using the velocity-density relationship (Brocher, 2005). The model is refined further keeping these density values and seafloor depth unchanged, and by changing the Moho depth and thickness of different layers slightly to get a reasonably good fit with computed and observed gravity anomalies.

Once a reasonably good fit for the gravity model is obtained, attempt has been made to derive the magnetic source bodies fitting within the crustal configuration derived from the gravity anomalies. This is achieved by carrying out the forward modelling of magnetic data based on Talwani and Heitzler (1964) method. For this, we considered that the magnetic anomalies are resulted due to the presence of volcanic intrusives present in the crust, in light of the understanding on tectonic framework of the study area. The paleomagnetic studies (Storey et al. 1995; Torsvik et al. 1998) carried out in the Madagascar mainland and coastal regions revealed the wide-spread volcanism during the Late Cretaceous. Based on the radiometric age determination (~84–90 Ma), the genesis of these volcanics has been attributed to the Marion hotspot volcanism (Storey et al. 1995; Torsvik et al. 1998). Since this timing falls within the Cretaceous normal superchron, the volcanic intrusives are of normal polarity (Torsvik et al. 1998). We have taken the average values of inclination and declination (Average Remnant Inclination = -65°; Average Remnant Declination = 358°) derived from the paleomagnetic data (Torsvik et al. 1998). The magnetic susceptibility values are considered within the range of 2.5-4.0 A/m. Once these parameters are fixed, the shape and extent of the intrusive bodies are adjusted to obtain a good fit between observed and calculated magnetic anomalies through several iterations. The derived crustal model (Fig. 8) suggests that the crust underlying the Mozambique and Mascarene Basin can be explained in terms of two-layered oceanic crust with an average thickness of 6–7 km. The model suggests a crustal thickness of ~16–17 km for the Northern Madagascar Ridge, with its moho located at ~22 km. The magnetic anomalies over the Northern Madagascar Ridge can be explained in terms of volcanic intrusions occurred during a normal polarity. Therefore, considering the density and magnetic structures and the thickness of the crustal layers, we infer that the crust underlying the Northern Madagascar Ridge can reasonably be explained in terms of thinned continental crust intermingled with volcanic intrusives.

Crustal configuration of the ATTC

To derive the crustal configuration of the ATTC, a profile ABC (profile AB extracted from satellite-derived free air gravity anomalies / global bathymetry and profile BC representing shipborne data along SK221-03) has been selected that cut across a portion of the Laccadive Basin, ATTC and continental shelf (Fig. 3b). While constructing the initial model along this profile, we adopted all the constraints from the crustal model derived for ATTC and the adjacent regions along SK221-05 from Yatheesh et al. (2013). As in the case of Northern Madagascar Ridge, as first step, we carried out forward modelling of gravity data and then incorporated the magnetic source bodies based on forward modelling of magnetic data. The prominent magnetic anomalies along the profile SK221-03 can be considered to have caused by volcanic intrusives within the ATTC region since a large number of volcanic rocks formed by Marion hotspot volcanism have been identified within the proximity of this region. This constraint is adopted from the paleomagnetic studies carried out in the Indian mainland (Radhakrishna and Joseph, 2012) as well as the St. Mary Island (Torsvik et al. 2000), which revealed the normal magnetization characteristics of the volcanic intrusives. The volcanic intrusives are included as dykes and sills, in which dyke is extended to the Moho derived through modelling. Besides, the magnetic properties of the intrusives are limited to a depth of ~22 km, based on the Curie point temperature of ~580 °C. All intrusive bodies are considered with an average remanent inclination of -56° and declination of 315°, by averaging of all normally magnetized bodies.

The derived crustal model (Fig. 9) suggests that, in the continental shelf region, moho is at a depth of 33 km and it shallows down to ~22 km in the boundary between ATTC and the Laccadive Basin. Therefore, the derived model suggests a crustal thickness of ~30 km under the continental shelf region thinning to ~16–17 km in the westernmost extent of the ATTC. Therefore, considering the density and magnetic structures and the thickness of the crustal layers, we infer that the crust underlying the Alleppey-Trivandrum Terrace Complex can reasonably be explained in terms

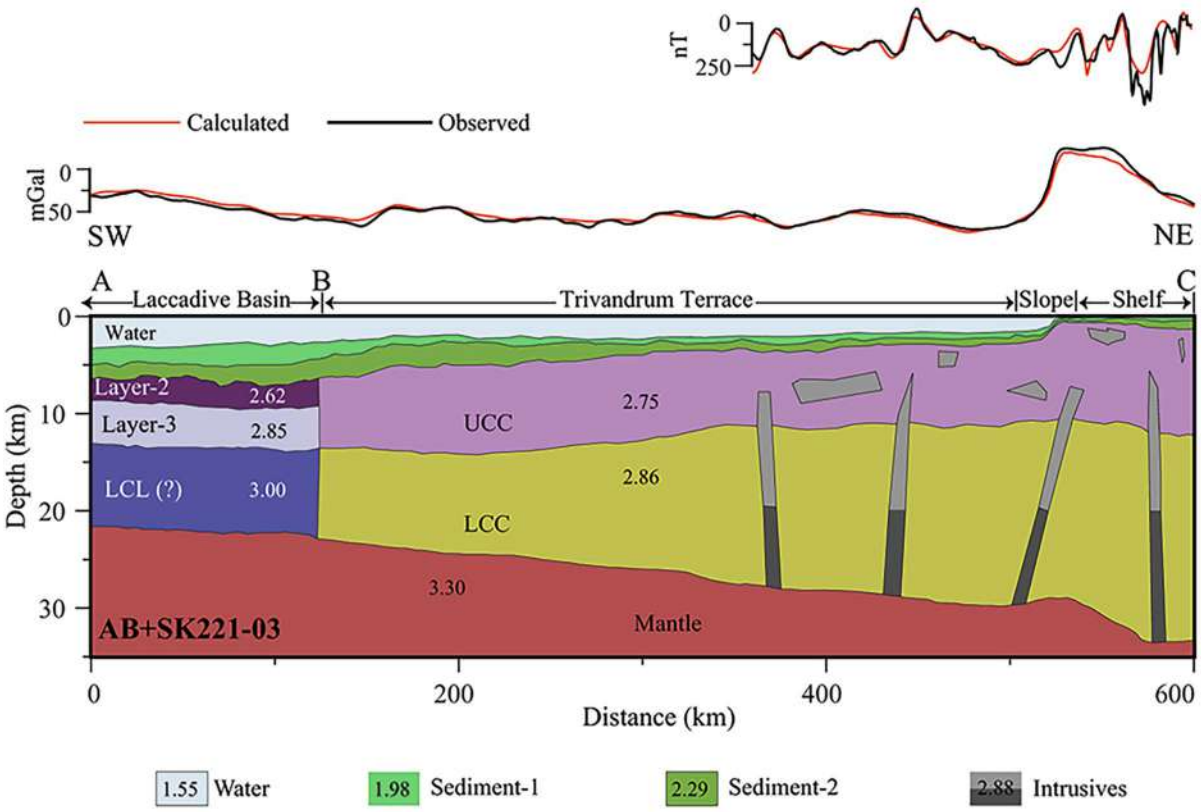

Fig. 9 Crustal model of the ATTC derived based on integrated gravity-magnetic modelling along the profile ABC (AB + SK221-03). UCC: Upper continental crust; LCC: Lower continental crust; LCL: High velocity lower crustal layer

of thinned continental crust intermingled with volcanic intrusives.

Comparison of crustal structure of NMR and ATTC

The revised plate tectonic reconstruction model shows that the Alleppey-Trivandrum Terrace Complex fits well in a bathymetric notch on the Northern Madagascar Ridge in the immediate pre-drift scenario, at ~ 88.0 Ma (Fig. 10a). This implies that geometries of both these features were formed after ~ 88 Ma, and prior to this period, both these features form a single unit of a crustal block. If the postulated juxtaposition of these features based on plate tectonic reconstruction is correct, then both these features should show a very similar crustal structure, even though some modifications might occur due to the geodynamic events occurred after their separation.

Our exercise to derive the crustal configuration of these postulated conjugate features reveals that both these features can be explained in terms of thinned continental crust intermingled with volcanics. The derived crustal model for the Northern Madagascar Ridge suggests a two-layered continental crust with a total thickness of ~ 16–17 km in the eastern side at the continent-ocean boundary between the NMR and the Mascarene Basin (Fig. 10b). Similarly, the derived crustal model for the Alleppey-Trivandrum Terrace Complex suggests a two-layered continental crust with a total thickness of ~ 16–17 km in the continent-ocean boundary between ATTC and the Laccadive Basin (Fig. 10c). The derived model for NMR further shows that the magnetic anomalies over the Northern Madagascar Ridge can be explained in terms of volcanic intrusion within the thinned continental crust. Similarly, the derived crustal model for ATTC suggests that the magnetic anomalies over this feature also can reasonably be explained in terms of volcanic intrusion within the thinned continental crust. Therefore, the above observations, complemented by the postulated juxtaposition observed from the plate tectonic reconstruction, strongly support that both these features existed as a single unit prior to ~ 88.0 Ma and this feature fragmented and broke away soon after ~ 88.0 Ma, possibly by the Marion hotspot activity. This age constraint comes from the

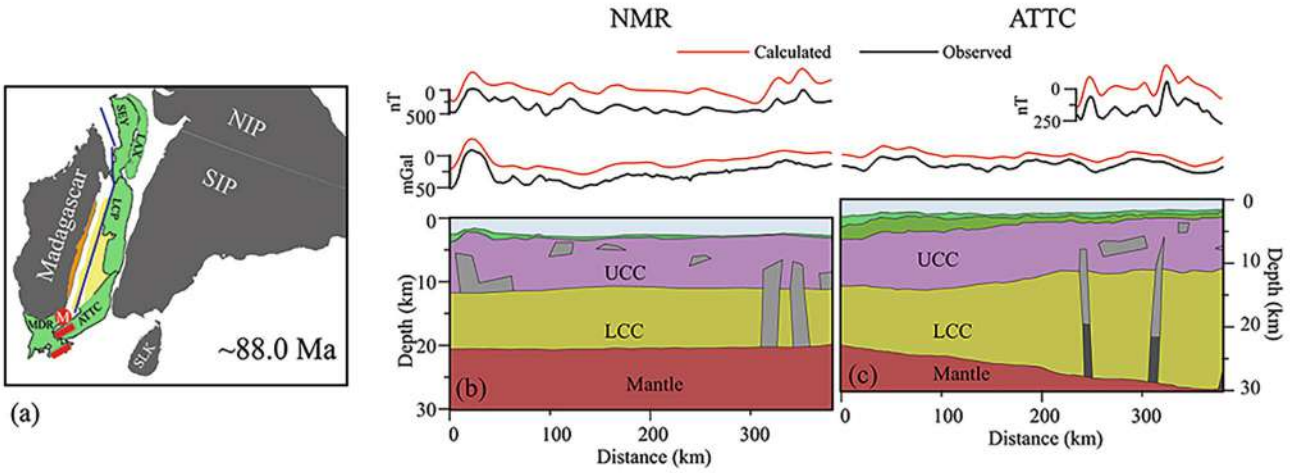

Fig. 10 (a) Plate tectonic reconstruction map (in fixed Madagascar reference frame) showing relative configuration of India and Madagascar in their pre-break up scenario (~ 88 Ma) with location of the profiles (shown as thick lines) along which the section of the crustal model presented as (b) and (c); (b) Selected portion of the crustal model derived in the eastern side of NMR near inferred continent-ocean boundary; (c) Selected portion of the crustal model derived in the southern end of ATTC near inferred continent-ocean boundary. Other details are as in Figs. 8 and 9

age of the volcanic rocks identified from Madagascar side (Storey et al. 1995; Torsvik et al. 1998; Torsvik et al. 2000) and Indian side (Valsangkar et al. 1981; Radhakrishna et al. 1994; Radhakrishna et al. 1999; Anilkumar et al. 2001; Pande et al. 2001; Melluso et al. 2009; Radhakrishna and Joseph, 2012; Mohan et al. 2016; Sheth et al. 2017).

Conclusions

The present study is aimed to compare the crustal configurations of the Northern Madagascar Ridge and the Alleppey-Trivandrum Terrace Complex to evaluate their postulated conjugate nature. For this, we analyzed multibeam bathymetry, gravity and magnetic data and carried out forward modelling of gravity and magnetic profiles. The derived crustal model for the NMR suggests that the moho is nearly flat at a level of ~ 22 km with a crustal thickness of ~ 16–17 km and the magnetic anomalies can be explained in terms of volcanic intrusives. Similarly, the derived crustal configuration of the ATTC suggests that the moho is at a level of ~ 32 km in the landward side of ATTC, shallowing to a level of ~ 22 km (with a thickness of ~ 16–17 km) at the boundary where the continental-oceanic crustal transition occurs between ATTC and the Laccadive Basin. The magnetic anomalies over the ATTC also have been interpreted in terms of volcanic intrusions. Comparison of the crustal configuration derived for these features reveal that both these features can be explained in terms of ~ 16–17 km thick thinned continental crust intermingled with volcanic intrusives. Therefore, based on these observations derived from the integrated interpretation of geophysical data, complemented by the postulated juxtaposition observed from the plate tectonic reconstruction, we support the earlier interpretation (Yatheesh et al., 2006; Yatheesh et al., 2013; Bhattacharya and Yatheesh, 2015) that the NMR and ATTC represent conjugate features that was proposed based on the fitting of shape and size of the bathymetric notch observed in the southeastern continental margin of Madagascar with a bathymetric protrusion observed in the southwestern continental margin of India in the India-Madagascar pre-drift scenario. These features remained as a single unit prior to ~ 88 Ma and subsequently got separated during the India-Madagascar breakup.

Acknowledgements The authors are grateful to Dr. M. Ravichandran, Director, National Centre for Polar and Ocean Research (NCPOR), Goa, and Prof. Sunil Kumar Singh, Director, CSIR-National Institute of Oceanography (CSIR- NIO), Goa, for their permission to publish the present work. This study forms a part of the PhD work of CMB at Goa University. We thank Dr. K.A. Kamesh Raju and Dr. G.N. Nayak for their constructive comments at various stages of the present work. We are indebted to two anonymous reviewers for their valuable comments, which helped us to improve the readability of the paper. We are grateful to Dr. Claudio Lo Iacono for the editorial handling of the manuscript. We thank the shipboard scientific party, officers and crew members of the MGS-03, MGS-04, and MGS-08 expeditions conducted onboard MGS Sagar, and SSD-059 expedition onboard RV Sindhu Sadhana, for extending their support. Directorate General

of Hydrocarbons, New Delhi is thanked for providing the multichannel seismic reflection sections used in the present study. For plotting the figures presented in this paper, we used Generic Mapping Tools (GMT) software (Wessel et al. 2019). This is NCPOR contribution J-79/2021-22 and NIO contribution 6887.

Funding Ministry of Earth Sciences (MoES), Government of India provided the financial support to carry out the work through the 'Geoscientific Studies of Exclusive Economic Zone of India' Programme under grant no. MoES/EFC/28/2018-PC-II.

Data Availability Datasets generated during the current study are confidential and is deposited at the Marine Geoscientific database being managed by NCPOR.

Code Availability Not applicable.

Declarations

Conflict of interest The authors declare no competing interests.

Ethics approval Not Applicable.

Consent to participate Not Applicable.

Consent for publication Certified that all authors have seen and approved the final version of the manuscript being submitted.

References

Anilkumar, Pande K, Venkatesan TR, Rao YJB (2001) The Karnataka Late Cretaceous Dykes as products of the Marion Hot Spot at the Madagascar - India Breakup Event: Evidence from 40Ar-39Ar geochronology and geochemistry. Geophys Res Lett 28:2715–2718. https://doi.org/10.1029/2001GL013007

Bhattacharya GC, Yatheesh V (2015) Plate-tectonic evolution of the deep ocean basins adjoining the western continental margin of India - A proposed model for the early opening scenario. In: Mukherjee J (ed) Petroleum Geoscience: Indian Contexts. Springer International Publishing, pp 1–61

Bijesh CM, John Kurian P, Yatheesh V et al (2018) Morphotectonic characteristics, distribution and probable genesis of bathymetric highs off southwest coast of India. Geomorphology 315:33–44. https://doi.org/10.1016/j.geomorph.2018.04.015

Brocher TM (2005) Empirical relations between elastic wavespeeds and density in the Earth's crust. Bull Seismol Soc Am 95(6):2081–2092

Fowler CMR (2005) The Solid Earth: an Introduction to Global Geophysics. Cambridge University Press, Cambridge

GEBCO Compilation Group (2020) GEBCO 2020 Grid, doi:https://doi.org/10.5285/a29c5465-b138-234d-e053-6c86abc040b9

Goslin J, Recq M, Schlich R (1981) Structure profonde du plateau de Madagascar: relations avec le plateau de crozet. Tectonophysics 76:75–97

Goslin J, Segoufin J, Schlich R, Fisher RL (1980) Submarine topography and shallow structure of the Madagascar Ridge, Western Indian Ocean. GSA Bull 91:741–753

IOC-IHO-BODC (2003) Centenary Edition of the GEBCO Digital Atlas, published on CD-ROM on behalf of the Intergovernmental Oceanographic Commission and the International Hydrographic Organization as part of the General Bathymetric Chart of the Oceans. British Oceanographic Data Centre, Liverpool, UK

Leinweber VT, Klingelhoefer F, Neben S et al (2013) The crustal structure of the Central Mozambique continental margin - Wide-angle seismic, gravity and magnetic study in the Mozambique Channel, Eastern Africa. Tectonophysics 599:170–196. https://doi.org/10.1016/j.tecto.2013.04.015

Maus S, Barckhausen U, Berkenbosch H et al (2009) EMAG2: A 2–arc min resolution Earth Magnetic Anomaly Grid compiled from satellite, airborne, and marine magnetic measurements. Geochem Geophys Geosyst 10:Q08005. https://doi.org/10.1029/2009GC002471

Melluso L, Sheth HC, Mahoney JJ et al (2009) Correlations between silicic volcanic rocks of the St Mary's Islands (southwestern India) and eastern Madagascar: implications for Late Cretaceous India–Madagascar reconstructions. J Geol Soc London 166:283–294. https://doi.org/10.1144/0016-76492007-147

Mohan MR, Shaji E, Satyanarayanan M et al (2016) The Ezhimala Igneous Complex, southern India: Possible imprint of Late Cretaceous magmatism within rift setting associated with India-Madagascar separation. J Asian Earth Sci 121:56–71. https://doi.org/10.1016/j.jseaes.2016.02.003

Nathaniel DM (2013) Hydrocarbon Potential of Sub-Basalt Mesozoics of Deepwater Kerala Basin, India. 10th Biennial International Conference & Exposition Kochi 2013, 1–7

Pande K, Sheth HC, Bhutani R (2001) ^{40}Ar–^{39}Ar age of the St. Mary's Islands volcanics, southern India: record of India–Madagascar break-up on the Indian subcontinent. Earth Planet Sci Lett 193:39–46

Radhakrishna T, Dallmeyer RD, Joseph M (1994) Palaeomagnetism and $^{36}Ar/^{40}Ar$ vs. $^{39}Ar/^{40}Ar$ isotope correlation ages of dyke swarms in central Kerala, India: Tectonic implications. Earth Planet Sci Lett 121:213–226

Radhakrishna T, Joseph M (2012) Geochemistry and paleomagnetism of Late Cretaceous mafic dikes in Kerala, southwest coast of India in relation to large igneous provinces and mantle plumes in the Indian Ocean region. GSA Bull 124:240–255. https://doi.org/10.1130/B30288.1

Radhakrishna T, Maluski H, Mitchell JG, Joseph M (1999) $^{40}Ar/^{39}Ar$ and K/Ar geochronology of the dykes from the south Indian granulite terrain. Tectonophysics 304:109–129

Sandwell D, Müller D, Smith W et al (2014) New global marine gravity from CryoSat-2 and Jason-1 reveals buried tectonic structure. Science 346:65–67. https://doi.org/10.1126/science.1258213

Sheth H, Pande K, Vijayan A et al (2017) Recurrent Early Cretaceous, Indo-Madagascar (89–86 Ma) and Deccan (66 Ma) alkaline magmatism in the Sarnu-Dandali complex, Rajasthan: $^{40}Ar/^{39}Ar$ age evidence and geodynamic significance. Lithos 284–285:512–524

Shuhail M, Yatheesh V, Bhattacharya GC et al (2018) Formation and evolution of the Chain-Kairali Escarpment and the Vishnu Fracture Zone in the Western Indian Ocean. J Asian Earth Sci 164:307–321. https://doi.org/10.1016/j.jseaes.2018.06.022

Storey M, Mahoney JJ, Saunders AD et al (1995) Timing of hot spot-related volcanism and the breakup of Madagascar and India. Science 267:852–855. https://doi.org/10.1126/science.267.5199.852

Straume EO, Gaina C, Medvedev S et al (2019) GlobSed: Updated total sediment thickness in the World's Oceans. Geochem Geophys Geosyst 20:1756–1772. https://doi.org/10.1029/2018GC008115

Talwani M, Heirtzler JR (1964) Computation ofmagnetic anomalies caused by two di- mensional structures of arbitrary shape. In: Parks GA (ed) Computers in the Mineral Industries. Stanford University, pp. 464–480

Talwani M, Worzel JL, Landisman M (1959) Rapid gravity computations for two-dimensional bodies with application to the Mendocino submarine fracture zone. J Geophys Res 64:49–59

Torsvik TH, Tucker RD, Ashwal LD et al (1998) Late Cretaceous magmatism in Madagascar: Palaeomagnetic evidence for a stationary

Marion hotspot. Earth Planet Sci Lett 164:221–232. https://doi.org/10.1016/S0012-821X(98)00206-4

Torsvik TH, Tucker RD, Ashwal LD et al (2000) Late Cretaceous India–Madagascar fit and timing of break-up related magmatism. Terra Nova 12:220–224

Valsangkar AB, Radhakrishnamurthy C, Subbarao KV, And Beckinsale RD (1981) Palaeomagnetism and Potassium - Argon age studies of acid Igneous rocks from the St.Mary Islands. In: Subbarao KV, Sukeshwala RN (eds) Deccan Volcanism, vol 3. Mem. Geol. Soc. India, pp 265–276

Wessel P, Luis JF, Uieda L et al (2019) The Generic Mapping Tools Version 6. Geochem Geophys Geosyst 20:5556–5564

Yatheesh V (2020) Structure and tectonics of the continental margins of India and the adjacent deep ocean basins: Current status of knowledge and some unresolved problems. Episodes 43:586–608. https://doi.org/10.18814/epiiugs/2020/020039

Yatheesh V, Bhattacharya GC, Mahender K (2006) The terrace like feature in the mid-continental slope region off Trivandrum and a plausible model for India-Madagascar juxtaposition in immediate pre-drift scenario. Gondwana Res 10:179–185. https://doi.org/10.1016/j.gr.2005.11.021

Yatheesh V, Bhattacharya GC, Shuhail M (2020) Revised plate tectonic reconstruction model for the early opening of the Arabian Sea. In: Rossi P, François C, Miles P (eds) The Indian Ocean and its Margins. Commission for the Geological Map of the World, France, pp 11–12

Yatheesh V, Kurian PJ, Bhattacharya GC, Rajan S (2013) Morphotectonic architecture of an India-Madagascar breakup related anomalous submarine terrace complex on the southwest continental margin of India. Mar Pet Geol 46:304–318. https://doi.org/10.1016/j.marpetgeo.2013.07.005